UNIVERSITY OF LEEDS

Long-Term Flexural Performance of Cracked Reinforced Concrete Beams Incorporating Recycled Aggregate and Steel Fibres

A thesis submitted in accordance with the requirements of School of Civil Engineering for the degree of

DOCTOR OF PHILOSOPHY

by

Lamen Saleh Mohamed Sryh

B. Sc., Civil Engineering

M. Sc., Structural Engineering

The University of Leeds

Faculty of Engineering

School of Civil Engineering

October, 2017

The candidate confirms that the work submitted is his own and that appropriate credit has been given within the thesis where reference has been made to the work of others.

This copy has been supplied on the understanding that it is copyright material and that no quotation from the thesis may be published without proper acknowledgement.

© 2017 The University of Leeds and Lamen Saleh Mohamed Sryh

PAPERS PRODUCED FROM THIS THESIS

Papers published in international conferences:

- SRYH, L. AND FORTH, J., 2015. Experimental investigation on the effect of steel fibres on the mechanical properties of recycled aggregate concrete. *In Proceedings of: the International Conference on the Fibre Concrete*. 10 – 11 September 2015, Prague, Czech Republic.
- SRYH, L. AND FORTH, J., 2016. Effect of Steel Fibres and Recycled Aggregate on Drying Shrinkage and Creep Deformations of Concrete. *In Proceedings of: The 9th International Concrete Conference*, 4 – 6 July 2016, Dundee, United Kingdom.

Papers submitted to journals:

- SRYH, L. AND FORTH, J., 2016. Long-term Flexural Behaviour of Reinforced Concrete Beams with Recycled Aggregate. Submitted for publishing in the *Engineering Structures Journal*, Elsevier.

Papers are in preparation:

- SRYH, L. AND FORTH, J., 2017. Long-term Loss of Tension Stiffening of Concrete Containing Recycled Aggregate and Steel Fibres. In preparation to be submitted for publishing in the *Construction and Building Material Journal*, Elsevier.
- SRYH, L. AND FORTH, J., 2017. The Feasibility of Adding Steel Fibres to Enhance the Long-term Flexural Performance of Reinforced Recycled Aggregate Concrete Beams. In preparation to be submitted for publishing in the *ACI Structural Journal*, American Concrete Institute.

ABSTRACT

The reuse of CDW as a coarse aggregate in the production of new concrete could potentially conserve natural resources, reduce the amount of landfill waste and reduce energy consumption; this would contribute to improved sustainability within the construction sector. The extensive scientific research conducted on this subject to date has concluded that in comparison to natural aggregate (NA), the quality of recycled aggregate (RA) is generally poorer and replacement with recycled aggregate has a negative impact on all concrete properties. The most noticeable effect is on time-dependent deformation (i.e. creep and shrinkage). This has meant that the use of recycled aggregate concrete in various construction applications has been restricted.

In this study, an experimental programme has been carried out to examine the effect of incorporating recycled aggregate and steel fibres on the mechanical properties, creep, shrinkage, long-term loss of tension stiffening and long-term flexural behaviour of beams under sustained loads. The results obtained from the tests indicated that replacement with recycled aggregate reduced all concrete properties but the addition of steel fibres proved to be highly beneficial and, in fact, countered the detrimental effect of the recycled aggregate. For instance, it was found that the addition of 0.5% and 1.0% steel fibres to concrete containing 50% and 100% recycled aggregate, respectively, resulted in concrete with almost the same performance as normal concrete.

An analytical investigation was also conducted to evaluate the suitability of existing code procedures for predicting the long-term deflection of concrete beams incorporating recycled aggregate and steel fibres. It was found that there were shortcomings within the existing codes when analysing these materials and modifications to the Eurocode 2 method were thus proposed. A numerical analysis program was developed using MATLAB language for predicting the long-term deflection of beams based on the proposed modifications. The program was used for validating the modifications by using the experimental results from this research and previous studies in the literature.

In addition, a 3D finite element analysis was carried out using the commercial software Midas FEA which included the development of a novel approach for predicting the long-term deflection of cracked reinforced concrete beams containing recycled aggregate and steel fibres. The approach was verified by comparing the finite element analysis predictions with the experimental results from this study and data selected from previous investigations. Sensitivity and parametric studies were carried out to investigate the effect of some model and structural parameters.

ACKNOWLEDGMENTS

I would like to express my sincere gratitude to my supervisor **Prof. John Forth** for his critical review and valuable comments which have had a great impact on the quality of this research. His assistance, patience and great guidance are highly appreciated.

I express my sincere thanks to Dr. Nikolaos Nikitas for his comments and great advice which really improved this thesis.

Special thanks also go to Prof. Jianqiao Ye and Dr. Konstantinos Tsavdaridis for their valuable comments and feedback on assessing this thesis.

I would like to express my appreciation to the School of Civil Engineering at the University of Leeds for the facilities and practical assistance. I am deeply grateful to the technicians in the Casting Shop Mr. George Flatt and in the George Earle Laboratory Mr. Norman Harmon, Mr. Stephen Holmes, Mr. Marvin Wilman and Mr. Robert Clarke for their efforts throughout the experimental work.

The financial support from the Ministry of Higher Education in Libya is gratefully acknowledged. The support provided by the Bureau of the Cultural Attaché at the Libyan Embassy in London, UK, is also highly appreciated.

Finally, I would like to extend my sincere thanks to my wonderful family, friends and colleagues for their support and encouragement, which have made this work possible.

Lamen Sryh

Leeds, 2017

DEDICATION

I wish to dedicate this work with all my love

To

The souls of my father "Saleh"

and grandfather "Mohamed"

To

My beloved mother "Saleha"

To

My lovely wife "Dania" and cute son "Muhab"

To

My dear brothers and sister

To

My uncle and all the members of my family

To

My friends and colleagues

TABLE OF CONTENTS

ABSTRACT ..... **i**

ACKNOWLEDGMENTS ..... **ii**

DEDICATION ..... **iii**

TABLE OF CONTENTS ..... **iv**

LIST OF FIGUERS ..... **ix**

LIST OF TABLES ..... **xv**

Chapter 1 : Introduction **1**

1.1 Motivation 1

1.2 Research Aim and Objectives 3

1.3 Research Strategy 4

1.4 Research Significance 4

1.5 Layout of this Thesis 5

Chapter 2 : Properties of Concrete Incorporating Recycled Aggregate and Fibres **7**

2.1 Introduction 7

2.2 Construction Waste; How it is Generated and Environmental Concerns 7

2.3 Preparation and Production of CDW aggregate 8

2.4 Composition and Classification of CDW aggregate 9

2.5 Properties of CDW as Recycled Aggregate 11

2.5.1 Attached mortar content in CDW aggregate 12

2.5.2 Density 12

2.5.3 Water absorption 13

2.5.4 Porosity 16

2.6 Properties of Recycled Aggregate Concrete 17

2.6.1 Workability 17

2.6.2 Compressive strength 19

2.6.3 Tensile strength 22

2.6.4 Flexural strength 25

2.6.5 Modulus of elasticity 26

2.7 Flexural Behaviour of Reinforced RAC Beams 27

2.8 Steel Fibre Reinforced Concrete 31

2.9 Properties of Steel Fibre Reinforced Concrete 33
2.9.1 Compressive strength 34
2.9.2 Tensile strength 34
2.9.3 Flexural strength 36
2.9.4 Modulus of elasticity 37
2.10 Flexural Behaviour of SFRC Beams 38
2.11 Effect of Adding Fibres on the Properties of RAC 44
2.12 Economic and Energy Aspects 48
2.13 Summary 50
Chapter 3 : Long-term Performance of Concrete Incorporating Recycled Aggregate and Steel Fibres 52
3.1 Introduction 52
3.2 Creep and Shrinkage 52
3.2.1 Effect of recycled aggregate 53
3.2.2 Effect of steel fibres 62
3.3 Long-term Flexural Behaviour of Beams 67
3.3.1 Effect of recycled aggregate 67
3.3.2 Effect of steel fibres 71
3.4 Tension Stiffening 74
3.4.1 Definition 74
3.4.2 Re-evaluation of experiments 77
3.4.3 Factors affecting tension stiffening 79
3.4.4 Long-term loss of tension stiffening 82
3.4.5 Effect of recycled aggregate and steel fibres 88
3.5 Summary 90
Chapter 4 : Experimental Programme 93
4.1 Introduction 93
4.2 Experimental Programme 93
4.3 Material Properties 95
4.3.1 Cement 95
4.3.2 Fine aggregate 95
4.3.3 Coarse aggregate 96
4.3.4 Water 99
4.3.5 Superplasticisers 99
4.3.6 Reinforcement bars 99

4.3.7 Steel fibres....100
4.4 Concrete Mixes....101
4.5 Test Specimens....102
4.6 Casting and Curing....103
4.7 Test Procedures....106
4.7.1 Compressive strength test....106
4.7.2 Tensile strength test....106
4.7.3 Flexural strength test....108
4.7.4 Modulus of elasticity test....108
4.7.5 Shrinkage test....109
4.7.6 Compressive creep test....111
4.7.7 Tensile creep test....111
4.7.8 Long-term tension stiffening test....112
4.7.9 Long-term flexural bending test....114
4.8 Summary....116
Chapter 5 : Experimental Results and Discussion....118
5.1 Introduction....118
5.2 Mechanical Properties of Concrete....118
5.2.1 Compressive strength....119
5.2.2 Tensile strength....121
5.2.3 Flexural strength....123
5.2.4 Modulus of elasticity....124
5.3 Time-dependent Deformations of Concrete....125
5.3.1 Drying shrinkage....125
5.3.2 Compressive creep....128
5.3.3 Tensile creep....132
5.4 Long-term Loss of Tension Stiffening....134
5.4.1 Effect of recycled aggregate....135
5.4.2 Effect of steel fibres....139
5.5 Short-term Deflection and Cracking Pattern of Beams....144
5.5.1 Effect of recycled aggregate....144
5.5.2 Effect of steel fibres....147
5.6 Long-term Deflection of Beams....150
5.6.1 Effect of recycled aggregate....150

5.6.2 Effect of steel fibres 153
5.7 Conclusion 158
Chapter 6 : Analytical Investigation 160
6.1 Introduction.....160
6.2 Existing Code Procedures for Long-term Deflection 160
6.2.1 ACI-318 161
6.2.2 ACI-435 163
6.2.3 CSA 165
6.2.4 AS3600.....165
6.2.5 Eurocode 2 168
6.3 Comparison of the Code Procedures.....172
6.4 Limitations and Modifications.....173
6.4.1 Cracked section analysis approach.....173
6.4.2 Elastic analysis approach.....182
6.5 Numerical Analysis Program 186
6.6 Comparison of the Proposed Modifications.....186
6.7 Conclusion 189
Chapter 7 : Finite Element Analysis 191
7.1 Introduction.....191
7.2 Description of Finite Element Model 191
7.2.1 Geometry modelling.....191
7.2.2 Constitutive models for materials 192
7.2.3 Property of sections 197
7.2.4 Element types.....197
7.2.5 Meshing 199
7.2.6 Loading and Boundary conditions 200
7.2.7 Analysis case.....201
7.3 Development of the FEA Approach 203
7.4 Results and Verification.....207
7.4.1 Long-term deflection 207
7.4.2 Concrete surface strains 209
7.4.3 Verification.....209
7.5 Investigation of Model Parameters 213
7.5.1 Mesh size 213

7.5.2 Effective reduction in stiffness....215
7.5.3 Shrinkage effect at cracking....215
7.5.4 Depth of cracking....217
7.6 Parametric Study....217
7.6.1 Compression reinforcement amount....218
7.6.2 Concrete cover....219
7.6.3 Experimental and predicted shrinkage and creep....219
7.7 Conclusion....221
Chapter 8 : Conclusions and Recommendations for Further Research....221
8.1 Introduction....223
8.2 Conclusions....223
8.2.1 Concluding remarks from the experimental investigation....223
8.2.2 Concluding remarks from the analytical investigation....223
8.2.3 Concluding remarks from the finite element analysis....224
8.3 Recommendations for Further Research....225
REFERENCES....228
APPENDIX....239

LIST OF FIGUERS

Figure 2-1 Total waste generation by sector in the EU (EEA 2015)..... 8

Figure 2-2 The typical CDW recycling plant (Eguchi et al., 2007)..... 9

Figure 2-3 Average composition of CDW (Fisher and Werge, 2009)..... 11

Figure 2-4 Proportions of CDW materials (Corinaldesi and Moriconi, 2009a)..... 11

Figure 2-5 Relationship between attached mortar content and bulk density (De Juan and Gutiérrez, 2009) 13

Figure 2-6 Relationship between attached mortar content and absorption of CDW (De Juan and Gutiérrez, 2009) 14

Figure 2-7 Normal (NMA) and two-stage (TSMA) mixing approaches adopted by Tam et al. (2007)..... 16

Figure 2-8 Reduction ratio in compressive strength due to increase of CDW content at 28 days (Pepe, 2015)..... 20

Figure 2-9 Effect of crushed brick content in RA on the splitting tensile strength (Yang et al., 2011)..... 24

Figure 2-10 Load-deflection curves of the full scale test beams (Arezoumandi et al., 2015) 28

Figure 2-11 Flexural behaviour of beams with different levels of RCA (Knaack and Kurama, 2014) 29

Figure 2-12 Crack patterns at faluir load in the middle of the span of normal and recylced aggregate beams (Ignjatović et al., 2013) 30

Figure 2-13 Commonly available types of steel fibres 33

Figure 2-14 Effect of steel fibre content on compressive strength of concrete (Ashour et al., 2000)..... 34

Figure 2-15 Influence of steel fibres content on tensile strength of concrete (Johnston and Coleman, 1974)..... 35

Figure 2-16 Effect of steel fibre content on splitting tensile strength of concrete with different grades (Ashour et al., 2000) 36

Figure 2-17 Effect of steel fibre content on modulus of rupture (Ashour et al., 2000)37

Figure 2-18 Effect of steel fibre volume fraction and aspect ratio on modulus of elasticity of concrete (Gul et al., 2014) 38

Figure 2-19 Load-deflection behaviour of plain and fibre reinforced concrete and the mechanism of strength enhancement in flexure (Monteiro, 2006) 39

Figure 2-20 Effect of steel fibres on the toughness and ductility of concrete (Li, 2011) 40

Figure 2-21 Load-deflection curves for SFRC beams (Ashour et al., 2000)..... 41

Figure 2-22 Steel fibre content and aspect ratio effect on load-deflection relationship of beams (Alsayed, 1993) 42

Figure 2-23 Load-deflection curves for SFRC beams (Ashour et al., 1997)..... 44

Figure 2-24 Effect of RCA and steel fibres on the compressive strength and flexural toughness of concrete (Jalilifar et al., 2016) 45

Figure 2-25 Effect of steel fibres on the compressive and flexural strength of RAC (Heeralal et al., 2009)..... 47

Figure 2-26 Increase in the mechanical properties of RAC due to the addition of glass fibres (Prasad and Rathish Kumar, 2007) 48

Figure 3-1 Creep test results (Knaack and Kurama, 2015a)..... 54

Figure 3-2 Shrinkage test results (Knaack and Kurama, 2015a) 55

Figure 3-3 RAC shrinkage and creep curves (Fan et al., 2014)..... 57

Figure 3-4 Shrinkage strains for different replacement levels of RCA (Domingo et al., 2010) 59

Figure 3-5 Creep deformations for different replacement levels of RCA (Domingo et al., 2010)..... 59

Figure 3-6 Influence of crimped steel fibres on the free shrinkage of concrete (Mangat and Azari, 1984)..... 63

Figure 3-7 Influence of steel fibres on c (Mangat and Azari, 1985)..... 64

Figure 3-8 Creep coefficients of SFRC (Tan et al., 1994a)..... 65

Figure 3-9 Shrinkage strains of SFRC (Tan et al., 1994a)..... 65

Figure 3-10 Effect of steel fibres volume fraction on shrinkage of concrete (Chern and Young, 1990) 67

Figure 3-11 Long-term deflection of beams with different ages and levels of loading (Knaack and Kurama, 2015b) 68

Figure 3-12 Long-term deflections of NC and RAC beams (Łapko and Grygo, 2010) 70

Figure 3-13 Long-term deflection of SFRC beams (Tan et al., 1994b) 71

Figure 3-14 Effect of steel fibres on the total long-term deflection of beams with various reinforcement ratios (Ashour et al., 1997) 73

Figure 3-15 Moment-curvature relationship for a reinforced concrete member in bending (Gilbert, 2012) 75

Figure 3-16 Stages of cracking of reinforced concrete members in tension (Gribniak et al., 2009)..... 76

Figure 3-17 Axial stress distribution and crack formation for reinforced concrete members in tension (Gribniak et al., 2009)..... 77

Figure 3-18 Equivalence between tension and flexural members (Whittle and Jones, 2004) 78

Figure 3-19 Effect of concrete strength on the reduction in tension stiffening under axial tensile loading (Khalfallah and Guerdouh, 2014) 80
Figure 3-20 Effect of the modulus of elasticity of concrete on tension stiffening for different reinforcement ratios (Khalfallah and Guerdouh, 2014) 81
Figure 3-21 Reinforcement strains versus time (Scott and Beeby, 2005) 84
Figure 3-22 Reinforcement strains along the length of the bar (Scott and Beeby, 2005) 84
Figure 3-23 Decay of concrete tensile stress (Scott and Beeby, 2005) 86
Figure 3-24 Effect of steel fibre content on the load-strain relationship of concrete specimens in tension (de Oliveira Júnior et al., 2016) 89
Figure 3-25 Load-strain curves of plain and steel fibre reinforced concrete (Bischoff, 2000) 90
Figure 4-1 Plan of the experimental programme 94
Figure 4-2 Grading of the fine aggregate 96
Figure 4-3 Samples of the coarse aggregate 98
Figure 4-4 Grading of the coarse aggregate 98
Figure 4-5 Composition of the recycled aggregate used in this research 98
Figure 4-6 Reinforcement of beam specimens 99
Figure 4-7 Uni-axial tensile test of steel bars 100
Figure 4-8 Hooked-end steel fibres (Dramix 3D) 100
Figure 4-9 Mechanical drum mixer 103
Figure 4-10 Casting and curing of specimens 105
Figure 4-11 Compressive strength tests 106
Figure 4-12 Splitting tensile strength test 107
Figure 4-13 Direct tensile strength test 107
Figure 4-14 Flexural strength test 108
Figure 4-15 Modulus of elasticity test 109
Figure 4-16 Shrinkage test 110
Figure 4-17 Environmental conditions of the Laboratory 110
Figure 4-18 Compressive creep test 111
Figure 4-19 Tensile creep test 112
Figure 4-20 Specimens of tension stiffening test 113
Figure 4-21 Test rig for tension stiffening specimens 113
Figure 4-22 Tension stiffening test 114
Figure 4-23 Details of beam dimensions and reinforcement 114
Figure 4-24 Flexural bending test 115

Figure 5-1 Compressive strength results of cubes 120
Figure 5-2 Compressive strength results of cylinders.....120
Figure 5-3 Effect of steel fibres during loading of cubic and cylindrical specimens121
Figure 5-4 Results of splitting tensile strength.....122
Figure 5-5 Results of direct tensile strength 122
Figure 5-6 Results of flexural strength 123
Figure 5-7 Results of modulus of elasticity.....124
Figure 5-8 Effect of recycled aggregate on drying shrinkage.....126
Figure 5-9 Effect of steel fibres on drying shrinkage.....127
Figure 5-10 Effect of incorporating recycled aggregate on compressive creep 129
Figure 5-11 Effect of adding steel fibres on compressive creep 130
Figure 5-12 Compressive creep coefficient results.....131
Figure 5-13 Effect of incorporating recycled aggregate on tensile creep 132
Figure 5-14 Effect of adding steel fibres on tensile creep.....133
Figure 5-15 Effect of RA on the reduction in tension stiffening over time.....135
Figure 5-16 Concrete tensile stress as a function of time for NC and RAC specimens 136
Figure 5-17 Effect of recycled aggregate on crack distribution 138
Figure 5-18 Influence of the steel fibres on the reduction rate of tension stiffening over time 140
Figure 5-19 Effect of steel fibres on the concrete tensile stresses as a function of time 142
Figure 5-20 Effect of steel fibres on crack distribution.....143
Figure 5-21 Effect of recycled aggregate on short-term deflection 145
Figure 5-22 Effect of recycled aggregate on cracking pattern 146
Figure 5-23 Effect of steel fibres on the short-term deflection 148
Figure 5-24 Effect of steel fibres on the cracking pattern 149
Figure 5-25 Effect of recycled aggregate on long-term deflection.....151
Figure 5-26 Effect of recycled aggregate on the development of concrete surface strains in the compression and tension zones.....153
Figure 5-27 Effect of steel fibres on long-term deflection 155
Figure 5-28 Concrete surface strains of beams in compression zone 156
Figure 5-29 Concrete surface strains of beams in tension zone.....157
Figure 6-1 ACI multiplier factor for long-term deflection 162
Figure 6-2 Comparison of the experimental and predicted long-term deflection of NC and RAC beams tested 175

Figure 6-3 Time-dependent strain distribution for SFRAC beams after 360 days under sustained load (Nakov, 2014).....178

Figure 6-4 Comparison of the experimental and predicted long-term deflection of beams with 0.5% steel fibres.....180

Figure 6-5 Comparison of the experimental and predicted long-term deflection of beams with 1.0% steel fibres.....181

Figure 6-6 Comparison between the experimental and elastic analysis results for the long-term deflection of NC, SFC-0.5 and SFC-1.0 beams.....183

Figure 6-7 Comparison between the experimental and elastic analysis results for the long-term deflection of RAC-50, SFRAC-50-0.5 and SFRAC-50-1.0 beams183

Figure 6-8 Comparison between the experimental and elastic analysis results for the long-term deflection of.....183

Figure 6-9 Comparison between experimental and predicted results.....187

Figure 7-1 Modelling of concrete and reinforcement 192

Figure 7-2 Definition of the creep function (MIDAS, 2010) 193

Figure 7-3 Creep function of concrete.....194

Figure 7-4 Shrinkage function of concrete.....196

Figure 7-5 Linear and Quadratic shape functions of solid elements (MIDAS, 2010)198

Figure 7-6 Mesh of the beam model 200

Figure 7-7 Loading and boundary conditions of the beam model.....201

Figure 7-8 Composing of construction stages (MIDAS, 2010).....202

Figure 7-9 Composition of the construction stages 203

Figure 7-10 Comparison between experimental results for NC with FEA predictions using an elastic model for the concrete 204

Figure 7-11 Definition of shrinkage as a non-uniform compressive stress.....207

Figure 7-12 Comparison between the experimental and FEA results for long-term deflection 208

Figure 7-13 Comparison between the experimental and FEA results for concrete surface strains in the compression zone 210

Figure 7-14 Comparison between the experimental and FEA results for concrete surface strains in the tension zone.....211

Figure 7-15 Mesh sensitivity of the predictions for long-term deflection 214

Figure 7-16 Mesh sensitivity of the predictions for concrete surface strains in the compression and tension zones.....214

Figure 7-17 Effect of reduction value in stiffness on the predictions for long-term deflection 215

Figure 7-18 Effect of shrinkage in the cracked region on the predictions for long-term deflection 216

Figure 7-19 Influence of crack depth on the predictions for long-term deflection..217
Figure 7-20 Effect of the compression reinforcement amount on the long-term deflection of SFRAC-50-1.0 specimen 218
Figure 7-21 Effect of concrete cover on the long-term deflection of SFRAC-50-1.0 specimen 219
Figure 7-22 Comparison of experimental and predicted shrinkage for NC specimen 220
Figure 7-23 Comparison of experimental and predicted creep for NC specimen..220
Figure 7-24 Effect of using the experimental and predicted shrinkage and creep values on the long-term deflection for NC specimen 221

LIST OF TABLES

Table 2-1 Distribution of CDW material content (Coelho and de Brito, 2011) 10

Table 2-2 Reduction in compressive and tensile strength of concrete containing CDW 23

Table 2-3 Reduction in modulus of elasticity of concrete containing CDW 26

Table 2-4 Specifications for steel fibres from ASTM A820 32

Table 3-1 Proposed constants for creep and shrinkage strains of SFRC (Tan et al., 1994a)..... 66

Table 3-2 Results of concrete tensile stresses (Scott and Beeby, 2005) 87

Table 4-1 Chemical compounds and physical properties of the cement..... 95

Table 4-2 Grading of the fine aggregate..... 96

Table 4-3 Grading of the coarse aggregate..... 97

Table 4-4 Properties of the fine and coarse aggregate..... 97

Table 4-5 Properties of steel bars 100

Table 4-6 Design of concrete mixes.....101

Table 4-7 Specimens used for the different tests 102

Table 4-8 Results of the slump tests.....104

Table 5-1 Experimental results for concrete mechanical properties 119

Table 5-2 Effect of RA on the concrete tensile stress.....138

Table 5-3 Concrete tensile stress results 144

Table 5-4 Short-term and long-term deflections of beams tested 150

Table 5-5 Details of cracks at stabilised cracking stage 152

Table 6-1 Values of the multiplier factor $\boldsymbol{St}$ for long-term deflection calculations ..165

Table 6-2 Predictions from the existing code procedures for the long-term deflection of NC beams.....172

Table 6-3 Calibration of experimental and predicted long-term deflections using the cracked section analysis approach.....179

Table 6-4 Long-term deflection results of elastic analysis approach.....184

Table 6-5 Comparison between experimental and predicted results using the proposed calculation method 188

Table 7-1 Values of the reduction factor $\boldsymbol{K}*$ for the elastic analysis.....206

Table 7-2 Comparison between experimental and predicted results using the modified FEA approach.....212

Chapter 1 : Introduction

1.1 Motivation

Concrete is the most common structural material, as it is used in all types of construction work. It has been reported that approximately 10 billion tonnes of concrete are consumed annually worldwide (De Brito and Saikia, 2012). The corresponding quantity of aggregate, which is the main component of concrete, is in the range of 8 to 12 billion tonnes. The continued growth in demand for concrete raises two main concerns regarding: first, the availability of the natural resources needed for its component materials and second, the vast size of the landfills required for disposal of construction and demolition waste. These two factors mean concrete is not an environmentally friendly construction material.

Concrete structures usually last for several decades, but sometimes their demolition is unexpected and unavoidable for reasons such as structural or material deterioration, natural disasters, construction development or war-inflicted damage. Recently, the Environmental Protection Agency (EPA, 2014) has estimated that the generation of rubble from construction and demolition waste (CDW) and renovation of buildings is close to 170 million tonnes annually in the USA; whereas, according to European Environment Agency (EEA, 2015) it is about 850 million tonnes in the EU; and based on data published by the Government Statistical Services (WRAP, 2015) it is roughly 110 million tonnes in the UK alone.

These figures have attracted much attention in the research community of civil engineering. The reuse of CDW as a coarse aggregate in the production of new concrete could potentially conserve natural resources, eliminate landfills and reduce energy consumption which would contribute to greater sustainability in the construction sector. Indeed, extensive scientific research on this subject has been carried out over the last 20 years. However, these studies have concluded that in comparison to natural aggregate (NA), the quality of recycled aggregate (RA) is generally poorer and replacing NA by RA has a negative impact on all concrete

properties. The most noticeable effect is on the time-dependent deformation (i.e. creep and shrinkage) as opposed to the mechanical properties. This had made the use of RA in various construction applications is restricted.

All of the studies to date have suggested that the presence of adhered mortar and other material such as clay bricks and tiles in RA, which are already poorer than NA, is the cause of the deterioration in properties observed. These materials make RA more porous and more liable to absorb high amounts of water. The high porosity and water absorption capacity of RA substantially reduce the properties of the resulting concrete.

For this reason, British Standard (BS 8500-2, 2006) only allows a maximum replacement of 20% of the total aggregate in concrete with crushed RA. Likewise, the German Committee for Reinforced Concrete (DAfStB, 2008) and the Italian Code for Constructions (NTC, 2008) allow a 25-35% of replacement. Higher percentages have been permitted by other international codes but these are dependent on the required grade of concrete to be produced and the type of application (i.e. non-structural or structural). However, it is still not enough to reuse all the amount of the construction waste and overcome the environmental issues.

Several researchers have found that the use of mineral additions in the production of recycled aggregate concrete (RAC) such as fly ash, silica fume, furnace slag and fibres can enhance the properties of the resulting concrete. These studies have tended to focus more on the mechanical properties than the time-dependent deformation and the structural behaviour of concrete members. More research in this area is important to understand the effect of such additions on the full range of properties of RAC.

Therefore, this experimental study will investigate the long-term flexural performance of cracked reinforced concrete beams incorporating recycled aggregate and steel fibres. The addition of steel fibres to RAC to produce ‘steel fibres recycled aggregate concrete’ (SFRAC) is expected to exhibit improved strength properties, time-dependent deformation and long-term flexural behaviour over RAC. Hopefully, SFRAC will prove to be a viable alternative which will allow for increased use of RA in constructions.

1.2 Research Aim and Objectives

The aim of this research is to investigate the feasibility of using the recycled aggregate and steel fibres to enhance the long-term flexural performance of reinforced concrete. It is expected that the conclusions will be of use for developing design guidelines which potentially can expand the use of RAC and SFRAC in various structural applications. In order to achieve this aim, the following objectives were set:

- To study the effects of recycled aggregate and steel fibres on the strength properties of concrete, and the time-dependent deformation and the long-term flexural behaviour of cracked reinforced beams. More specifically, the following aspects were investigated experimentally to gain a better understanding:
    - Mechanical properties of concrete.
    - Creep and shrinkage of concrete.
    - Long-term loss of tension stiffening.
    - Short-term deflection of reinforced concrete beams and cracking patterns.
    - Long-term deflection of cracked reinforced concrete beams and their cracking behaviour.
- To evaluate, through an analytical investigation, the suitability of the existing code procedures for estimating the long-term curvature and deflection of beams containing recycled aggregate and steel fibres.
- To develop modifications to the analytical methods presented in Eurocode2 to make it suitable for estimating the long-term deflection of recycled and fibre reinforced concrete beams.
- The experimental and analytical findings also allowed a secondary aim to be achieved: to determine whether a combination of recycled aggregate and steel fibres can be used to produce reinforced concrete suitable for structural applications.
- To develop, through finite element analysis (FEA), an optimum 3D finite element model approach which can be used to simulate the long-term

flexural performance of cracked reinforced concrete beams containing different levels of recycled aggregate and steel fibres.

1.3 Research Strategy

To achieve the aforementioned aim and objectives, the work was completed in five stages as follows:

Stage one: included the collection of resources, data and reports from previous studies that are related to the research topic. Reviewing and summarising this information was the most significant part of this stage as it provided a background to and highlighted the potential contribution of the current research.

Stage two: was the setting up of the experimental programme and included constructing and testing the specimens used in this research. The analysis, presentation and discussion of the experimental results were also part of this stage.

Stage three: included the evaluation of the suitability of the existing analytical code procedures for estimating the long-term deflection of reinforced concrete beams. This evaluation also included the proposal of modifications to the Eurocode 2 methods for better prediction of SFRAC beams flexural performance. Developing a numerical analysis program using the MATLAB language to include the proposed modifications was also conducted in this stage.

Stage four: comprised developing a 3D finite element analysis (FEA) approach using the commercial software Midas FEA. Comparisons between the results obtained from the developed FEA approach and those obtained from the experimental work of this study and from previous investigations were made for verification purposes. Sensitivity and parametric studies were also carried out to investigate the effect of some model and structural parameters.

Stage five: included the writing of this thesis, presenting papers at international conferences and publishing the results of the study in international journals.

1.4 Research Significance

The volume of construction and demolition waste (CDW) generated around the world increases every year. At the same time, the extraction of natural aggregate to be used for construction and building purposes also increases. These issues mean

there is an increasing need for large spaces for landfills for waste disposal and a threat to the limited supply of natural resources available both of which raise concerns over the environmental friendliness of concrete. Reusing CDW as recycled aggregate to produce new concrete can potentially conserve natural resources and reduce energy consumption. However, the low density and high water absorption and porosity of CDW can result in a low quality of the resulting concrete (low strength properties and high creep and shrinkage deformations) which restricts its use as a structural material.

The addition of mineral admixtures may overcome some of the negative effects of using recycled aggregate. This research investigates the effects of using a combination of recycled aggregate and steel fibres on the mechanical properties of concrete, the time-dependent deformations and the long-term loss of tension stiffening, and the resulting influence on the flexural performance of cracked beams. The present research has the following significance:

- The findings of this research will provide valuable experimental results for the effect of recycled aggregate and steel fibres on the properties of concrete and the long-term flexural behaviour of reinforced beams.
- Researchers and engineers will have a better understanding about these effects and the feasibility of using SFRAC in various applications.
- The analytical method developed will help to improve code guidelines to expand the scope of using SFRAC for structural applications.
- The FEA approach developed could be used for further parametric studies to provide more insight into the behaviour of concrete structures and conditions.

1.5 Layout of this Thesis

This thesis consists of the following chapters:

Chapter 1 gives an introduction and background to the topic of the research. The aim, objectives, significance and strategy of the research are also presented.

Chapter 2 presents a review of the literature on the use of recycled aggregate and steel fibres in concrete. Their effects on the properties of the resultant concrete and short-term flexural behaviour of reinforced beams are summarised and discussed.

Chapter 3 presents a background to the effects of recycled aggregate and steel fibres on the time-dependent deformations of concrete and the long-term flexural behaviour of beams. The concept of tension stiffening and its effect on the flexural performance of cracked reinforced concrete beams are also presented and illustrated.

Chapter 4 describes the experimental programme adopted in this study to examine the mechanical properties, creep, shrinkage and tension stiffening of concrete, and the long-term flexural behaviour of beams. Details of the materials properties, mixes, preparation of specimens and test procedures are also described.

Chapter 5 presents and discusses the results obtained from the experimental work. The effects of incorporating recycled aggregate and steel fibres are assessed with a view to the objectives of this research.

Chapter 6 describes the analytical investigation carried out as part of this study. The theory behind the existing code procedures for predicting the long-term curvature and deflection of beams under sustained loads is described. Comparisons between the experimental results obtained and the analytical predictions from these theories are presented. An evaluation of the suitability of Eurocode 2 methods for predicting the long-term deflection of RAC and SFRC beams and proposed modifications to account for that are also included.

Chapter 7 includes details of the 3D finite element analysis performed using the Midas FEA software and describes the development of the existing approach for predicting the long-term deflection of cracked reinforced concrete beams. This chapter also discusses the verification of the proposed approach using the experimental results obtained in this study and from previous investigations. The results of sensitivity and parametric studies for some parameters also discussed and presented.

Chapter 8 presents the main conclusions and findings of this study and suggests some recommendations for further research.

Chapter 2 : Properties of Concrete Incorporating Recycled Aggregate and Fibres

2.1 Introduction

The main aim of this research is to investigate the effect of recycled aggregate and steel fibres on the long-term flexural performance of cracked reinforced concrete beams. Initially, the effect of these materials on the concrete is considered and thus this chapter presents a detailed review of the following aspects:

- A background to the use of recycled aggregate in construction; how it is generated and why re-use would be beneficial.
- The preparation, composition and classification of construction and demolition waste (CDW) used as aggregate.
- The properties of the CDW used as recycled aggregate.
- The effect of recycled aggregate on the properties of concrete.
- The properties of the steel fibres currently used in concrete.
- The effect of steel fibres on the properties of concrete.
- The effect of adding fibres to RAC.

2.2 Construction Waste; How it is Generated and Environmental Concerns

Over the past few decades, the growth of the world's population has increased disproportionately, and there has been a significant expansion of urban and industrialised areas. As a result, existing infrastructure has had to be demolished to make way for expansion and this has generated a huge amount of rubble. In addition, this growth has resulted in increasing concerns over natural balance and the resources required for construction materials.

The European Environment Agency (EEA, 2015) has reported the contribution to the overall generation of waste of a number of industrial sectors in 15 of the member states of the European Union; this data is shown in Figure 2-1. From this figure, it can be seen that the largest percentage (48%) of waste is attributed to construction and demolition waste (CDW); this was estimated to be around 850

million tonnes per year. In the UK, based on data published by the Government Statistical Services (WRAP, 2015), approximately 200 million tonnes of general waste was generated in 2012 and 50% of this was CDW. In the USA, the generation of debris from the demolition and renovation of existing infrastructure is close to 170 million tonnes annually, as reported by the Environmental Protection Agency (EPA) in 2014.

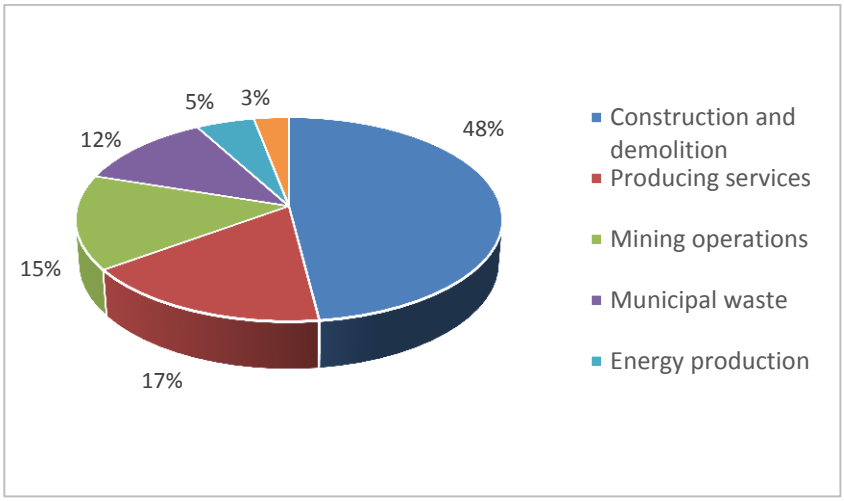

Figure 2-1 Total waste generation by sector in the EU (EEA 2015)

Regardless of the variation between different regions and the dependence on construction activity levels, the high levels of CDW generation need to be addressed around the world and more effort to reuse CDW as a recycled aggregate is needed; its incorporation in new concrete is one potential avenue. Reusing CDW in new concrete can help with many environmental issues such as reducing the use of natural materials, saving natural resources and reducing the need for large spaces for landfill. Reusing this material will also make concrete a more environmentally friendly and sustainable material.

2.3 Preparation and Production of CDW aggregate

In many countries, recycling plants have been established to produce CDW aggregate and some countries have even passed laws and approved regulations to promote recycling. In the preparation of CDW aggregate, the first step is normally crushing waste concrete elements mechanically into small-sized pieces. After crushing, the different sized pieces are screened using a range of sieving devices.

The rubble is often contaminated with other substances such as wood, plastics, metals and glass. These impurities can be detrimental and are unsuitable for concrete production, therefore in most cases, they must be separated and removed when producing CDW aggregate for future use. The CDW aggregate production process used can significantly affect its quality and composition. The actual concrete and construction waste used to make the CDW aggregate also plays a very important role in the final aggregate properties. Additional processing and higher quality sources of waste result in better quality aggregate (Nagataki et al., 2004). A schematic of a typical CDW recycling plant is presented in Figure 2-2 (Eguchi et al., 2007).

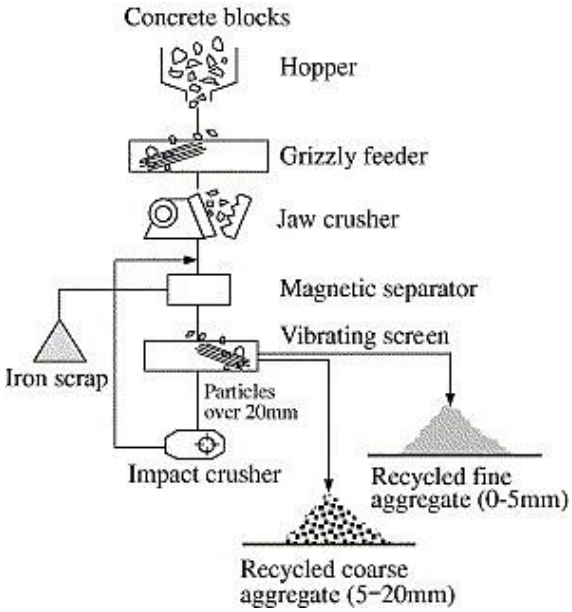

Figure 2-2 The typical CDW recycling plant (Eguchi et al., 2007)

2.4 Composition and Classification of CDW aggregate

In the literature, two types of CDW aggregate have been studied. The first type contains natural aggregate with adhered mortar; this is produced from recycled precast concrete and test specimens. The second type contains a variety of contaminants such as bricks, tiles and bitumen mixtures in minor amounts in combination with the natural aggregate and adhered mortar; this type is of the most interest due to its high availability. In the United Kingdom, BS 8500-2 (2006) defines two specific types of the recycled aggregate (RA): recycled concrete aggregate

(RCA), which contains a minimum of 95% crushed concrete, and construction and demolition waste (CDW) which contains 100% crushed masonry-based material.

The composition of CDW aggregate depends on the type of construction and demolition waste used for its production. Typical CDW aggregate prepared from normal concrete blocks contains 65-70% of coarse and fine normal aggregate and is 30-35% cement paste (Poon et al., 2004b). In addition, CDW aggregate produced from concrete used for bituminous road construction may contain organics.

The distributions of the various materials contained in some construction and demolition wastes as reported in a number of published works were summarised by Coelho and de Brito (2011) and are presented in Table 2-1.

The presence of other crushed materials such as bricks, tiles, wood and glass have also been observed and their presence depends on the source of the CDW. In 2009, Fisher and Werge (2009) and Corinaldesi and Moriconi (2009a) reported the average composition of CDW collected from a number of recycling plants; their data is presented in Figures 2-3 and 2-4.

Table 2-1 Distribution of CDW material content (Coelho and de Brito, 2011)

Materials	Amount in %			
	Pereira (2002)	Costa and Ursella (2003)	Reixach et al. (2000)	Franklin Associates (1998)
Concrete and ceramics	58.3	84.3	85	24
Metals	8.3	0.08	1.8	2
Wood	8.3	-	11.2	42
Plastics	0.83	-	0.2	32
Bituminous concrete	10	6.9	-	-
Other waste	14.2	8.8	1.8	-

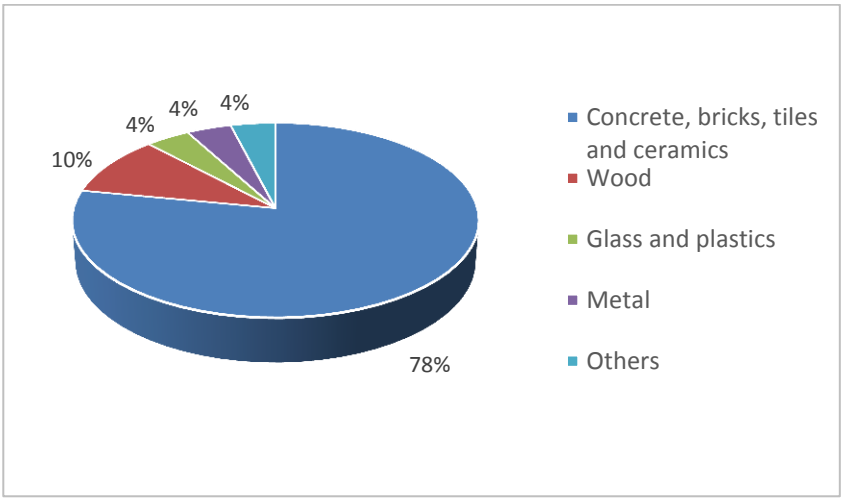

Figure 2-3 Average composition of CDW (Fisher and Werge, 2009)

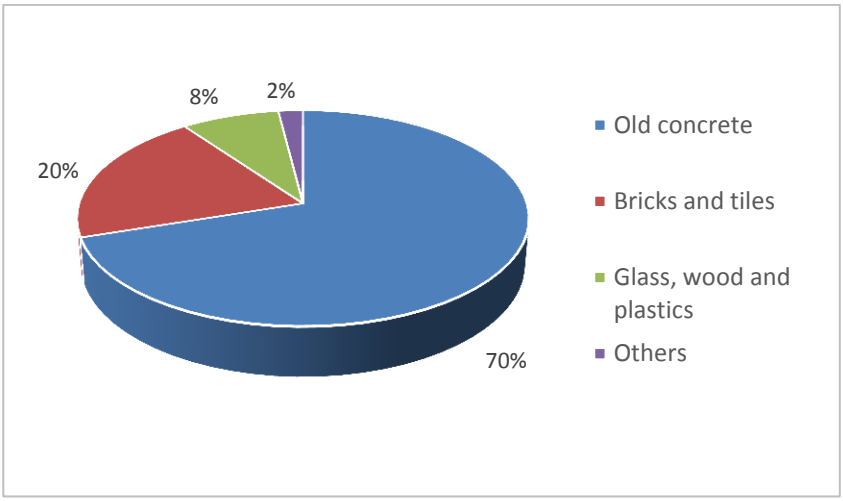

Figure 2-4 Proportions of CDW materials (Corinaldesi and Moriconi, 2009a)

2.5 Properties of CDW as Recycled Aggregate

Due to environmental concerns, the need to improve management of construction wastes and the potential benefits of using recycled aggregate, investigation of the reuse of CDW as aggregate in new concrete has seen significant interest worldwide. Aggregate occupies more than 75% of the volume of a concrete mix. Thus, the characteristics of concrete are strongly influenced by the properties of the aggregate employed. In this section, the most important properties of recycled aggregate are presented and evaluated in comparison to those of natural aggregate.

2.5.1 Attached mortar content in CDW aggregate

The properties of CDW aggregate are significantly influenced by the mortar content. The amount of mortar in CDW depends on the type and number of crushing processes carried out during production. Increasing the number of crushing processes can reduce the amount of attached mortar. However, increasing the number of crushing processes can also increase the cost of production.

Attached mortar levels of 33-55% and 23-44% on 4-8mm and 8-16mm particles of CDW respectively were measured by De Juan and Gutiérrez (2009) using a thermal method. In the literature, many authors (Etxeberria et al., 2007, Zaharieva et al., 2003, Katz, 2003) have found that CDW aggregate produced from high strength concrete contains a greater amount of adhered mortar than that produced from low strength concrete. This can be owed to the greater amount of the cement in such this type of concrete.

Several different methods of determining attached mortar content have been described. One of these methods, used by Nagataki et al. (2000), employs a solution of dilute hydrochloric acid to dissolve the cement paste. This can only be used when the acid does not affect the aggregate particles. Certain aggregates, such as limestone or similar, can also be dissolved by the dilute acid and therefore with these aggregates, this method would not be appropriate. In another method, a coloured cement is used to produce a new concrete with the CDW aggregate. The mortar can then be easily detected in slice specimens (Sri and Tam, 1985). De Juan and Gutiérrez (2009) adopted a different method which involved soaking CDW aggregate in water and then heating it for several cycles in order to remove the attached mortar from the surface of the natural aggregate particles.

In addition to increasing the mechanical processing steps during production, other methods have been suggested for removing the mortar content from the aggregate and therefore improving the quality of the final material (Akbarnezhad et al., 2011). These include thermal treatment, mechanical treatment, acid soaking, chemical-mechanical treatment and microwave-assisted treatment.

2.5.2 Density

Density is one of the key properties of aggregates and is an important parameter for the design of concrete mixes. It affects many of the properties of the resulting

concrete. In general, previous studies have concluded that the density of recycled aggregate produced from CDW is lower than that of natural aggregate. Depending on the origin and size of the CDW, the resulting aggregate may have a different density and specific gravity. Researchers have attributed this to variations in the amount of adhered mortar in the CDW. Indeed, the relationship between the density of aggregate and the amount of attached cement paste is inversely proportional, which means that the higher the amount of adhered mortar paste on the surface of the aggregate, the lower the density (Yehia et al., 2015). This is because the cement paste is much more porous and less dense than the natural aggregate particles (Ferreira et al., 2011).

De Juan and Gutiérrez (2009) published a study on the influence of attached mortar content on the properties of recycled concrete aggregate. Based on their observations, they stated that the average bulk densities of NA and RA are 2546 Kg/m^3 and 1600 kg/m^3 respectively and the relationship between density and adhered mortar content is as shown in Figure 2-5. Ferreira et al. (2011) found the bulk density of CDW is generally in the range of 1150-1400 Kg/m^3 which they attributed to the greater volume of voids between the particles in CDW.

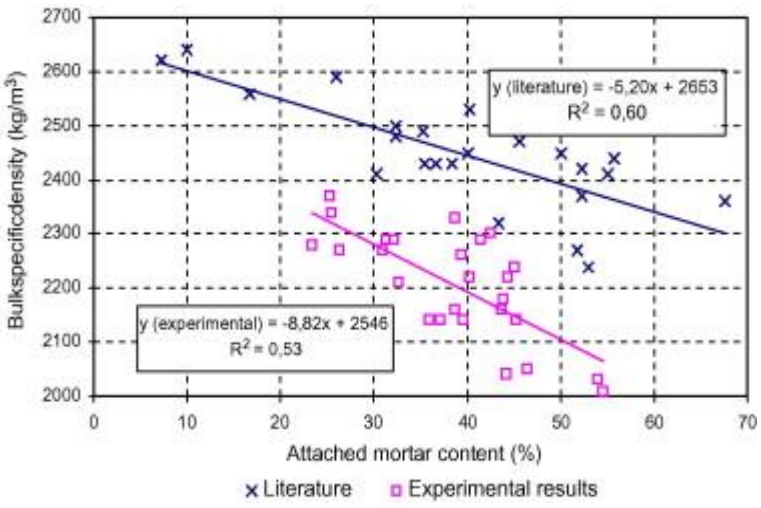

Figure 2-5 Relationship between attached mortar content and bulk density (De Juan and Gutiérrez, 2009)

2.5.3 Water absorption

The water absorption ratio of aggregate is a fundamental parameter which can affect concrete mixes and the resulting concrete properties. As mentioned earlier,

the cement paste attached to the surface of CDW aggregate is very porous; this makes CDW more liable to absorb high amounts of water. Consequently, the water absorption capacity of CDW aggregate is higher than that of normal aggregate (which for almost types of natural aggregate is normally less than 1%).

The experimental results reported in various references have shown that the water absorption ratio of CDW depends on the cement paste content. Moreover, the content of other components such as crushed clay brick and tiles, which also have a very high water absorption capacity, can also influence this ratio (De Brito and Saikia, 2012). Experimental data for the inverse relationship between the attached mortar content and the water absorption capacity of CDW, as noted by De Juan and Gutiérrez (2009), is presented in Figure 2-6.

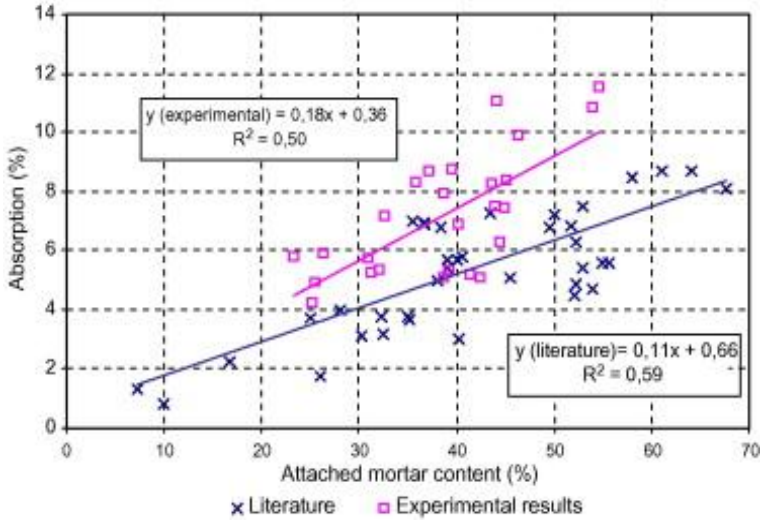

Figure 2-6 Relationship between attached mortar content and absorption of CDW (De Juan and Gutiérrez, 2009)

In 2004, de Juan and Gutiérrez (2004) reported that the water absorption capacity of NA is in range of 0% to 4%, while it is between 16% to 17% for adhered mortar. This means the water absorption capacity of CDW is generally between 0.8% and 13% and is on average 5.6%. This is clearly much higher than that of NA. De Brito and Saikia (2012) summarised the results of several experimental studies from the literature and confirmed these values.

Data from Vieira et al. (2011) for the water absorption of CDW as a function of time revealed that 80% of absorption occurs during the first 5 min of immersion. After

this period, the increase in the amount of water absorbed is much slower and only 84% absorption was recorded after 30 min. Similar results were also presented by de Juan and Gutiérrez (2004) who measured 70-90% of the water absorption of CDW occurs within the first 10 min of soaking.

As the water absorption of CDW is much greater and faster than that of NA, it can significantly affect the degree of workability for concrete of the same w/c ratio. Therefore, special mixing procedures are necessary for RAC to meet workability requirements. Pre-soaking CDW before mixing concrete can prevent the absorption of the mixing water (Zaharieva et al., 2003). However, complete saturation of the CDW may influence the mechanical performance of the resulting concrete due to the formation of a weak interfacial transition zone (ITZ) between the saturated recycled aggregate and the new cement paste, see Etxeberria et al. (2007). In addition, it can increase bleeding during mixing of the concrete (Poon et al., 2004a). Ferreira et al. (2011) stated that newly hardened concrete produced using the pre-soaking method exhibits slightly poorer properties but has significantly greater time-dependent deformations.

In other studies, a number of methods have been investigated to compensate for water absorption, to control the workability of the mix, and to improve the properties of the resulting concrete. In one method, an additional quantity of water is added to the concrete mix corresponding to the water absorption capacity of the CDW (Matias and de Brito, 2004, de Oliveira and Vazquez, 1996, Santos et al., 2002). This method was called the mixing water compensation method. In this method, the amount of additional water added depends on the initial water content and the absorption capacity of the CDW aggregate.

The mixing water compensation method has the advantage that it can be used to design mixes for concrete with either NA or CDW aggregates in a similar way. However, de Oliveira and Vazquez (1996) noted that the pores of the CDW aggregate can become filled with cement paste during mixing which can reduce the water absorption capacity of the CDW and may lead to extra water in the mix. This results in an undesirable increase in the effective water to cement ratio. To compensate for this, Tam et al. (2007) adopted a two-stage mixing approach (TSMA). A flowchart of their procedure is presented in Figure 2-7. In this approach,

half of the required water is added first to saturate the aggregate before the cement is added. The authors found that a stronger ITZ was formed which effectively improved some of the strength properties of the final concrete.

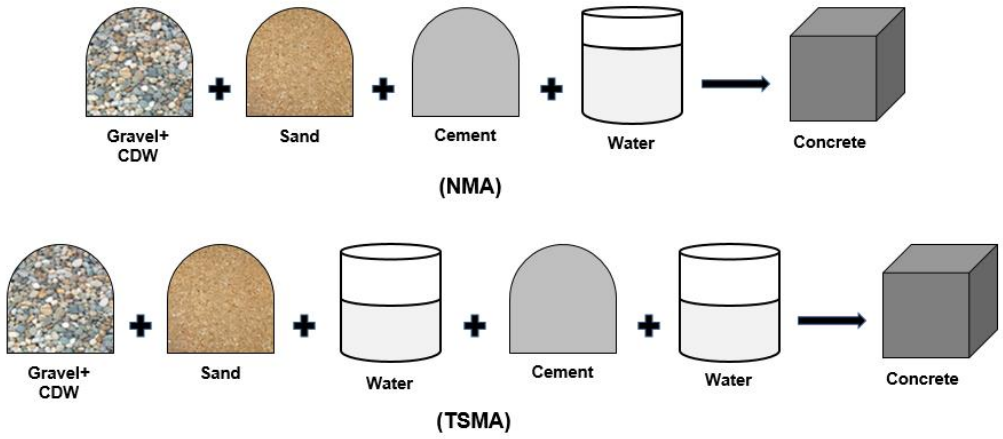

Figure 2-7 Normal (NMA) and two-stage (TSMA) mixing approaches adopted by Tam et al. (2007)

Ferreira et al. (2011) followed a different procedure to maintain the effective water to cement ratio in different concrete mixes containing CDW aggregate so as to ensure the right level of compensation was achieved during the mixing process. In their method, the quantity of water they expected to be absorbed by the CDW aggregate was added directly to the concrete mix during the mixing process form 5 minutes before adding the cement.

2.5.4 Porosity

As previously stated, CDW aggregate has a high water absorption capacity due to the presence of cement paste attached to the surface of the aggregate particles. The large proportion of adhered mortar results in a high porosity of the overall aggregate. A close examination of the microstructure of CDW aggregates shows that they are more porous than natural aggregate (Yehia et al., 2015). The high porosity of the CDW aggregate can lead to a weak bond between the aggregate particles and the cement paste. This negatively affects the microstructure of the paste-aggregate interfacial transition zone (ITZ) and increases the number of micro cracks in this region (Poon et al., 2004b).

2.6 Properties of Recycled Aggregate Concrete

Using recycled aggregate to produce new concrete has attracted much interest in the civil engineering research community worldwide. Therefore, many studies have been conducted to examine the effects of replacing natural aggregate with recycled aggregate on the different properties of concrete.

As mentioned earlier, the quality and the properties of recycled aggregate are poorer than those of natural aggregate which can significantly affect the properties of the resulting concrete. This section aims to present the most notable results from different researchers on the effects of recycled aggregate on the fresh and hardened properties of concrete.

2.6.1 Workability

The workability of fresh concrete is considered to be the most significant property for recycled aggregate concrete as it affects several other the properties of both fresh and hardened concrete. The importance of workability for the performance of concrete has led many researchers to investigate how it is affected by using recycled aggregate. The slump test is the most common method used in the literature to determine the workability of RAC.

Even without the high absorption capacity of RA, the slump value of RAC containing any type of RA would be expected to be lower than that containing natural aggregate as the higher water absorption capacity, surface texture and angularity of CDW aggregates all have a significant effect on the workability of RAC (Buyle-Bodin and Hadjieva-Zaharieva, 2002). A slump of 100mm and 75mm was observed by Topcu (1997) for concrete mixes prepared from natural and recycled coarse aggregate respectively. A similar reduction in workability of RAC was also reported by many authors in the literature and the addition of extra water to control the workability of RAC mixes was therefore proposed (Topcu, 1997, Khan, 1984, Mukai and Kikuchi, 1978, Malhotra, 1978, Hansen and Narud, 1983).

A number of different mixing approaches have been developed to meet workability requirements and to overcome the high water absorption capacity of CDW aggregate (De Brito and Saikia, 2012), for example:

1- Adding extra water during mixing to compensate for the absorption of CDW.

2- Pre-soaking of the CDW aggregate in water for 10-20 min or for 24 hrs before use.
3- Increasing the moisture content of the CDW to 70-80% of its total water absorption capacity 24hrs before use and covering it in plastic sheets to prevent water loss due to evaporation.
4- Using a super-plasticiser in the concrete mix.
5- Increasing the amount of cement in the concrete mix.

These procedures have been evaluated by many researchers and their results and conclusions are presented in the literature. For example, the pre-soaking of CDW aggregate prior to mixing to prevent absorption of the mixing water was tested and some negative effects were observed. Poon et al. (2004a) stated that complete saturation of CDW aggregate may increase bleeding during the preparation of the concrete mix which can significantly influence the mechanical properties of the resulting concrete. These findings were supported by Etxeberria et al. (2007) who concluded that pre-soaking CDW aggregate can cause formation of a weak ITZ.

In concrete produced from natural and recycled aggregate with the same ratio of water to cement in a mix containing 1.2% super-plasticiser, González-Fonteboa and Martínez-Abella (2008) found that the cement content needed to be increased by 6.2% in the 50% NA-50% RA concrete mix to obtain the same average slump as the 100% NA mix. Etxeberria et al. (2007) tested a number of different concrete mixes and added greater amounts of super-plasticiser to the concrete mixes containing CDW aggregate in order to control the workability and keep the water to cement ratio constant.

The composition of the CDW aggregate employed also plays an important role in the slump of fresh concrete. Concrete containing CDW aggregate that has more crushed bricks and tiles has a lower slump than other types of CDW aggregate concrete. The water absorption capacity of aggregate prepared from waste with a greater percentage of crushed brick and tiles is notable higher than that of aggregate with a greater crushed concrete content (Gomes and de Brito, 2009). Yang et al. (2011) observed a reduction in slump of 27% when 100% pre-saturated recycled concrete aggregate (RCA) was used, and this reduction increased to

about 40% when a mix of 20% recycled crushed bricks (CCB) and 80% RCA was used. The reduction increased even further to 70% when NA was replaced by 50% CCB and 50% RCA.

In another study, Li et al. (2009) observed that mixes prepared using RCA which was coated with pozzolanic powder had a higher slump than those containing conventional RCA. This was attributed to the pozzolanic powder coating the surface of the RCA particles and reducing the amount of water absorption. The addition of silica fume (SF) and metakaolin (MK) have also been found to reduce the slump of concrete mixes prepared with RCA (Kou et al. (2011b). In contrast, the addition of fly ash (FA) and granulated blast furnace slag (GBFS) increased slump.

2.6.2 Compressive strength

The compressive strength of concrete is arguably the most important of its mechanical properties. Many other mechanical properties can be correlated with the compressive strength. In general, the presence of attached mortar on the surface of CDW particles and the poor quality of the particles themselves influence the concrete porosity and lead to a zone of weakness at the interface between the new cement paste and the aggregate. This means that when NA is replaced by RA, the resulting concrete has a lower compressive strength.

For concrete prepared with natural aggregate, the main parameters that affect compressive strength are: w/c ratio, type and content of cement, type and quality of aggregate and curing conditions. However, when recycled aggregate is employed, other factors need to be considered such as the replacement ratio. Several experimental investigations have been carried out to study the influence of these factors on mechanical performance, and have particularly focused on the reduction in compressive strength. A summary of the results from investigations of the effect of replacing coarse natural aggregate with CDW and RCA by up to 100% is presented below.

Pepe (2015) provided a summary of the results from previous experimental studies available in the literature. Figure 2-8 shows data from this review for the reduction in compressive strength at 28 days as the replacement ratio of recycled aggregate increases. All the results shown are average compressive strengths obtained from testing cubic specimens. Reductions are presented as a ratio between the results

for the recycled aggregate specimens to those for the corresponding normal concrete specimens. The reductions represent purely the effect of replacement percentage on the compressive strength as there were no changes to any of the other parameters (e.g. w/c, type and content of cement, curing conditions).

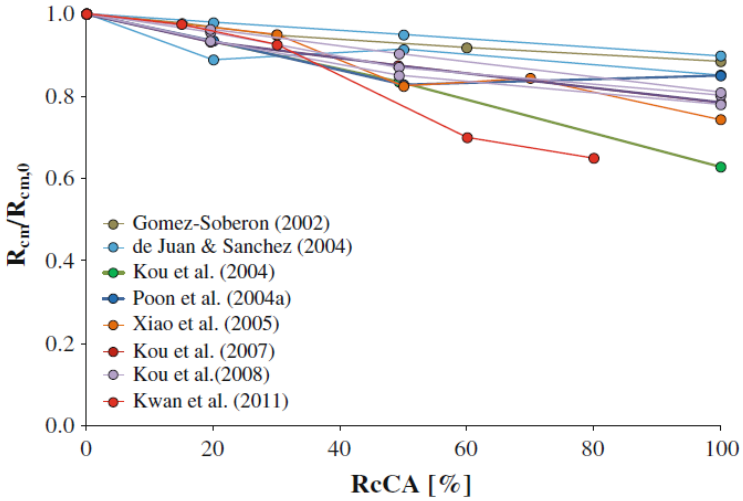

Figure 2-8 Reduction ratio in compressive strength due to increase of CDW content at 28 days (Pepe, 2015)

It is clear that for replacement percentages up to 50%, the loss of compressive strength is in the range of 5-20% and the loss becomes much more significant when 100% of the aggregate is substituted. The scatter in the results is mainly due to other factors such as the origin of the recycled aggregate and its basic properties.

In other studies, typical results indicated that the reduction in compressive strength is less than 5% when 25-30% of recycled CDW aggregate is employed, and increases to 12-25% when 100% of NA is replaced (Etxeberria et al., 2007, Rahal, 2007, Li et al., 2009, Corinaldesi, 2011, Alengaram et al., 2011).

The development of compressive strength over time is another important area that has been studied. Rao et al. (2011) observed a higher early strength gain during the period from 0-7 days in RAC specimens as compared to NA specimens. They attributed this to the high water absorption capacity of the old attached cement paste and the rough texture of RA. However, they recorded an 8% development in compressive strength between 28 and 90 days of curing for specimens with 25%

NA replacement compared with a 12% development for specimens of conventional concrete. There was no corresponding increase in specimens with replacement ratios of 50% and 100%.

Alengaram et al. (2011) results showed that more than 80% of the 28-day compressive strength is achieved after 7 days' curing for both natural and recycled aggregate concrete. Similarly, Fonseca et al. (2011) observed 80% and 95% of the 56-day compressive strength was achieved for natural and recycled aggregate concrete after 7 and 28 days respectively. In contrast, Etxeberria et al. (2007) recorded a development of compressive strength of the order of 12-15% between 7 and 28 days of curing with RAC specimens produced by replacing 25, 50 and 100% of NA in comparison to an ~20% gain for control specimens of NC. A similarly low rate of development of compressive strength with time during the first seven days for RAC was noted by (Yehia et al., 2015).

It has been found that the reduction in compressive strength due to utilising CDW can be controlled by employing a number of techniques when producing a concrete mix. Adjustment of water to cement ratio, altering the mixing procedure, pre-treatment of the recycled aggregate and using mineral additives are the most common approaches presented in the literature (De Brito and Saikia, 2012). For example, no difference was observed by Sagoe-Crentsil et al. (2001) in the 28-day and 1-year compressive strengths when concrete mixes were prepared with pre-saturated RA and NA. Noticeable increases in the compressive strength of RAC were recorded when the cement content was increased by 5% or slag cement was used.

Ferreira et al. (2011) compared the compressive strength of RAC specimens produced using two different mixing methods: the pre-saturation method and the compensation method. The 7-day and 28-day compressive strengths of the specimens prepared using the pre-saturation method were lower than those of the specimens prepared using the compensation method. However, the difference in compressive strength became insignificant as the replacement percentage of RCCA increased.

The addition of mineral additives such as fly ash, metakaolin, silica fume and ground blast furnace slag has also been shown to have a beneficial effect on the

compressive strength of RAC. In particular, Kou et al. (2008) found that by replacing 25% of the ordinary cement with fly ash, an improvement in the 90-day compressive strength could be achieved. However, the incorporation of 35% fly ash has a negative effect. Corinaldesi and Moriconi (2009b) also recorded higher values of compressive strength when RAC was prepared by replacing Portland cement with 30% fly ash or 15% silica fume. The effect of silica fume was greater than that of fly ash and the compressive strength measured was even better than that for concrete containing NA.

Moreover, Kou et al. (2011a) noticed a reduction in the compressive strength of RAC when 55% and 35% of the cement was substituted by ground blast furnace slag and fly ash respectively. However, an improvement in the compressive strength was achieved due to the replacement of cement by 10% silica fume or 15% metakaolin. The compressive strengths of the RAC specimens containing silica fume and metakaolin were similar to that recorded for normal concrete.

2.6.3 Tensile strength

Although the compressive strength is the most important mechanical property for concrete, the tensile strength has a greater impact on serviceability conditions. Similar to the compressive strength, in general the tensile strength of concrete prepared with RA is lower than that of normal concrete. Increasing the aggregate replacement percentage increases the strength reduction. This is probably due to the properties of the recycled aggregate which reduce the aggregate-cement paste bond strength (Kou and Poon, 2008). There is great variation in the results in the literature which may be related to the variability in the experimental parameters and the sources and properties of the recycled aggregate used in the various studies. In particular, a 10% reduction in splitting tensile strength was noticed by Yehia et al. (2015) when 100% of NA was substituted with RA. Another study conducted by Kou et al. (2011a) showed a 10% and 7% decrease in splitting tensile strength for concrete containing RA and RCA in comparison to normal concrete. Results from other studies are summarised and presented in Table 2-2.

In contrast, some studies have shown that the splitting tensile strength of RAC improved substantially during later stages of curing and final strengths greater than those for NC were obtained. Kou et al. (2011b) investigated the long-term

mechanical properties of RAC and observed an increase in the splitting tensile strength of 56% between 28 days and 5 years of curing for RAC compared with 37% for NC. They concluded that this was due to an improvement in the cement paste-aggregate bond strength and the microstructure of the ITZ over time. Similar results were recorded in another study carried out by Kou and Poon (2008). Their results showed higher splitting tensile strengths for RAC specimens in comparison to NC specimens after 5 years of curing and that the development in strength increased with increasing replacement ratio.

Table 2-2 Reduction in compressive and tensile strength of concrete containing CDW

Reference	Type of aggregate	Reduction %		Replacement ratio %
		Compressive strength	Tensile strength	
Yang et al. (2011)	RCA	5.7	13.8	100
Rao et al. (2011)	CDW	7.4, 14.1, 17.5	13.9, 18.0, 23.2	25, 50, 100
González-Fonteboa et al. (2011)	RCA	10.7, 9.3, 10.6	17.2, 14.8, 9.9	20, 50, 100
Kou et al. (2011a)	RCA	21.7	9.0	100
	CDW	18.7	7.0	100
Etxeberria et al. (2007)	CDW	3.5	9.3	25

The effect of the water to cement ratio on the splitting tensile strength of concrete produced using RA has also been studied. González-Fonteboa et al. (2011) observed lower tensile strengths in RAC specimens than in NC specimens for a w/c ratio of 0.65. On the other hand, with a w/c ratio of 0.5, the tensile strength of RAC was higher than that of NC. Moreover, an increase in the water absorption capacity and porosity of the concrete prepared with RA aggregate resulted in a decrease in splitting tensile strength (Kou et al., 2011a, Yang et al., 2011, Gomez-Soberon, 2002).

An increase in RA impurity content due to the presence of crushed clay brick and ceramic material was also found to have a negative effect on the tensile strength of the resulting concrete as shown in Figure 2-9. According to Yang et al. (2011) results, replacing 20% and 50% of RA by crushed brick decreased the 7-day and 28-day splitting tensile strengths of the resulting concrete compared to conventional RAC. They attributed this to the higher porosity and poor strength of crushed brick in comparison to the natural particles in aggregate as in their experiments, most of the tensile failures occurred within the brick particles.

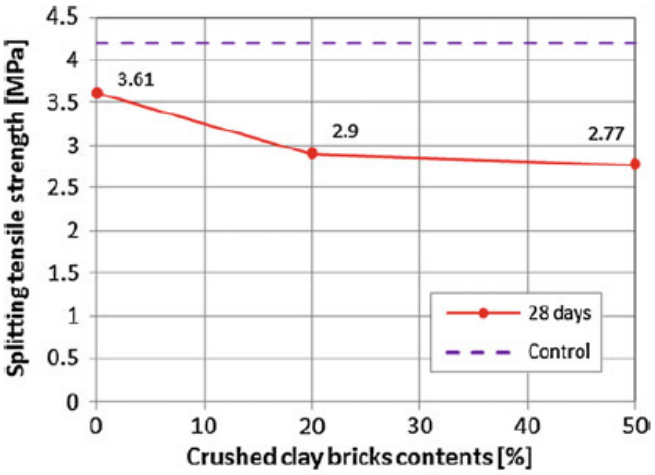

Figure 2-9 Effect of crushed brick content in RA on the splitting tensile strength (Yang et al., 2011)

Unlike compressive strength, the effect of adding mineral admixtures such as silica fume, fly ash and ground blast furnace slag on the splitting tensile strength was minimal. In a study conducted by González-Fonteboa and Martínez-Abella (2008), an improvement of 6% in splitting tensile strength due to the addition of silica fume was recorded for specimens prepared with RA compared to an improvement of 12% gained in compressive strength. Similar results were recorded by Ajdukiewicz and Kliszczewicz (2002).

Kou et al. (2011a) noted that the substitution of Portland cement by 10% silica fume or 15% metakaolin resulted in higher splitting tensile strengths for concrete mixed by replacing 50% and 100% of NA after 7, 28 and 90 days' curing compared to normal concrete. However, the RAC produced by replacing 35% and 55% of the Portland cement with fly ash and ground blast furnace slag respectively had lower

strengths than RAC containing 100% Portland cement. They stated that this was due to the increased hydration from adding the silica fume and metakaolin which improved the microstructure of the ITZ and increased the bond strength between the RA and the new cement paste.

2.6.4 Flexural strength

The flexural strength of concrete beams is usually determined by testing with loading applied at different points according to the standard used. Experimental data has shown that there is no significant difference in the flexural strengths of NC and RAC prepared with up to a 50% RA replacement. However, a notable decrease in the flexural strength of up to 20-40% occurs when utilising more than 50% CDW. Flexural strength results vary depending on a number of factors such as replacement ratio, origin and quality of CDW, and w/c ratio. The decay in flexural strength has been attributed by many researchers to the lower modulus of elasticity of recycled aggregate compared to normal aggregate (Pepe, 2015).

In an experimental investigation of the influence of the amount of recycled aggregate used on the properties of concrete, Mas et al. (2012) observed reductions of 13%, 20% and 30% in flexural strength due to replacing 75% of NA by RA in three concrete mixes prepared with 0.72, 0.65 and 0.45 w/c ratios respectively. James et al. (2011) noted a 28-day flexural strength about 2.5% lower due to a substitution of 25% of RA at a w/c ratio of 0.55. Lower flexural strengths were recorded at higher w/c ratios. A similar trend was observed by Yang et al. (2011) with reductions of 7.5-13.8%, and Casuccio et al. (2008) with reductions of 5-21% in flexural strength noted at various ages of curing due to replacement of 100% of NA by CDW.

In contrast, some studies have found that some RAC specimens had either similar or higher flexural strengths than NC (Safiuddin et al., 2013, Chen et al., 2010, Limbachiya et al., 2004). The authors suggested that this could be attributed to the angularity and surface roughness of some types of CDW which can improve interfacial bonding and mechanical interlocking.

The addition of mineral admixtures to RAC and their effects on flexural strength have also been investigated. Gupta et al. (2011) replaced 10% and 20% of the Portland cement in RAC mixes with fly ash and recorded a 3% higher flexural

strength compared to the 6% reduction which was recorded when 100% Portland cement was used. The improved flexural strength due to incorporation of 10% and 15% fly ash was also noted by James et al. (2011). They found that specimens prepared with a w/c ratio of 0.55 had higher flexural strengths than normal concrete.

2.6.5 Modulus of elasticity

Similar to the other mechanical properties discussed above, the incorporation of CDW in concrete also reduces the modulus of elasticity. This reduction increases as the content of CDW in the concrete increases. In several studies, it was indicated that the reduction in modulus of elasticity is due firstly, to the lower modulus of elasticity of the recycled aggregate itself; and secondly, to the loss of concrete stiffness arising from porosity, aggregate-cement paste bonding and mortar stiffness, all of which deteriorate due to the addition of CDW (De Brito and Saikia, 2012).

Depending on different factors such as replacement percentage, origin and quality of CDW, composition of CDW and w/c ratio of the mix, the modulus of elasticity of RAC can decrease to as low as 50% of the modulus of NC. Some typical results from the literature are summarised and presented in Table 2-3.

Table 2-3 Reduction in modulus of elasticity of concrete containing CDW

Reference	Type of aggregate	Reduction %	Replacement ratio %
Yehia et al. (2015)	CDW	15, 45	30, 100
Safiuddin et al. (2013)	RCA	17.7	100
González-Fonteboa et al. (2011)	RCA	3.8, 14.9, 29.2	20, 50, 100
Rao et al. (2011)	RCA	14.3, 14.4, 15.4	25, 50, 100
Corinaldesi (2011)	CDW	17	30
Berndt (2009)	RCA	15	100
Etxeberria et al. (2007)	RCA	4, 12, 15	25, 50, 100

Although mineral additions normally improve concrete strength properties, in some studies it was found that the inclusion of certain mineral additions did not influence the modulus of elasticity of RAC. This is because the modulus of elasticity of concrete relies on the properties of the aggregate particles more than the strength of the cement paste (Tangchirapat et al., 2008). González-Fonteboa and Martínez-Abella (2008) replaced 8% of Portland cement with silica fume and did not notice any improvement in the modulus of elasticity for concrete specimens containing varying amounts of RA. Berndt (2009) observed a lower modulus of elasticity when 50% and 70% of Portland cement was replaced by blast furnace slag. However, a slight increase was recorded by Kou et al. (2008) due to a 25% replacement of Portland cement by fly ash in concrete mixes containing 20%, 50% and 100% RA.

2.7 Flexural Behaviour of Reinforced RAC Beams

As stated previously, the utilisation of recycled aggregate has a negative effect on the properties of concrete. The higher the replacement percentage, the poorer the properties of the concrete. In addition to the studies above on mechanical properties of concrete itself, several investigations have been carried out to understand and evaluate the flexural performance of RAC beams.

Arezoumandi et al. (2015) carried out an experimental investigation of the flexural strength of full-scale beams constructed using 100% recycled aggregate. They concluded that the cracks in RAC beams are more closely spaced and open wider compared to those in NC beams. In terms of the cracking moment and flexural capacity, the RAC beams had a 7% lower cracking moment than NC beams but had a comparable ultimate flexural capacity. The RCA beams had 13% higher deflections and lower stiffness after cracking as shown in Figure 2-10. A comparison of the experimental results with predictions from ACI-318, Eurocode2 and the Modified Compression Field Theory (MCFT) showed that the predictions were either comparable to or underestimated the experimental results.

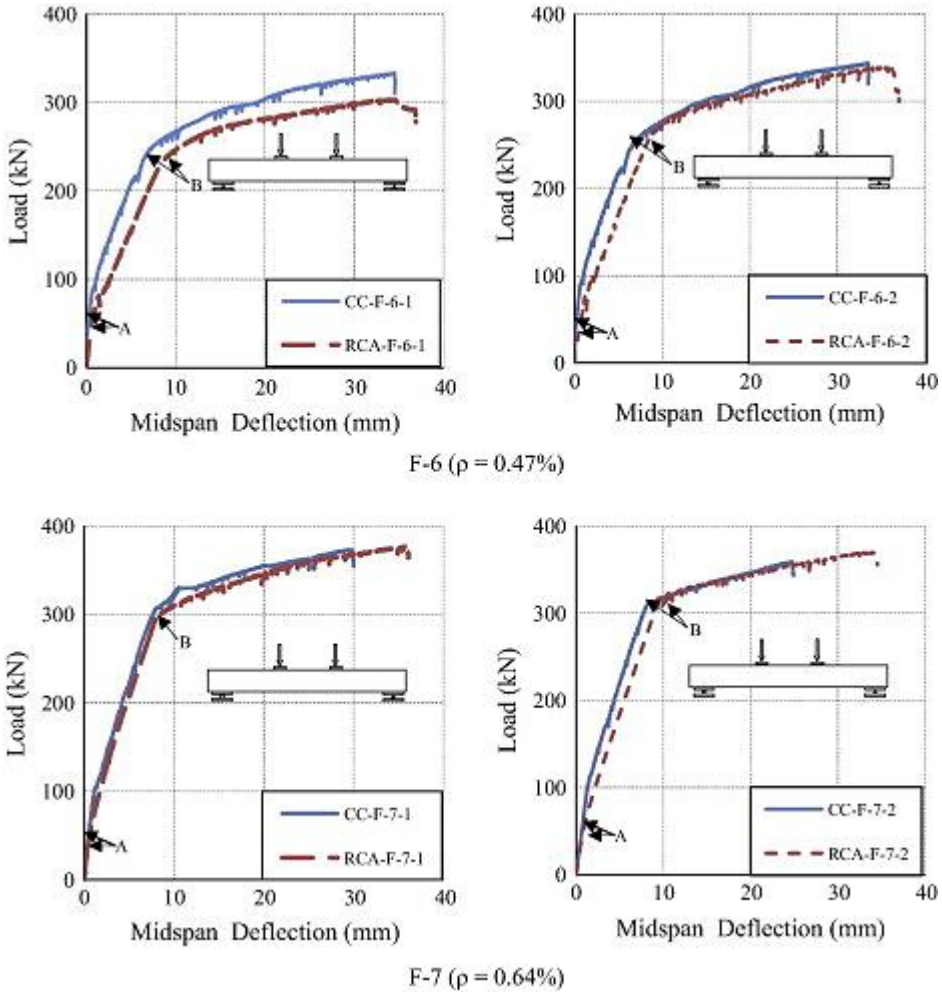

Figure 2-10 Load-deflection curves of the full scale test beams (Arezoumandi et al., 2015)

Twelve beams were tested by Knaack and Kurama (2014) to investigate the flexural behaviour of reinforced concrete beams prepared with 0%, 50% and 100% aggregate replacement levels. It was found that the effect of using RCA on the ultimate flexural strength was small, however a clear reduction in the initial stiffness and an increase in the deflection were observed as the amount of the RCA was increased as shown in Figure 2-11. The authors concluded that the existing analytical models and code procedures for normal concrete could be used for predicting the ultimate flexural strength of RAC beams, whereas those for calculating deflections needed to be developed.

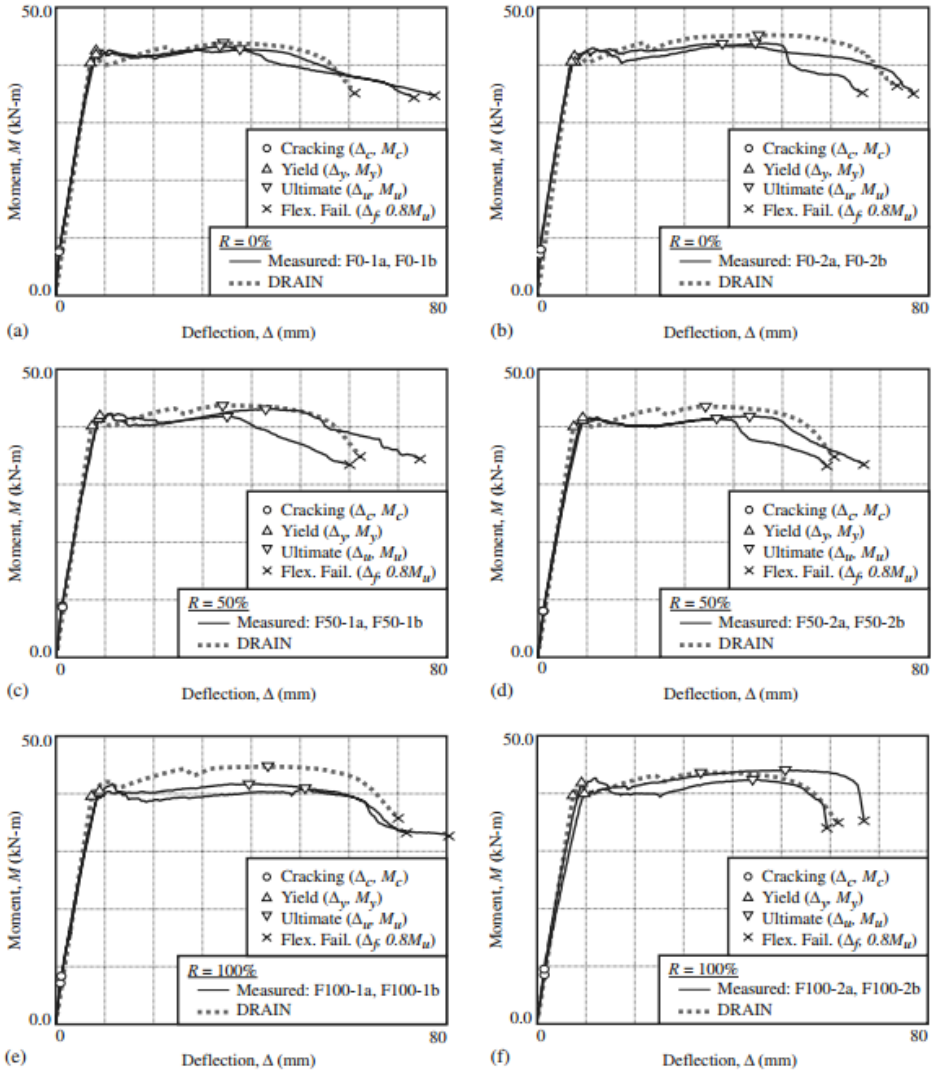

Figure 2-11 Flexural behaviour of beams with different levels of RCA (Knaack and Kurama, 2014)

Kang et al. (2014) explored the flexural behaviour of RAC beams and the potential for application of RAC in concrete structures. Compared to NAC beams, RAC beams have a greater number of cracks and a lower cracking moment, however the general overall crack patterns are similar and the flexural behaviour is not influenced significantly by replacing up to 30% NA with RCA. The authors presented a comparison between their and other researchers' results regarding the applicability of ACI-318 for RAC design and indicated that the current flexural design procedure may be considered valid at replacement ratios of up to 30%.

However, for reliable design with RCA replacement ratios greater than 30%, additional flexural testing would be needed.

In another study performed by Ignjatović et al. (2013), nine full-scale beams with three levels of aggregate replacement (0%, 50% and 100%) were tested. They recorded no noticeable difference in the load-deflection behaviour, service load deflection and ultimate flexural strength of RAC and NC. However, they observed higher levels of concrete destruction at failure in beams with higher levels of recycled aggregate as shown in Figure 2-12.

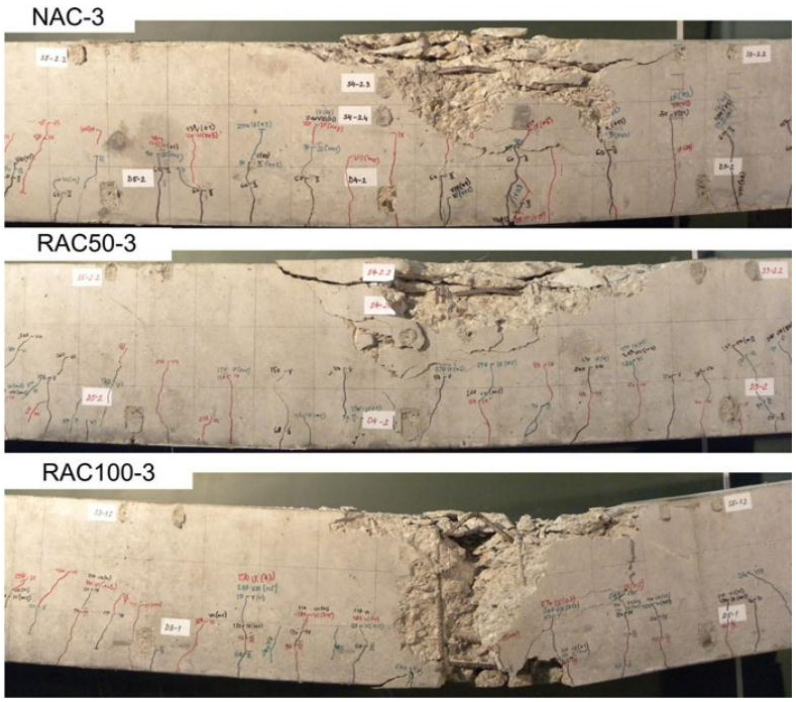

Figure 2-12 Crack patterns at faluir load in the middle of the span of normal and recylced aggregate beams (Ignjatović et al., 2013)

Bai and Sun (2010) tested beams with different replacement ratios of recycled coarse aggregate (0%, 50%, 70% and 100%) and different percentages of reinforcement (0.68%, 0.89% and 1.13%). They found that the cracking moment and the ultimate flexural capacity of the RAC beams were almost the same as those of NC beams which was owed to the lower effect of RA on the compressive strength of concrete. However, the crack widths increased with increasing replacement level. The authors concluded that calculating the ultimate bending moments and cracking moments of RAC beams can be carried out following the

procedures in the China Concrete Structure Design Code, but the approach used to calculate deflections needs modification.

Sato et al. (2007) reported that RAC beams have larger deflections than normal concrete NC beams. They concluded that the ACI-318 equation for deflections can be used to predict immediate deflections of RAC beams with full replacement for low levels of loading. In terms of cracks, they found that RAC beams have wider cracks, however no significant difference was observed with regards crack spacing and almost identical ultimate moments were recorded for RAC and NC beams

The same conclusion was drawn by Ajdukiewicz and Kliszczewicz (2007) based on their tests of 2.6m long rectangular beams with a 200x300mm cross-section with partial and full replacement of NA with recycled aggregate. Their results showed that RAC beams have slightly lower moment capacities and higher deflections compared with NC beams. Maruyama et al. (2004) also tested beams with RA and observed that the cracks in RAC beams were wider and more closely spaced. Once again, they recorded larger deflections for RAC beams than NC beams but no significant difference in flexural capacity.

All of the studies discussed above have concluded that the existing code methods for predicting initial cracking and ultimate flexural loads are applicable for RAC beams but the methods for predicting deflection need modification. However, there has been no discussion of how these methods could be developed to take into account the effect of RA on short-term deflections.

2.8 Steel Fibre Reinforced Concrete

The use of different types of fibres in the matrix of building materials has a long history. In recent years, steel, glass and polypropylene have been the most common types of fibre used in concrete. The main aims of adding fibres to concrete are to:

- Improve the rheology of concrete in its early age fresh state after casting to reduce plastic cracking.
- Improve the compressive strength.
- Improve the tensile and flexural performance.
- Increase the impact strength and toughness.

- Control the cracking and reduce crack propagation.
- Enhance the ductility and control the mode of failure.
- Enhance the durability.

The term “Steel Fibre Reinforced Concrete (SFRC)” refers to concrete with short and randomly oriented steel fibres. SFRC is defined by the American Concrete Institute (ACI) as “a normal concrete which contains discontinuous discrete steel fibres” (ACI 544.1R, 2009). Fibres in low dosages of 0.25-2.0% by volume of concrete can easily be added to concrete during mixing.

Steel fibres are most common and are used widely to improve concrete properties, most notably the mechanical properties (Kosmatka et al., 2011). Steel fibres are generally short and are available with a variety of cross sections (ACI 544.1R, 2009). They can be straight or wavy, and sometimes have hooked ends or flattened ends to improve their ability to transfer load to the cement matrix. Typical fibres have lengths of 6-76mm and diameters of 0.1-1.0mm and fibre contents are normally 0.25-2.0% by volume of concrete. If the volume exceeds 2%, the workability of the concrete and fibre dispersion are reduced and special mix designs or concrete placement techniques are required (Kosmatka et al., 2011). ASTM A820 (2004) gives specifications for standards of steel fibres as shown in Table 2-4. Figure 2-13 shows some commonly available types of steel fibres.

Table 2-4 Specifications for steel fibres from ASTM A820

Length (mm)	Diameter (mm)	Aspect ratio	Specific Gravity	Tensile strength (MPa)	Modulus of elasticity (MPa)	Strain at failure (%)
6-76	0.1-1.0	20-100	7.80	500-2600	210,000	0.5-3.5

Although there are many advantages to using steel fibres in concrete, they can cause problems with workability and it is difficult to achieve a uniform distribution of the fibres. These are considered to be the most difficult challenges of making SFRC (Bentur and Mindess, 2006). One of the reasons why it is difficult to obtain a uniform fibre distribution is that the steel fibres have a tendency to clump together

and reduce workability. A number of factors that may cause clumping have been identified as follows:

- The fibres may be clumped together before they are added to the mix.
- Fibres may be added too quickly and therefore they do not disperse within the mix.
- The fibre content added may be too high.
- The mixer itself may be ineffective for dispersing the fibres.
- The fibres may be added to the mixer before the other ingredients.

The current technology available for mixing, placing and finishing SFRC is described in detail in ACI 544.3R (2009).

Figure 2-13 Commonly available types of steel fibres

2.9 Properties of Steel Fibre Reinforced Concrete

According to the design guidelines for steel fibre reinforced concrete provided by the ACI Committee 544.4R (2009), the properties of SFRC are influenced by a number of factors:

- The type and geometry of the fibres.
- The aspect ratio of the fibres (length to diameter ratio (l/d)).
- The amount of fibres included “volume fraction” (V_f).
- The orientation and distribution of the fibres within the matrix.
- The size of the aggregate.
- The size of the specimen.
- The method of specimen preparation.

2.9.1 Compressive strength

Recent studies have revealed that the addition of steel fibres does little to improve the compressive strength of concrete in comparison to their effect on other mechanical properties. An increase in compressive strength of 0-25% has been observed due to the addition of steel fibres up to 2% by volume (Bentur and Mindess, 2006).

Soutsos et al. (2012) investigated the flexural performance of fibre reinforced concrete with different types of steel fibre. They found that increases in compressive strength were of the order of 4-5MPa when 30-50 Kg/m^3 of steel fibres were included. Sarsam and Al-Azzawi (2010) also reported that fibre additions of 1.5% by volume resulted in small increases of 6% and 17.5% in compressive strength for straight and hooked steel fibres respectively.

Similar results were also observed by Thomas and Ramaswamy (2007). In their study, the maximum increase in compressive strength due to the addition of steel fibres was relatively small (less than 10%). Ashour et al. (2000) also found that adding 1.0% by volume of hooked-end steel fibres increased the compressive strength by 14, 11.3 and 8.8% for concrete prepared to achieve compressive strengths of 49, 79 and 102MPa respectively as shown in Figure 2-14.

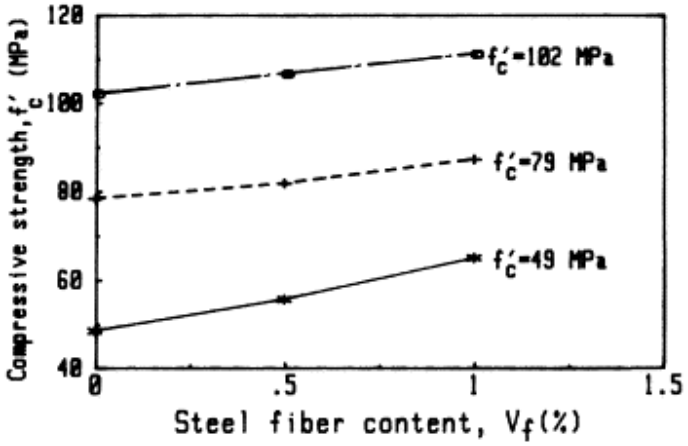

Figure 2-14 Effect of steel fibre content on compressive strength of concrete (Ashour et al., 2000)

2.9.2 Tensile strength

A uniform distribution of fibres aligned in the direction of tensile stresses can increase the direct tensile strength of concrete by up to 133%. However, a more

random distribution of fibres results in a much smaller increase in tensile strength of around 60% (Shah and Rangan, 1971, Hughes, 1981, Johnston and Coleman, 1974). Figure 2-15 shows the increase in tensile strength due to an increase in fibre content for different types of steel fibre.

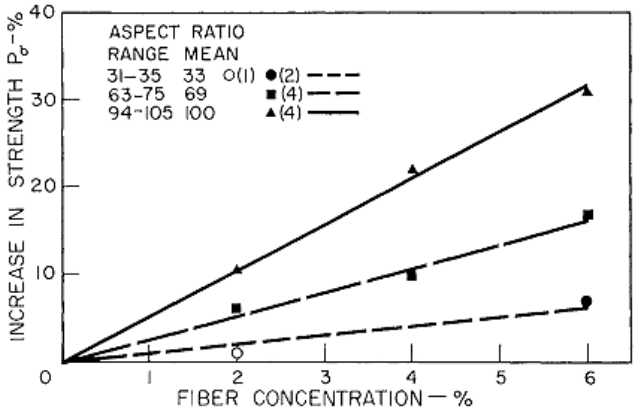

Figure 2-15 Influence of steel fibres content on tensile strength of concrete (Johnston and Coleman, 1974)

An experimental study of the properties of steel fibre reinforced concrete was conducted by Shende et al. (2012). They tested specimens prepared with a concrete grade of 40MPa containing hooked-end steel fibres with volume fractions of 0, 1, 2 and 3%. The steel fibres used in their study had a range of aspect ratios: 50, 60 and 67; the fibres had lengths of 35, 30 and 30mm and diameters of 0.70, 0.50 and 0.40 respectively. They found that the splitting tensile strength increased by 3% to 41% as a result of adding different types and amounts of steel fibres.

Moreover, Sarsam and Al-Azzawi (2010) found that the addition of 1.5% by volume of straight steel fibres resulted in an increase of 32% in splitting tensile strength compared to a 99% increase for hooked steel fibres. Thomas and Ramaswamy (2007) have also tested the mechanical properties of steel fibre reinforced concrete. In their study, concrete with grades of 35, 65, and 85MPa was used to cast specimens with hooked-end glued steel fibres with a length of 30mm and aspect ratio of 55. Fibre dosages varied between 0% and 1.5% by volume. Their results showed that the maximum increase in spilt tensile strength was 40% for the grades of concrete studied.

In 2000, (Ashour et al., 2000) presented a paper on the effects of concrete compressive strength and tensile reinforcement ratio on the flexural behaviour of fibrous concrete beams. They showed that an increase in fibre content from 0% to 1.0% increased the splitting tensile strength by 82.1, 52.3 and 45.4% for concrete specimens having 49, 79 and 102MPa compressive strengths respectively as shown in Figure 2-16.

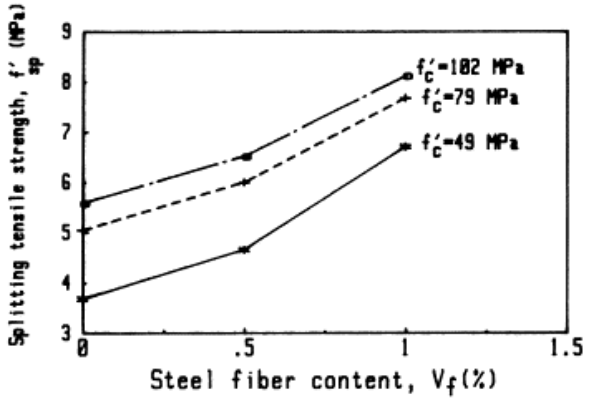

Figure 2-16 Effect of steel fibre content on splitting tensile strength of concrete with different grades (Ashour et al., 2000)

2.9.3 Flexural strength

The effect of steel fibres on the flexural strength of concrete has been found to be much greater than the effect on either the compressive or tensile strengths. It has been reported that the increase in flexural strength can exceed 100% (Bentur and Mindess, 2006). High fibre volumes and high fibre aspect ratios lead to larger increases in strength and straight and smooth fibres are less effective than deformed fibres. Shende et al. (2012) observed an increase in flexural strength of up to 49% due to the addition of steel fibres.

Sarsam and Al-Azzawi (2010) found that the addition of 1.5% by volume of steel fibres increased the modulus of rupture of concrete by 24.5% for straight fibres and 77% for hooked-end fibres. Ashour et al. (2000) results indicated that the modulus of rupture of SFRC increased by 41, 38.5 and 20% due to the addition of 1.0% of hooked-end steel fibres for concrete specimens having compressive strengths of 49, 79 and 102MPa respectively. Figure 2-17 shows Ashour et al.'s data for the effect of fibre content on the modulus of rupture of concrete.

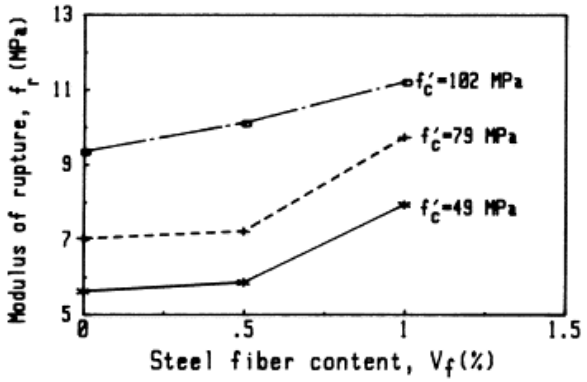

Figure 2-17 Effect of steel fibre content on modulus of rupture (Ashour et al., 2000)

2.9.4 Modulus of elasticity

The elastic modulus of concrete is a very important property and it reflects the ability of concrete to deform elastically. To make full use of the compressive strength of concrete, structures using high strength concrete tend to be slimmer and thus require a higher elastic modulus of the concrete to maintain the stiffness of the structure.

Inclusion of steel fibres in the concrete matrix has a small effect on the modulus of elasticity. Gul et al. (2014) tested the elastic modulus of concretes incorporating hooked-end steel fibres with aspect ratios of 50 and 71 at fibre contents of 0.5, 1.0 and 1.5% by volume. The results obtained showed that the addition of steel fibres increases the modulus of elasticity and that the increase was directly related to the fibre volume fraction and aspect ratio as shown in Figure 2-18.

In investigations carried out by PAWADE et al. (2011) and Elsaigh and St Kearsley (2002), a slight increase in the modulus of elasticity was recorded due to the inclusion of steel fibres for varying fibre contents. Al-Owaisy and Shallal (2007), however, observed a noticeable increase in the modulus of elasticity due to the addition of steel fibres. In their study, the inclusion of 0.5% and 1.0% steel fibres resulted in 5.4% and 29.2% increases in the modulus of elasticity respectively. They suggested that this was due to the interlocking of fibres in the matrix locking the large pieces of aggregate together thus preventing the propagation of micro cracks and inhibiting crack growth.

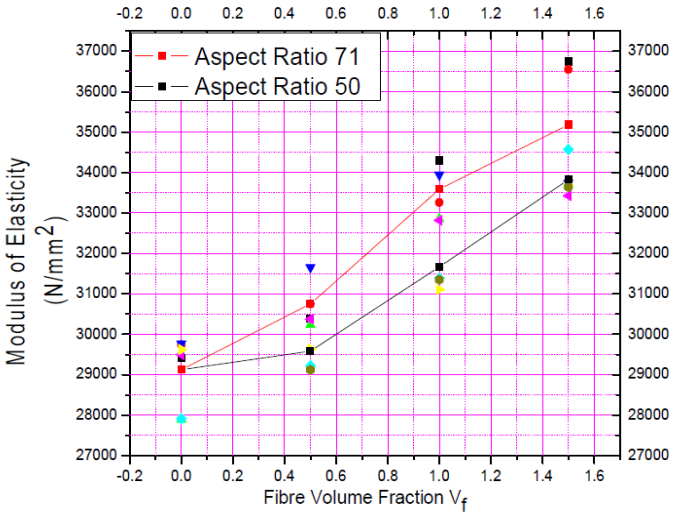

Figure 2-18 Effect of steel fibre volume fraction and aspect ratio on modulus of elasticity of concrete (Gul et al., 2014)

2.10 Flexural Behaviour of SFRC Beams

As mentioned earlier, the effect of incorporating steel fibres in the concrete matrix on the flexural performance is much greater than on other properties. This can be attributed to the ability of fibres to carry load due to the stress transfer from the matrix to the fibres through a combination of interfacial shear stress and mechanical interlock. Prior to the point of matrix cracking, loads are carried by both the matrix and the fibres, but once cracking of the matrix occurs, the fibres bridge the cracks and continue to carry the load until they are pulled out (Bentur and Mindess, 2006).

Figure 2-19 shows typical load-deflection curves for plain concrete and fibre reinforced concrete. The plain concrete fails suddenly once the load reaches the ultimate flexural strength, but the fibre-reinforced concrete continues to bear loads even in excess of the fracture load of the concrete matrix.

Unlike the failure behaviour of plain concrete under flexural loading, fibre reinforced concrete specimens do not fail immediately after the first crack occurs; they continue to carry load while the pull-out resistance of the fibres is greater than the applied load. In the region adjacent to the crack face, the matrix does not carry any load. The fibres transfer the load to the matrix away from the crack face through

interfacial bond stresses. This continues until either the fibres fail or they de-bond and are pulled out (Balugaru and Shah, 1992).

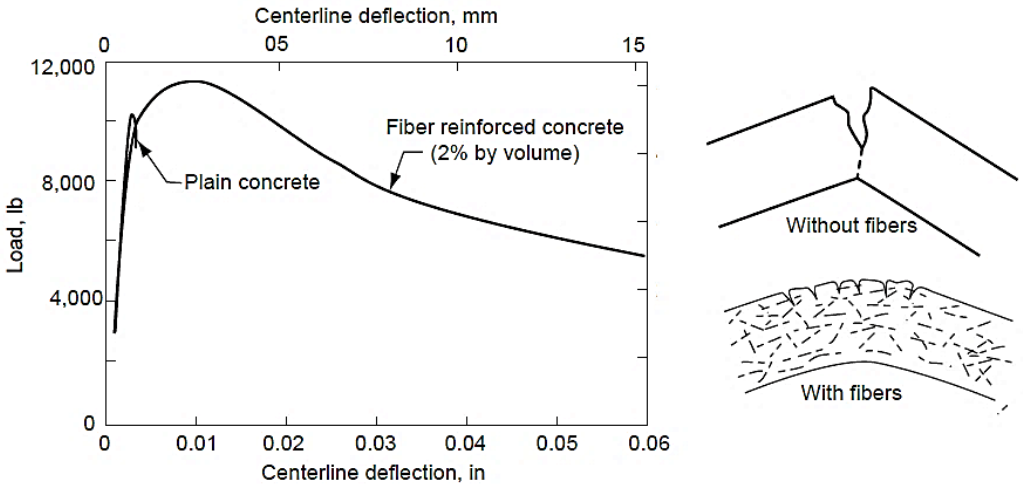

Figure 2-19 Load-deflection behaviour of plain and fibre reinforced concrete and the mechanism of strength enhancement in flexure (Monteiro, 2006)

According to Report 544 by the ACI Committee, toughness is defined as the ability to absorb energy and deform plastically without fracture. Mathematically, it is measured by the area under the load-deflection or stress-strain curve. The results of previous studies have demonstrated an increase in the toughness and ductility of concrete members under flexural loads due to the addition of steel fibres, see Figure 2-20. It has been found that the total energy absorbed by steel fibre reinforced concrete is at least 10-40% higher than plain concrete. The degree of toughness enhancement is strongly dependent on the fibre content, fibre characteristics and fibre pull-out resistance (Bentur and Mindess, 2006).

In 2012, Meda et al. (2012) published an investigation of the flexural behaviour of RC beams containing fibre reinforced concrete. The results from tests of 7 full-scale reinforced concrete beams indicated that the presence of steel fibres could change the failure mode such that collapse was determined by steel rupture as opposed to concrete crushing (more ductile). It is clear that both flexural toughness and ductility are strongly influenced by the addition of steel fibres.

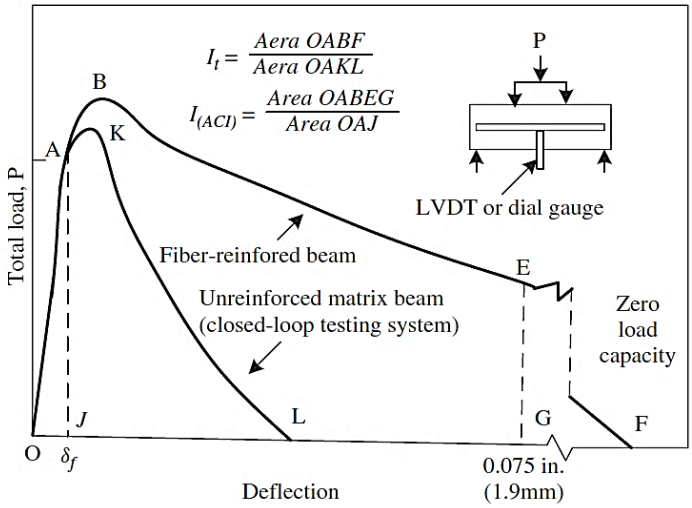

Figure 2-20 Effect of steel fibres on the toughness and ductility of concrete (Li, 2011)

Kang et al. (2012) have also studied the behaviour of steel fibre reinforced concrete beams. Their test results showed that increases of 30% to 200% were observed in flexural ductility and toughness by the addition of 0.5% to 0.75% steel fibres by volume. Altun et al. (2007) examined the effects of steel fibres on the mechanical properties of concrete and RC beams. They concluded that both the ultimate loads and flexural toughness of concretes with compressive strengths of 20 and 30MPa increased appreciably with the addition of steel fibres at dosage levels of 30 and 60 Kg/m^3.

Ashour et al. (2000) tested 27 reinforced concrete beams to study the influence of a number of factors on the flexural behaviour. Fibre contents of 0, 0.5 and 1.0% by volume were added to different specimens with concrete compressive strengths of 49, 79 and 102MPa and tensile reinforcement ratios of 1.18, 1.77 and 2.37%. The results showed that the fibres contributed significantly to the response of the beams by increasing the flexural rigidity and enhancing the post cracking stiffness and ductility of all the beams.

Figure 2-21 shows the load-deflection curves for all the beams tested in their study. Modifications were proposed to a formula from the literature for the estimation of the effective moment of inertia in order to take into account the effects of reinforcement ratio and concrete compressive strength as well as fibre content.

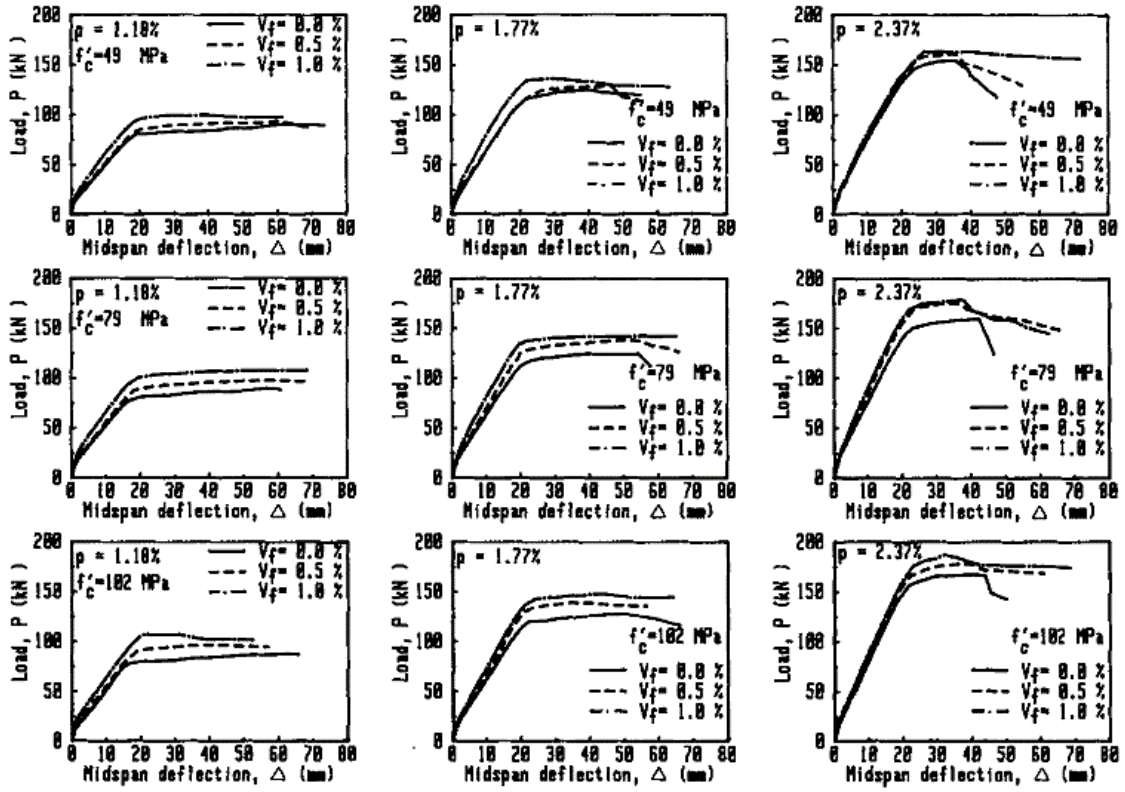

Figure 2-21 Load-deflection curves for SFRC beams (Ashour et al., 2000)

A total of nine beams were tested by Chunxiang and Patnaikuni (1999) to investigate the influence of fibre reinforcement on the mechanical behaviour of reinforced concrete beams. They observed that the addition of steel fibres improves the mechanical properties of concrete and enhances its resistance to cracking. Moreover, increases in first crack loads and reduced deflections were recorded.

Alsayed (1993), Lim et al. (1987), and Swamy and Sa'ad (1981) proposed analytical models for estimating the instantaneous deflection of SFRC beams. It has been shown that the effect of steel fibres on the flexural rigidity (EI) of beams is much greater than their effect on elastic modulus. This is due to the ability of steel fibres to act as crack arrestors and control crack propagation. One theoretical model which has been proposed to calculate the flexural rigidity of SFRC beams is as follows:

$$I_{ef} = \frac{E_c}{E_f}(I_e + KI_g) \qquad \textbf{(2-1)}$$

Where:

I_{ef} = effective moment of inertia of the fibre reinforced concrete section.

E_c = modulus of elasticity of plain concrete.

E_f = modulus of elasticity of fibre reinforced concrete.

I_e = effective moment of inertia of plain concrete section.

I_g = gross moment of inertia of plain concrete section.

K = theoretical function

$$K = 0.45(V_f \frac{l}{d})^2 \left(\frac{M_{cr}}{M}\right)^{1.25} \quad \textbf{(2-2)}$$

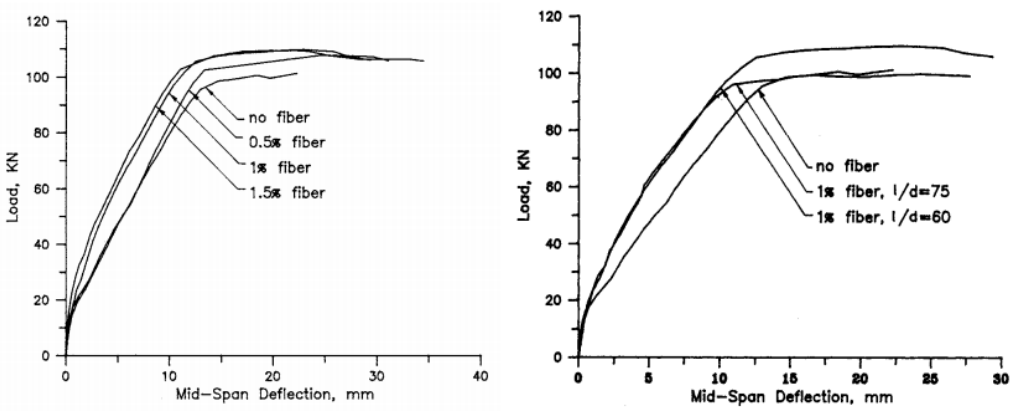

Figure 2-22 Steel fibre content and aspect ratio effect on load-deflection relationship of beams (Alsayed, 1993)

The value of I_{ef} calculated using this expression can be used in the ACI-318 method for calculating short-term deflections. The proposed expression was verified by calculating the ratio between predicted deflections and data for experimental deflections from several studies in the literature; mean deflection ratios were 102% with a variation coefficient of 0.33%.

A combined experimental and analytical investigation of SFRC was carried out by Tan et al. (1994b). Five steel fibre reinforced beams were prepared and tested to the point of flexural failure. The addition of steel fibres was found to significantly increase the first-crack loads and post-cracking flexural stiffness of the resulting concrete beams. A 30% reduction in defections was noted due to the inclusion of 2.0% steel fibres by volume. Based on these experimental results, an empirical approach following the ACI-318 method was developed and the following expression proposed for calculating short-term deflections:

$$\Delta_i = \frac{5wl^4}{384EI_e} \qquad (for\ uniform\ loading\ w) \tag{2-3}$$

$$I_e = \left(\frac{M_{cr}}{M_a}\right)^3 I_g + \left[1 - \left(\frac{M_{cr}}{M_a}\right)^3\right] I_{cr} \ \leq I_g \tag{2-4}$$

$$M_{cr} = \frac{\varphi_{cf} I_g}{y_t} \tag{2-5}$$

$$\varphi_{cf} = 0.843 f_r V_m + 2.93 V_f \frac{l_f}{d_f} \tag{2-6}$$

$$I_{cr} = \frac{bx^3}{3} + nA_s(d-x)^2 + (n-1)A_s`(x-d`)^2 + n_f A_f \frac{(h-x)^2}{3} + (n_f - 1)A_f` \frac{x^2}{3} \tag{2-7}$$

$$E_{cf} = (1 - \eta_1 \eta_0 V_f) E_c + \eta_1 \eta_0 V_f E_f \tag{2-8}$$

$$A_f = \eta_1 \eta_0 V_f (h-x) \tag{2-9}$$

$$A_f` = \eta_1 \eta_0 V_f bx \tag{2-10}$$

Where:

φ_{cf} = first-crack flexural strength of fibre reinforced concrete.

V_m = volume fraction of matrix.

V_f = volume fraction of fibres.

n = modulus of elasticity ratio of concrete = E_s/E_{cf}

η_1 = length efficiency factor.

η_0 = orientation factor.

The predictions from this method were verified by comparison with the available experimental test results of SFRC beams in the literature. The predicted deflections had reasonable agreement with the experimental results. All results were within a range of ±20%; the average ratio was 1.06 with a standard deviation of 0.103.

In 1997, Ashour et al. (1997) published an experimental and theoretical study of the influence of steel fibres and compression reinforcement on the deflection of high strength concrete beams. Their experimental results showed that the inclusion of steel fibres significantly enhanced the flexural rigidity of the beams and reduced the deflection as shown in Figure 2-23.

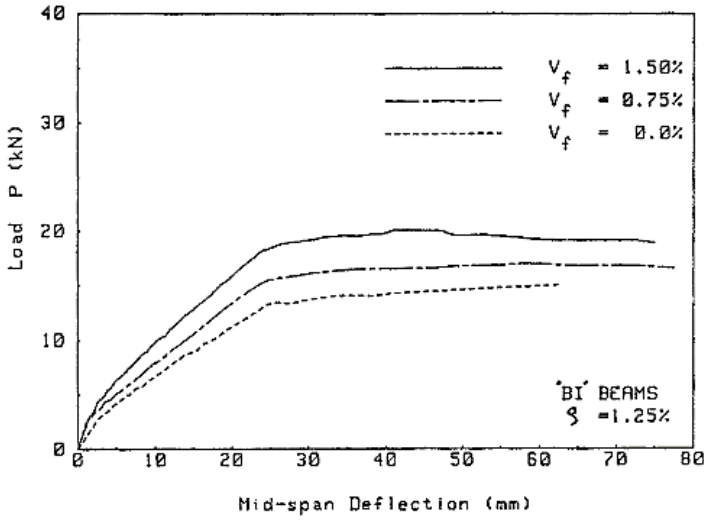

Figure 2-23 Load-deflection curves for SFRC beams (Ashour et al., 1997)

They proposed a theoretical model for calculating the effective moment of inertia of steel fibre reinforced concrete beams to use in the ACI-318 approach for predicting immediate deflections as follows:

$$I_u = \frac{bh^3}{12} + bh\left(\frac{h}{2} - y_u\right)^2 + (n-1)A_s`(y_u - d`)^2 + (n-1)A_s(d - y_u)^2 + \frac{\alpha}{3}V_f b(m-1)(h - y_u)^3 \quad \textbf{(2-11)}$$

$$I_{cr} = \frac{by_c{}^3}{12} + (n-1)A_s`(y_c - d`)^2 + nA_s(d - y_c)^2 + \frac{\alpha}{3}V_f bm(h - y_c)^3 \quad \textbf{(2-12)}$$

$$I_e = \left(\frac{M_{cr}}{M_a}\right)^3 I_u + \left[1 - \left(\frac{M_{cr}}{M_a}\right)^3\right] I_{cr} \leq I_u \quad \textbf{(2-13)}$$

2.11 Effect of Adding Fibres on the Properties of RAC

Although the quantity of construction and demolition waste generated worldwide increases annually and large quantities of natural aggregate are extracted to be used in construction, the utilisation of recycled aggregate in new concrete production and structural applications is limited and not authorised. This can be attributed to the poor quality and properties of recycled aggregate which affects the properties of the concrete produced. To improve the environmental performance of concrete and encourage the use of recycled aggregate in various applications, the addition of different types of fibres to RAC has been investigated. The main aim is

to enhance the properties of the concrete to overcome the negative effects of using recycled aggregate.

Jalilifar et al. (2016) investigated the influence of steel fibre content on the compressive and flexural strength of concrete prepared with RCA obtained from a 45-year-old building. The RCA replacement percentages of 0, 30, 50 and 100% and fibre contents of 0, 0.5, 1.0 and 1.50% were the main variables in their study. Significant reductions in the compressive and flexural strengths of the resulting concrete were observed due to the replacement of the aggregate. The addition of steel fibres, however, increased these strengths as well as the flexural toughness. Figure 2-24 shows the effect of incorporating both RCA and steel fibres on the compressive strength and flexural toughness of concrete.

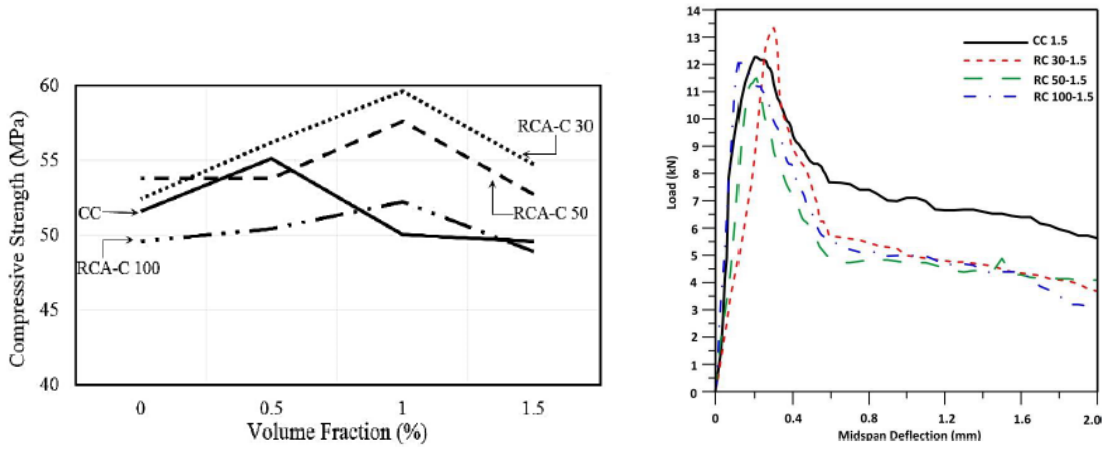

Figure 2-24 Effect of RCA and steel fibres on the compressive strength and flexural toughness of concrete (Jalilifar et al., 2016)

In 2015, Krishna (2015) published the results of an experimental investigation on the flexural behaviour of recycled aggregate fibre reinforced concrete. He also examined the possibility of using recycled aggregate with steel fibres for structural members. The test results showed that by replacing natural aggregate with recycled aggregate and adding steel fibres, the compressive strength improved with increasing fibre percentage and the load-deflection relationship of the beams prepared with recycled aggregate and steel fibres was similar to that for concrete prepared with natural aggregate.

Carneiro et al. (2014) carried out an experimental investigation of the influence of steel fibres on the stress-strain behaviour of concrete made with CDW aggregate. The natural coarse and fine aggregates were replaced by recycled aggregate and hooked-end steel fibres with a length of 35mm and aspect ratio of 65 were added. They noticed that the incorporation of steel fibres in the RAC improved the mechanical strength and changed the fracture process. The recycled aggregate made the concrete more brittle, however the addition of steel fibres enhanced the toughness of the RAC and its behaviour under compressive loads became more similar to that of fibre reinforced natural aggregate concrete.

Another experimental investigation was carried out by Akinkurolere (2010) to study the effect of adding steel fibres on the compressive and tensile strengths of recycled aggregate concrete. The main variables considered included the water/cement ratio, the recycled aggregate percentage, the fly ash content and the steel fibre content. The effects of these varialbes on the compressive and tensile strengths were discussed and the results indicated that the addition of steel fibres enhanced the 28-day compressive and splitting tensile strengths of RAC by 10-30% and 27-41% respectively.

The flexural characteristics of steel fibre reinforced recycled aggregate concrete was studied by Heeralal et al. (2009). They concluded that replacement of natural aggregate with recycled aggregate decreases the compressive and flexural strengths of concrete, and the addition of steel fibres can marginally increase the compressive strength and signficantly increase the flexural strength as shown in Figure 2-25. Furthermore, the results showed that there is an increase in the number of cycles to failure with increased replacement percentages of RA and in the case of the steel fibre reinforced specimens, failure occurred due to multiple minor cracks. The fibre reinforced specimens also exhibited a greater toughness and energy absorpotion capacity.

Younis and Pilakoutas (2013) examined the effect of various parameters on the performance of recycled aggregate concrete including the influence of the addition of recycled tyre steel fibres (RTSFs). Their results showed that inclusion of 2% RTSF enhanced the compressive strength of RAC by 30% and controlled the propagation of microcracks.

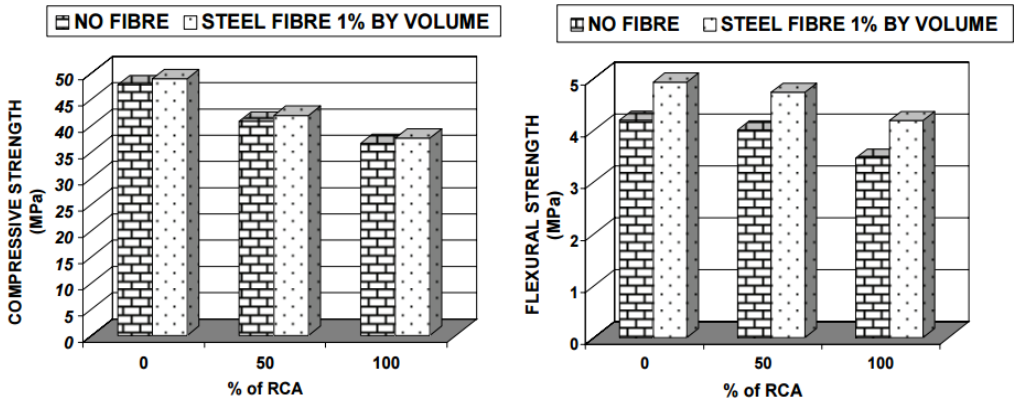

Figure 2-25 Effect of steel fibres on the compressive and flexural strength of RAC (Heeralal et al., 2009)

The addition of different types of fibres has also been studied. For example, Kumar et al. (2014) published an experimental study on the properties of recycled aggregate concrete with polypropylene fibres. Concrete mixes prepared with 25, 30 and 35% of recycled aggregate and 0, 0.5 and 1% of polypropylene fibres (5cm in length) were tested to determine the 1-, 7- and 28-day compressive and tensile strengths. The results indicate that the samples with 1% fibres and 25% recycled aggregate had the highest strengths. The authors concluded that in general the fibres improved the elasticty of the concrete and reduced shrinkage cracking.

Vytlačilová (2011) carried out an experimental program to investigate the combined effects of the incorporation of recycled construction and demolition waste and synthetic fibres on the properties of concrete. Synthetic polypropylene fibres (FORTA FERRO®), Polymer BeneSteel fibres (made from a mixture of polypropylene and polyethylene) and fibres cut from waste PET bottles were used in the experiments. Based on the results, it was concluded that the use of these fibres in structural materials was beneficial especially under tensile loading due to the increase in ductility.

Glass Fibre Reinforced Recycled Aggregate Concrete (GFRRAC) was developed by Prasad and Rathish Kumar (2007). Although the addition of glass fibres leads to a marginal increase in the compressive strength in the range of 2-3%, noticeable increases in the splitting tensile strength and flexural strength of 10-17% and 10-14% respectively were observed as shown in Figure 2-26. Moreover, a higher

toughness was observed for the GFRRAC specimens due to an increased energy absorption capacity.

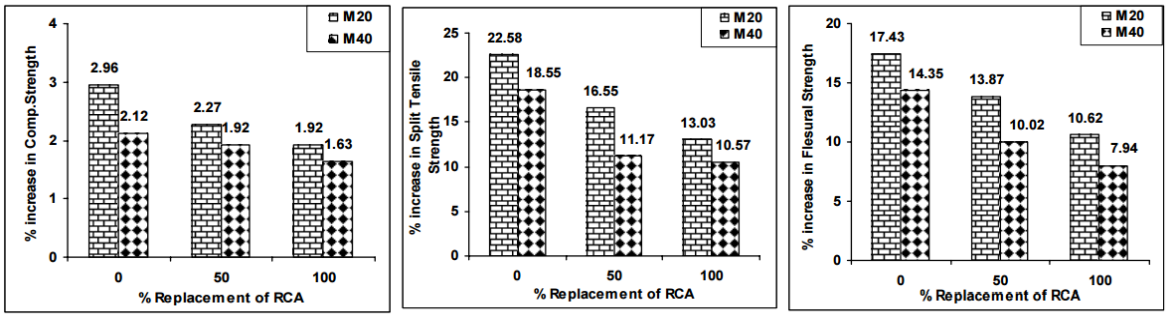

Figure 2-26 Increase in the mechanical properties of RAC due to the addition of glass fibres (Prasad and Rathish Kumar, 2007)

2.12 Economic and Energy Aspects

It is obvious that many environmental issues can be solved by reusing CDW as a coarse aggregate in producing concrete. However, some researchers have given more attention to investigating the economic and energy advantages.

According to the US EPA (2002), reusing CDW in concrete production makes good economic and business sense and, at the same time, can improve production efficiency, profits, good neighbour image, employee participation, product quality and environmental performance. The benefits come from all the direct, indirect and intangible benefits of reusing and recycling waste materials, although there are also direct, indirect and intangible costs involved in reusing and recycling on site.

Begum et al. (2006) performed a cost benefit analysis (CBA) to estimate the economic feasibility of reusing CDW in terms of cost savings. This study concluded that reusing the waste is economically feasible and also plays an important role in reducing concrete production costs. The net benefit from reusing CDW was estimated at 2.5% of the total budget for this section.

Tam (2008) studied the cost and benefit of the current practice of dumping construction waste in landfills and producing new natural materials for new concrete production. A method of recycling construction waste as aggregate for new concrete production was proposed and it was found that this concrete recycling method could result in a considerable saving. Therefore, recycling concrete waste

for new production is a cost-effective method that also helps to protect the environment and to achieve construction sustainability.

Regarding the energy aspects, Copple (2008) compared the energy required for production of recycled aggregate concrete with that required for the production of conventional concrete with virgin aggregate. The energy requirements which are unique to conventional concrete mixes were considered, including the haulage and disposal of old concrete, production of virgin aggregate and haulage of virgin aggregate. The energy requirements which are unique to RAC mixes were also taken into account, including moving crushers to the job site, crushing and screeing processes, and transporting old concrete to the recycling site and then to the production site. The results demonstrated that energy savings are realised for the RAC, even when virgin aggregate must be hauled for only a few miles.

Hameed and Chini (2010) examined the feasibility of recycled aggregate concrete over virgin aggregate in terms of both cost and energy. The goal was to determine the extent to which transportation distance impacts the cost and energy. The results from this study show that different approaches can be taken for the use of demolished concrete. Three cases were studied. In the first case, a portable crusher was used to recycle the concrete and use the recycled concrete aggregate at the project site, and this was the most cost-effective and energy-efficient option. The second case, in which the demolished concrete was landfilled and new virgin aggregate was bought, was the least cost-effective and energy-efficient option. Therefore, crushing waste concrete at the demolition site where the aggregate is reused is the most economic and energy-efficient option.

The results of this study also showed that transportation distance has a major impact on cost and energy consumption. When the distance between the job site and the recycling plant was increased by increments of 5 km, there was a point at which virgin aggregate became a more favourable option in terms of cost and/or energy consumption than using a RCA from a recycling plant.

Although the benefits of adding steel fibres to concrete are well recognised and have been extensively studied individually, few recent efforts have focused on the combination of both RA and steel fibres as a structural material. Therefore, more experiments and structural tests are required to provide a better understanding of

this combination. There is also a lack of research focusing on the economic feasibility of this mixture, despite the predictions of several environmental benefits with the use of RA.

Senaratne et al. (2016) presented a study analysing the cost-effectiveness of the combination of RA and steel fibres for beams. An experimental investigation was carried out to determine the optimum combination, which was followed by a CBA to find out the direct/indirect costs and benefits of using RA. The optimum combination found through the experimental phase was 30% recycled aggregate replacement with the addition of 0.6% steel fibres. The CBA showed that, in the typical beam design considered, the saving per beam from RA replacement was nearly 2.5 times more than the cost increase of adding the steel fibres. These results confirmed that the additional cost increase of utilising steel fibres could be offset considerably by the quantified sustainable benefits of using RA in the mixture. However, these findings were based on using a low replacement percentage of RA (30%).

2.13 Summary

The concluding remarks of this review are summarised below:

- The results of previous research have shown that the properties of recycled aggregate are poorer than those of natural aggregate.
- The presence of cement paste which is attached to the surface of the RA and other materials such as clay bricks and tiles increase the porosity of RA and it is thus more liable to absorb large amounts of water.
- Based on the experimental results reviewed, properties of both fresh and hardened recycled aggregate concrete are significantly influenced by the poor properties of RA.
- Reinforced RAC beams develop more closely spaced and wider cracks than reinforced NC beams under flexural loading. There are no significant reductions in cracking and ultimate moment values due to the inclusion of RA, however greater deflections were observed with RAC beams.
- The existing analytical models and code procedures for conventional normal concrete can be used to predict ultimate bending moments for RAC, but they need to be modified to predict instantaneous deflections.

- Most studies to date have investigated the effect of incorporating RCA on the properties of concrete; the effect of using CDW as recycled aggregate has received little attention.
- There has been extensive investigation of the effects on the properties of concrete of the addition of steel fibres. It has been found that adding steel fibres leads to significant enhancements in the properties of concrete.
- The addition of steel fibres to the concrete matrix has a much greater effect on the flexural behaviour of beams than on other properties. The results of beam tests have shown that steel fibres contribute significantly to material response by increasing flexural rigidity and toughness and enhancing post cracking stiffness and ductility.
- Steel fibre reinforced concrete beams have higher cracking and ultimate loads and reduced deflections. The fibres also increase the resistance to crack propagation, control crack widths and change the failure mode from sudden crushing to a more ductile mode of failure.
- The addition of mineral admixtures and fibres to RAC such as silica fume, fly ash, ground blast furnace slag, steel fibres, polypropylene fibres and glass fibres on the fresh and hardened properties of concrete could overcome the negative effects of including RA. These additions have been investigated and several advantages have been identified.

In sum, it is well documented that the addition of steel fibres can enhance the performance of concrete. However, studies have not sufficiently addressed the combination of both recycled aggregate and steel fibres for structural purposes. Furthermore, there is also a lack of research focused on the economic feasibility of this mixture.

Chapter 3 : Long-term Performance of Concrete Incorporating Recycled Aggregate and Steel Fibres

3.1 Introduction

Recently, there has been an increasing trend for designing more serviceable buildings. Serviceability is one of the most significant aspects to be considered in the design of concrete structures and attention must be paid to controlling cracking and limiting deflections to acceptable levels. However, at the design stage, the long-term properties of concrete cannot be predicted accurately as its behaviour under service loads is non-linear and complicated (Gilbert, 2001b).

There are three principal phenomena which are considered to be the main reasons for the nonlinearities in concrete response to sustained loads: creep, shrinkage and tension stiffening. These materials behaviours lead to the widening of cracks and crack propagation, and the subsequent increase in deflection of concrete members over time (Scott and Beeby, 2012). For practical purposes, it is more valuable to understand the long-term rather than the short-term deflections of structures. Therefore, it is important that the long-term performance of concrete should be taken into account at the design stage.

In this chapter, the effect of incorporating recycled aggregate and steel fibres on the time-dependent deformations of concrete and the long-term flexural performance of beams is presented. Moreover, the concept of loss of tension stiffening and its effect on the flexural performance of concrete structures are presented.

3.2 Creep and Shrinkage

The creep and drying shrinkage of concrete lead to time-dependent deformations and are considered to be the main contributors to the long-term deflection of concrete structures. Creep is defined as deformation which occurs under sustained stresses (compressive or tensile) while drying shrinkage is defined as the deformation which occurs due to the volume change of concrete when it is exposed

to drying conditions. As reported in ACI 209-1R, these deformations are dependent on various factors including the following:

- Materials properties (especially of the aggregate).
- Mix proportions (e.g. water, aggregate and cement content).
- Temperature and relative humidity of the surrounding environment.
- Period of curing.
- Age of loading.
- Size and shape of specimens.

Many studies have been carried out to investigate the effect of these factors on the creep and shrinkage deformations of concrete. Moreover, methods for reducing these deformations through adding mineral admixtures to the concrete have also been examined. In this section, the effect of the incorporation of recycled aggregate and steel fibres on creep and shrinkage will be presented and discussed.

3.2.1 Effect of recycled aggregate

As the type, properties and quantity of aggregate included are some of the main factors affecting the creep and shrinkage of concrete, in this section, the effect of using recycled aggregate on creep and shrinkage will be examined in detail. A number of factors related to RA which affect creep and shrinkage have been investigated by researchers of which the replacement percentage of aggregate is the most common.

In general, according to the results presented in the literature, as replacement of NA with RA increases, the creep and shrinkage deformations of concrete also increase. However, with the incorporation of RA at low levels, specifically up to 30%, an equivalent or negligibly greater shrinkage in comparison to that of the corresponding normal concrete is observed.

Knaack and Kurama (2015a) carried out an experimental investigation of the creep and shrinkage of normal strength concrete with recycled concrete aggregates (RCA) as a replacement for coarse natural aggregates. Three RCA sources and two aggregate replacement levels were used for testing different parameters including curing conditions, loading age and applied stress levels. They concluded that the creep and shrinkage strains of concrete increase significantly with

increasing replacement percentage of aggregate (RP) as illustrated in Figures 3-1 and 3-2.

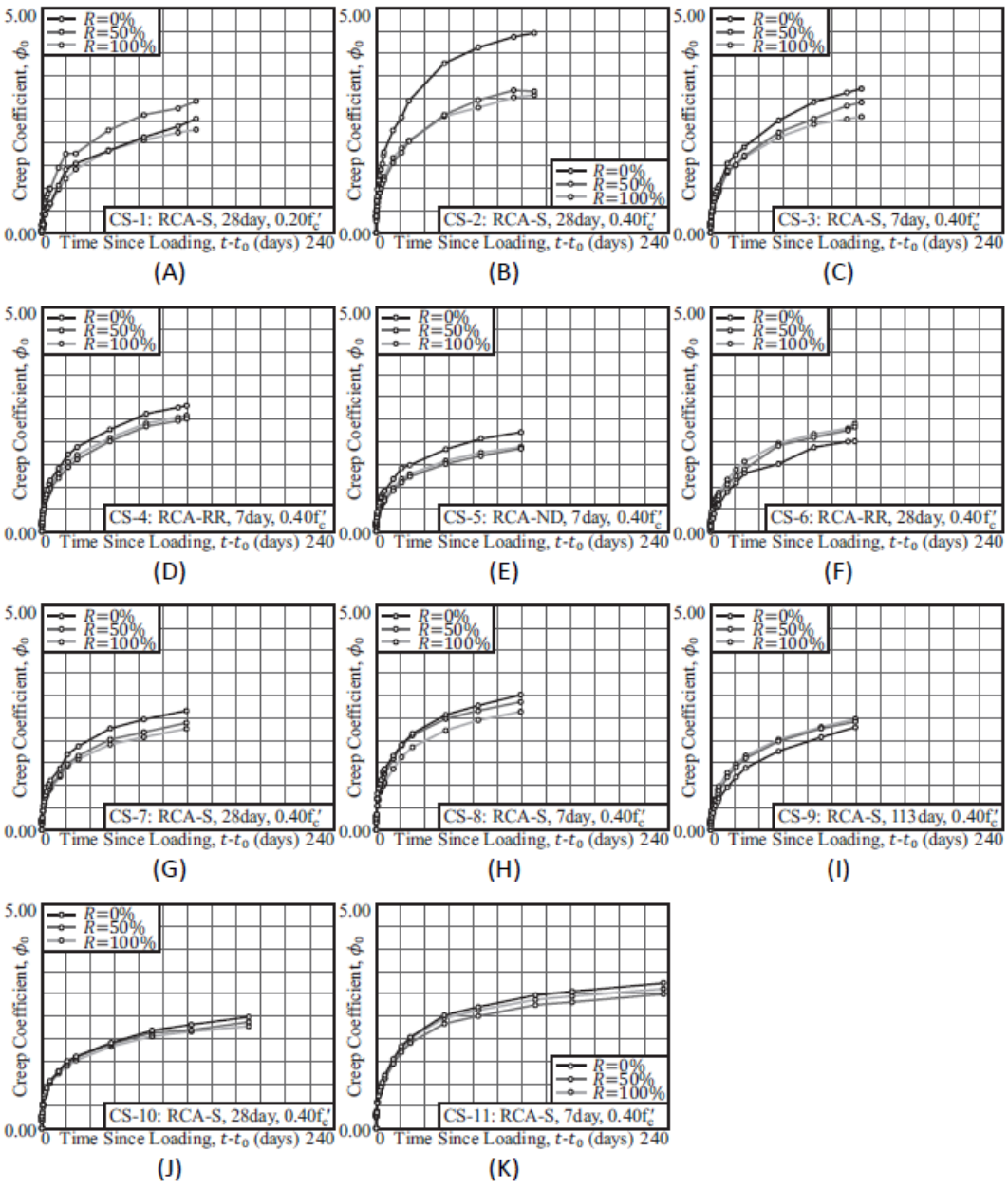

Figure 3-1 Creep test results (Knaack and Kurama, 2015a)

Based on an average of the test results, the ratios between the total creep strain of RCA concrete and NA concrete after testing for approximately 7.5 months were 1.31 and 1.61 for RPs of 50% and 100% respectively. The corresponding average ratios for the shrinkage strains were 1.21 and 1.71 for RPs of 50% and 100%. They attributed these results to the presence of the attached mortar and the resulting

reduction in modulus of elasticity and increase in porosity and water absorption capacity. It was also concluded that as the age of loading increased, the creep compliance increased and samples with the lowest concrete compression strength exhibited the lowest creep compliance. Adjustment factors were proposed to improve the accuracy of code-based creep models for RCA concrete.

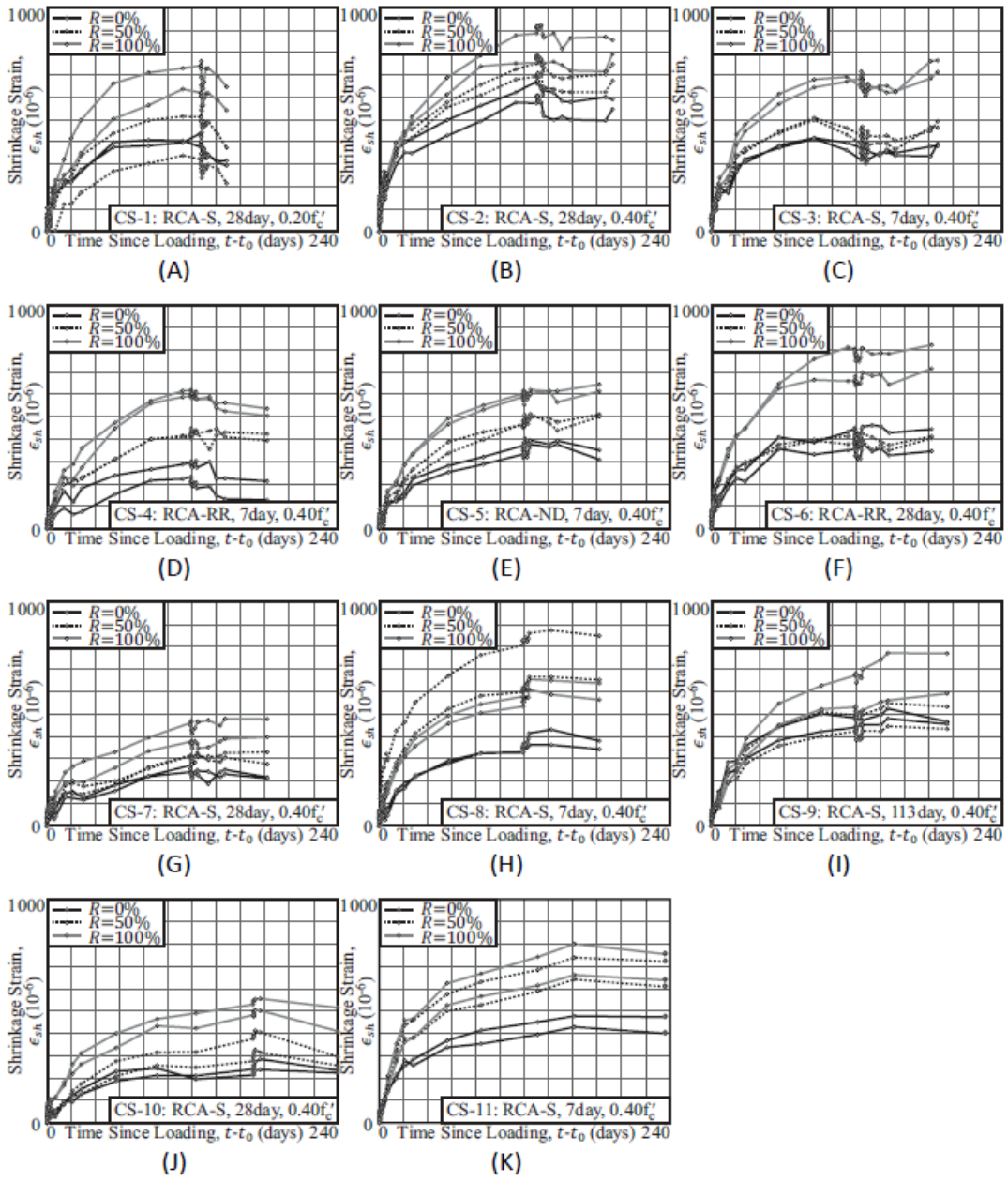

Figure 3-2 Shrinkage test results (Knaack and Kurama, 2015a)

Based on statistical nonlinear regression analysis, the authors found that RCA concrete creep and shrinkage strains can be reasonably predicted by using the

normal concrete models in ACI-209R in combination with an adjustment factor t_0. The proposed equations for calculating the creep coefficient at time $t = t_0$ and the ultimate creep coefficient for RAC under constant stress are given as:

$$\phi_{0,rca}(t) = \frac{(t - t_0)^{\psi_{cr1}}}{[\psi_{cr2} + (t - t_0)^{\psi cr1}]}\phi_{u,na} \quad \textbf{(3-1)}$$

$$\phi_{u,rca} = \frac{\alpha_{cr}(\phi_{u,na} + 1)E_{c,rca}}{E_{c,na} - 1} \quad \textbf{(3-2)}$$

$$\alpha_{cr} = \beta_{cr0} + \beta_{cr1}\frac{fc`_{rca}}{fc`_{na}} + \beta_{rc2}R \quad \textbf{(3-3)}$$

Where:

$\psi_{cr1}$and ψ_{cr2} = creep time-function factors.

$\phi_{u,na}$ = ultimate creep coefficient of normal concrete.

α_{cr} = proposed creep adjustment factor.

β_{cr0}, β_{cr1} and β_{cr2} = un-normalised creep regression coefficients.

$E_{c,na}$ and $E_{c,rca}$ = modulus of elasticity of normal and recycled aggregate concrete.

$fc`_{na}$ and $fc`_{rca}$ = compressive strength of normal and recycled aggregate concrete.

R = aggregate replacement ratio in decimal form.

Similarly, a constrained linear regression analysis was performed to determine the shrinkage adjustment factors for RAC. Based on the shrinkage model proposed by ACI-209R, the equations developed are:

$$\varepsilon_{sh_{rca}}(t) = \frac{(t - t_0)}{[\psi_{sh} + (t - t_0)]}\varepsilon_{sh_{u,na}} \quad \textbf{(3-4)}$$

$$\varepsilon_{sh_{u,rca}} = \frac{\alpha_{sh}(\varepsilon_{sh_{u,na}} + 1)E_{c,rca}}{E_{c,na} - 1} \quad \textbf{(3-5)}$$

$$\alpha_{sh} = \beta_{sh0} + \beta_{sh1}\frac{fc`_{rca}}{fc`_{na}} + \beta_{sh2}R \quad \textbf{(3-6)}$$

Where:

ψ_{sh}= shrinkage time-function factor.

$\varepsilon_{sh_{u,na}}$ = ultimate shrinkage of normal concrete.

α_{sh} = proposed shrinkage adjustment factor.

β_{sh0}, β_{sh1} and β_{sh2} = un-normalised shrinkage regression coefficients.

Fan et al. (2014) studied the effect of the replacement of NA by recycled crushed concrete aggregate (RCA) on creep and shrinkage deformations. Concrete with a 30MPa compressive strength was used to produce the RCAC and the replacement percentages were 33%, 66% and 100%. Similar to the previous study, Fan et al. (2014) observed that the creep and shrinkage of RCA concrete increased with increasing substitution levels. More specifically, the creep increased by 28.7%, 75% and 103.3% at day 200 of testing for replacement percentages of 33%, 66% and 100% respectively. Moreover, the shrinkage of the RCA was approximately 2.6%, 15.4% and 26.9% higher than that of NAC as shown in Figure 3-3. The creep and shrinkage response was attributed to the presence of the old mortar and its volume content. A numerical model for predicting RAC creep was proposed which took into account the effect of the mechanical properties and creep behaviour of the old adhering mortar.

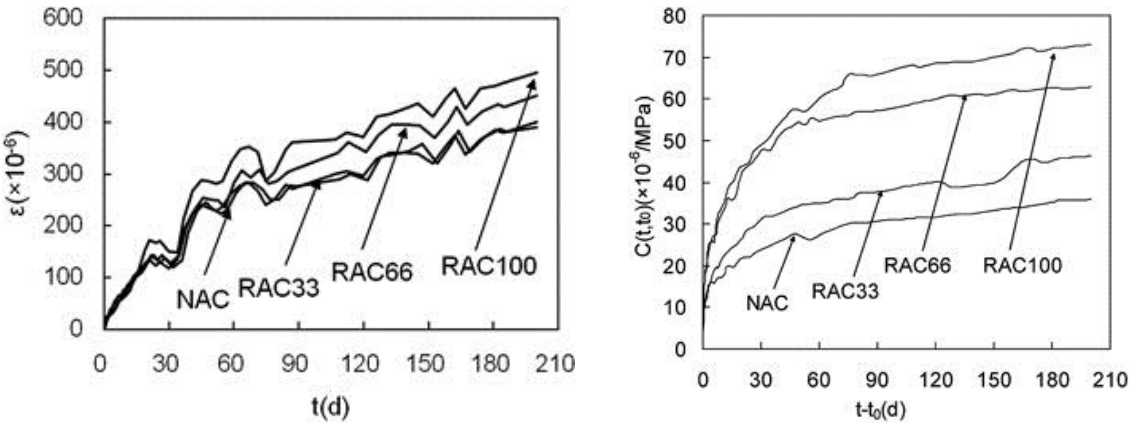

Figure 3-3 RAC shrinkage and creep curves (Fan et al., 2014)

The authors modified existing creep and shrinkage models for normal concrete for predicting the creep and shrinkage when RA is incorporated. The modifications were developed based on phenomenological models which treat the concrete as a two-phase material (aggregate and cement paste). The resulting formulas are as follows:

$$C_{RAC} = C_m(1 - g_{R-NCA})^{\alpha_{R-NAC}} \quad \textbf{(3-7)}$$

$$\alpha_{R-NAC} = \frac{3(1-\mu_{RAC})}{1+\mu_{RAC}+2(1-2\mu_{NAC})E_{RAC}/E_{NCA}} \quad \textbf{(3-8)}$$

$$g_{R-NCA} = \frac{m_{RCA}(1-MRC)}{SG_{NCA}} \quad \textbf{(3-9)}$$

Where:

C_{RAC} = creep of recycled aggregate concrete.

g_{R-NCA} = volume fraction of NCA in recycled aggregate concrete.

μ_{RAC} = Poisson`s ratio of recycled aggregate concrete.

μ_{NAC} = Poisson`s ratio of normal concrete.

E_{RAC} = elastic modulus of recycled aggregate concrete.

E_{NCA} = elastic modulus of normal concrete.

m_{RCA} = mass of recycled aggregate concrete.

MRC = mass fraction of old adhering mortar in RCA.

SG_{NCA} = apparent density of normal concrete.

In another study, Domingo et al. (2010) measured the creep and drying shrinkage deformations of recycled aggregate concrete. A control specimen of 40MPa compressive strength concrete was cast for comparison with specimens prepared with replacement levels of 0%, 20%, 50% and 100% RCA. All specimens were cured for 7 days and tested for 180 days. 35%, 42% and 51% higher total creep and 4%, 20% and 70% higher shrinkage strains were measured for the 20%, 50% and 100% RA samples of RCA respectively as shown in Figures 3-4 and 3-5.

The increase in shrinkage was attributed to the old adhered mortar in the recycled aggregate. In particular, the presence of attached mortar on the surface of the RCA increases the volume of the cement paste in the concrete. This can lead to higher drying shrinkage as the w/c ratio has a significant effect on shrinkage. Increasing the volume of cement paste leads to a greater volume of pores thus increasing the porosity of the resulting concrete. This porosity combined with the difference in relative humidity between the concrete and the surrounding environment cause a greater loss of water which significantly increases the drying shrinkage. Moreover, it was noted that an increase in the RA replacement level means there is a decrease in the aggregate-to-cement ratio as RA includes additional mortar which is attached

to the surface of the particles. This can result in reducing the density and greatly increasing the porosity of the concrete which also causes more drying shrinkage.

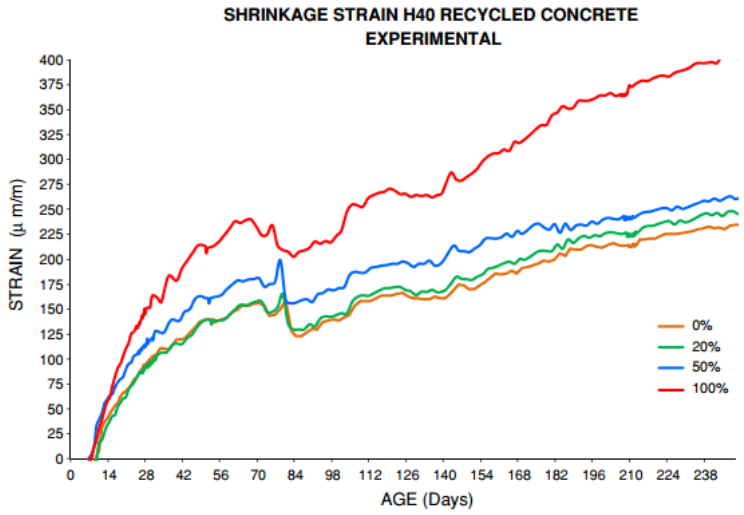

Figure 3-4 Shrinkage strains for different replacement levels of RCA (Domingo et al., 2010)

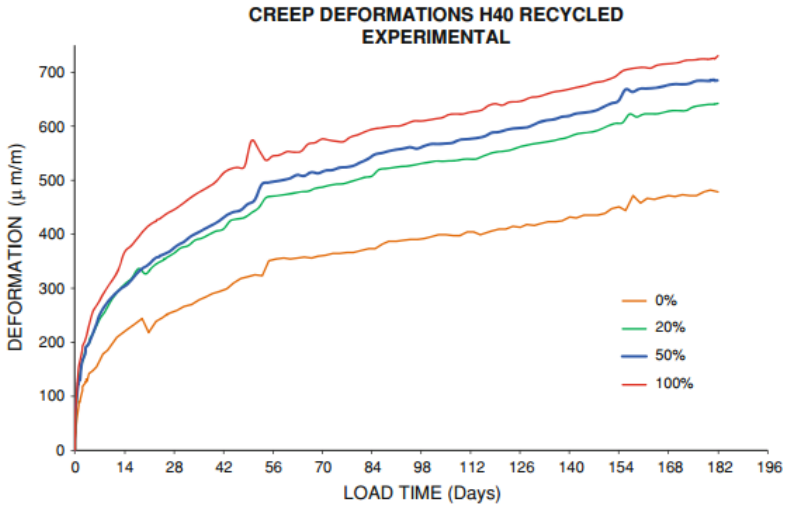

Figure 3-5 Creep deformations for different replacement levels of RCA (Domingo et al., 2010)

With regards creep, the authors found that the mechanism of creep observed was related to the loss of water from the C-H-S gel in the cement paste and micro-cracking due to the applied loads. As mentioned previously, due to the presence of attached mortar, RAC has a greater volume of cement paste and a lower aggregate-to-cement ratio. Therefore, as the creep deformation occurs in the

cement paste, recycled aggregate concrete has higher creep strains than normal concrete. Furthermore, the lower elastic modulus of the recycled aggregate and the higher porosity of the resulting concrete were considered by the authors to be significant reasons for the observed increase in creep.

A variety of other factors that affect the creep and shrinkage deformations of concrete when recycled aggregate is incorporated have been investigated. A systematic review of the literature on the effect of using recycled aggregate on shrinkage was presented by Silva et al. (2015). Their conclusion was that an increase in the amount of the RA leads to higher concrete shrinkage strains and that the two are linearly related. It was noted that using the water compensation method when mixing could reduce shrinkage by 30% compared to the pre-saturated method. This result was confirmed by Ferreira et al. (2011). In addition, the authors found that similar to conventional concrete, the use of water-reducing admixtures can allow for control of shrinkage, and that the modulus of elasticity of the RA employed has a noticeable influence on shrinkage.

Xiao et al. (2014) studied the long-term properties of recycled aggregate concrete and reported that the increased drying shrinkage of RAC is initially rapid and slows down over time. They also found that creep and shrinkage deformations increase with increasing RCA substitution levels and with the strength class of the concrete used. Some techniques, such as the new mixing approach called the Equivalent Mortar Volume Method (EMV) or the addition of various mineral admixtures, e.g. fly ash or slag, can effectively improve the long-term behaviour of RCAC.

The effect of using alternative mixing approaches on the creep and shrinkage characteristics of RAC was investigated by Fathifazl et al. (2011). Laboratory tests were carried out to examine the effect of a new method of mixture proportioning called the Equivalent Mortar Volume Method (EMV). In this method, the RA is treated as a composite material comprised of particles of natural aggregate and adhered mortar. The properties and amounts of these two components are considered individually when calculating the proportions of the concrete mixtures. The authors used two different types of aggregate denoted as RCA-M and RCA-V which were obtained from different recycling plants and had residual mortar contents of 41% and 21% respectively.

Generally it was found that the specimens prepared and proportioned using the EMV method (EM and EV) had lower or comparable creep and shrinkage strains to the normal concrete mix specimens (CL and CG) while the specimens prepared with a conventional method (CM and CV) had higher creep and shrinkage strains. The authors proposed a modification factor, the “residual mortar factor”, for use with the existing ACI and CEB models for predicting creep and shrinkage of RCAC.

The creep and shrinkage expressions derived by the authors were based on a model proposed by Neville (1995) and are as follows:

$$\alpha_{RCA-concrete} = \frac{3(1-\mu_{NAC})}{1+\mu_{NAC}+2(1-2\mu_{NA})\frac{E_{RCA}}{E_{NAC}}\times\frac{E_{NAC}}{E_{NA}}} \quad \textbf{(3-10)}$$

$$C_{RCA-concrete} = \frac{(1-V_{NA}^{RCA-concrete})^{\alpha_{RCA-concrete}}}{(1-V_{NA}^{NAC})^{\alpha_{NAC}}} C_{NAC} \quad \textbf{(3-11)}$$

$$S_{RCA-concrete} = \left(\frac{1-V_{NA}^{RCA-concrete}}{1-V_{NA}^{NAC}}\right)^{n} S_{NAC} \quad \textbf{(3-12)}$$

Where:

$C_{RCA-concrete}$ = creep coefficient of recycled aggregate concrete.

$S_{RCA-concrete}$ = shrinkage of recycled aggregate concrete.

$V_{NA}^{RCA-concrete}$ = total volume fraction of natural aggregate in recycled aggregate concrete.

V_{NA}^{NAC} = total volume fraction of natural aggregate in normal concrete.

μ_{NAC} = Poisson`s ratio of normal concrete.

μ_{NA} = Poisson`s ratio of natural aggregate.

E_{RCA} = elastic modulus of recycled aggregate concrete.

E_{NAC} = elastic modulus of normal concrete.

E_{NA} = elastic modulus of natural aggregate.

Kou and Poon (2012) studied the effect of adding fly ash and recycled aggregate on concrete creep and shrinkage. Specimens were cast with aggregate replacement percentages of 0%, 20%, 50% and 100% and fly ash contents of 0%, 25% and 35% of the weight of cement. In the first series of specimens (Series I), the w/c ratio was constant; in the second series (Series II) it was reduced as the fly ash content increased. The drying shrinkage of one set of specimens was measured for 112 days and the creep specimens of the other set were measured for 120 days.

The results showed that the drying shrinkage and creep strains increased as the amount of recycled aggregate used increased. The authors attributed this to the presence of old attached mortar. However, the addition of fly ash significantly reduced both the drying shrinkage and creep strains. The authors stated that this reduction was due to the dilution of the fly ash particles which was confirmed in another study by Limbachiya et al. (2012). Furthermore, the difference in the results between the Series I and Series II specimens indicates that the decrease in water-to-binder ratio leads to noticeably reduced drying shrinkage and creep strains. Finally, the authors concluded that the incorporation of fly ash as a cement replacement in recycled aggregate concrete can enhance the durability of the resulting concrete and allow for use of a higher percentage of RA.

To date, the studies reported in the literature have examined the effect of incorporating RCA on the creep and drying shrinkage deformations of concrete, while the effect of adding CDW as a recycled aggregate on time-dependent deformation has received little attention.

3.2.2 Effect of steel fibres

Recently, the use of steel fibre reinforced concrete (SFRC) has become more popular in various construction applications as adding steel fibres significantly enhances concrete strength properties. In this section, test results from the literature related to the effect of steel fibres on creep and drying shrinkage deformations are presented and discussed.

The effect of steel fibres on the free shrinkage of cement-based matrices has been experimentally and analytically investigated by (Mangat and Azari, 1984, Mangat and Azari, 1988). Tests were carried out on cement paste, mortar and two different concrete mixes for a period of up to 520 days. Crimped, hooked and melt extract steel fibres were added to the concrete specimens at volume contents between 1% and 3%. It was found that deformed fibres can reduce concrete shrinkage by up to 40% and that the reduction increases with an increase in fibre content as shown in Figure 3-6. The authors pointed out that fibre geometry is significant, and deformed fibres have a greater effect than straight and smooth ones.

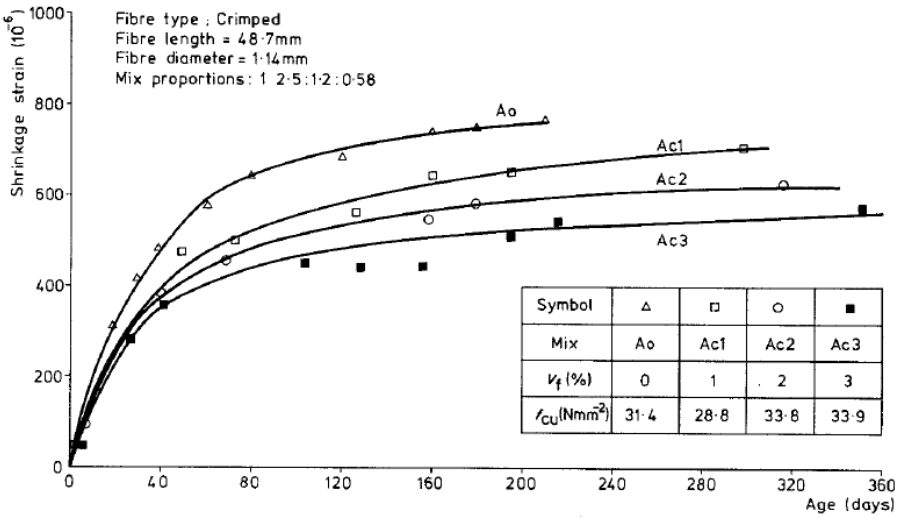

Figure 3-6 Influence of crimped steel fibres on the free shrinkage of concrete (Mangat and Azari, 1984)

The authors modified a theoretical model of the shrinkage of normal concrete to predict the free shrinkage of concrete when randomly oriented steel fibres are incorporated. Their model takes into account the equivalent aligned length and geometry of the fibres and the effect of these on bond strength and the fibres' ability to restrain shrinkage. The model was validated with extensive experimental data obtained from adding different types of steel fibres to both cement mortar and concrete. The expression for the free shrinkage of SFRC derived is as follows:

$$\varepsilon_{fs} = \varepsilon_{os}\left(1 - 2.45\mu V_f \frac{l}{d}\right) \quad \textbf{(3-13)}$$

Where:

ε_{fs} = free shrinkage of SFRC.

ε_{os} = free shrinkage of normal plain concrete.

μ = coefficient of friction between fibres and matrix (ranging from 0.04 for smooth and straight fibres to 0.12 for deformed fibres).

V_f= volume fraction of fibres, %.

l/d = aspect ratio (length over diameter) of fibres.

In 1985, Mangat and Azari (1985) also studied the effect of steel fibres on concrete creep and concluded that the addition of steel fibres had only a small influence as shown in Figure 3-7. They proposed another theoretical model to predict the creep

of SFRC based on the creep of normal plain concrete. This model was also validated for different geometries of steel fibre. The expression derived for creep strain is as follows:

$$\varepsilon_{fc} = \varepsilon_{oc}(1 - 1.96\mu V_f \frac{l}{d}) \quad \textbf{(3-14)}$$

Where:

ε_{fc} = creep strain of the SFRC.

ε_{oc} = creep strain of normal plain concrete.

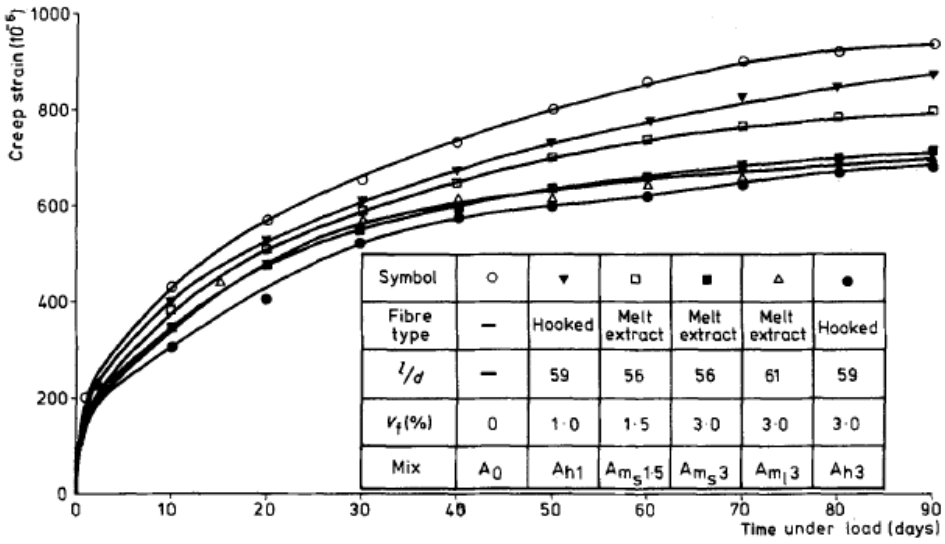

Figure 3-7 Influence of steel fibres on c (Mangat and Azari, 1985)

Another experimental investigation of the creep and shrinkage properties of SFRC was carried out by Tan et al. (1994a). In this study, concrete cylinders and prisms were prepared and cured with different fibre volume fractions (V_f = 0%, 0.5%, 1%, 1.5% and 2%) and compressive creep response and drying shrinkage were measured. It was concluded that with increasing fibre content, both the creep coefficient and shrinkage strains decreased as shown in Figures 3-8 and 3-9.

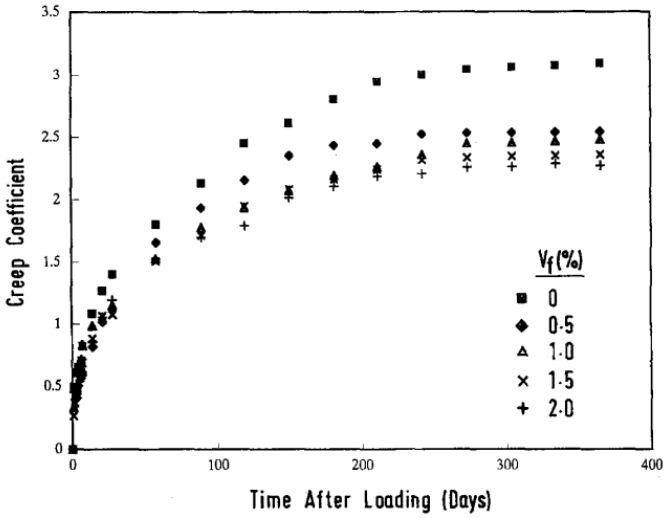

Figure 3-8 Creep coefficients of SFRC (Tan et al., 1994a)

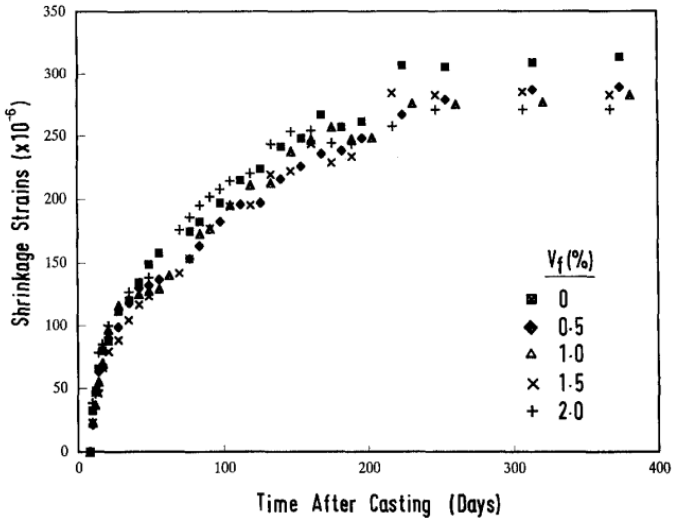

Figure 3-9 Shrinkage strains of SFRC (Tan et al., 1994a)

Experimental constants were proposed by the authors for use in the ACI 209R models of creep and shrinkage of normal concrete to include the effects of steel fibres. The constants presented in Table 3-1 are for use in the following equations:

$$\varphi_f(t,t_0) = \frac{(t-t_0)^c\, b}{a+(t-t_0)^c} \qquad \textbf{(3-15)}$$

$$\varepsilon_{shf}(t,t_0) = \frac{t}{\alpha` + t}\varepsilon_{sh,u} \qquad \textbf{(3-16)}$$

Table 3-1 Proposed constants for creep and shrinkage strains of SFRC (Tan et al., 1994a)

V_f %	Creep coefficient			Shrinkage strain	
	a	***b***	***c***	α`	$\varepsilon_{sh,u}$ $x10^{-6}$
0	16.67	5.65	0.526	56.95	354.02
0.5	16.64	3.55	0.663	61.29	331.06
1.0	14.07	5.06	0.452	48.06	288.25
1.5	13.60	3.56	0.576	67.06	337.42
2.0	12.58	3.31	0.582	34.80	297.52

Other test results reported by Chern and Young (1990) indicate that the shrinkage of steel fibre reinforced concrete is lower than that of conventional plain concrete as shown in Figure 3-10. These authors concluded that the reduced shrinkage observed in older specimens could be attributed to an effective increase in interfacial bond strength between the fibres and the matrix with time. The authors also stated that a volume fraction of steel fibres in excess of 2% may cause poor workability, impair the strength of the resulting concrete and decrease the effectiveness of the fibres for reducing shrinkage. In addition, their results showed that samples with fibres with higher aspect ratios had less shrinkage. Similarly, Swamy and Stavrides (1979) reported that the drying shrinkage of normal and lightweight aggregate concrete was reduced by about 15-20% due to the addition of 1.0% steel fibres.

Although experimental results for the strength properties of concrete have shown that steel fibres enhance the tensile and flexural response of concrete more than the compressive response, the studies reported here have focused on the effect of steel fibres on compressive creep as opposed to tensile creep. To date, little attention has been given to the tensile creep behaviour of SFRC and as a result, there is a lack of understanding regarding the long-term structural behaviour of SFRC members.

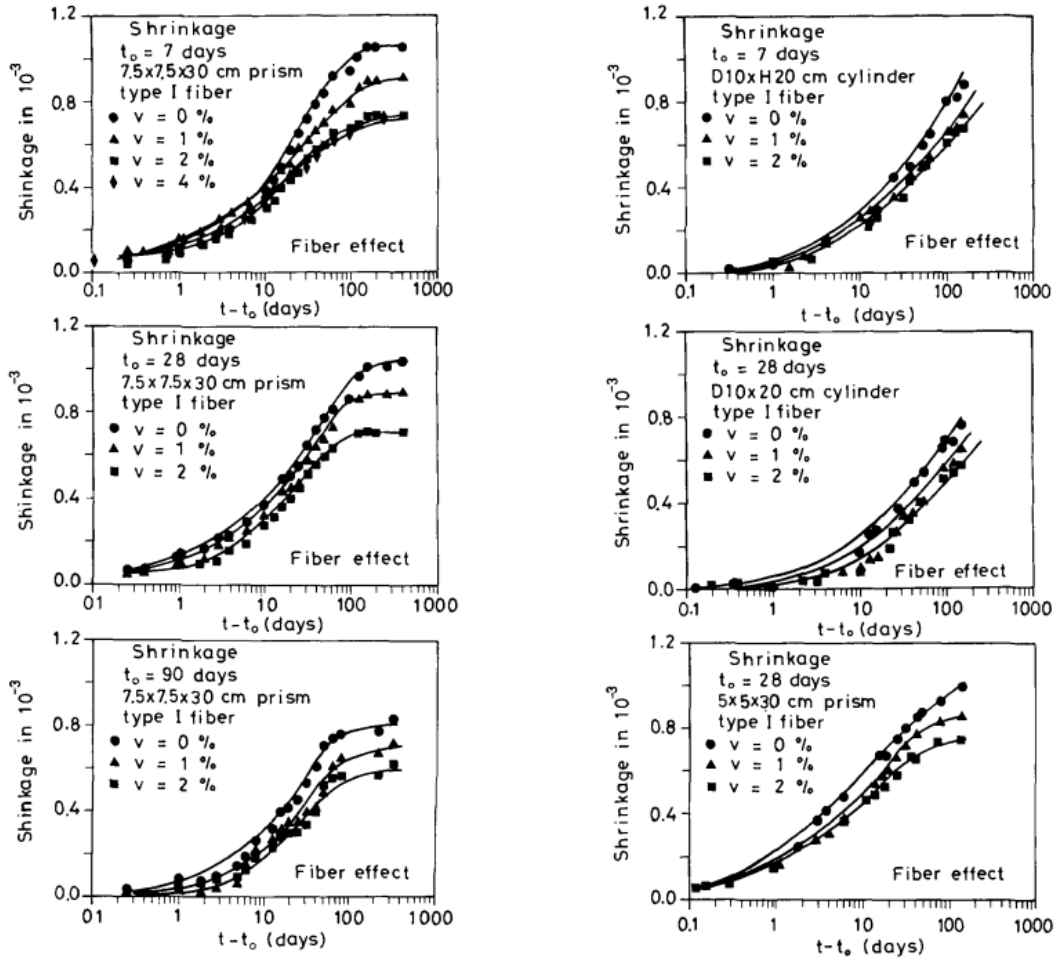

Figure 3-10 Effect of steel fibres volume fraction on shrinkage of concrete (Chern and Young, 1990)

3.3 Long-term Flexural Behaviour of Beams

Several investigations have been carried out to identify the factors which affect the long-term flexural performance of concrete structures. In this section, the effect of incorporating recycled aggregate and steel fibres on the long-term flexural behaviour of reinforced concrete beams will be presented and discussed.

3.3.1 Effect of recycled aggregate

In comparison to NC beams, there has been little attention given to the time-dependent behaviour of RAC beams under sustained loads. Knaack and Kurama (2015b) have compared the time-dependent sustained service-load behaviour of beams with normal and recycled aggregate. The variables in their study included the aggregate replacement ratio, amount of reinforcement, concrete age at loading

and level of loading for un-cracked and cracked beams. Their findings revealed that an increase in the RA replacement ratio resulted in increased immediate and long-term deflections as shown in Figure 3-11.

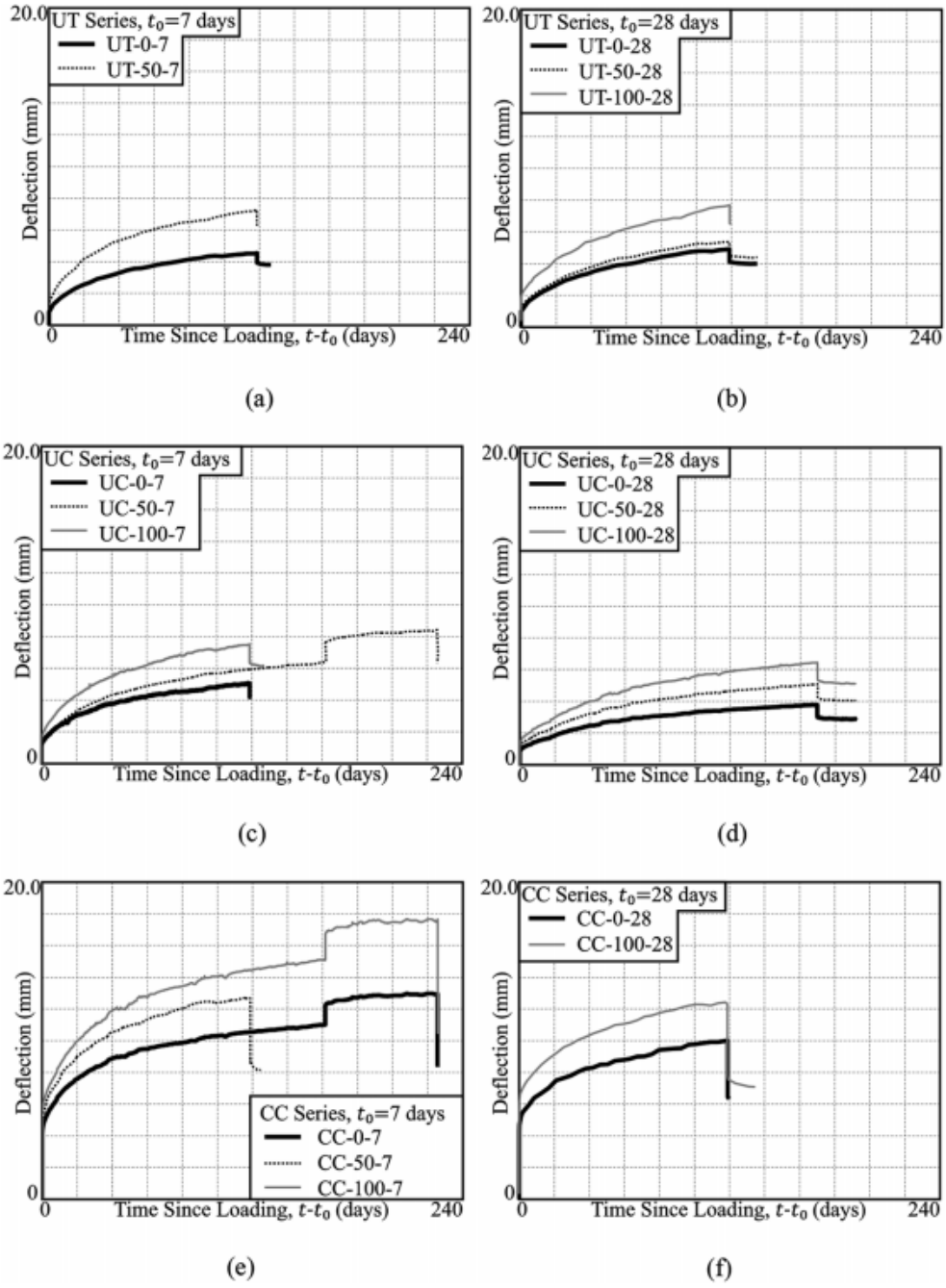

Figure 3-11 Long-term deflection of beams with different ages and levels of loading (Knaack and Kurama, 2015b)

They observed an increase in the number of cracks in the RAC specimens which they attributed to the lower modulus of rupture of RAC. Furthermore, it was

concluded that similar to conventional concrete beams, the long-term deflection of RAC beams was influenced by the age of the concrete at loading, the amount of compression reinforcement and the level of cracking. More specifically, beams loaded at an age of 7 days had larger long-term deflections than those loaded at 28 days. They also found that beams with greater compression reinforcement tended to have lower long-term deflections. Regarding the level of cracking, the RAC beams that were designed as un-cracked deflected more those that were designed as cracked.

The authors observed that ACI-318 and Eurocode 2 gave reasonable predictions for the immediate deflections of NC beams, however the predictions were less accurate for cracked RAC beams; specifically, ACI-318 underestimated the deflections of cracked RAC beams, whilst Eurocode 2 overestimated them. In addition, both ACI-318 and Eurocode 2 significantly underestimated the long-term deflections of un-cracked RAC beams. Close examination of their work suggests that they may have miscalculated the short-term deflections of the RAC beams and this error was carried forward into the calculations for the long-term deflections. As a result, it is difficult to make any assessment of the accuracy of the code prediction methods at this stage. Knaack and Kurama (2015b) made no attempt to explain the inaccuracies of the code predictions or to propose any empirically-based modifications to the models to help improve accuracy.

Another experimental study was performed by Choi and Yun (2013) in order to investigate the long-term deflection and flexural behaviour of reinforced concrete beams with recycled aggregate. In their study, three reinforced beams were prepared: one with 100% natural aggregate, one with 100% recycled coarse aggregate and one with 50% recycled fine aggregate. The beams were subjected to a sustained load equivalent to 50% of the nominal flexural capacity of the control specimens for 380 days. The authors found that the immediate and total long-term deflections of the beam prepared with 100% recycled coarse aggregate were the smallest. In addition, the ratios between the long-term and immediate deflections of the RAC beams were smaller than the equivalent ratios for the NC beam.

The experimental results were compared to predictions from the ACI-318 method and a modified formula was proposed to predict the long-term deflection of

reinforced beams prepared with recycled aggregate. The modification was based on including a reduction factor α (equal to 0.92 and 0.86 for recycled coarse and fine aggregate concrete respectively) for the modulus of rupture which can be used for calculating both short-term and long-term deflections.

Their comparison between experimental results and calculated predictions showed good agreement. However, regardless of the agreement obtained, this modification only takes into account the effect of RA on the properties of the concrete. This type of modification is certainly an agreed way forward for calculating crack spacing in a flexural element, and the cracking theory proposed by Beeby (1990) clearly illustrates the relationship between tensile strength and crack spacing. It could be argued that this approach is valid for crack width calculations and thus for modifying the ACI method for calculating deflections. However, when predicting deflections, a more appropriate property to consider may be tension stiffening, as this not only represents the material properties but also the interaction between the concrete and steel elements.

Łapko and Grygo (2010) tested two series of beams with natural and recycled aggregate under short- and long-term loading. The results of the short-term tests showed that RAC beams have a 7% lower flexural capacity and 42% greater deflection than NC beams, and the long-term test results showed that RAC beams have a 20% greater deflection and 46% greater strains in the compression zone than NC beams as shown in Figure 3-12.

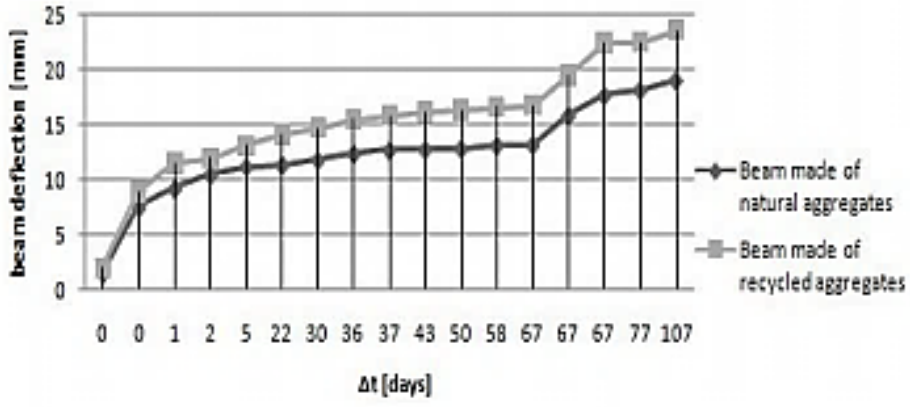

Figure 3-12 Long-term deflections of NC and RAC beams (Łapko and Grygo, 2010)

3.3.2 Effect of steel fibres

Although steel fibres have been recognised as suitable for use in structural materials and the behaviours of SFRC members in bending and shear are well understood, there is limited information available about the long-term behaviour of cracked SFRC structural members under sustained loads.

Tan et al. (1994b) reported the results from their study of the instantaneous and long-term deflections of steel fibre reinforced concrete beams. Fourteen SFRC beams 100x125x2000mm in size with different fibre contents (0%, 0.5%, 1.0%, 1.5% and 2.0%) were tested. Nine were subjected to sustained loads of 0.35%, 0.5%, 0.65% and 0.8% of their design ultimate load of flexure. The results indicated that the inclusion of 2% steel fibres could reduce long-term deflections by 20% as shown in Figure 3-13. Furthermore, the effect of steel fibres was noted to be more effective for reducing long-term deflections with sustained loads greater than 50% of the design ultimate load of flexure.

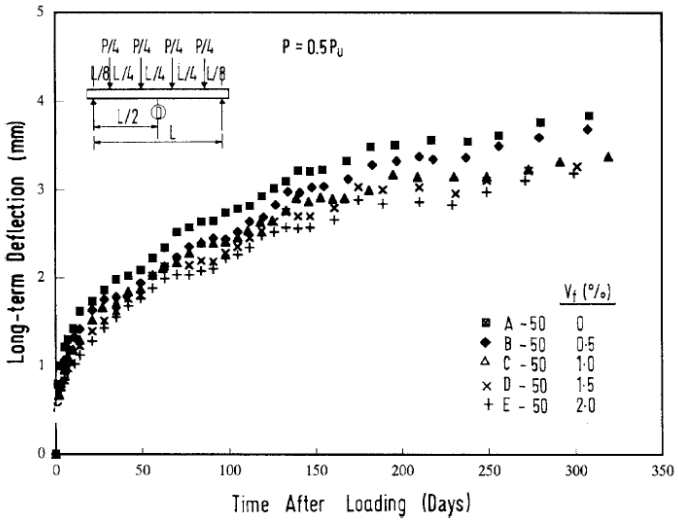

Figure 3-13 Long-term deflection of SFRC beams (Tan et al., 1994b)

Based on the ACI-318 method, an empirical expression was developed for predicting the long-term deflections of SFRC beams as follows:

$$\Delta_l = \left(1 - c\mu \frac{l_f}{d_f} V_f\right) \lambda \, \Delta_i \qquad \textbf{(3-17)}$$

$$\lambda = \frac{\xi}{1 + 50\rho`} \qquad \textbf{(3-18)}$$

Where:

c = a constant determined from linear regression analysis of test data = 0.96

μ = coefficient of friction between the fibres and the concrete = 0.04 for plain fibres and 0.12 for deformed fibres

Tan and Saha (2005) presented the results from a ten year study on steel fibre reinforced concrete beams under sustained loads. In this study, nine reinforced concrete beams of the dimensions 100x125x2000mm with steel fibre contents between 0% and 2% were subjected to sustained loads of between 0.35% and 0.8% of the ultimate flexural capacity for a period of 10 years. The results showed 34% and 58% reductions in long-term deflections and maximum crack widths respectively due to the addition of 2% steel fibres. Furthermore, empirical expressions were developed for predicting long-term deflections and maximum crack widths for SFRC as follows:

Long-term deflection:

$$\Delta_l = \alpha\lambda\,\Delta_i \quad \textbf{(3-19)}$$

$$\lambda = \frac{\xi}{1 + 50\rho`} \quad \textbf{(3-20)}$$

$$\alpha = \begin{cases} 1 - 0.69V_f & (for\ V_f \leq 1.5\%) \\ 0.897 & (for\ V_f > 1.5\%) \end{cases} \quad \textbf{(3-21)}$$

Long-term maximum crack width:

$$w_{if} = \left(1 - 0.22V_f\right)w_i \quad \textbf{(3-22)}$$

$$w_{lf} = \left(0.19 + 0.1V_f\right)w_{if} \quad \textbf{(3-23)}$$

Where:

w_{if} = initial crack width of SFRC.

w_i= initial crack width of NC.

w_{lf}= long-term crack width of SFRC.

Ashour et al. (1997) also studied the effects of steel fibres and compression reinforcement on the long-term deflection of high strength concrete beams. They stated that the inclusion of steel fibres could reduce total long-term deflections of

reinforced concrete beams as shown in Figure 3-14. They proposed modification of the multiplier factor λ in the ACI-318 method to include the effect of steel fibres on the strength of concrete:

$$\Delta_l = \lambda\, \Delta_i \qquad \textbf{(3-24)}$$

$$\lambda = \frac{\mu_m \alpha_m \xi}{1 + 50 \mu_s \alpha_s \rho`} \qquad \textbf{(3-25)}$$

Where:

$$\mu_m = 1.29 - 0.0000755 f_c`(psi) \qquad \textbf{(3-26)}$$

$$\mu_s = 1.48 - 0.000107 f_c`(psi) \qquad \textbf{(3-27)}$$

$$\alpha_m = 1 - 40 V_f + 4000 V_f^2 \qquad \textbf{(3-28)}$$

$$\alpha_s = 1 - 40 V_f \qquad \textbf{(3-29)}$$

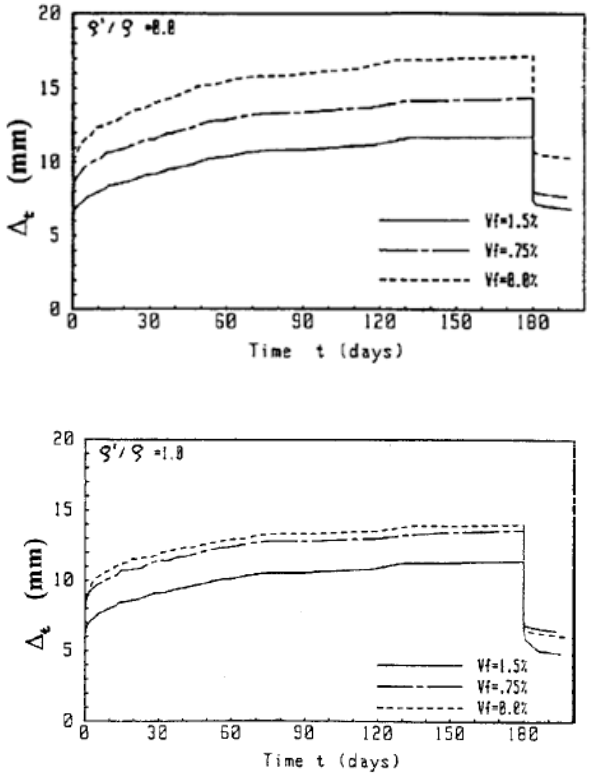

Figure 3-14 Effect of steel fibres on the total long-term deflection of beams with various reinforcement ratios (Ashour et al., 1997)

All of the theoretical modifications proposed in the literature have been based on the ACI-318 method. However, this simple method for calculating long-term deflections does not separate the effects of all the parameters that influence long-

term deflections. Instead, there is one factor ζ which takes into account the combined effect of all of the parameters including the compression reinforcement ratio. This does not improve the fundamental understanding of the effect of steel fibres on the long-term flexural behaviour of concrete structures even if there is good agreement between predictions and experimental results. This will be discussed in details in Chapter 6.

Zerbino and Barragán (2012) published a paper about the long-term behaviour of cracked steel fibre reinforced concrete beams under sustained loading. The beams tested were 150x150x600mm in size, and were made of 45MPa compressive strength concrete with 0.5% by volume hooked-end steel fibres of length 50mm and diameter 1mm. The beams were subjected to a range of loads for approximately 21 months and stable crack opening rates were observed throughout the duration of the tests.

Vasanelli et al. (2013) published a paper on the long-term behaviour of FRC flexural beams with a mixure of steel and polyester fibres. The experimental programme included the measurement of crack widths and flexural displacements under sustained loads as well as chemical analysis. Their results showed that flexural displacements, crack widths and carbonation depths were reduced by the addition of fibres.

3.4 Tension Stiffening

3.4.1 Definition

When calculating the flexural behaviour of reinforced concrete structures, it is assumed that concrete only carries compressive loads and tensile loads are carried purely by the steel reinforcement. However, concrete does have the capacity to carry tensile loads. Even though the tensile strength of concrete is about one tenth of its compressive strength, it still makes a considerable contribution to the flexural behaviour of beams (Scott and Beeby, 2012).

When the load applied to the concrete in a structural member exceeds its tensile strength, the concrete starts cracking and as the load increases, the number of cracks increases. Immediately after cracking occurs, the concrete in the vicinity of the crack cannot carry any tensile load. However, the cracks appear at discrete

positions and the concrete which is away from the cracks can continue to carry some tensile load (Scott and Beeby, 2012). This results in a decrease in the load that the reinforcement bars have to carry which reduces the deformation of the steel bars, and hence the total deformation of the reinforced concrete member. The reduction in deformation means that the member is stiffer than would be expected based on the assumption that concrete does not carry tensile loads. The additional stiffness resulting from the concrete carrying tensile loads after initial cracking occurs is referred to as “tension stiffening” (Scott and Beeby, 2012).

To explain tension stiffening in more detail, Figure 3-15 illustrates the relationship between the applied moment and the curvature of a reinforced concrete member under uniform bending loads (Gilbert, 2012). At applied moments less than the cracking moment (M_{cr}), the element is un-cracked and the relationship is linear with a slope related to the second moment of area of the un-cracked section (I_u). When the applied moment reaches the cracking moment, initial cracks start forming and there is a sudden change in the relationship with a reduction in the stiffness of the concrete member. As the applied moment increases further, the flexural stiffness of the member decreases significantly and the slope of the curve is more directly related to the second moment of area of the cracked transformed section (I_{cr}).

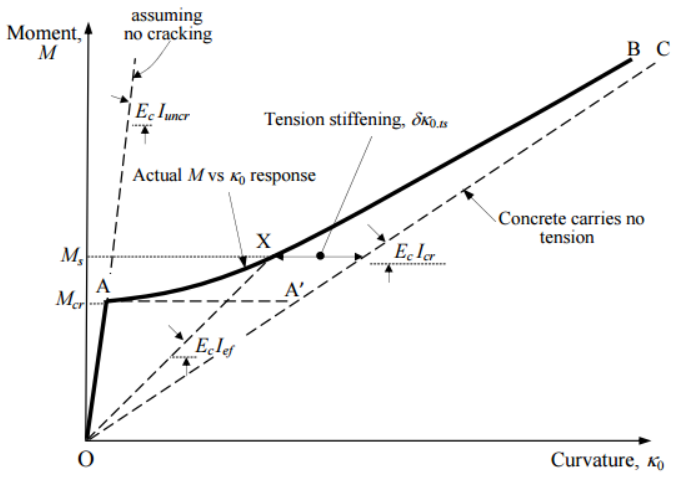

Figure 3-15 Moment-curvature relationship for a reinforced concrete member in bending (Gilbert, 2012)

The actual flexural rigidity of the section (EI) falls in the region between that of the un-cracked section ($E_c I_u$) and a fully-cracked section ($E_c I_{cr}$) which is due to the contribution of the concrete to carrying the tensile loads after cracking. The difference between the actual response and the response predicted based on the assumption of no tensile capacity of the concrete is what is called tension stiffening.

A typical load-strain curve for reinforced concrete members under pure tension is shown in Figure 3-16. The tensile response of reinforced concrete members can be divided into three phases (Gribniak et al., 2009). The first phase is the un-cracked phase and covers the period from the onset of loading to the formation of the first crack. At this stage, the section is considered to be homogenous and exhibits an elastic behaviour with a linear relationship between load and strain.

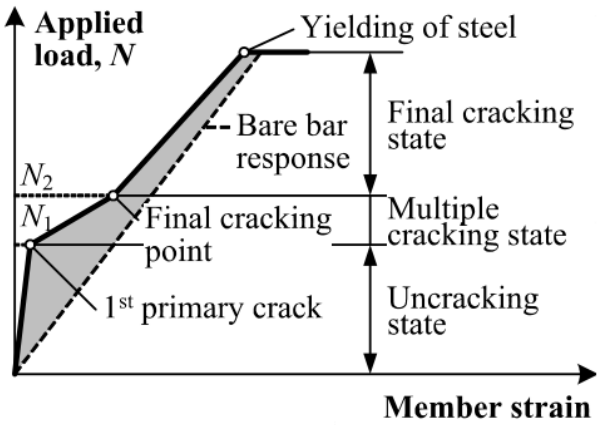

Figure 3-16 Stages of cracking of reinforced concrete members in tension (Gribniak et al., 2009)

The second phase is called the cracked phase and covers the period from the first crack appearing until all of the cracks have appeared. During this phase, the stress in the concrete decreases due to the presence of the cracks. At the location of the cracks, the stress is zero but due to the bond between the concrete and the reinforcement, the stress in the concrete increases as the distance from the crack increases. The distance between cracks (l) is called the “Transfer Length” and the distance from the point of cracking to the point where the crack does not influence the stress in the concrete is (S). At the location of the crack, the stress in the

concrete is zero and it reaches its maximum value at a distance S from the crack as shown in Figure 3-17 (Gribniak et al., 2009).

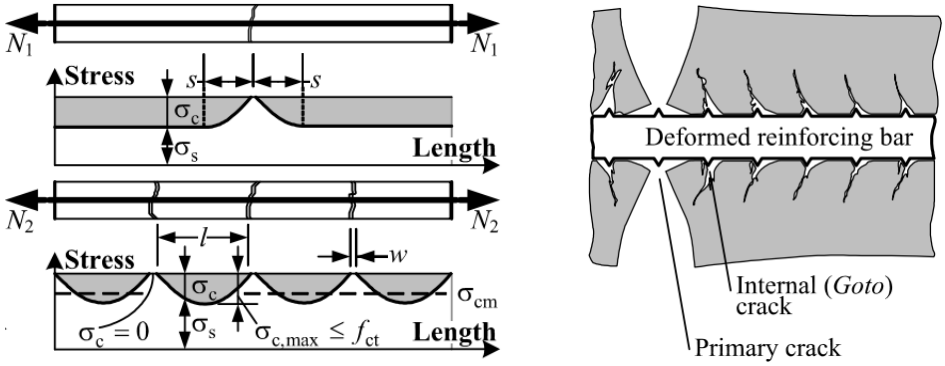

Figure 3-17 Axial stress distribution and crack formation for reinforced concrete members in tension (Gribniak et al., 2009)

Slip at the interface between the steel bar and the concrete leads to crack opening. As loads increase, more cracks are formed at regular intervals (l) along the length of the member where $S < l < 2S$. The stabilised cracking stage is reached when no more cracks can be formed and any increase in load only causes an increase in crack widths. As the number of cracks increases, the stiffness of the concrete reduces slightly and thus the contribution of the concrete to carrying the tensile loads decreases.

However, the intact concrete sections in between the cracks can still carry some tension although this is less than the tensile strength of the concrete. Therefore, although the cracking of the concrete causes a reduction in the concrete`s tensile stress, the stress is in fact non-zero. The third phase covers the period from the point of final cracking to the yielding of the reinforcement bar.

3.4.2 Re-evaluation of experiments

There has been extensive experimental investigation of the tension stiffening of reinforced concrete members under flexural loading. The majority of this experimental work has focused on short-term rather than long-term behaviour which does not reflect the loading of reinforced concrete members in practice (Scott and Beeby, 2005). Moreover, most of the previous work has been based on the flexural behaviour of reinforced concrete members in order to assess actual

behaviour which is significantly different from the behaviour of concrete under pure axial tension. The relationship between the tensile and flexural response cannot be fully understood because the flexural response of members is influenced by other factors. The relationship becomes even more complicated when considering long-term response due to the effects of creep and shrinkage.

The method of testing square prisms of concrete reinforced with one central steel bar under uni-axial tension loads shows great improvement over other methods for assessing the tension stiffening of concrete. This is due to the fact that the average stress generated in the steel bar and on the surface of the concrete can be measured directly and the use of a load cell can provide accurate data for the tensile loads applied. In addition, the portion of the concrete that causes the observed tension stiffening can be clearly identified. The presence of a single bar offers another advantage in that there is no interaction between adjacent bars and there is no ambiguity in the results for the load carried by the concrete (Scott and Beeby, 2005).

Whittle and Jones (2004) conducted an experimental study and assumed that the results of pure tension tests are applicable to the understanding of flexural response. More specifically, they assumed the concrete in the area surrounding the reinforcing bars in a tension test are equivalent to sections in the concrete of a flexural member as shown in Figure 3-18. In their study, slabs were designed and cast such that the area of the concrete surrounding each of the bars was identical to that in the tension specimens.

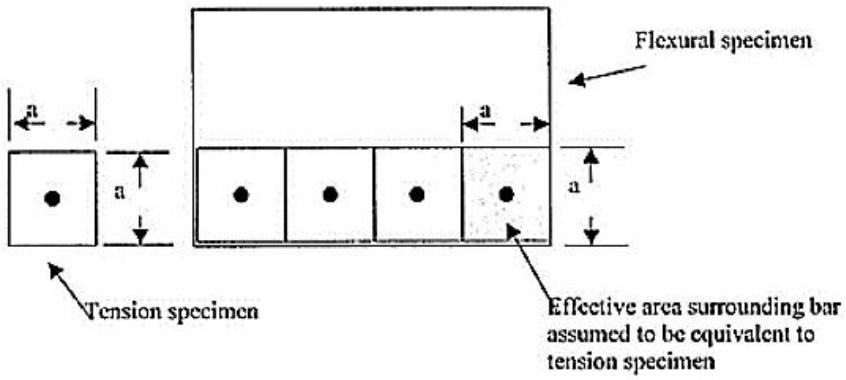

Figure 3-18 Equivalence between tension and flexural members (Whittle and Jones, 2004)

The slabs were subjected to point loading such that the stress generated in the reinforcing bars at the crack locations was similar to that in the tension tests. It was expected that the behaviour of the concrete in the tensile region of the slabs and the concrete in the tension specimens would be similar. Scott and Beeby (2005) used the same assumption in their work and stated that accurate assessment of the tension stiffening of concrete could be helpful for understanding its flexural behaviour.

3.4.3 Factors affecting tension stiffening

Tension stiffening is related to the stiffness of concrete as it arises from the interaction between the reinforcement and the concrete and it enhances structural performance. Internal phenomena such as slip between the concrete and the reinforcing bars and the development of primary cracks around the reinforcement cause a reduction in tension stiffening. It is thus the properties of the concrete and reinforcement that are the main factors which affect tension stiffening.

The majority of the research in the literature regarding the factors that influence the tension stiffening of reinforced concrete members has been based on flexural tests and few investigations have examined the performance of members subjected to pure axial tension. In this section, a review of the data available regarding the factors affecting tension stiffening under pure axial loads is presented.

3.4.3.1 Influence of concrete strength

As mentioned earlier, the properties of the concrete employed are the main factors that influence tension stiffening. Some of the studies in the literature have examined this in detail. Khalfallah and Guerdouh (2014) presented an experimental and analytical investigation of the effect of various parameters on the tension stiffening of reinforced concrete members. One of these parameters was the concrete strength, and samples with concrete of strength classes C21 and C40 were tested. It was observed that the higher compressive strength specimens had less of a reduction in tension stiffening under axial tensile loading as presented in Figure 3-19.

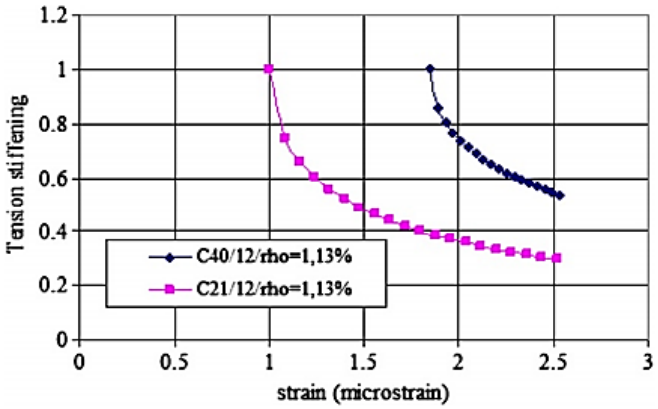

Figure 3-19 Effect of concrete strength on the reduction in tension stiffening under axial tensile loading (Khalfallah and Guerdouh, 2014)

Lee and Kim (2009) also carried out an experimental study of 35 specimens subjected to direct tension and prepared with 25, 60 and 80MPa strength concrete. They found that during the stabilised cracking stage, the high strength concrete had a much smaller reduction in tension stiffening compared to the normal strength concrete. In contrast, Fields and Bischoff (2004) tested large-scale specimens prepared with 40 and 80MPa concrete under pure axial tension and their results showed a greater reduction in tension stiffening for the high strength concrete specimens. The authors suggested that this was due to other factors such as shrinkage.

3.4.3.2 Influence of concrete modulus of elasticity

As tension stiffening is related to the stiffness of the concrete, the modulus of elasticity of the concrete is another factor which has been investigated. As part of their study, Khalfallah and Guerdouh (2014) also examined the effect of the concrete modulus of elasticity on tension stiffening for different ratios of reinforcement. As can be seen in Figure 3-20, the effect is negligible when the reinforcement ratio is small. However, with more reinforcement, the modulus of elasticity of the concrete has a greater effect. More specifically, with higher reinforcement ratios, an increase in the concrete modulus of elasticity led to less reduction in the tension stiffening during loading.

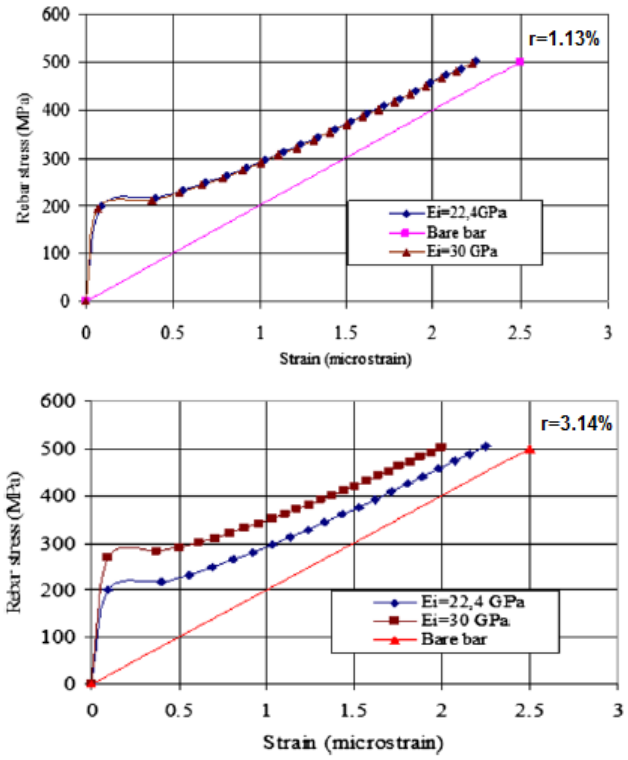

Figure 3-20 Effect of the modulus of elasticity of concrete on tension stiffening for different reinforcement ratios (Khalfallah and Guerdouh, 2014)

3.4.3.3 Influence of shrinkage

As the reduction in tension stiffening of concrete is related to deformation, the effect of shrinkage has also been studied. Wu and Gilbert (2008) presented an experimental study which aimed to investigate the tension stiffening in reinforced concrete members under short-term and long-term loads. They concluded that the amount of shrinkage is inversely related to the load-deformation relationship prior to and during the application of load. Prior to loading, shrinkage is restrained by the reinforcement which generates tensile stresses in the concrete and reduces the amount of external load needed to crack the concrete. Under long-term loading in the concrete away from the cracks, shrinkage can also cause a reduction in the tension stiffening as a function of time. Bischoff (2001) also studied the influence of shrinkage on the tension stiffening of concrete and found that shrinkage significantly affected the tension stiffening. Therefore, shrinkage is addressed to be a significant factor which affects the behaviour of tension and flexural concrete members in service.

3.4.3.4 Influence of reinforcement ratio

As mentioned earlier, the tension stiffening of concrete members can be influenced by the interfacial bonding and slip between the reinforcing bars and the surrounding concrete. The reinforcement ratio has thus been studied as a factor which can affect the degree of tension stiffening. Khalfallah and Guerdouh (2014) tested specimens with reinforcement ratios of 1.13% and 3.14% and found that the reduction in tension stiffening is greater for the samples with less reinforcement. The same conclusion was drawn by Bischoff (2001) who tested specimens with reinforcement ratios of 1-2%.

3.4.4 Long-term loss of tension stiffening

Although some of the existing code procedures consider loss of tension stiffening in calculations for long-term concrete response, this consideration is limited and is based on current knowledge which does not include the effect of time. Investigation of this issue only began in 2005 when Scott and Beeby initiated an extensive experimental program to study the rate of reduction of tension stiffening with time. Their study aimed to provide a suitable modification to the current design codes to take into account this rate and to introduce alternative limits for acceptable deflections.

Their experimental program was conducted at Durham University and the University of Leeds. At Durham, tension specimens were cast and tested in pairs using two test rigs. All the specimens were the same size and had a cross section of 120x120mm and a length of 1200mm. The specimens were reinforced centrally by a single bar with a diameter of either 12, 16 or 20mm, and each bar had 85 internal strain gauges distributed along the full length. This arrangement was chosen to avoid affecting the bonding between the concrete and the steel bar and to provide accurate data for the distribution of strain along the length of the bar. Another two strain gauges were placed outside the concrete at each end of the bar in order to measure the value of the applied load accurately. The surface strains of the concrete were measured using hand-held mechanical strain gauges and Demec points that were placed on two opposite sides of the concrete every 200mm along the length.

Three different concrete mixes with compressive strengths of 30, 70 and 100MPa were used. A total of 14 specimens were prepared with different concrete compressive strengths and reinforcing bar sizes. They were tested in pairs using two rigs: B and R. One specimen of each pair was tested in Rig B under a constant load of 72KN for a period of 3-4 months, while the second was tested in Rig R under three levels of load: 43, 58 and 72KN, where each load was applied for a period of one month. Some of the specimens were unloaded at the end of the test to assess whether there was any tension stiffening recovery.

At Leeds, three sets of three rigs were built to allow up to nine specimens to be tested at the same time. Identical specimens were prepared using the same materials, mixture proportions and reinforcing bar sizes. To link the rate of tension stiffening reduction and the long-term flexural behaviour, the slab specimens were constructed and tested based on the assumption that the concrete areas in the slabs were equivalent.

The difference between the Durham and Leeds test methods was the approach to measuring the strain distribution in the reinforcing bars. A limited number of specimens were tested at Durham due to the expense of the internal gauged reinforcing bars. However, the amalgamation of the results from the tests performed at the two sites provided a significant quantity and range of quantitative data.

The results obtained by averaging the strain gauge readings gave a good representation of each specimen’s overall behaviour. The readings from the hand-held mechanical strain gauges were averaged for every loading stage. Figure 3-21 shows the strain distributions versus time for two specimens with different applied loads and Figure 3-22 shows the distribution of strains along the length of the reinforcing bar. All of the data in Figures 3-21 and 3-22 are from tests performed at Durham. The detailed data shows a clear variation in the strain measured at the positions of the cracks and in between the cracks.

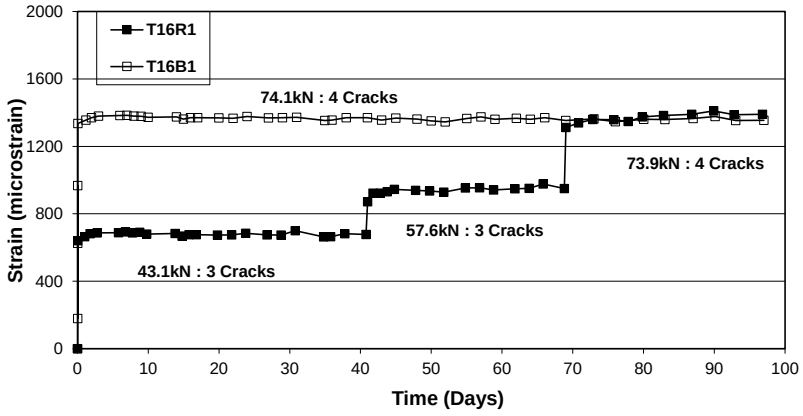

Figure 3-21 Reinforcement strains versus time (Scott and Beeby, 2005)

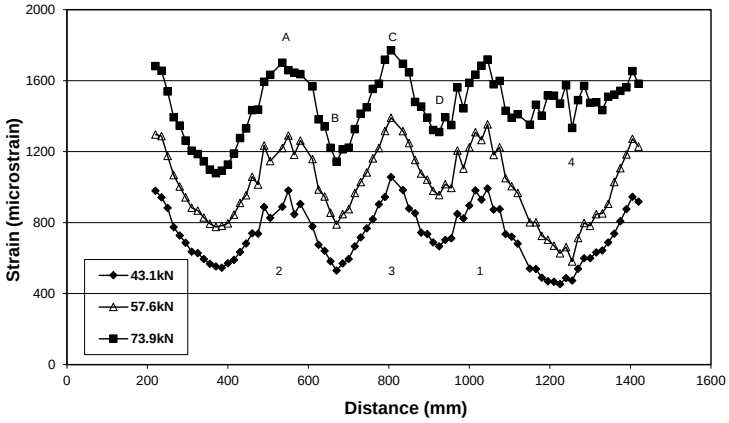

Figure 3-22 Reinforcement strains along the length of the bar (Scott and Beeby, 2005)

The strain data obtained from the tension tests were used to calculate the concrete tensile stresses using three different methods. The difference between the three methods was related to how the measured strain values were used to calculate the average strain (ε_s) and thus the force in the steel bar (F_s). Once the force in the steel bar was known, the concrete tensile stresses were calculated for all three methods by employing the following equation:

$$\sigma_c = (F - F_s)/A_c \qquad \textbf{(3-30)}$$

Where:

σ_c = concrete tensile stress

F = applied force

F_s = force in steel bar

A_c = cross-sectional area of concrete (area of steel bar is deducted)

As stated above, the difference between the three methods was in the way the strain in the steel bar (ε_s) was determined from the experimental results. All three methods were used for analysing the data obtained from the tests at Durham, while only Method 1 was used for the data from Leeds.

Method 1:

This method is based on the assumption of strain compatibility between the steel bar and the surrounding concrete. Therefore, the average of the concrete surface strains (ε_c) obtained from the hand-held mechanical strain gauge readings plus the shrinkage strains of the concrete were assumed to be equal to the average strain in the steel bar, i.e.:

$$\varepsilon_s = \varepsilon_c \qquad \textbf{(3-31)}$$

The stress in the steel bar (σ_s) was then determined from the strain in the steel bar (ε_s) using the modulus of elasticity of steel, which is a constant, as follows:

$$\sigma_s = E_s \times \varepsilon_s \qquad \textbf{(3-32)}$$

The force in the steel bar (F_s) was then calculated by multiplying the stress in the bar by the area of the bar:

$$F_s = \sigma_s \times A_s \qquad \textbf{(3-33)}$$

The force in the steel bar (F_s) was subtracted from the applied load (F) to obtain the total force carried by the concrete in tension. This value was then divided by the cross-sectional area of the concrete (A_c) to compute the average tensile stress in the concrete. The area of the concrete was obtained by subtracting the area of the steel bar from the gross area of the specimen section.

Method 2:

For this method, the reinforcement strain gauge readings were used to calculate the bar stresses and forces at the location of each of the strain gauges. The concrete stress was also calculated at each position and these values were averaged over the full length of the specimen to obtain the average concrete tensile stress. The same equations in method 1 were then followed and no additional assumptions were required.

Method 3:

This method is similar to method 2 in that it directly uses the steel strains to calculate the concrete stresses by employing the same equations. The difference between the two methods is that the average concrete tensile stress in this method is computed for each section of concrete between pairs of adjacent cracks not over the full length of the specimen. Therefore in this case, when the strain gauges are very close to cracks, no calculations can be made.

The results from Scott and Beeby's (2005) long-term rate of tension stiffening reduction tests were plotted as concrete stress as a function of time as shown in Figure 3-23. It can be observed that the tension stiffening initially reduced rapidly and became stable after approximately 2 weeks of loading and that the rate of reduction was quite dramatic during the first day of loading.

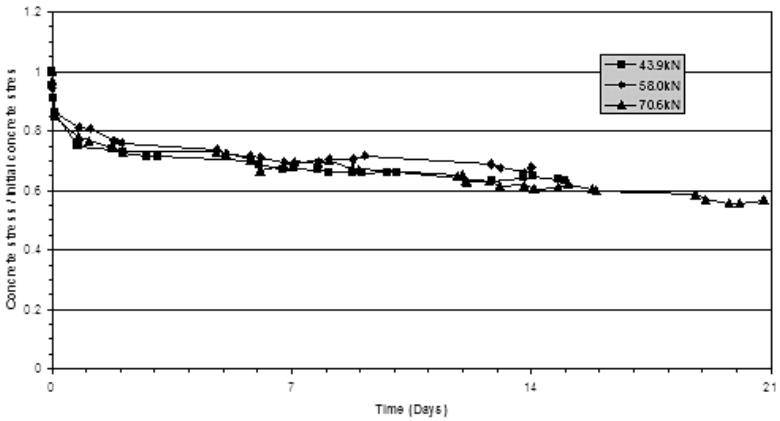

Figure 3-23 Decay of concrete tensile stress (Scott and Beeby, 2005)

The results from the three methods for calculating the average concrete tensile stress are summarised in Table 3-2 where it can be seen there are some differences in the results. Method 1 which uses the hand-held mechanical strain gauge results gave the highest value of concrete stress and Method 3 which uses the average value for each section of the concrete between cracks gave the lowest. The reasons for this discrepancy are not clear as noted by Scott and Beeby (2005). However, the ratios between the long-term and short-term stresses were more similar. In addition, the overall average of the short-term and long-term stresses are

approximately 1.0 and 0.6MPa which are in good agreement with the values of 1.0 and 0.55MPa given in Part 2 of BS8110.

From the calculation methods above, the authors suggested that Method 1 was the most appropriate for examining global specimen behaviour because it is relatively inexpensive. They also stated that Method 3 may be more applicable when there is a well-established distribution of cracks.

Table 3-2 Results of concrete tensile stresses (Scott and Beeby, 2005)

Method of calculation	Short-term stress (MPa)	Long-term stress (MPa)	Ratio of long/short
Hand-held mechanical strain gauges (over 1000mm)	1.22	0.84	0.69
Strain gauges (over 1000mm)	0.93	0.55	0.60
Strain gauges (over crack spacing)	0.65	0.35	0.54

The results from both the Durham and Leeds tests indicated that the tensile stress in the concrete is roughly stable after a period of between 6h and 30 days. The exact time was variable and could not be attributed to any particular parameters, although the specimens with a higher reinforcement ratio tended to have shorter decay times. In comparison, the slabs tested in flexion had longer decay times than those tested in tension which was attributed to the level of stress applied.

In 2008, an experimental study was conducted by Wu and Gilbert (2008) to investigate the behaviour of reinforced concrete members in tension and the mechanism of tension stiffening. Six reinforced concrete prisms of dimensions 100x100x1100mm with a single reinforcing bar located at the centre were constructed and tested under axial tension. In order to monitor the strains in the reinforcing bar, 25 strain gauges were attached to the middle 600mm of the bar. Four specimens were loaded with a monotonic axial tensile load up to failure immediately after curing before any drying shrinkage could occur. The final two specimens were tested under sustained axial tension loads for a period of 2

months. Strain gauges were placed along the length of the reinforcing bars to monitor the strain distribution. The strains measured were used to calculate the tensile stress carried by the reinforcing bar and hence the concrete tensile stress along the specimen. As a result of this study, a theoretical method was proposed for calculating the short-term and long-term concrete tensile stresses. The experimental results showed that under sustained loads, the average concrete tensile stress in the specimens dropped to 81.2% of its initial value in the first 50 days. Furthermore, it was concluded that shrinkage has a significant influence on the load-deformation behaviour and crack development of reinforced concrete members in tension which is in line with the results of the previously discussed studies.

3.4.5 Effect of recycled aggregate and steel fibres

As mentioned in the previous sections, tension stiffening is related to the stiffness of the concrete and the characteristics of the bond between the reinforcement and the concrete matrix. Therefore, it would be expected that the incorporation of recycled aggregate or steel fibres in concrete would have a significant effect on the behaviour of reinforced concrete members under tensile loads. This hypothesis is based on the well-known fact that the incorporation of recycled aggregate and steel fibres effects the strength properties of concrete (in particular the tensile strength), the bond and slip characteristics of the reinforcement-matrix interface and the time-dependent (creep and shrinkage) deformation of concrete.

To date, there have been no reports in the literature of investigations into the effect of recycled aggregate on the tension stiffening of concrete. Similarly, there has been little attention given to the effect of adding steel fibres on the short-term tension stiffening behaviour of concrete, let alone the long-term response. There is therefore a lack of data for long-term loss of tension stiffening which would enable a clear understanding of the long-term flexural performance of reinforced concrete members with recycled aggregate and steel fibres.

Regarding to the effect of steel fibres, de Oliveira Júnior et al. (2016) investigated the influence of the addition of steel fibres on tension stiffening. The tension stiffening coefficient was assessed from tensile test data for the full load-strain relationship. According to the test results, the addition of steel fibres reduces the

strain in the reinforcement and affects crack widths. This leads to an increase in the stiffness of the cracked concrete and hence increases the tension stiffening. The reason for this is the ability of steel fibres to carry tensile forces across cracks. Figure 3-24 shows the load-strain curves from a variety of steel fibre reinforced concrete members in tension. The authors also proposed an empirical model to predict the tension stiffening coefficient of steel fibre reinforced concrete based on reinforcement strains.

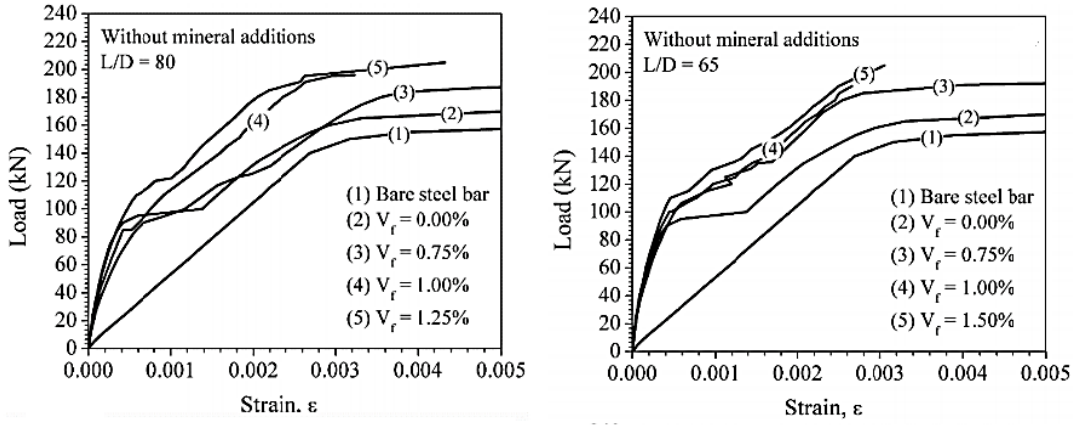

Figure 3-24 Effect of steel fibre content on the load-strain relationship of concrete specimens in tension (de Oliveira Júnior et al., 2016)

In another study, the tensile behaviour of steel fibre reinforced concrete members with conventional deformed reinforcing bars was investigated by Lee et al. (2013). The analytical investigation was based on the assumption that the total resistance to applied tensile loads can be separated into three parts: namely, that due to the reinforcement, the steel fibres, and the bond between the reinforcement and the concrete matrix. This was contrary to previous investigations in which the tension stiffening of the concrete was evaluated by removing only the load carried by the reinforcing bar from the total tensile load which means the contribution of the steel fibres was included in the part attributed to the interfacial bond. A simple constitutive model was derived as part of this study for the tension stiffening of steel fibre reinforced concrete members. A modifying factor to take into account the effect of the steel fibres was introduced, which was determined based on the variables considered in the parametric study. It was presented that the proposed tension stiffening model was able to estimate the experimental data for the tensile

behaviour of FRC members well. The proposed constitutive model can be easily implemented in a sectional or finite element model as it is based on the Smeared Crack Model.

Bischoff (2000), (2003) studied the post-cracking tensile behaviour of axially reinforced concrete members made with both plain and steel fibre reinforced concrete. The results of these studies provided information about the tensile stress carried by the cracked concrete in reinforced members when steel fibres are added. It was concluded that the addition of steel fibres could effectively enhance the tension stiffening and reduce the crack spacing. This was attributed to the combined contribution of the steel fibres at the crack locations and in between the cracks. Figure 3-25 shows the results for the tension stiffening of plain and steel fibre reinforced concrete for comparison.

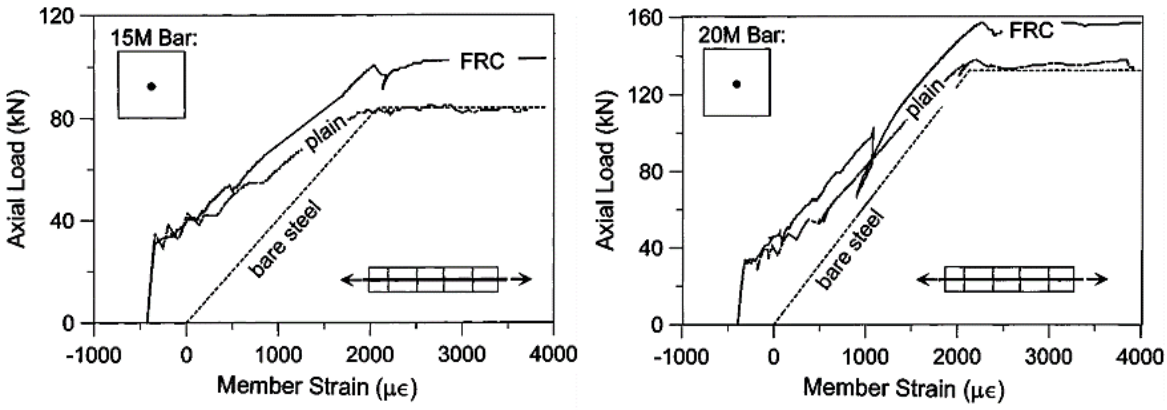

Figure 3-25 Load-strain curves of plain and steel fibre reinforced concrete (Bischoff, 2000)

Similar findings and conclusions were presented by Mitchell et al. (1996) based on the results of their tension testing of normal and high strength steel fibre reinforced concrete specimens. The results show the significant contribution of the steel fibres in enhancing the tension stiffening of the concrete after cracking of the concrete and yielding of the reinforcing bar.

3.5 Summary

In this chapter, a review of the literature regarding the long-term performance of concrete has been presented. The following summary can be drawn:

- In general, it can be concluded that with increasing the replacement percentage of RA, the creep and shrinkage deformations increase. All of the researchers agreed that the main reason for this increase is the presence of old adhered mortar in the RA.
- The review of the available literature showed that all studies of the creep and drying shrinkage deformations of concrete have investigated the effect of incorporating RCA, and to date the effect of adding CDW has not been examined.
- A number of empirical models have been proposed to predict the creep and shrinkage of recycled aggregate concrete which were developed from models for conventional concrete.
- The results showed that mineral admixtures can be used to control creep and shrinkage when RA is incorporated.
- The inclusion of steel fibres in concrete can significantly reduce shrinkage strains. In contrast, no noticeable effect of steel fibres on compressive creep response has been recorded.
- RAC beams have a much greater long-term deflection than NAC beams. As the replacement percentage of RA increases, the long-term deflection and the width of the cracks in the concrete also increase.
- The suitability of some code procedures has been examined and it was found that they give inaccurate long-term deflection predictions for RAC. Modifications have been proposed to develop the calculation steps in order to obtain more accurate results.
- The addition of steel fibres has a significant influence on the long-term deflection of beams and cracking development over time.
- A number of theoretical approaches have been proposed based on the ACI-318 procedure to estimate the long-term deflection of SFRAC beams. However, these approaches do not separate the effects of all the parameters influencing long-term deflection (e.g. creep, shrinkage and tension stiffening).
- The benefits of adding steel fibres to enhance the long-term performance of concrete have been well identified. However, there are few recent attempts

have been made to investigate the feasibility of combining RA with steel fibres as structural and sustainable material.

- Some of the existing code procedures consider loss of tension stiffening with time in calculations of long-term deflection. Nevertheless, this consideration is still limited and based on current knowledge of the amount and rate of reduction in tension stiffening for conventional normal concrete.

Although a better understanding of both the rate and amount of reduction in tension stiffening which occurs with normal concrete has been achieved, there is a lack of information about concrete which contains recycled aggregate and steel fibres. The absence of any data regarding the effect of recycled aggregate and steel fibres on the long-term tension stiffening response of concrete members means there is a lack of understanding about the long-term flexural behaviour of reinforced concrete members containing recycled aggregate and steel fibres. This gab of knowledge will be the main objective of this research.

Chapter 4 : Experimental Programme

4.1 Introduction

An experimental programme was carried out as the core part of this research. It was designed to investigate the effects of construction and demolition waste (CDW) as recycled aggregate and steel fibres on the long-term flexural behaviour of reinforced concrete beams under sustained loading. Three different recycled aggregate replacement percentages (RP%= 0%, 50% and 100%) and three steel fibre contents (V_f%= 0%, 0.5% and 1.0%) were considered as the main variables. A series of tests were performed on beam, cube, cylinder and prism specimens.

This chapter presents details of the experimental plan, material properties, concrete mixes, preparation of the specimens and test procedures.

4.2 Experimental Programme

The plan for the experimental programme is shown in Figure 4-1. The programme consisted of testing 9 full-scale beams (150x300x4200mm) with supplementary tests of cubes (100x100x100mm), cylinders (150x300mm), prisms (100x100x500mm) and bobbins (75x365mm) to determine the mechanical properties of the concrete for each mix. In addition, square prisms (120x120x1200mm) reinforced with a single central bar of ∅16mm were used to study the loss in tension stiffening over time with corresponding samples in the form of small prisms (75x75x200mm) and bobbins (75x365mm) for shrinkage and creep tests.

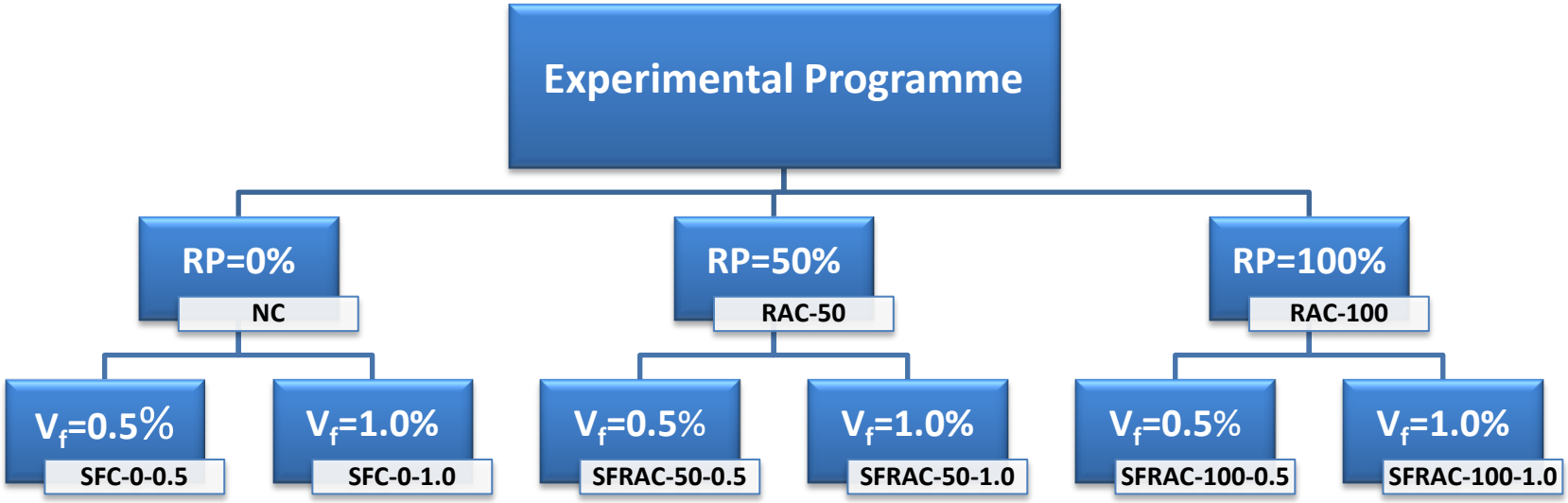

Figure 4-1 Plan of the experimental programme

RP% = Replacement percentage of recycled aggregate

V_f% = Steel fibres content

NC = Normal concrete

RAC = Recycled aggregate concrete

SFC = Steel fibres concrete

SFRAC = Steel fibres recycled aggregate concrete

4.3 Material Properties

4.3.1 Cement

The cement used throughout this research was high strength Portland cement (C 52.5) obtained from the Hanson Group. This cement is manufactured to comply with the requirements of BS EN 197-1 (2011). The bags come in waterproof and air-tight packaging to protect the cement and prevent it from deterioration over time. Table 4-1 shows the chemical composition of the cement and the physical properties of the cement mortar as provided by the manufacturer.

Table 4-1 Chemical compounds and physical properties of the cement

Property	Value	Unit	Requirements of standard
Initial setting time	110	min	≥ 45
Soundness (expansion)	1.1	mm	≤ 10
Compressive strength 2 days	27	MPa	≥ 20
Compressive Strength 28 days	58	MPa	≥ 52.5
C3S	51.33	%	-
C2S	21.14	%	-
C4AF	8.86	%	-
C3A	7.49	%	-

4.3.2 Fine aggregate

Natural river sand with a maximum particle size of 5mm was used as the fine aggregate (FA) for this research. Table 4-2 and Figure 4-2 show the grading results of the fine aggregate and the standard requirement limits according to BS 882 (1992). As can be seen from the data, the obtained grading curve complied with the requirements of the standard. The same batch of FA was used for all mixes to avoid any effects of variation in the aggregate on the results.

Table 4-2 Grading of the fine aggregate

Sieve size	Passing (%)	BS 882 Limits
10.0 mm	100	100
5.0 mm	95	89-100
2.36 mm	76	60-100
1.18 mm	59	30-100
600 µm	34	15-100
300 µm	13	5-70
150 µm	3	0-15
75 µm	0.6	-

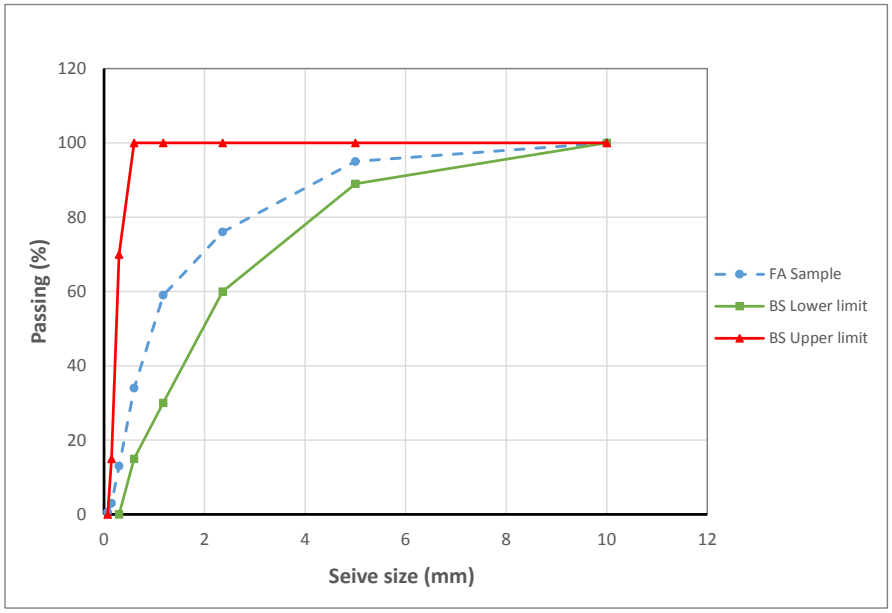

Figure 4-2 Grading of the fine aggregate

4.3.3 Coarse aggregate

Based on the aims of this research, two types of coarse aggregate were used as shown in Figure 4-3. An un-crushed limestone aggregate with a maximum size of 20mm was used as natural coarse aggregate (NA), and a crushed washed construction and demolition waste (CDW) aggregate with a maximum size of 20mm

was used as recycled aggregate (RA). The recycled aggregate was ordered from Yorkshire Aggregate Ltd.

Some preliminary tests such as sieve analysis, specific gravity, bulk density, porosity and water absorption were carried out to obtain the properties of the aggregates. The results of these tests correlated well with the data provided by the supplier. The grading and properties of both types of aggregate conformed to the standard requirements of BS 882 (1992) and BS 8500-2 (2006) as shown in Tables 4-3 and 4-4, and Figures 4-3 and 4-4. Figure 4-4 shows that the grading curves fall within the acceptable range from the standard. The composition of the recycled aggregate as provided by the supplier is presented in Figure 4-5.

Table 4-3 Grading of the coarse aggregate

Sieve size	Passing (%)		BS 882 Limits
	NA	RA	
37.50 mm	100	100	100
20.0 mm	100	88	85-100
14.0 mm	66	24	0-70
10.0 mm	15	3	0-25
5.0 mm	1	1	0-5

Table 4-4 Properties of the fine and coarse aggregate

Properties	FA	NA	RA
Specific gravity	2.64	2.62	2.48
Bulk density (Kg/m^3)	1680	1600	1360
Water absorption ratio (%)	1.06	0.89	4.78
Porosity (%)	-	38	46

(a) Natural aggregate

(b) Recycled aggregate

Figure 4-3 Samples of the coarse aggregate

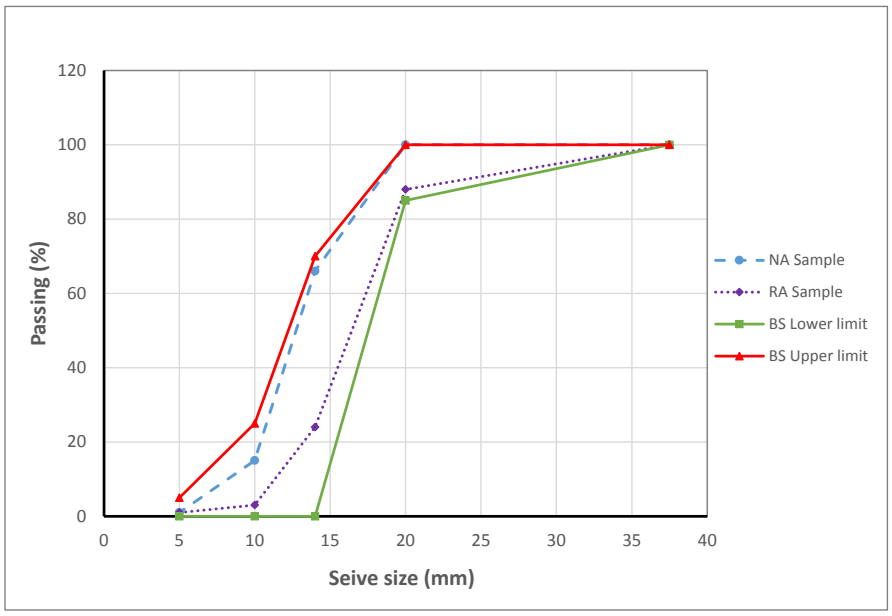

Figure 4-4 Grading of the coarse aggregate

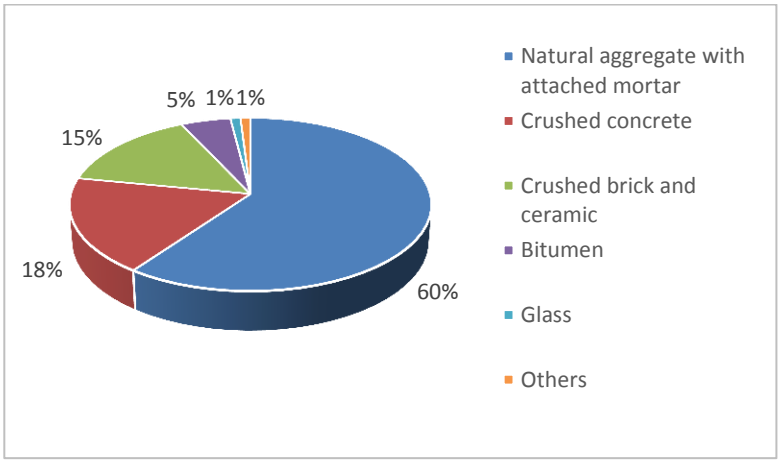

Figure 4-5 Composition of the recycled aggregate used in this research

4.3.4 Water

Leeds tap drinking water which meets the BS EN 1008 (2002) standard was used as the mixing water throughout this research. Neville (1995) reported that there is no clear standard for the quality of mixing water for concrete, however, it should be clean and not include too high a level of organic or inorganic substances.

4.3.5 Superplasticisers

A superplasticiser (SP), known as a high range water-reducing admixture, was used to improve the workability of the concrete mixture and reduce the water/cement ratio. In this research, Sika®ViscoCrete 25MP, provided by Sika, was used in all mixes containing steel fibres. This product meets the requirements of BS EN 934-2 (2009).

4.3.6 Reinforcement bars

Deformed steel bars of ∅16mm and ∅12mm were used for bottom and top longitudinal reinforcement respectively in all the full-scale beam tests. Deformed bars with a diameter of ∅8mm were used for the shear links which were located in the shear zones at 150mm c/c as shown in Figure 4-6.

Uni-axial tensile tests were carried out on samples of the steel bars according to BS EN 10002-1 (2001) to determine the mechanical properties of the steel reinforcement (see Figure 4-6); the results are summarised in Table 4-5.

Figure 4-6 Reinforcement of beam specimens

Figure 4-7 Uni-axial tensile test of steel bars

Table 4-5 Properties of steel bars

Nominal diameter (mm)	Area (mm^2)	Modulus of elasticity (MPa)	Yielding stress (MPa)
16	201	200,000	500
12	113		
8	50		

4.3.7 Steel fibres

Glued discontinued hooked-end steel fibres (Dramix 3D 65/35BG) as shown in Figure 4-8 were obtained from Bekaert were used in this research. The fibres have an aspect ratio of 65, length of 35mm and diameter of 0.55mm, and an ultimate tensile strength of 1180MPa. Their other properties, as received from the supplier, meet the requirements of BS EN 14889 (2006) and ASTM A820 (2010).

Figure 4-8 Hooked-end steel fibres (Dramix 3D)

4.4 Concrete Mixes

A total of 9 different concrete mixes were designed and produced with varying levels of recycled aggregate replacement and fibre contents. This matrix of mixes was set up in order to study the effects of the main variables on the objectives of this research and determine proper statistical relationships.

All mixes had the same effective water-to-cement ratio of w/c = 0.42. The mixing water compensation method was used to account for the effect of the recycled aggregate, and additional water was added to the RAC mixes to compensate for the high water absorption capacity of the RA and to achieve the required workability. The amount of additional water was calculated based on the amount of aggregate and its initial water content.

As mentioned earlier, Sika®ViscoCrete was used in the steel fibre concrete mixes to control the workability and to keep the w/c ratio constant for all mixes. Details of the mix proportions are given in Table 4-6.

Table 4-6 Design of concrete mixes

Mix	Specimen	Mix proportions (Kg/m^3)						
		W	C	FA	CA	RA	SP	SF
M1	NC	177	422	754	1024	-	-	-
M2	SFC-0-0.5	177	422	754	1024	-	0.5	40
M3	SFC-0-1.0	177	422	754	1024	-	1.0	80
M4	RAC-50	177	422	754	512	512	-	-
M5	SFRAC-50-0.5	177	422	754	512	512	0.5	40
M6	SFRAC-50-1.0	177	422	754	512	512	1.0	80
M7	RAC-100	177	422	754	-	1024	-	-
M8	SFRAC-100-0.5	177	422	754	-	1024	0.5	40
M9	SFRAC-100-1.0	177	422	754	-	1024	1.0	80

Note: W = free water, C = cement, FA = fine natural aggregate, CA = coarse natural aggregate, RA = recycled coarse aggregate (CDW), SP = superplasticiser, SF = steel fibres.

4.5 Test Specimens

In order to complete the experimental programme (see Figure 4-1), beams (150x300x4200mm) were prepared and cast for flexural bending tests, and cubes (100x100x100mm), cylinders (150x300mm), prisms (100x100x500mm) and bobbins (75x365mm) were produced for testing the mechanical properties of the concrete. In addition, 8 square prisms (120x120x1200mm) reinforced with a single central bar of ∅16mm were produced for the tension stiffening tests along with small prisms (75x75x200mm) and bobbins (75x365mm) for the shrinkage and creep tests. Details of the specimens' sizes and respective tests are shown in Table 4-7.

Each specimen was labelled X-Y-Z according to its mix, where X indicated the type of concrete (NC for normal concrete, RAC for recycled aggregate concrete, SFC for steel fibre concrete or SFRAC for steel fibre concrete with recycled aggregate), Y indicated the replacement percentage of the recycled aggregate (50% or 100%) and Z indicated the fibre content (0.5% or 1.0%). For example, SFRAC-50-1.0 referred to samples that were cast with 50% recycled aggregate and contained 1.0% steel fibres.

Table 4-7 Specimens used for the different tests

Test	Mould type	Specimen dimensions mm
Compressive strength	Cube	100x100x100
Splitting tensile strength	Cylinder	150x300
Direct tensile strength	Bobbin	75x365
Flexural strength	Prism	100x100x500
Modulus of elasticity	Cylinder	150x300
Flexural bending	Beam	150x300x4200
Shrinkage	Prism	75x75x200
Compressive creep	Prism	75x75x200
Tensile creep	Bobbin	75x365
Tension stiffening	Prism	120x120x1200

4.6 Casting and Curing

Concrete mixing was performed in accordance with BS 1881−125 (2002). A 200 litre mechanically driven drum mixer was used as shown in Figure 4-9. For each mix, the materials were prepared and weighed in the required proportions. The concrete quantity for each mix was increased by 10% to account for losses.

Based on the discussion presented in Chapter 2 about the different mixing procedures for concrete with recycled aggregate, it was decided that the mixing water compensation method would be used. The materials were therefore poured into the drum mixer in the following order: 1) half of the required quantity of coarse aggregate; 2) the full quantity of fine aggregate; 3) the full quantity of cement; and 4) the remaining quantity of coarse aggregate. These materials were mixed dry for the first minute to homogenise the batch, then the total amount of water (free + additional) was added and wet mixing continued for a couple of minutes. For the steel fibre concrete, the superplasticiser was added to the water prior to the water being added to the dry mix.

Figure 4-9 Mechanical drum mixer

The workability of the fresh concrete was evaluated using the slump test according to BS EN 12350−2 (2000). The test was carried out using a dampened metal cone mould which was filled with concrete in three layers. The cone was of the following dimensions: top diameter 100mm, base diameter 200mm and height 300mm. Each

of the filled layers was compacted with 25 strokes from a cylindrical rod of ∅16mm and length 600mm. After filling and compacting the concrete, the top surface of the mould was levelled using a tamping rod. The mould was then carefully removed in the vertical direction and, after cleaning the surrounding concrete, the slump was measured by comparing the height of the moulded concrete with the height of the mould.

The results of the slump tests are summarised in Table 4-8. As can be seen, the slump did not influence by replacing the aggregate. This is due to following the mixing water compensation method in the design process which kept the same effective w/c ratio in all the mixes. In contrast, the slump decreased slightly with increasing the steel fibres content even by using the superplasticiser. However, the reduction is not considerable and does not has a significant effect on the properties of concrete.

Table 4-8 Results of the slump tests

Mix	Specimen	Slump mm
M1	NC	120
M2	SFC-0-0.5	110
M3	SFC-0-1.0	105
M4	RAC-50	120
M5	SFRAC-50-0.5	110
M6	SFRAC-50-1.0	110
M7	RAC-100	120
M8	SFRAC-100-0.5	120
M9	SFRAC-100-1.0	110

As specified by BS EN 12390−2 (2000), the remainder of the concrete was placed in the prepared moulds immediately after measuring the slump. The moulds were filled in layers and compacted using a vibrating table or hand-held mechanical vibrator. Care was taken to avoid segregation of the concrete. The specimens were

then covered by wet mats and plastic sheets to prevent the evaporation of water and left for at least 24 hours. The following day, the specimens were demoulded and transferred to the controlled fog room to be cured for 28 days prior to testing. Figure 4-10 presents some pictures of the casting and curing of the specimens used for this research.

Figure 4-10 Casting and curing of specimens

4.7 Test Procedures

4.7.1 Compressive strength test

Six cubes (100x100x100mm) and three cylinders (150x300mm) were cast and cured for the compression testing of each mix. The samples were tested at an age of 28 days to determine the concrete compressive strength following the procedure specified in BS EN 12390-3 (2009). Before testing, the surface of the samples was wiped and the specimens were then left for at least 1 hour in the laboratory. The machine used for compression testing is shown in Figure 4-11. The load was increased at a constant rate (3KN/sec) and failure loads were recorded; average values of compressive strength (f_{cu} and f_c) from the cube and cylinder tests were calculated.

(a) Cube (b) Cylinder

Figure 4-11 Compressive strength tests

4.7.2 Tensile strength test

The tensile strengths of the different concrete mixes were evaluated using two tests: the indirect tensile strength test (splitting test) and the direct tensile strength test.

For the splitting test, three cylinders (150x300mm) were cast from each mix and tested at an age of 28 days. A compressive load was applied along the sample length as specified by BS EN 12390-6 (2009) and shown in Figure 4-12.

The specimen was initially fixed in a special jig which ensured the sample was accurately located at the centre of the machine. After the samples were placed in

the testing machine, the compressive load was applied. The load was increased at a constant rate (0.2KN/sec) and the failure load (P) was recorded. The tensile splitting strength (f_{spt}) was calculated in MPa using the following equation:

$$f_{spt} = \frac{2\,P}{\pi\,L\,D} \qquad \textbf{(4-1)}$$

Where:

L and D are the length and diameter of the test specimen in mm, respectively.

Figure 4-12 Splitting tensile strength test

Two bobbins (75x365mm) from each mix were cast for the direct tensile test and tested at an age of 28 days. The samples were cast in a special mould and subjected to a direct tensile load as shown in Figure 4-13. The direct tensile strength (f_t) was calculated in MPa by dividing the failure load (P) by the area of the specimen at the failure position (A).

Figure 4-13 Direct tensile strength test

4.7.3 Flexural strength test

In accordance with BS 12390-5 (2009), three prisms (100x100x500mm) were cast from each mix and tested at an age of 28 days to determine the flexural strength of the concrete (modulus of rupture). The simply supported specimens were subjected to a 4-point load as shown in Figure 4-14; the clear span length was 300mm. The load was increased at a constant rate (0.1KN/sec) until failure. The flexural strength (f_b) was calculated in MPa from the following equation:

$$f_b = \frac{P\,L}{b\,d^2} \qquad \textbf{(4-2)}$$

Where:

P is the failure load and L, b and d are the length, width and height of the test specimen in mm, respectively.

Figure 4-14 Flexural strength test

4.7.4 Modulus of elasticity test

Three cylinder specimens were tested to determine their static modulus of elasticity at an age of 28 days according to the procedures specified in BS 12390-13 (2009) and ASTM C469 (2012). The sample surfaces were smoothed and two Electrical Resistance Strain (ERS) gauges were placed on the vertical faces of the cylinders at opposing polar positions, i.e. 180º apart. Deformations were measured under compressive loads as shown in Figure 4-15. The value of the elastic modulus was calculated using the average of the strain readings in the following equation:

$$E_c = \frac{\sigma_2 - \sigma_1}{\varepsilon_2 - 50 \times 10^{-6}} \qquad \textbf{(4-3)}$$

Where:

σ_2 is the stress corresponding to 40% of the ultimate load, σ_1 is the stress corresponding to a longitudinal strain of 50×10^{-6} and ε_2 is the longitudinal strain produced by stress σ_2.

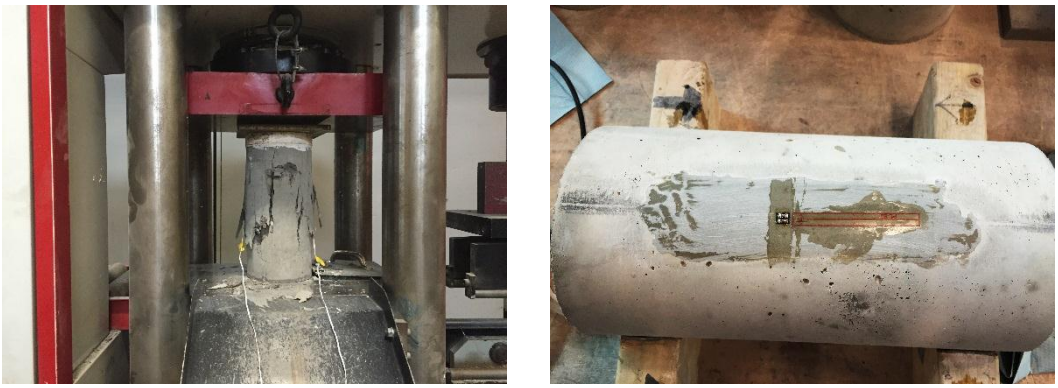

Figure 4-15 Modulus of elasticity test

4.7.5 Shrinkage test

Two small prisms (75x75x200mm) were used to measure drying shrinkage for each mix as shown in Figure 4-16. Demec points were placed on two opposite sides of the specimens (not on the floated face) and strains were measured over time using a hand-held mechanical strain gauge.

The specimens were cast and cured at the same time as the beams used for long-term testing. They were then stored in a control room and after exactly 28 days of curing, shrinkage was measured starting on the same day as the testing of the beams. The average shrinkage of the two specimens was calculated. The control room was maintained at 20ºC (±2ºC) and 45% (±5%) relative humidity. These environmental conditions were close to the average ambient conditions of the laboratory where the beams were tested (see Figure 4-17).

The effect of fluctuations in the environmental conditions was considered and no major influence was noticed; all fluctuations were within the acceptable range of ±5% for this type of test. In order to address any potential effect of the fluctuations in environmental conditions, smoothed curves are presented for all the results of time-dependent behaviours.

Figure 4-16 Shrinkage test

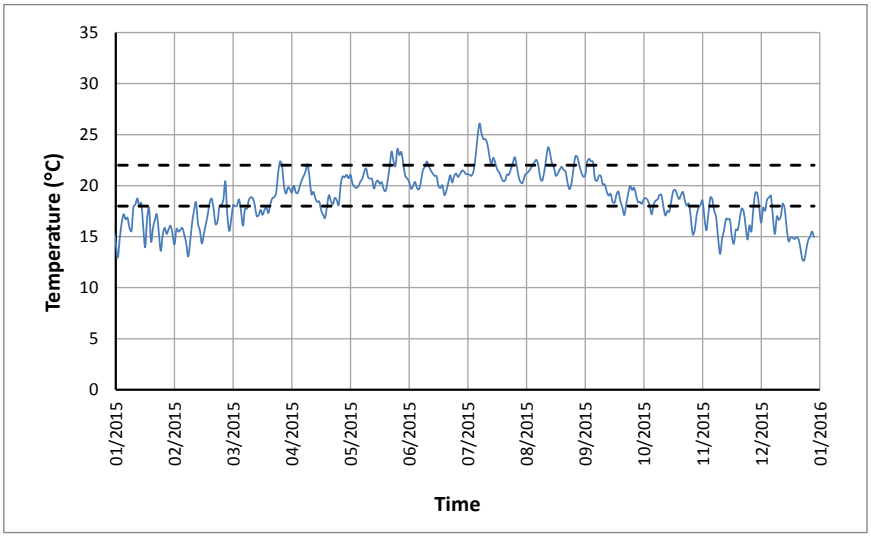

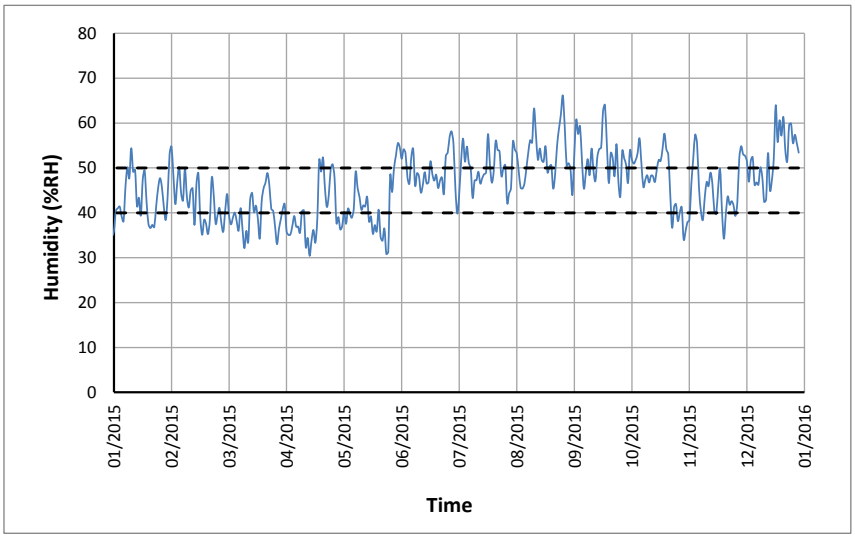

Figure 4-17 Environmental conditions of the Laboratory

4.7.6 Compressive creep test

As creep is considered to be one of the most significant time-dependent deformations that affects the long-term flexural behaviour of concrete, another two small prisms (75x75x200mm) from each mix were cast, cured and loaded at an age of 28 days to identify the compressive creep properties. Demec points were fixed on two opposite sides (not on the floated face) of the specimens in order to measure deformations over time. Specimens were subjected to a constant compressive stress of 10MPa (which is equivalent to $0.2f_c$` of the control specimen), as shown in Figure 4-18. The load cells were calibrated prior to applying the load. The initial elastic strain due to the applied load was measured and then additional strain readings were recorded over time.

Tests were carried out in the controlled environment room under the same conditions as were used for the shrinkage specimens. The compressive creep strains and coefficients were calculated based on the average results from the two specimens after removing the elastic strain and taking into account shrinkage.

Figure 4-18 Compressive creep test

4.7.7 Tensile creep test

The tensile creep of all the concrete mixes was measured using bobbin specimens (75x365mm) and the test rig shown in Figure 4-19. Demec points were attached to the specimens and a 1MPa tensile stress was applied. Specimens were first cured in a fog room before being tested in the control room under the same environmental conditions as the shrinkage specimens. The load cells were first calibrated before being used to apply the load. The initial elastic strain due to the applied load was

determined and the creep deformation was measured over time. As with the compressive creep results, elastic strain and shrinkage were considered in the final calculation of the tensile creep strain.

Figure 4-19 Tensile creep test

4.7.8 Long-term tension stiffening test

Square section prisms (120x120x1200mm) reinforced with a central bar of ∅16mm were used for the long-term tension stiffening tests as shown in Figure 4-20. A total of 16 specimens, two specimens from each mix, were prepared, cast and tested. The first specimen was subjected to a sustained load to measure tension stiffening, while the second specimen was unloaded and used to measure shrinkage.

In the first specimen, three strain gauges were placed every 300mm along the steel reinforcement bar to measure the strains in the bar at different positions. This was done to monitor the strain in the steel bar after concrete cracking. Seven Demec points were also fixed on two opposite sides of the concrete specimens every 150 mm in order to measure the surface strains of the concrete. After curing, the specimens were placed in a special rig, as shown in Figures 4-21 and 4-22. This rig was designed and built specifically for this test and was based on the test rig used by Scott and Beeby (2005).

A direct tensile load was applied to the steel bar and kept at a constant value of 45KN using a hydraulic jack and load cell. This load was equivalent to a stress of 200MPa in the bar, which was the same as the tensile stress induced in the steel reinforcement in the beam tests. Immediately after the load was applied, the initial elastic deformation was determined; the measurements of the strain in the steel

bars and on the concrete surfaces were then recorded for a period of 35 days. A hand-held mechanical strain gauge was used to take regular readings; a data logger was used to record the ERS strains and the load applied by the load cell over time.

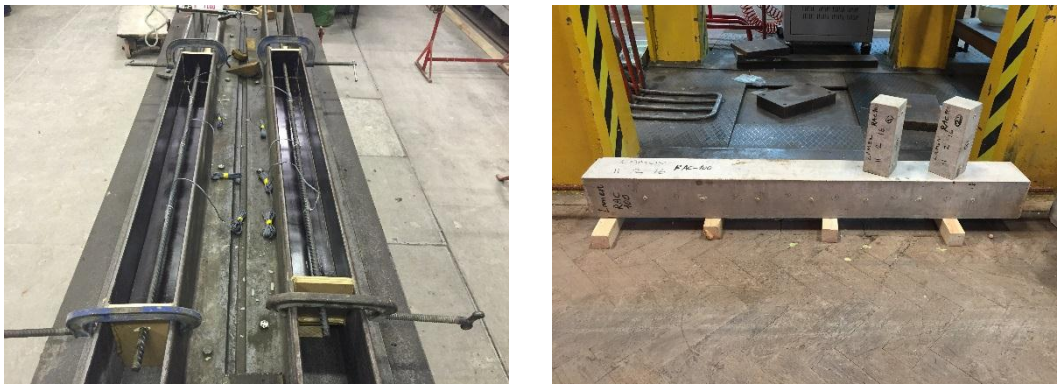

Figure 4-20 Specimens of tension stiffening test

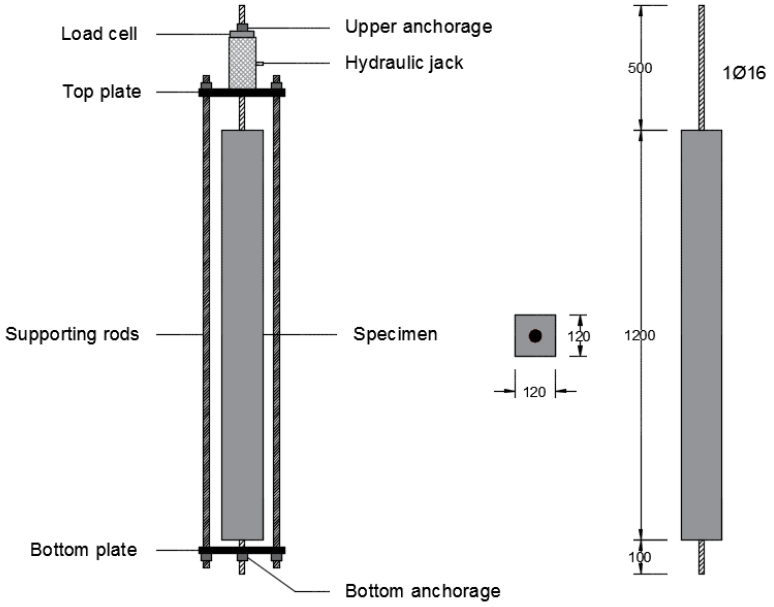

Figure 4-21 Test rig for tension stiffening specimens

The second specimen was stored next to the first specimen and used to measure shrinkage as this was necessary to determine the degree of tension stiffening. The strain data was used to calculate the time-dependent reduction in the ratio between the concrete tensile stress measured over time due to the sustained load and the

initial concrete tensile stress recorded directly after applying the load. The strain data was analysed in accordance with the methods proposed by Scott and Beeby (2005).

Figure 4-22 Tension stiffening test

4.7.9 Long-term flexural bending test

As mentioned previously, 9 long-term beam (150x300x4200mm) bending tests were performed. Initially, steel forms were built to accommodate the required reinforcement cages. The same amount and arrangement of reinforcement were used for all the beams, as shown in Figure 4-23. The reinforcement cages were placed inside the forms after the internal walls of the forms were cleaned and brushed with oil to facilitate removal after casting of the concrete. The reinforcement cage was supported by small pieces of concrete (packers) to maintain a 25mm clear concrete cover. Three Electric Resistance Strain (ERS) gauges were placed on the top of the middle of the reinforcing bars and connected to a data logger in order to record steel strains over time.

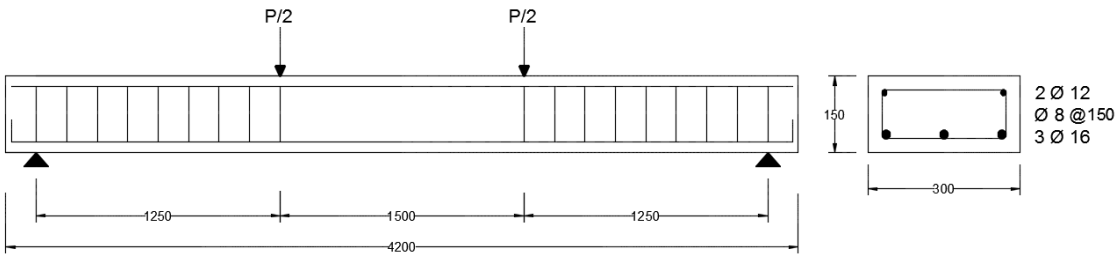

Figure 4-23 Details of beam dimensions and reinforcement

Before testing, Demec points were placed on the two sides of the beam in the constant moment zone. Four rows of Demec points were fixed at 36, 63, 90, and 116mm from the bottom of the beam and at 150mm centres along the length of the constant moment zone in order to measure the concrete surface strains. The bottom and top rows of Demec points (at 36mm and 116mm respectively) were in line with the height of the bottom and top steel reinforcement.

Each beam was painted white to facilitate monitoring of the crack patterns. In addition, a linear variable differential transformer (LVDT) was placed in the middle of the beam to record the central displacement, as shown in Figure 4-24.

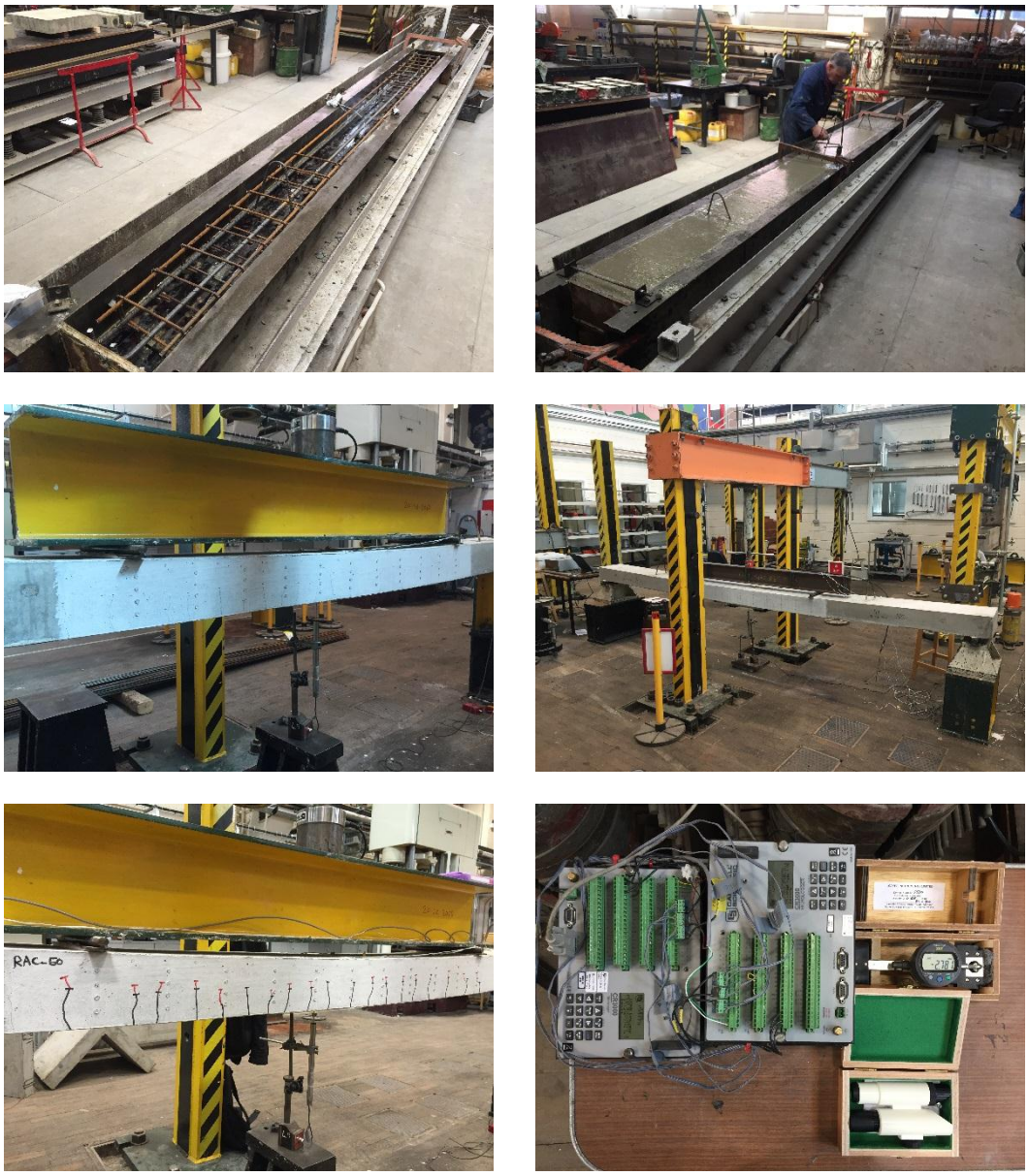

Figure 4-24 Flexural bending test

All of the beams were loaded at a constant rate up to 23KN. This applied load corresponded to 50% of the failure load of the control specimen. The applied load generated a tensile stress in the steel reinforcement of 200MPa which is the stress normally associated with stabilised cracking pattern for these types of beam loaded in flexure. As can be seen from Figure 4-24, a 4-point loading system was used and the beams were simply supported.

All load, deflection and steel strain measurements were recorded automatically using an electronic data logger. Concrete surface strains were measured using a hand-held mechanical strain gauge. The development of crack patterns and crack propagation were observed and marked on the beams; crack widths were measured using a hand-held optical microscope as shown in Figure 4-24.

4.8 Summary

This chapter has described the details of the experimental programme. The following points summarise the programme:

- Three different replacement percentages of recycled aggregate and three amounts of steel fibre contents were considered as the main variables of this research.
- The results of the preliminary tests of aggregate revealed that the CDW used in this research had poorer properties than the NA. However, it seemed to be of good quality in comparison to other types presented in the literature.
- A matrix of nine different concrete mixes was set up in order to study the effects of the main variables on the objectives of this research and to determine proper statistical relationships.
- The mixes were designed for the same target of workability. Therefore, the mixing water compensation method was used to account for the effect of the RA and superplasticiser was added in the steel fibres concrete mixes.
- The slump test results showed that replacing aggregate did not influence the degree of workability when the mixing water compensation method was followed. However, the slump decreased slightly with increased content of steel fibres.

- Several sets of specimens were cast and tested for various purposes in order to achieve the objectives of this research.
- The changes in environmental conditions were considered to be in an acceptable range of ±5% in order to reduce fluctuations in the results of time-dependent deformations.
- All the laboratory equipment was calibrated before use in this research to ensure the accuracy of the measurements.
- Electronic data loggers were used to record the measurements and Excel sheets were used for the calculations of the final results.

Chapter 5 : Experimental Results and Discussion

5.1 Introduction

The following chapter discusses the results obtained from the experimental tests carried out in this research. The results obtained address the following aspects:

1- Mechanical properties.
2- Creep and shrinkage deformations.
3- Long-term loss of tension stiffening.
4- Short-term deflection of reinforced concrete beams and cracking patterns.
5- Long-term deflection of cracked reinforced concrete beams and cracking development.

Each of these aspects will be discussed separately with regards the influence of recycled aggregate and steel fibres on performance with comparison to the control specimens of normal concrete tested.

5.2 Mechanical Properties of Concrete

In this section, the experimental results for the effects of recycled aggregate and steel fibres on the compressive strength, tensile strength, flexural strength and modulus of elasticity of concrete will be presented and discussed. The results are summarised in Table 5-1.

In general, the results obtained from the tests indicated that replacement with recycled aggregate reduced all concrete properties but the addition of steel fibres proved to be highly beneficial. Interestingly, it was found that the addition of 0.5% and 1.0% steel fibres to concrete containing 50% and 100% recycled aggregate, respectively, resulted in concrete with almost the same performance as normal concrete. However, in some cases i.e. when 1.0% steel fibres were added to the RAC with 50% replacement, the performance was better than the equivalent NC mix. This confirmed that incorporating steel fibres within the RAC mix is beneficial and can expand the use of RAC within various applications (e.g. bridge decks, foundations slabs, industrial floors, dams and retaining walls .. etc.).

Table 5-1 Experimental results for concrete mechanical properties

Specimen	f_{cu} (MPa)	f_c (MPa)	f_t (MPa)	f_{spt} (MPa)	f_{fb} (MPa)	E_c (MPa)
NC	51.57	41.50	2.25	4.17	5.25	30,550
SFC-0-0.5	52.92	43.72	2.52	4.68	6.12	31,840
SFC-0-1.0	54.20	47.12	2.83	5.62	6.98	33,470
RAC-50	49.15	39.00	1.96	3.65	4.75	25,240
SFRAC-50-0.5	50.38	41.56	2.20	4.08	5.54	26,330
SFRAC-50-1.0	51.53	44.18	2.46	5.02	6.42	27,600
RAC-100	47.32	37.43	1.74	3.23	4.28	22,460
SFRAC-100-0.5	48.67	39.88	1.95	3.64	4.98	24,780
SFRAC-100-1.0	49.69	42.04	2.18	4.43	5.81	26,020

5.2.1 Compressive strength

All the compressive strength results for NC and RAC with and without fibres were obtained after 28 days of curing. Tests were performed on both cubes and cylinders and the results are shown in Figures 5-1 and 5-2.

The results indicate that there is a similar trend for both types of specimen with and without recycled aggregate, i.e. a reduction in compressive strength of about 5% and 10% was measured for both types of specimen (cubes and cylinders) when 50% and 100% of the coarse aggregate was replaced, respectively. This can be owed to the lower strength of RA in comparison to NA as revealed in many studies.

As reported in the literature, adding steel fibres to NC and RAC has no significant effect on compressive strength especially when it is tested using cubic specimens. In this study, an approximate increase of 2% and 5% was obtained by adding 0.5% and 1.0% steel fibres respectively for all replacement percentages of RA. This is likely explained by the effect of adding a high fibre content to a small volume sample (e.g. a cube of 100×100×100mm) which means the mixture is neither homogenous nor well compacted.

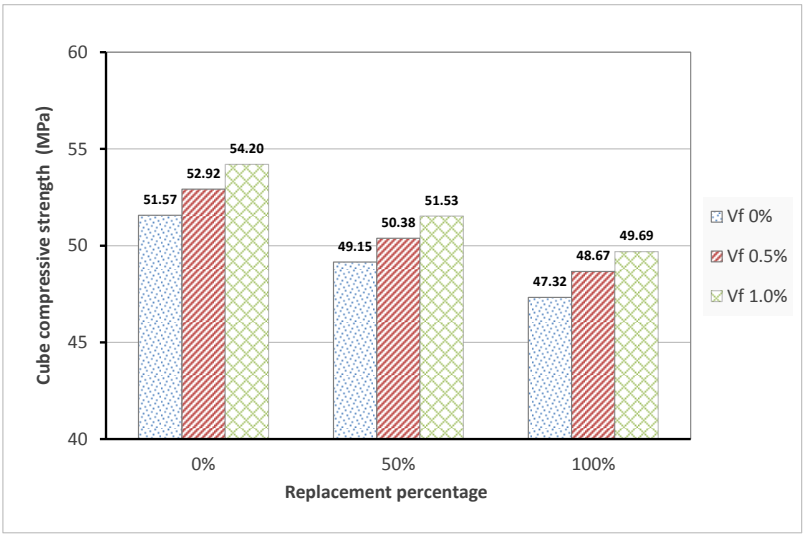

Figure 5-1 Compressive strength results of cubes

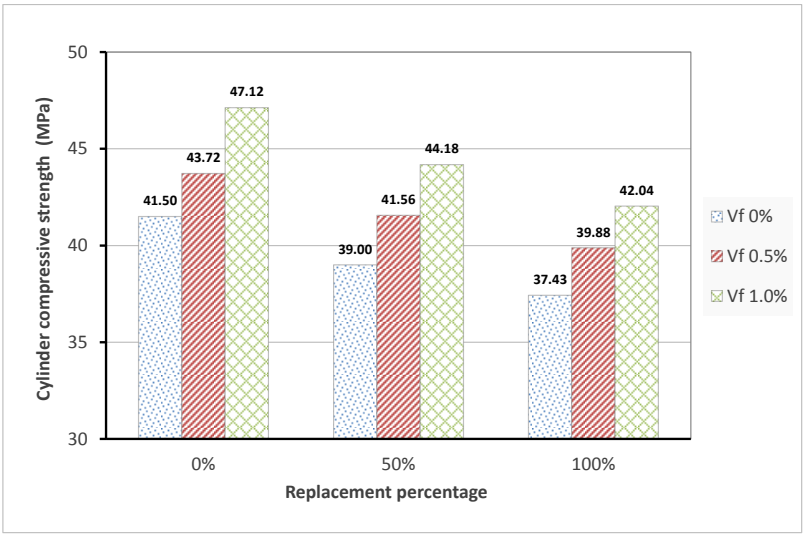

Figure 5-2 Compressive strength results of cylinders

Interestingly, the compressive strength results for the cylindrical specimens showed an increase of 5-6% and 12-13% when 0.5% and 1.0% steel fibres was added to the NC and RAC specimens. Figure 5-3 suggests a reason for the disparity between the behaviour of cubic and cylindrical specimens with steel fibres. With the cubic specimens, casting and compaction will most likely lead to the load being applied parallel to the length of the steel fibres. The tensile forces which govern failure are therefore perpendicular to the length of the fibres and not resisted by the steel fibres.

The opposite is observed in the cylinders where it is more likely the steel fibres will resist the tensile forces and help to bridge any cracks. Thus with the cylindrical specimens, the compressive strength increases noticeably with an increase in steel fibre content (see Figure 5-2). The different failure patterns observed for the cubic and cylindrical specimens also mean that the steel fibres work better in the cylindrical samples to enhance the compressive strength. Therefore, the cylindrical specimens are highly recommended to be used in the experiments of this type of concrete and their results should be considered in the design.

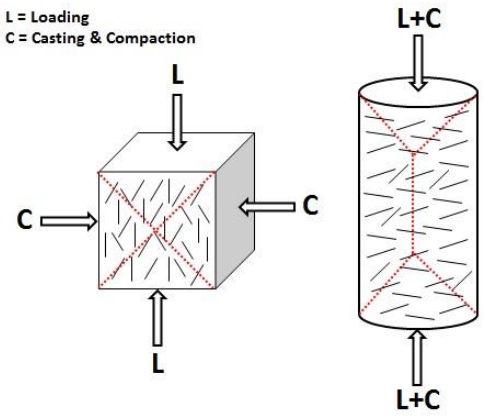

Figure 5-3 Effect of steel fibres during loading of cubic and cylindrical specimens

5.2.2 Tensile strength

Two different tensile strength tests were carried out as described in Chapter 4. The splitting tensile test was performed by applying a line compressive force along the sides of a cylindrical test specimen. Figure 5-4 shows the effect of adding steel fibres and RA replacement levels on the splitting tensile strength. The results clearly demonstrate a gradual reduction in splitting tensile strength of 15% and 30% with increasing RA percentage.

As expected, it was found that steel fibres significantly enhance the splitting tensile strength of both NC and RAC. The increase in tensile strength is greater than the corresponding increase in compressive strength. The reason this is expected is that fibres can reduce the development of tensile stress and delay the propagation of cracks. The increase observed was strongly dependent on the fibre content, i.e. adding 0.5% and 1.0% fibres increased the splitting tensile strength by 11-12% and 35-37% respectively for all RA replacement levels.

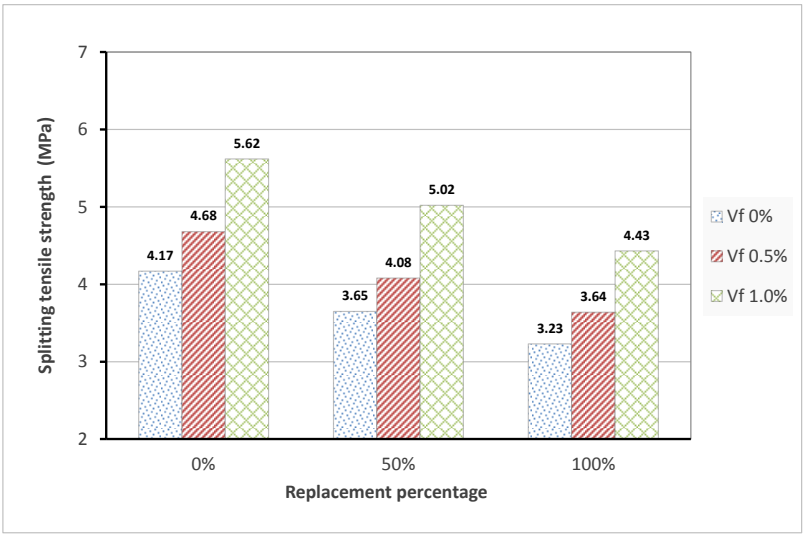

Figure 5-4 Results of splitting tensile strength

The second test carried out was the direct tensile strength test, where the specimen is subjected to a direct tensile load after 28 days of curing. Figure 5-5 shows the experimental results for the effects of steel fibres and recycled aggregate on the direct tensile strength.

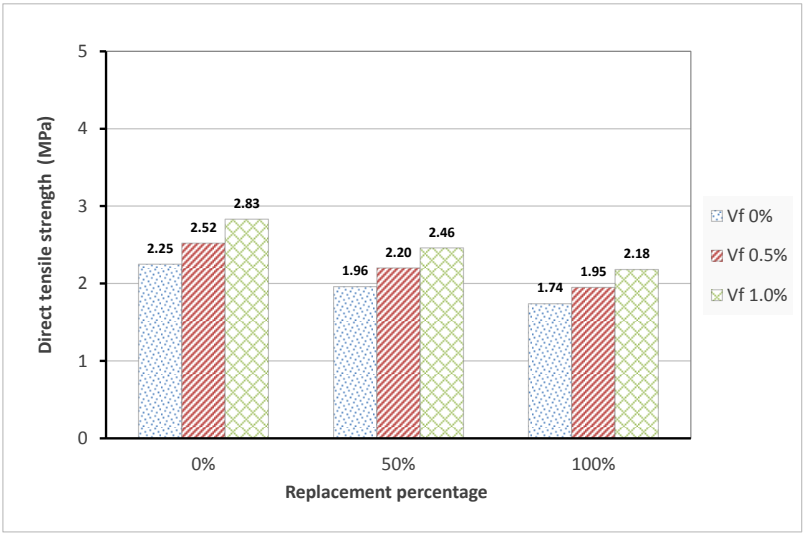

Figure 5-5 Results of direct tensile strength

Similar to the splitting tensile strength, 15% and 30% reductions in direct tensile strength were recorded for samples with 50% and 100% RA respectively. All of these reductions can be attributed to the poor properties of the recycled aggregate

compared to those of the natural aggregate as noted in the literature. Nevertheless, adding 0.5% and 1.0% steel fibres increased the direct tensile strength by 12% and 25% respectively. It is thought that the effectiveness of the steel fibres on improving indirectly the interfacial bond between the cement matrix and the aggregate is the main reason for this enhancement.

The results indicated that the ratio between the tensile and compressive strengths (f_{spt}/f_c) of all specimens was about 8-12%; this is usually 10% for normal concrete of such strength class. This ratio decreased with increasing RA replacement level and increased with increasing fibre content.

5.2.3 Flexural strength

The results for the flexural strength of the concrete specimens tested are shown in Figure 5-6. Similar to the compressive and tensile strength, the flexural strength decreased by 10% and 22% when 50% and 100% of the aggregate was replaced by RA respectively.

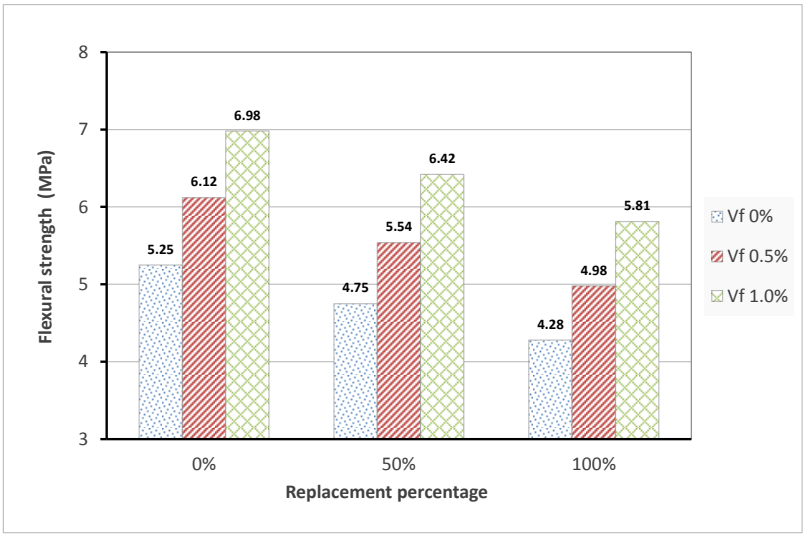

Figure 5-6 Results of flexural strength

Incorporation of steel fibres in the NC and RAC resulted in a considerable increase in flexural strength. Increments of 16% and 35% were recorded for additions of 0.5% and 1.0% steel fibres respectively for all RA replacement percentages. The great ability of steel fibres to enhance the stiffness of the concrete under flexural is considered the main reason for these increments as many previous studies

reported before. The ratio of flexural to compressive strength (f_{fb}/f_c) varied between 12-15%; it recorded 13% for the NC specimen and decreased with increasing RA replacement level and increased with increasing fibre content.

5.2.4 Modulus of elasticity

Cylindrical specimens were tested to determine the static modulus of elasticity of the materials after 28 days of curing. In comparison to normal concrete, the modulus of elasticity of the RAC specimens was lower by 20% and 30% when 50% and 100% of RA was used as shown in Figure 5-7. As the aggregate is the main factor which affects the modulus of elasticity of concrete, it was expected that the modulus would decrease with the addition of RA due to the presence of adhered mortar and other materials in the composition of RA.

This can both decrease the amount of natural aggregate particles in the matrix and increase the porosity. In addition to the lower stiffness and modulus of elasticity of the recycled aggregate itself, the presence of adhered mortar can influence the microstructure and the micro-cracking of the interfacial transition zone (ITZ) and thus affect the shape of the stress-strain curve. Moreover, the low density of the RA and the resulting concrete exacerbate this effect.

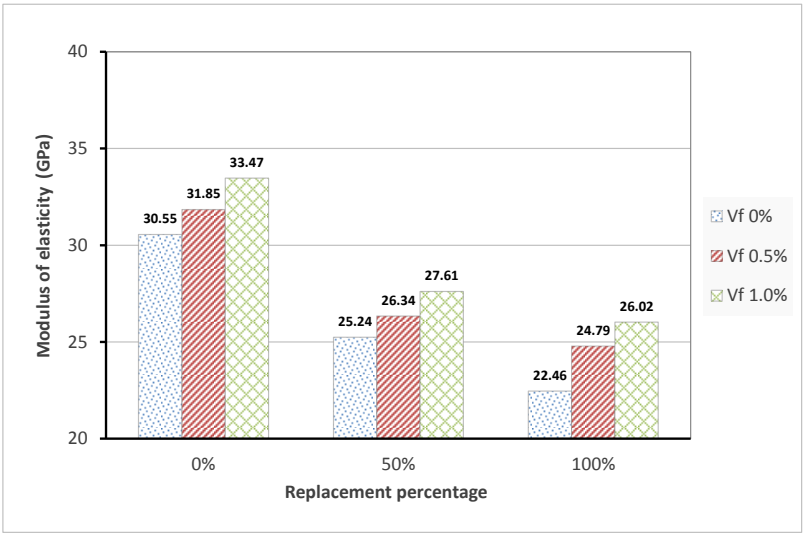

Figure 5-7 Results of modulus of elasticity

Figure 5-7 also shows the influence of the inclusion of steel fibres on the modulus of elasticity of NC and RAC specimens. In line with studies reported previously in

the literature, in this study, additions of 0.5% and 1.0% steel fibres increased the modulus of elasticity of NC and RAC by 4% and 10% respectively. The higher modulus of elasticity of the steel fibres (210,000 MPa) and the contribution of the fibres to enhance the strength of the concrete and reduce the deformation under applied load seems to play an important role in increasing the elasticity of the specimens tested. With increasing load and deformation, the steel fibres appear to enhance the stiffness of the concrete through the bridging of the macro cracks.

5.3 Time-dependent Deformations of Concrete

As concluded in the literature review, the incorporation of recycled aggregate has a more significant detrimental impact on the time-dependent deformation than on the short-term mechanical properties of concrete. Moreover, the possibility of adding steel fibres to reduce these negative effects was discussed with the view to increasing the use of recycled aggregate concrete in various structural applications. Therefore, laboratory tests were carried out as part of this study to investigate the effect of recycled aggregate and steel fibres on the drying shrinkage and compressive and tensile creep deformation of concrete.

5.3.1 Drying shrinkage

In this research, concrete shrinkage was measured after 28 days of curing. Figures 5-8 and 5-9 show the effects of recycled aggregate and steel fibres on shrinkage strains over time. As the aggregate restrains the shrinkage of the cement paste, thus the type of aggregate used plays an important role in affecting the potential shrinkage. It is clear from the data that there is a great influence on the shrinkage values due to increase the percentage of RA in the concrete. More specifically, drying shrinkage strains increased by 18% and 38% when 50% and 100% of aggregate were replaced respectively.

This can be attributed to the presence of adhered mortar and materials such as clay bricks and tiles in the composition of the RA which causes a decrease in the volume of NA particles in the resulting concrete. These materials have a lower stiffness and therefore provide less restraint to the shrinkage than the NA. Replacing the natural aggregate with recycled aggregate having a lower modulus of elasticity can also tend to cause a higher shrinkage (Silva et al., 2015, Fathifazl et al., 2011, Domingo et al., 2010). In addition, the existence of such materials within

the composition of the RA makes the concrete more porous and therefore more liable to absorb water. This can affect the evaporation of water from the concrete and lead to higher shrinkage strains (drying and autogenous shrinkage).

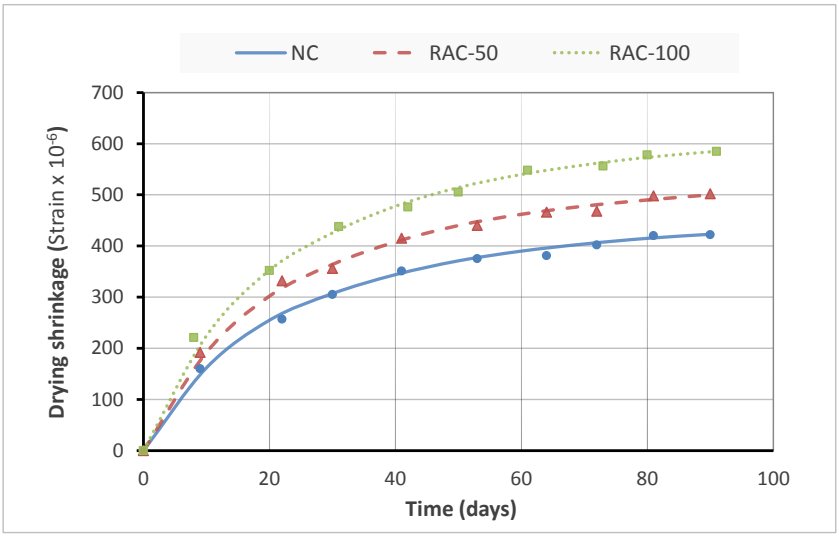

Figure 5-8 Effect of recycled aggregate on drying shrinkage

In contrast, adding steel fibres decreased the drying shrinkage strains of normal and recycled aggregate concrete. The drying shrinkage reduced more with increasing fibre volume fraction (V_f). Reductions of 7% and 15% were observed when 0.5% and 1.0% steel fibres were added respectively. The reasons for this are the ability of the steel fibres to restrain the volume changes of concrete by improving indirectly the bond between the cement matrix and the coarse aggregate as presented in Figure (5-9).

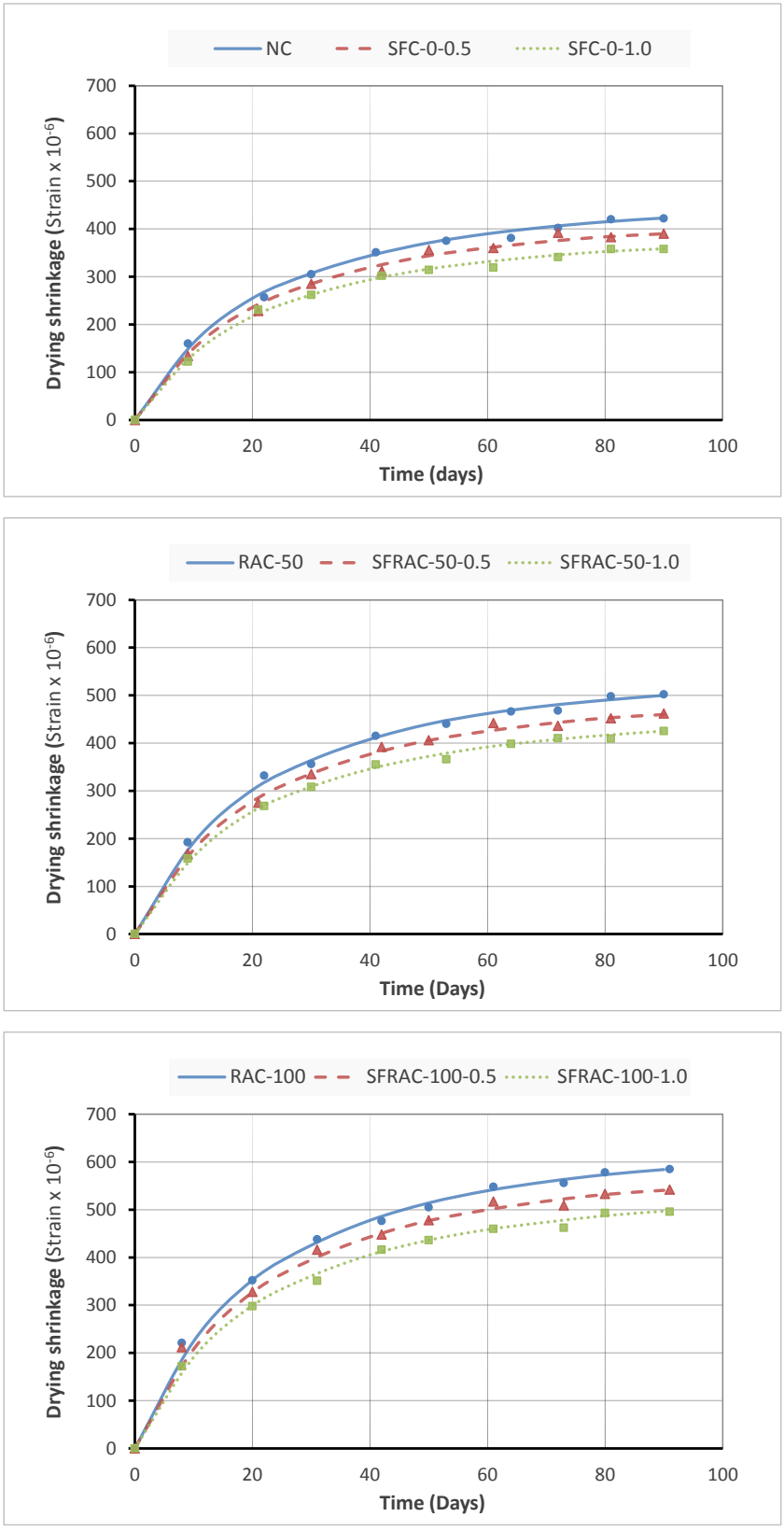

Figure 5-9 Effect of steel fibres on drying shrinkage

5.3.2 Compressive creep

In this research, specimens of prism were cured for 28 days and then subjected to sustained compressive stresses as described in Chapter 4. In general, the experimental results showed that when natural aggregate is replaced by recycled aggregate, the creep deformation increases. One reason for this is thought to be that the actual volume of natural aggregate is reduced due to the presence of adhered mortar and materials such as clay bricks and tiles in the composition of the RA. This makes the aggregate/cement ratio lower and increases the porosity of the resulting concrete (Knaack and Kurama, 2015a, Fan et al., 2014, Domingo et al., 2010).

In addition, the old attached mortar and the existence of other materials can amplify the ITZ between the new cement paste and the RA which degrades the properties of the concrete and causes more micro cracking in this region under sustained loads. The elastic modulus of the RA and the resulting concrete are lower than those of NA and conventional concrete. These factors can cause a significant increase in creep deformation (ACI 209, 2005).

The long-term compressive creep strain was obtained by subtracting the shrinkage and elastic strains from the total measured strain as follows:

$$C_c(t, t_0) = \varepsilon_t - \varepsilon_{sh} - \varepsilon_0 \qquad \textbf{(5-1)}$$

Where:

ε_t = total measured strain

ε_{sh} = shrinkage strain

ε_0 = instantaneous elastic strain

Figures 5-10, 5-11 and 5-12 show the results for the compressive creep strains of concrete with recycled aggregate and steel fibres. Similar to shrinkage strains, the compressive creep strains and coefficients increased by 15% and 29% when 50% and 100% of RA was used, respectively.

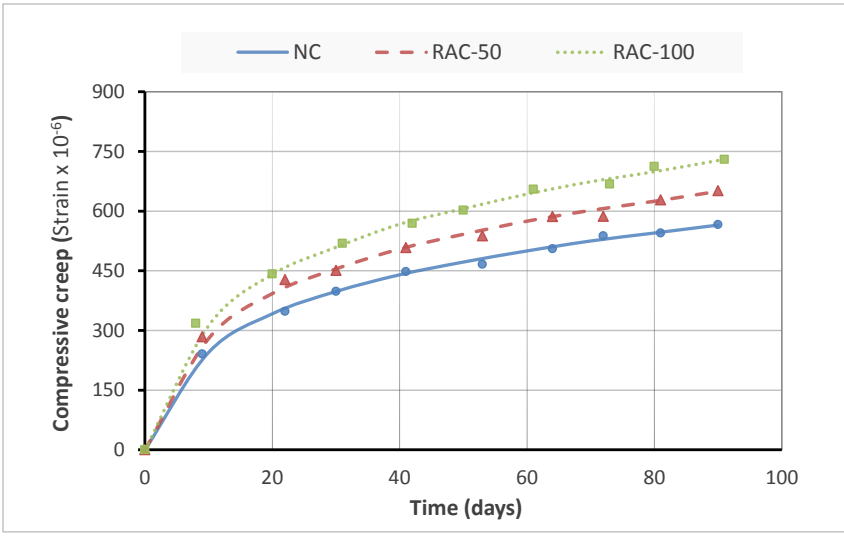

Figure 5-10 Effect of incorporating recycled aggregate on compressive creep

On the other hand, the results showed that there is no significant impact on the compressive creep strains and coefficients from the addition of steel fibres. Only 3% and 5% reductions in compressive creep results were observed when incorporating 0.5% and 1.0% steel fibres respectively. Although this time the fibres may take a parallel orientation to the direction of the applied load in the prism due to the casting and compaction processes, there is still no evidence of steel fibres resisting the compressive stresses. Similar results were observed for all the specimens of normal and recycled aggregate concrete.

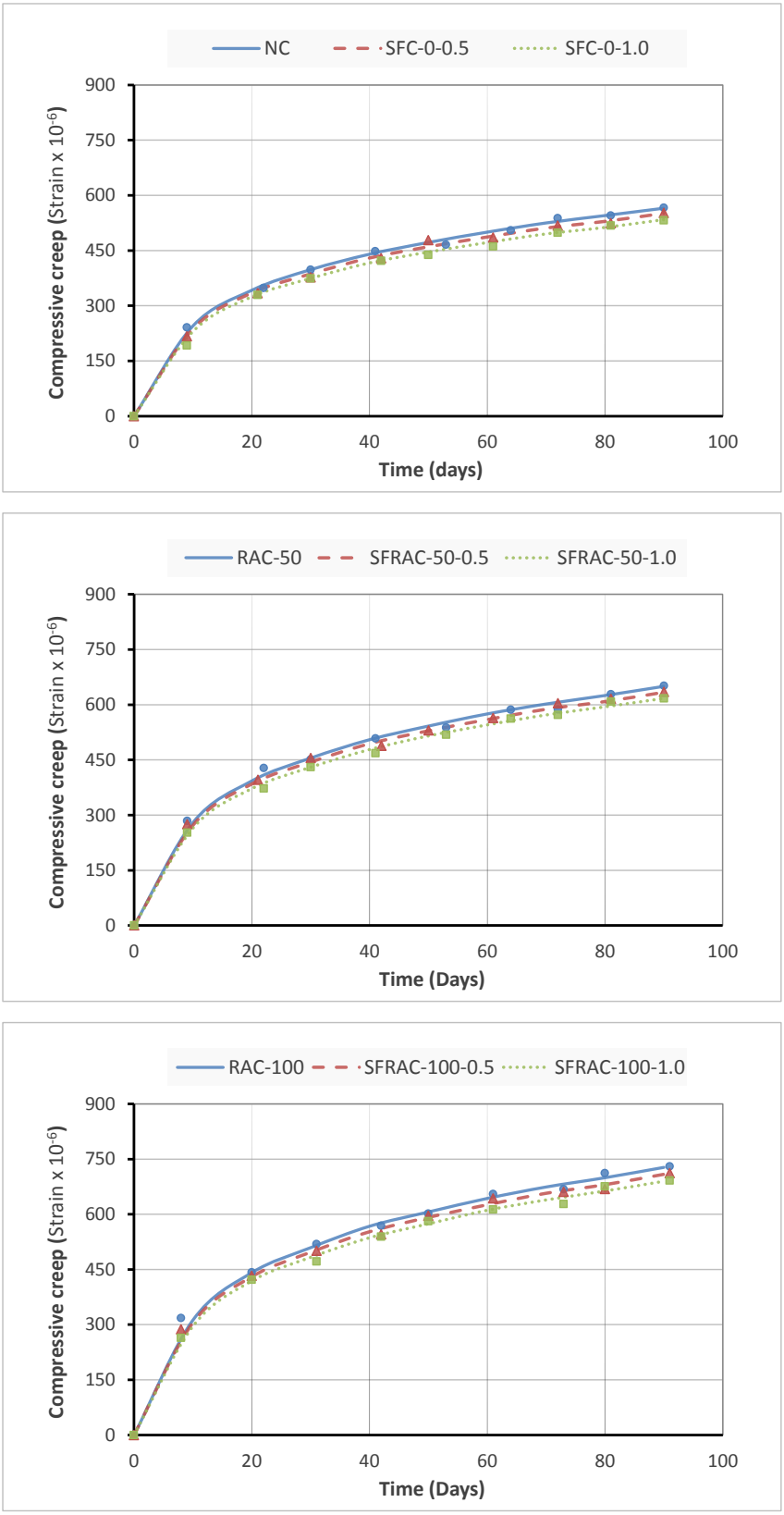

Figure 5-11 Effect of adding steel fibres on compressive creep

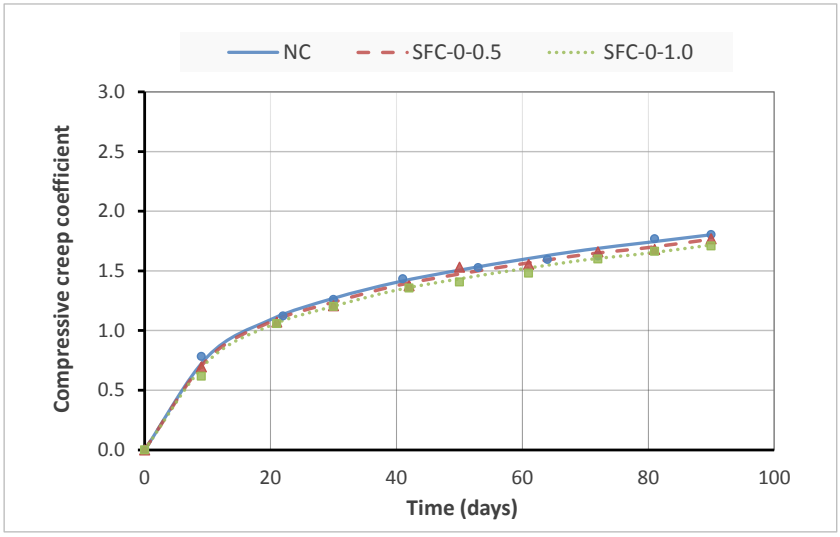

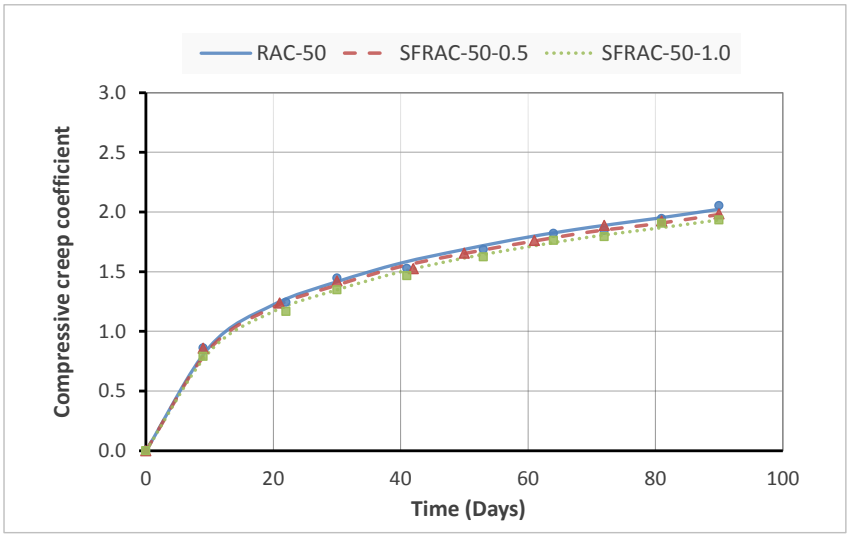

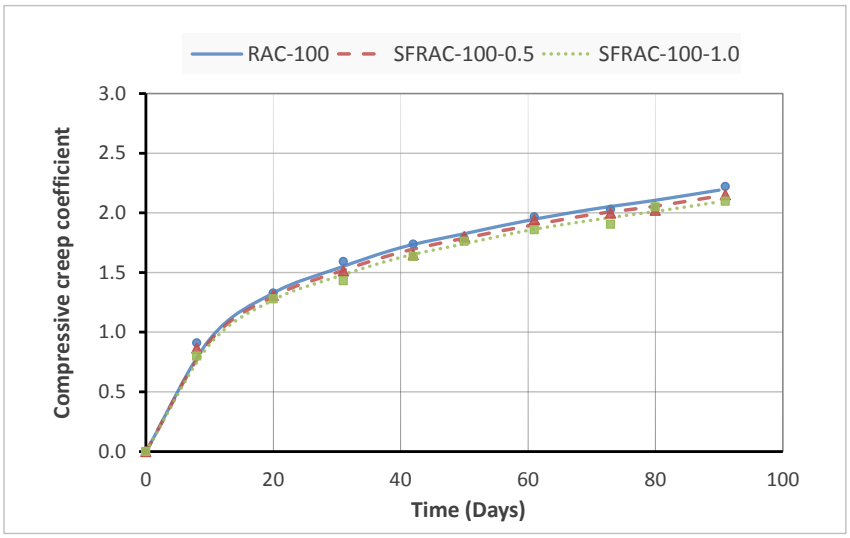

Figure 5-12 Compressive creep coefficient results

5.3.3 Tensile creep

As described earlier in Chapter 4, tensile creep response was tested using bobbin samples (75x365mm) under an applied tensile stress of 1MPa. Figures 5-13 and 5-14 present the experimental results for the effect of recycled aggregate and steel fibres on tensile creep strains. The long-term tensile creep data were obtained by adding the total measured strain to the shrinkage strain (since they act in opposite directions) and subtracting the instantaneous elastic strain as follows:

$$C_t(t, t_0) = \varepsilon_t + \varepsilon_{sh} - \varepsilon_0 \qquad \textbf{(5-2)}$$

Where:

ε_t = total measured strain

ε_{sh} = shrinkage strain

ε_0 = instantaneous elastic strain

As expected, similar to the results for drying shrinkage and compressive creep, replacing NA with RA by 50% and 100% increased the tensile creep strain by 8% and 15%, respectively. As the incorporation of RA has an impact on reducing the tensile strength and the modulus of elasticity of the concrete, it can be inferred that these are the main reasons for the increase in creep observed under the sustained tensile stress.

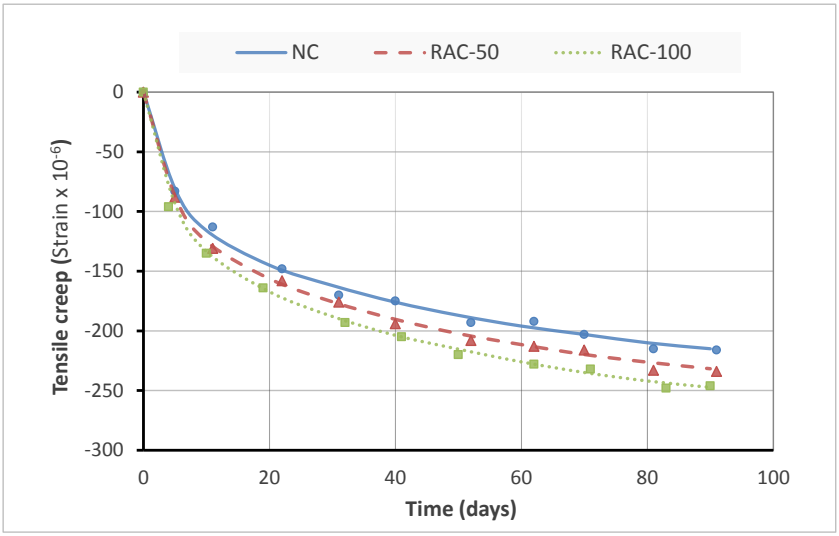

Figure 5-13 Effect of incorporating recycled aggregate on tensile creep

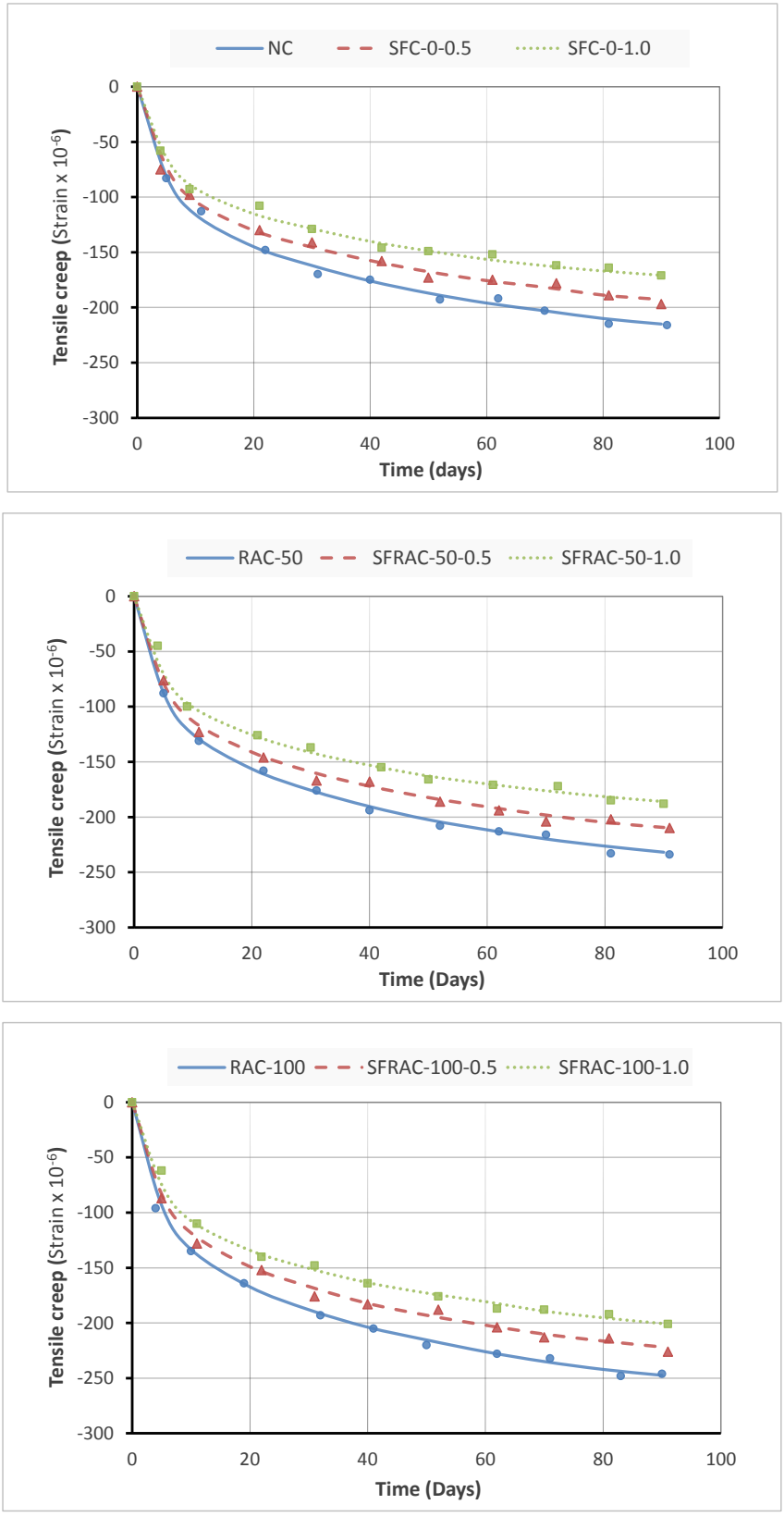

Figure 5-14 Effect of adding steel fibres on tensile creep

Interestingly, the effect of adding steel fibres on tensile creep was different to its effect on compressive creep. The results showed there was a noticeable effect on tensile creep strains reduced by 10% and 20% when 0.5% and 1.0% steel fibres were added, respectively. This can be attributed to the fact that steel fibres enhance the tensile strength of concrete more than the compressive strength. In addition, steel fibres can also contribute to improve indirectly the interfacial bond between the cement matrix and aggregate and enhance the cracking resistance.

The specific creep values were calculated by dividing the final compressive and tensile creep strains by the applied stress as follows:

$$C(t, t_0) = \frac{C_c \; or \; C_t}{\sigma} \qquad \textbf{(5-3)}$$

Where:

C_c = compressive creep strain

C_t = tensile creep strain

σ = applied stress

By applying the experimental results of creep strains in this equation, a comparison between the specific compressive and tensile creep responses at an equal applied stress can be conducted. This allows to illustrate the influence of recycled aggregate and steel fibres. The results of this comparison showed that the ratio between the specific tensile and compressive creep decreases with increasing replacement percentage of RA and increases with increasing steel fibres content. This can be attributed to the greater effects on the tensile strength than the compressive strength of concrete by replacing the aggregate and adding steel fibres. The range of this ratio was between 2.9 and 3.8 for the materials tested.

5.4 Long-term Loss of Tension Stiffening

The measured concrete surface strains and steel bar deformations were analysed to determine the long-term loss of tension stiffening in the beam specimens. As discussed in Chapter 3, Scott and Beeby (2005) carried out an extensive experimental study on loss of tension stiffening at Durham University and the University of Leeds. In their work, three methods were discussed and assessed for

calculating the reduction in concrete tensile stress with time. A brief description of these three methods is presented in Chapter 3.

The most important conclusion in the literature review which needs to be mentioned here concerns the effect of concrete shrinkage on the results. Scott and Beeby (2005) did not mention how this effect should be treated and therefore their results were criticised by Wu and Gilbert (2008). In this research, the strain readings from the shrinkage specimens were added to the strain readings of the tension stiffening specimens since they act in opposite directions.

5.4.1 Effect of recycled aggregate

This section presents and discusses the effect of incorporating RA on the reduction in tension stiffening over time. The experimental results for the specimens that were made with 50% and 100% RA replacement are analysed using calculation Method 1, presented in Chapter 3, to compare with the normal concrete specimen results.

Figure 5-15 shows the effect of incorporating RA on the long-term loss of tension stiffening. The ratio between the long-term concrete stress and the initial concrete stress is used for illustrating this loss. Figure 5-16 shows the data for the actual values of concrete tensile stress as a function of time for the NC and RAC specimens.

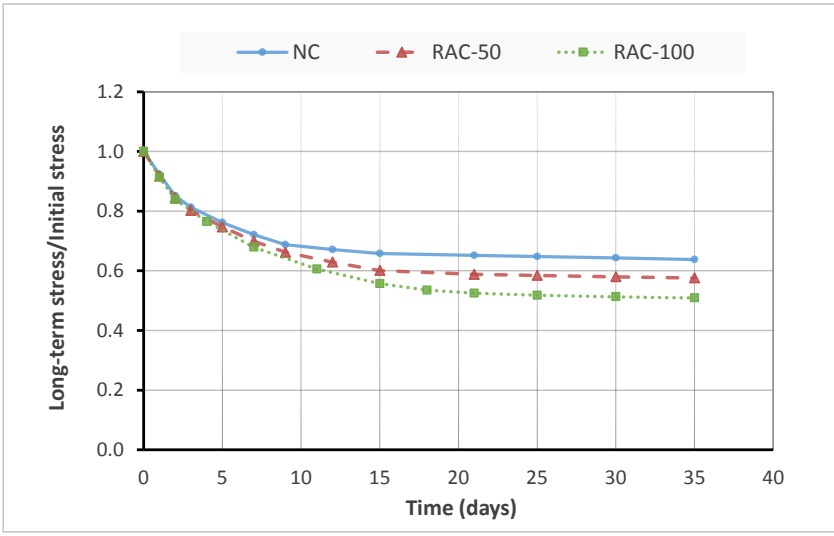

Figure 5-15 Effect of RA on the reduction in tension stiffening over time

As can be seen from both figures, there is a very rapid loss of tension stiffening in all the specimens at the beginning of the test. Up until the 5th day of testing, the percentage reduction in concrete tensile stress in the normal concrete and recycled aggregate concrete specimens is nearly the same (around 25%). After day 5, the data for the recycled aggregate specimens show a higher rate of tension stiffening reduction compared to the normal concrete specimen over time.

The figure also shows that the normal concrete specimen reached the stabilised cracking stage earlier than the RAC specimens which occurred at the 15th and 20th days respectively. After the stabilised cracking stage was reached, the loss of tension stiffening remained constant for all the specimens. On the final day of testing (35th day), the total reduction for the normal concrete specimen was 36.2% while for the RAC specimens, the reductions were 42.4% and 49.1% for the 50% and 100% RA specimens respectively. In other words, by substituting 50% and 100% of the aggregate with recycled aggregate, an increase in the loss of tension stiffening by 6.2% and 12.9% occurs, respectively.

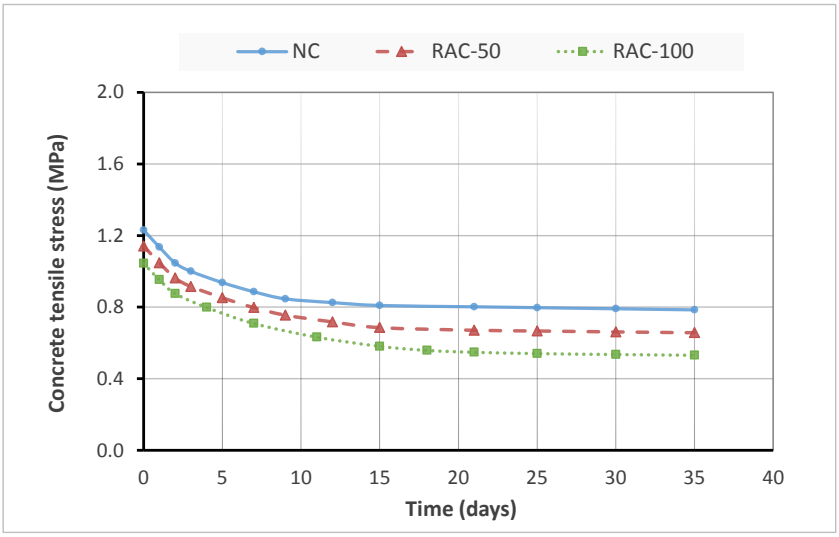

Figure 5-16 Concrete tensile stress as a function of time for NC and RAC specimens

According to the results presented in Figure 5-16, the incorporation of RA also reduced the initial tensile stress in the concrete. Directly after applying the load, tensile stresses of 1.14MPa and 1.04MPa were recorded for the 50% and 100% RA specimens in comparison to 1.23MPa obtained for the normal concrete specimen. This effect reflects the results obtained for the ultimate tensile strength of concrete.

In general, it can be concluded that the higher the replacement percentage of RA, the greater the loss of tension stiffening. This can be attributed to the effect of the inclusion of RA on the properties of the concrete, namely the tensile strength, which is the most significant factor affecting tension stiffening. The decrease in the concrete mechanical properties plays a significant role in the reduction of tension stiffening as mentioned in the literature (Khalfallah and Guerdouh, 2014). Furthermore, the effect of using RA on the microstructure of the ITZ and its influence on the micro-cracking of the concrete matrix under load, as discussed earlier with regards the results of the mechanical properties testing, can also cause the reduction in tension stiffening observed.

Another reason that has been proposed is that the increase in the amount of micro-cracking in the concrete matrix due to the use of RA can influence the bond strength between the concrete and the steel rebar thus having a significant effect on the tension stiffening. Both Ajdukiewicz and Kliszczewicz (2002) and Xiao and Falkner (2007) proposed this idea in their studies as they observed a reduction of 6-12% in bond strength when RA was used. This is also supported by the results of the tensile creep deformations measured in this research as the RAC specimens showed greater tensile deformations than the NC specimen.

Figure 5-17 shows the difference between the final crack distributions of the NC and RAC specimens. It is clear from the figure that a total of four cracks developed in the NC specimen while a total of five cracks developed in both of the RAC specimens. The cracks developed at relatively regular intervals varying between $s < l < 2s$ along the length of the specimen in full agreement with the discussion on crack formation and spacing in the literature (Gribniak et al., 2009). The position of the cracks with respect to the Demec points that were used to measure the strains in the concrete vary from specimen to specimen. However, taking the average strain over the full length of the specimen should ensure that maximum or minimum strain values have not been used when estimating concrete tensile stresses.

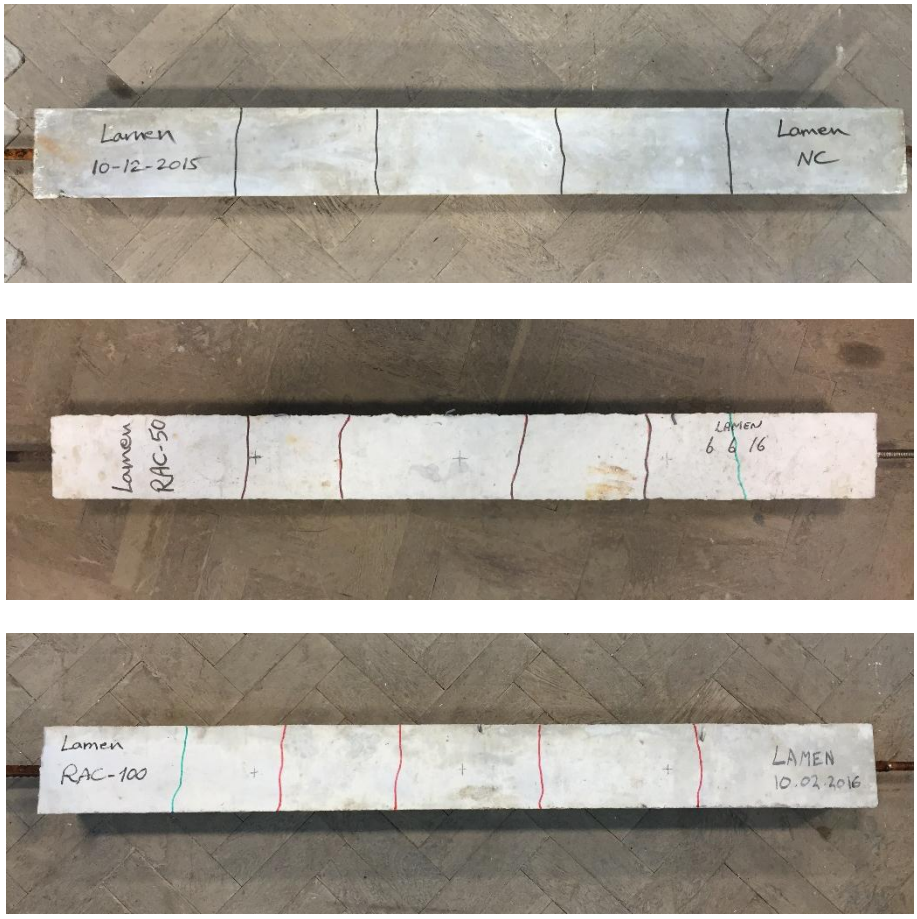

Figure 5-17 Effect of recycled aggregate on crack distribution

Table 5-2 summarises the short and long-term tensile stresses in the concrete for the NC and RAC specimens calculated using Method 1. It is clear from the results that increasing the substitution level of RA decreases the ratio between the long-term and short-term stresses.

Table 5-2 Effect of RA on the concrete tensile stress

Specimen	Short-term stress (MPa)	Long-term stress (MPa)	Ratio
NC	1.23	0.785	0.638
RAC-50	1.14	0.656	0.576
RAC-100	1.04	0.531	0.509

There is good agreement between the results of this research and the results of Scott and Beeby (2005) for normal concrete specimen; they measured short- and long-term stresses in NC specimens of 1.22MPa and 0.84MPa respectively with a ratio of 0.69.

5.4.2 Effect of steel fibres

In this section, the effect of adding steel fibres on the long-term loss of tension stiffening is presented and discussed. More specimens were cast and tested for comparison with the control specimens without fibres as presented in Chapter 4. The experimental results were analysed using Method 1 to assess the loss and to allow comparison between the specimens. The ratio between the long-term concrete stresses and the initial stresses are used to illustrate the loss over time.

Figure 5-18 shows the influence of adding different amounts of steel fibres to normal and recycled aggregate concrete on the reduction in tension stiffening over time. Also, the reductions in the actual concrete tensile stresses are presented as a function of time for all the specimens in Figure 5-19.

Although the specimen (SFRAC-50-0.5) was lost during the test, the statistical regression analysis showed a strong correlation between the other results in a linear relationship which makes this missing cannot influence the general understanding of the behaviour.

As can be observed from the figures, the reduction in tension stiffening follows a similar trend to that recorded for the specimens without steel fibres, however the inclusion of steel fibres has a significant influence on the rate of the reduction. More specifically, after 35 days of loading, the NC specimens that were prepared with 0.5% and 1.0% steel fibres recorded a long-term reduction in tension stiffening of 26.4% and 15.8% respectively, compared to a reduction of 36.2% for the specimen without steel fibres. In other words, reductions in the long-term loss of tension stiffening due to the addition of 0.5% and 1.0% steel fibres decreased by 9.8% and 20.4% respectively.

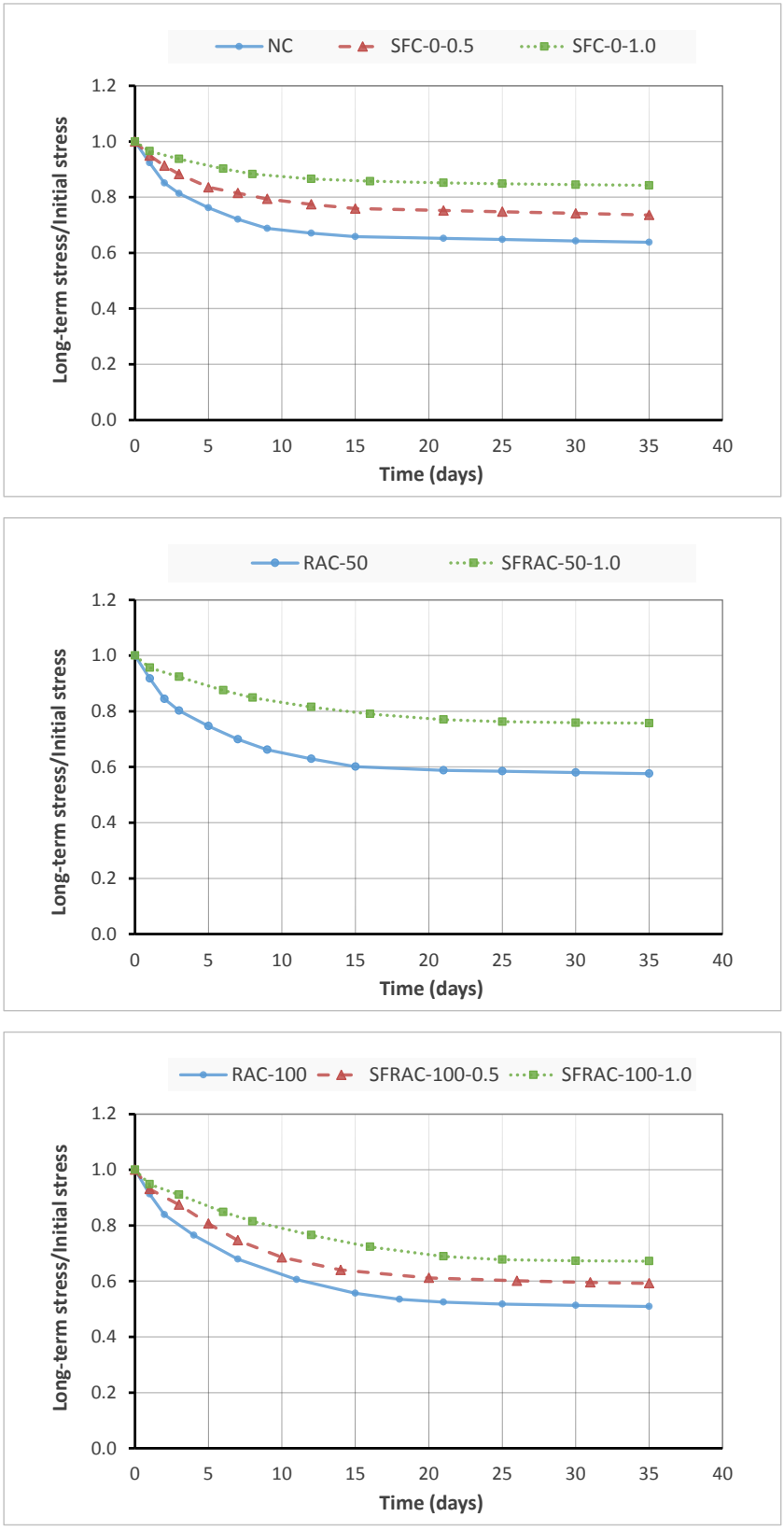

Figure 5-18 Influence of the steel fibres on the reduction rate of tension stiffening over time

For the recycled aggregate concrete specimens, slightly lower percentage reductions were recorded when the RA replacement percentage increased. For example, reductions of 40.8% and 32.8% were measured on the 35th day of testing when 0.5% and 1.0% steel fibres were added to the specimens of 100% RA concrete in comparison to 49.1% for the specimen without steel fibres. This corresponds to a lower reduction of 8.3% and 16.3% in the long-term loss of tension stiffening when 0.5% and 1.0% steel fibres were added, respectively, which is lower than the 9.8% and 20.4% achieved with the NC specimens. In addition, a reduction of 24.3% was calculated for the 50% RA specimens with 1.0% steel fibres which is an 18.1% lower reduction than that for the same sample without fibres.

Figure 5-19 shows the effect of steel fibres on the concrete tensile stress as a function of time. It can be noted that the addition of steel fibres to normal and recycled aggregate concrete enhances the initial tensile stress in the concrete measured directly after applying the load. Specifically, an increase in the initial tensile stress in the concrete of 15% and 30% was obtained due to the addition of 0.5% and 1.0% steel fibres, respectively. This enhancement was similar for both the normal and recycled aggregate concrete specimens and reflects the influence of steel fibres on the tensile strength of concrete.

Generally, the improved performance can be attributed to the contribution of the steel fibres to carrying the tensile load which reduces the strain in the reinforcing bars and hence increases the tension stiffening of the concrete. It arises from the ability of the steel fibres to bridge cracks which increases the stiffness of the concrete section. In this case, the contribution of the steel fibres is two-fold: firstly, at the position of the cracks, the steel fibres govern the crack widths and carry tensile loads across the crack; secondly, they enhance the strength of the concrete in the un-cracked regions. These reasons were discussed in Chapter 3 in the discussion of the short-term response of concrete presented in the literature (de Oliveira Júnior et al., 2016, Lee et al., 2013, Bischoff, 2003).

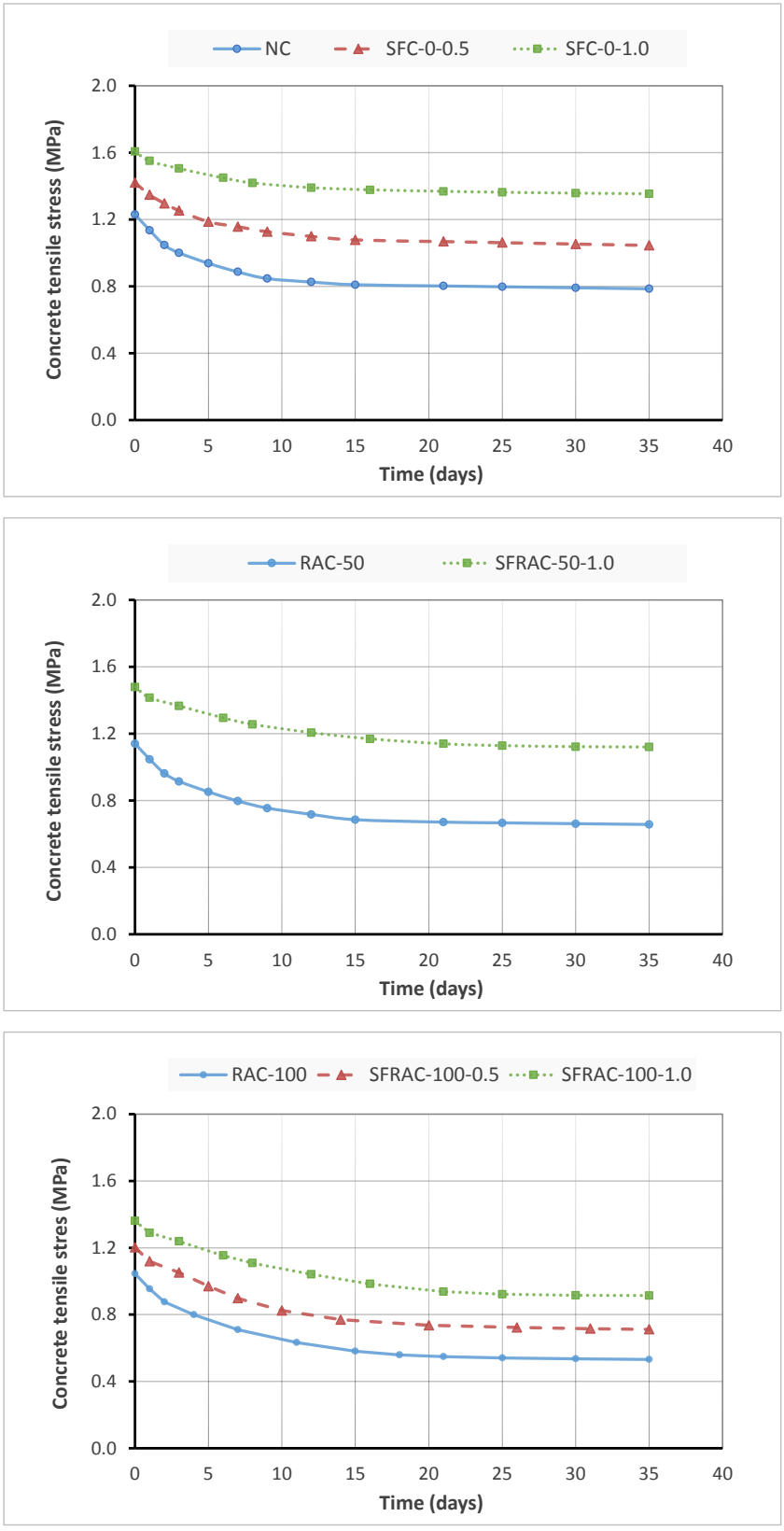

Figure 5-19 Effect of steel fibres on the concrete tensile stresses as a function of time

Figure 5-20 shows the final crack distribution in the normal concrete specimens that were prepared with and without steel fibres. It can be seen that the inclusion of steel fibres did not reduced the final number of cracks along the length of the concrete specimens. However, the contribution of steel fibres in reducing the crack widths and bridging them cannot be ignored in this case.

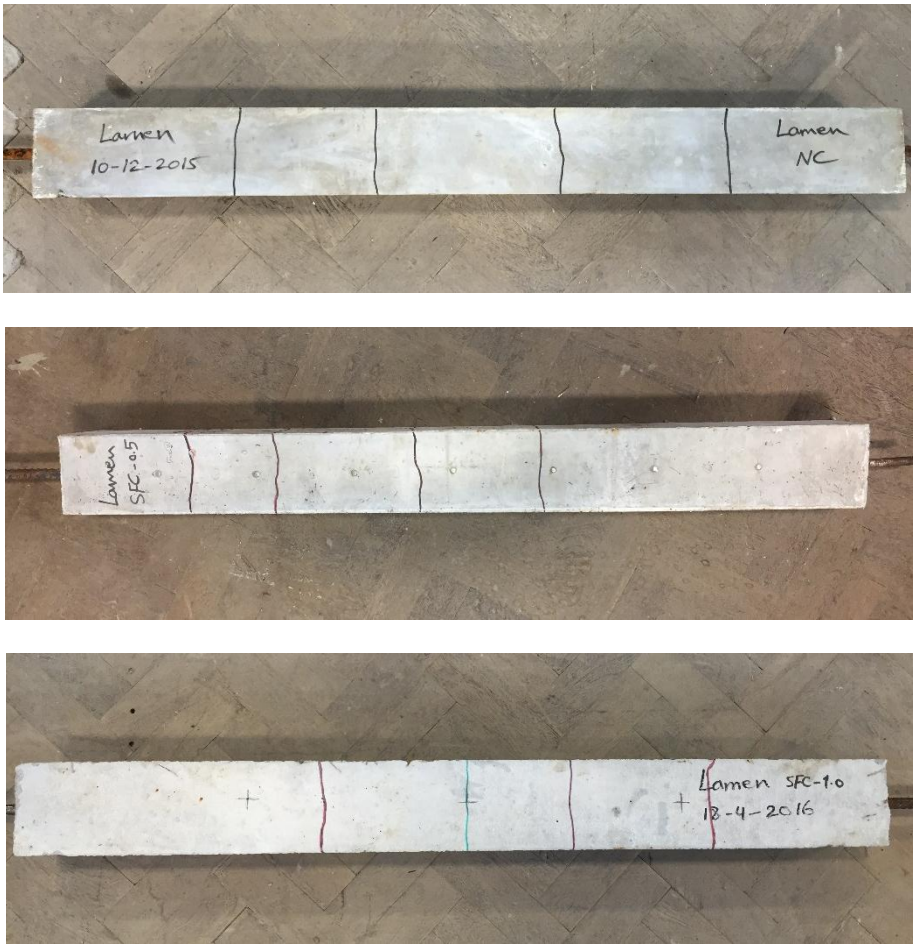

Figure 5-20 Effect of steel fibres on crack distribution

Table 5-3 summarises the short and long-term concrete tensile stresses for the specimens with and without steel fibres that were calculated using Method 1 from the averaged results. It can be concluded that the ratio between the long-term and short-term stress increases with increasing fibre content and decreases with increasing RA replacement percentage.

Table 5-3 Concrete tensile stress results

Specimens	Short-term stress (MPa)	Long-term stress (MPa)	Ratio
NC	1.23	0.785	0.638
SFC-0-0.5	1.42	1.045	0.736
SFC-0-1.0	1.60	1.353	0.845
RAC-50	1.14	0.656	0.576
SFRAC-50-1.0	1.48	1.026	0.693
RAC-100	1.04	0.531	0.509
SFRAC-100-0.5	1.20	0.712	0.592
SFRAC-100-1.0	1.36	0.914	0.672

5.5 Short-term Deflection and Cracking Pattern of Beams

In this section, the results for the short-term deflections and cracking patterns of reinforced concrete beams incorporating recycled aggregate and steel fibres are presented. The results are for the short-term mid-span deflections of beams subjected to an applied load from 0 to 23KN (the value of the sustained load). The effects of recycled aggregate and steel fibres on the results are discussed. The experimental results are summarised in Table 5-4.

5.5.1 Effect of recycled aggregate

Figure 5-21 shows the relationship between the applied load and the short-term mid-span deflection of the beams prepared with different replacement percentages of RA. The results indicate that the overall trend of the load-deflection curves for the concrete beams containing RA was similar to that of the normal concrete beam. However, the incorporation of RA had a noticeable effect on the magnitude of the short-term deflection. More specifically, the mid-span deflection increased by about 8% and 15% when 50% and 100% RA was used respectively. Furthermore, the first cracking loads measured for the beams containing RA were about 15% and 30%

lower than that for the normal concrete beam. This can be attributed to the effect of recycled aggregate on the strength properties of concrete, namely the tensile and flexural strength, as discussed previously.

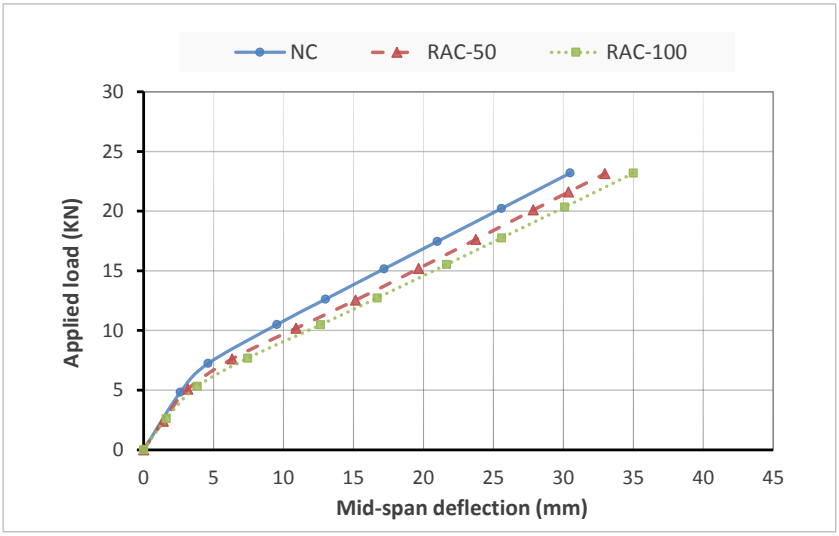

Figure 5-21 Effect of recycled aggregate on short-term deflection

Moreover, the RAC beams exhibited different cracking patterns to the NC beam. Wider and more closely spaced cracks were observed in the RAC specimens in the stabilised cracking stage as detailed in Table 5-5 and Figure 5-22.

The lower tensile strength measured for the RAC and the lower bond strength in RAC compared to NC observed in previous research (Ajdukiewicz and Kliszczewicz, 2002, Xiao and Falkner, 2007) were thought to be the main reasons for the differences in the observed cracking patterns.

Furthermore, an increased amount of cracking in the RAC beams was expected due to the decrease in the modulus of rupture when RA is incorporated in concrete (see section 5.2.3). The results obtained in this research are similar to those discussed in the literature.

Figure 5-22 Effect of recycled aggregate on cracking pattern

5.5.2 Effect of steel fibres

The effect of the addition of steel fibres to normal and recycled aggregate concrete on the short-term mid-span deflection is presented in Figure 5-23. The inclusion of 0.5% and 1.0% steel fibres had a very similar effect on the short-term defection of both NC and RAC beams. Specifically, reductions of about 11% and 20% in the short-term deflection were recorded when 0.5% and 1.0% steel fibres were incorporated.

In addition, the data show that the SFRC beams had greater first cracking loads. Approximately the same increase of 18% and 34% in the values of first cracking load were obtained when 0.5% and 1.0% steel fibres were incorporated respectively in NC and RAC. The ability of steel fibres to enhance the flexural rigidity of concrete structures is the main reason for the decrease in the short-term deflections of the beams. Moreover, the effect of the addition of steel fibres on the tensile and flexural strength of concrete (as presented in Sections 5.2.2 and 5.2.3) and their contribution to controlling crack development are the reasons for the observed increase in first cracking loads.

With regards the cracking pattern during the stabilised cracking stage, the SFRC beams had a lower number of narrower cracks as summarised in Table 5-5 and shown in Figure 5-24. This can be attributed to the role of steel fibres as crack arrestors in governing crack propagation (as discussed earlier in Section 2.10).

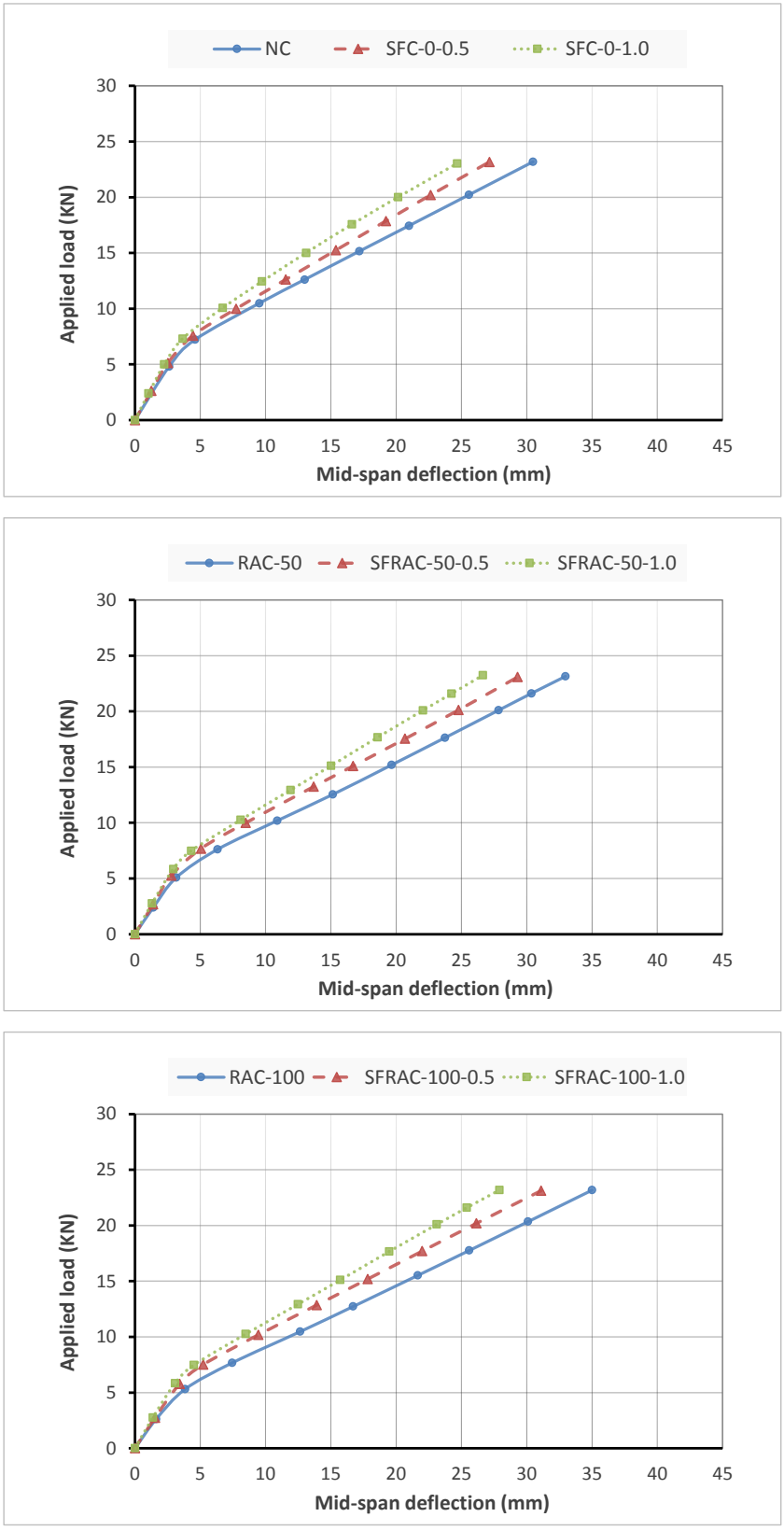

Figure 5-23 Effect of steel fibres on the short-term deflection

Figure 5-24 Effect of steel fibres on the cracking pattern

5.6 Long-term Deflection of Beams

As presented in Chapter 4, full-scale reinforced concrete beams (300x150x4200mm) were subjected to a sustained load for 90 days in order to examine the long-term flexural behaviour. The effect of incorporating recycled aggregate and steel fibres on long-term deflection was investigated. In this section, the experimental results summarised in Table 5-4 are presented and discussed.

Table 5-4 Short-term and long-term deflections of beams tested

Specimen	Short-term deflection (mm)	Long-term deflection (mm)
NC	30.49	18.30
SFC-0-0.5	27.15	16.40
SFC-0-1.0	24.68	14.94
RAC-50	32.97	21.99
SFRAC-50-0.5	29.29	19.72
SFRAC-50-1.0	26.65	17.98
RAC-100	35.00	25.36
SFRAC-100-0.5	31.10	22.78
SFRAC-100-1.0	27.91	20.79

5.6.1 Effect of recycled aggregate

Figure 5-25 shows the effect of incorporating recycled aggregate on long-term mid-span beam deflection. In general, the beams tested showed a similar trend in deflection over time, i.e. the deflection increased continuously with time. It is clear from the results that the increase in long-term deflection was much more rapid during the first 20 days of loading. The majority of the long-term deflection (about 65%) occurred during this time. Furthermore, the results indicate that increasing the replacement ratio of RA resulted in significant increases in long-term deflection. The long-term deflection increased by 20% and 38% as a result of replacing 50% and 100% of the aggregate, respectively. This was attributed to the effect of RA on the

properties of the concrete, in particular the time-dependent deformation (e.g. creep and shrinkage).

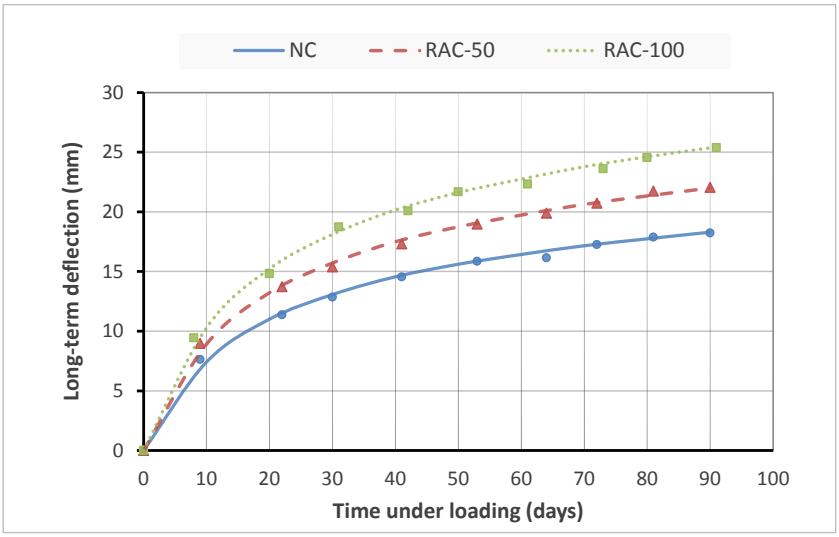

Figure 5-25 Effect of recycled aggregate on long-term deflection

In terms of crack development, the cracks in the RAC beams extended slightly further up the height of the section than those in the NC beams, as shown in Figure 5-22. Also, the cracks were wider in the RAC beams under sustained load, as summarised in Table 5-5, which agrees with the observations reported in the literature (Choi and Yun, 2013). It is clear from the results that the percentage increase in crack width decreased with increasing replacement ratio. This is because of the increased number of cracks with increasing RA replacement ratio which reduced the space between cracks and hence altered the distribution of the total displacement due to crack widening.

Figure 5-26 shows the effect of replacing the natural aggregate on the surface strains within the compression zone (measurements were taken at the compressive reinforcement level) and tension zone (measurements were taken at the tensile reinforcement level) of the beams over time. The strains presented are the long-term strains which occurred after the beams were loaded to 23KN (the initial strain was subtracted). The results show that the strain in all of the beams generally increased throughout the test duration. An increase in strain of 16% and 36% was observed in both zones when 50% and 100% of RA was used, respectively. This

increase is thought to be due to the effect of the RA on the creep, shrinkage and long-term loss of tension stiffening of the concrete.

The compressive strains increased continually during the first stage of loading (up to 20 days) after which they increased less rapidly. This is related to the effect of creep and shrinkage which were previously found to slow at this stage and reach a nearly constant increase. Within the early stages of loading (0-10 days), the tensile strains increased dramatically; however, after this initial activity, the rate of increase for all beams slowed. This can be attributed to the loss of tension stiffening with time similar to that seen in the experimental results discussed earlier which is in line with the conclusions of Whittle and Jones (2004) and Scott and Beeby (2005).

Table 5-5 Details of cracks at stabilised cracking stage

Specimen	Number of cracks	Space between cracks (mm)	Crack width (mm)	
			t_0	t_{90}
NC	16	110	0.10	0.16
SFC-0-0.5	14	120	0.08	0.12
SFC-0-1.0	13	125	0.06	0.10
RAC-50	18	90	0.16	0.24
SFRAC-50-0.5	16	100	0.14	0.20
SFRAC-50-1.0	14	115	0.12	0.16
RAC-100	20	70	0.20	0.30
SFRAC-100-0.5	19	80	0.17	0.25
SFRAC-100-1.0	17	95	0.15	0.20

** The results are the average of the readings from both sides of the specimens.*

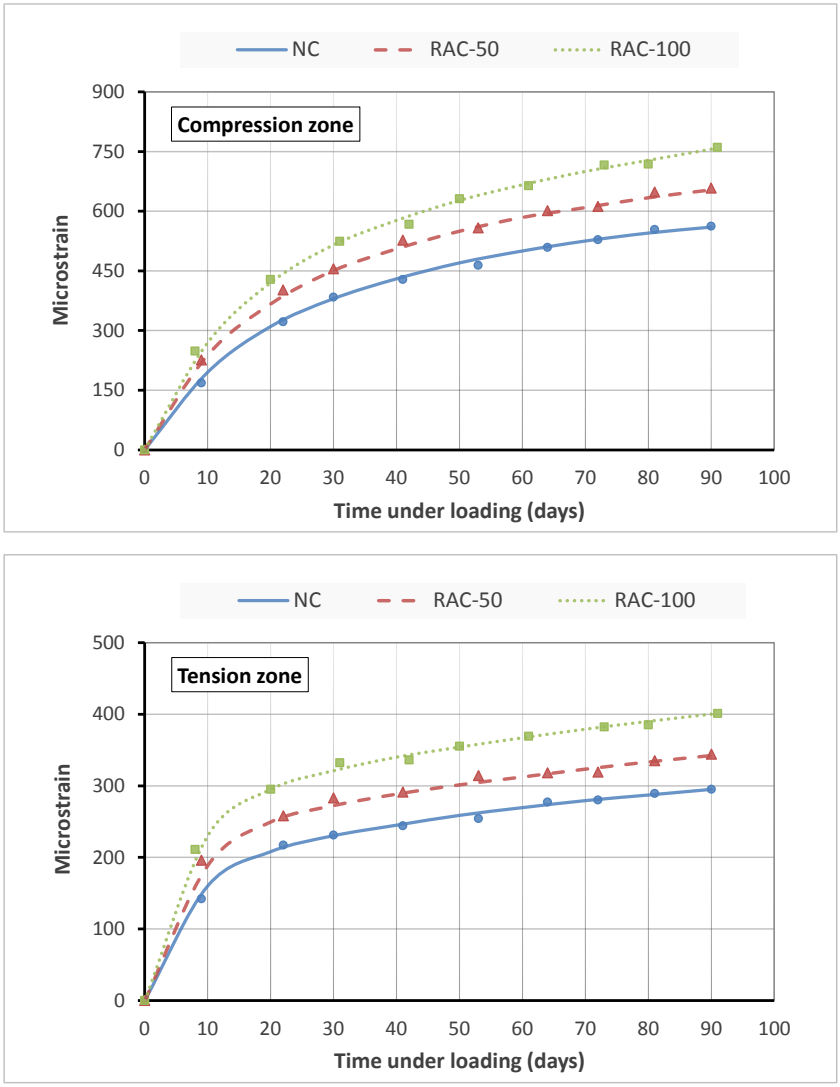

Figure 5-26 Effect of recycled aggregate on the development of concrete surface strains in the compression and tension zones

5.6.2 Effect of steel fibres

The effect of the addition of steel fibres to normal and recycled aggregate concrete beams on the long-term deflection is presented in Figure 5-27. In general, all the beams exhibited the same trend of increasing long-term deflection with time and the higher the steel fibre content, the smaller the long-term deflection. According to the figure and the results presented in Table 5-4, it can be deduced that the incorporation of steel fibres has a similar effect on the long-term deflection of both NC and RAC beams. More specifically, the addition of 0.5% and 1.0% steel fibres reduced long-term deflection by 10% and 20% respectively. In addition, with

increasing the steel fibre content, the cracks in the SFRC beams were shorter and narrower than those in the NAC and RAC beams without fibres as shown in Figure 5-24 and summarised in Table 5-5. This is due to the steel fibres enhancing the concrete properties, increasing the stiffness of the concrete members and governing crack development.

Figures 5-28 and 5-29 illustrate the effect of the addition of steel fibres on the development of concrete surface strains in the compression and tension zones. It is obvious that steel fibres have a similar effect on the strains in the NC and RAC beams. The same continual increase during the first 20 days was noticed in the compressive strain curves and the same dramatic increase during the first 10 days was noticed in the tensile strain curves for all the beams tested. As discussed before, this is due to the creep, shrinkage and loss of tension stiffening that affect the long-term behaviour of concrete members.

The addition of 0.5% and 1.0% steel fibres decreased the strains in the compression zone by 7% and 13% and in the tension zone by 13% and 25%, respectively. It is clear that the effect of the incorporation of steel fibres is greater in the tension zone than in the compression zone. This is thought to be due to the fact that steel fibres have a greater effect on the tensile response than on the compressive response of concrete. This effect was evident in the results of the compressive and tensile creep experiments. In addition, the steel fibres affect the loss of tension stiffening over time as discussed in earlier sections. This difference in behaviour may change the assumptions behind the theoretical methods used to calculate the long-term deflections of concrete beams which will be discussed in detail in the next chapter.

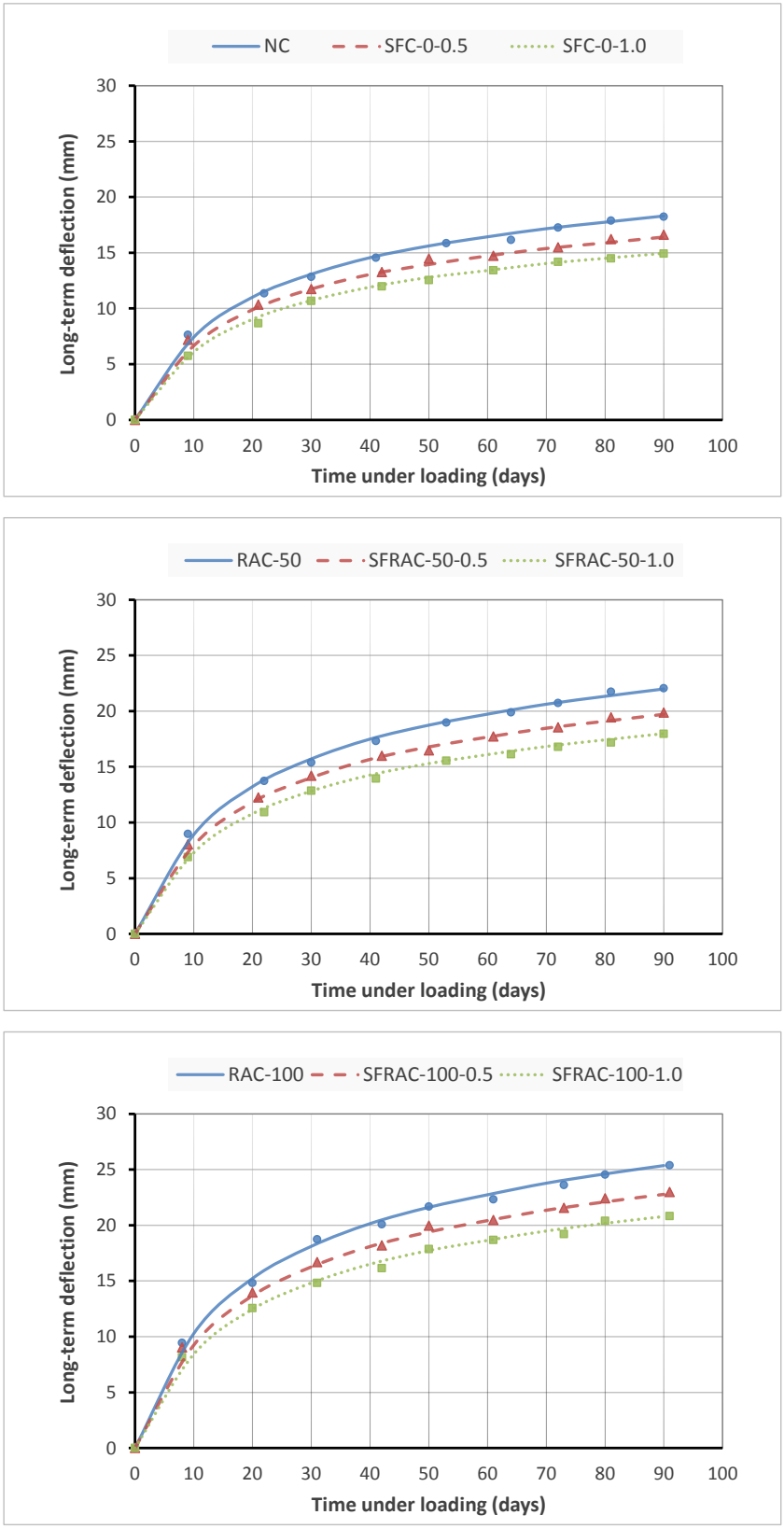

Figure 5-27 Effect of steel fibres on long-term deflection

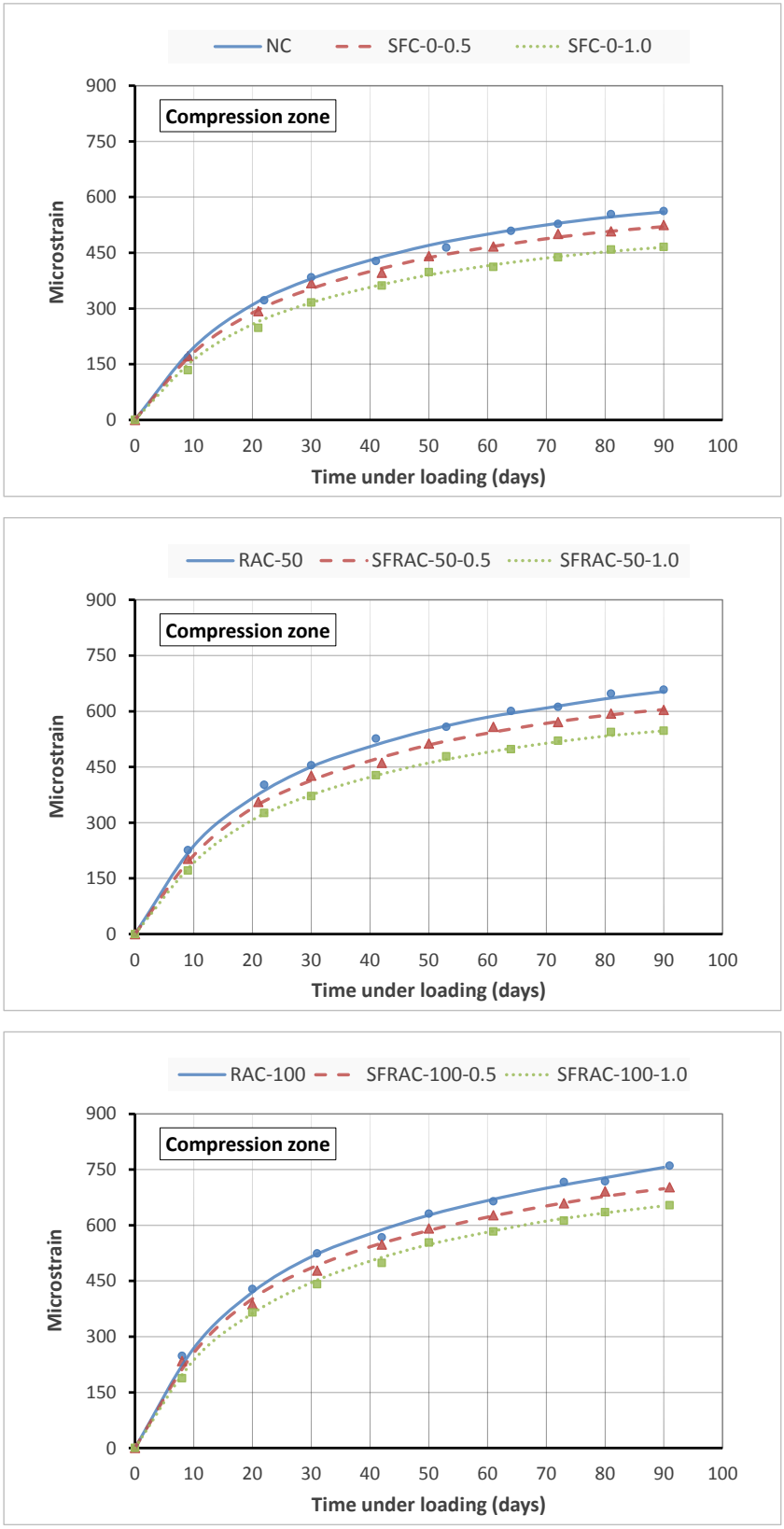

Figure 5-28 Concrete surface strains of beams in compression zone

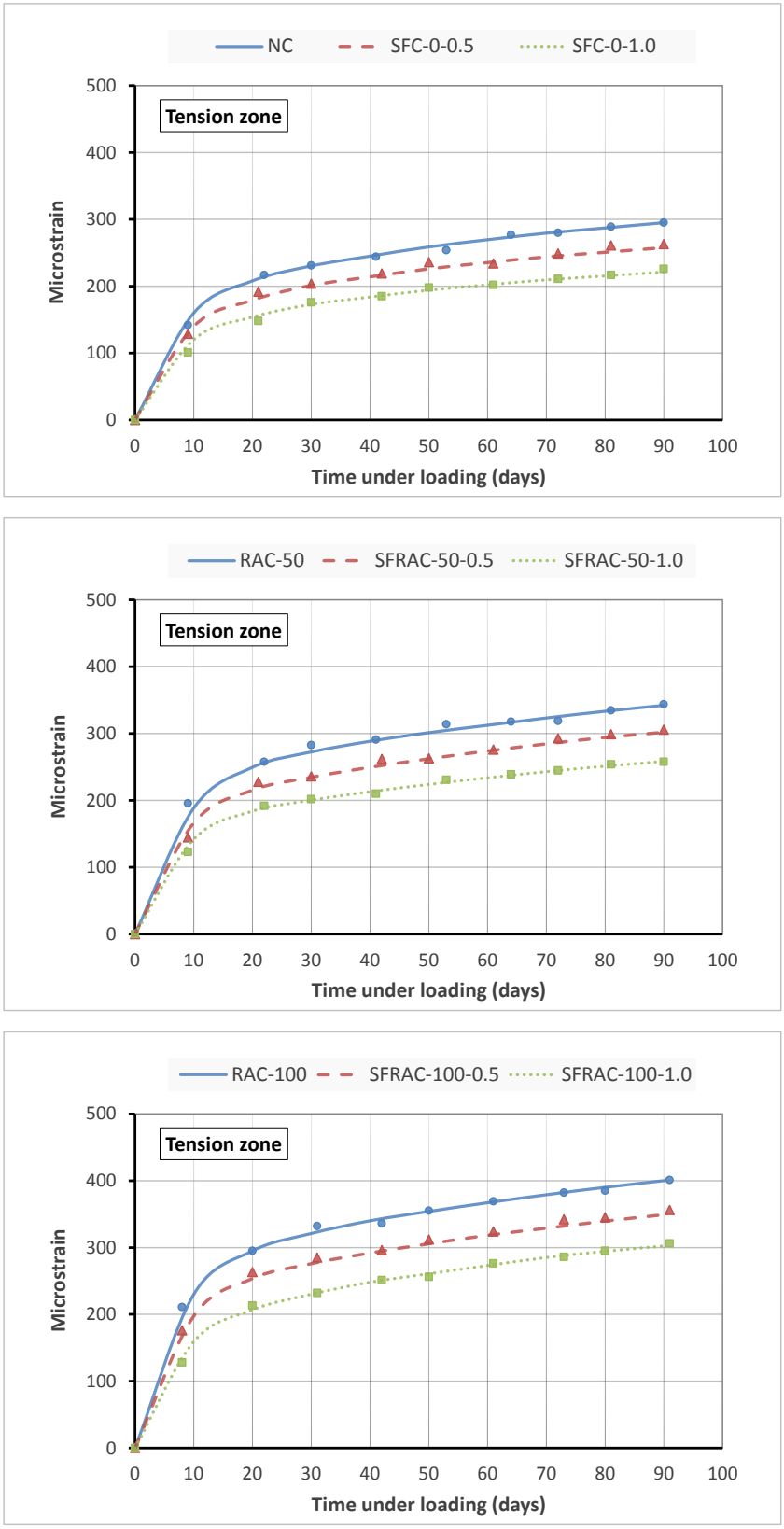

Figure 5-29 Concrete surface strains of beams in tension zone

5.7 Conclusion

The principal findings from the experimental results presented in this chapter are outlined below:

- In general, it can be deduced that the incorporation of 50% RA with 0.5% steel fibres or 100% RA with 1.0% steel fibres could result in concrete with strength properties, time-dependent deformations and flexural responses similar to equivalent conventional concrete. Improved properties were obtained when 50% RA and 1.0% steel fibres were incorporated.
- The addition of steel fibres to recycled aggregate concrete succeeded in enhancing the properties of the resulting concrete and the flexural behaviour of beams. In particular, the serviceability (short and long-term deflections and crack development) improved which could reduce the limitations on the use of RAC.
- The compressive strength of cylindrical specimens exhibited greater increase due to the addition of fibres than the increase observed for cubic specimens. The reason for this was thought to be the orientation of the fibres with respect to the applied load.
- Replacing the NA by RA had a negative effect on the drying shrinkage and creep deformation. With increasing the amount of RA the deformations increase. In contrast, adding steel fibres to the concrete resulted in significant reductions in drying shrinkage strains.
- Incorporating steel fibres resulted in significant reductions in tensile creep deformation. However, it had less effect on compressive creep.
- The substitution of NA by RA increased the loss of tension stiffening over time while the addition of steel fibres to NC and RAC had a significant influence on the reduction in tension stiffening over time.
- The experimental results indicated that the overall trend of load-deflection behaviour of the concrete beams containing RA was similar to the behaviour of the conventional concrete beam. However, the incorporation of RA had a noticeable effect on increasing the first cracking loads and the short-term deflection and the inclusion of steel fibres had considerable effect on reducing these aspects.

- With regards the cracking pattern at the stabilised cracking stage, the RAC beams showed different cracking patterns to the NC beam. Wider and more closely spaced cracks were observed in the RAC specimens. In contrast, the effect of the addition of steel fibres was the opposite. The SFRC beams made with NC and RAC had fewer and narrower cracks compared to those without steel fibres.
- The experimental results indicated that increasing the replacement percentage of RA resulted in significant increases in long-term deflection.
- The addition of steel fibres to the normal and recycled aggregate concrete beams significantly affected the long-term deflection and the higher the steel fibres content, the smaller the long-term deflection.
- Both recycled aggregate and steel fibres had a significant effect on crack development in beams under sustained loads. The cracks in the RAC beams extended further up the height of the section than those in the NC beams and were wider under sustained loads. Increasing the steel fibres content resulted in shorter and narrower cracks in the SFRC beams compared to those in the NC and RAC beams without fibres.
- Replacing the aggregate resulted in an increase in the surface strains in the compression and tension zones of the beams tested.
- The addition of steel fibres decreased the long-term strains in the compression and the tension zones in all types of beams tested. The effect of steel fibres on reducing the strains in the tension zone is greater than that in the compression zone.
- The difference in the effect of steel fibres on the tensile and compressive response of concrete was also clear in the results of the compressive and tensile creep tests. The role of steel fibres in enhancing tension stiffening will change the assumptions behind the theoretical calculations for the long-term deflection of concrete beams which will be discussed in detail in the next chapter.

Chapter 6 : Analytical Investigation

6.1 Introduction

In this chapter, the principal aim of the work presented is to evaluate the suitability of existing code procedures (ACI, CSA, AS3600 and Eurocode 2) for predicting the long-term deflection of normal reinforced concrete beams and to develop an appropriate approach for reinforced concrete beams incorporating recycled aggregate and steel fibres. Firstly, the code methods are evaluated in terms of the calculation steps and the parameters included in each method which affect the predictions of long-term flexural behaviour. This is followed by a discussion of the limitations of the method selected for use in this study and modifications are proposed based on a comparison between the experimental results and code predictions. In addition, a numerical program will be presented which has been developed in the MATLAB language to include the proposed modifications for predicting the long-term deflection of reinforced concrete beams. The experimental results from other studies available in the literature have also been used to validate the method developed.

6.2 Existing Code Procedures for Long-term Deflection

The deflection of reinforced concrete members under constant sustained loads is influenced by the following factors:

- Creep of the concrete.
- Shrinkage of the concrete.
- Non-symmetrical reinforcement.
- Crack development.
- Loss of tension stiffening.

The interaction between these complex factors makes the prediction of long-term deflections of reinforced concrete members complicated. Therefore, a number of approaches have been proposed in international design codes with different

degrees of simplification and accuracy. In this section, the calculation steps in the most common and reliable code procedures are presented and discussed.

6.2.1 ACI-318

The American Concrete Institute (ACI) proposed a method in ACI-318 for calculating the instantaneous deflections of reinforced concrete beams based on the elastic analysis of un-cracked and fully-cracked sections. In this method, the effect of tension stiffening is taken into account when calculating the effective second moment of inertia (I_e) of the beam, as proposed by Branson (1977), which is found by interpolating between the un-cracked (I_g) and cracked (I_{cr}) values, as follows:

$$I_e = \left(\frac{M_{cr}}{M_a}\right)^3 I_g + \left[1 - \left(\frac{M_{cr}}{M_a}\right)^3\right] I_{cr} \quad \leq I_g \qquad \textbf{(6-1)}$$

Where:

M_{cr} = the cracking moment

M_a = the applied moment

I_g = the second moment of area of the gross section

I_{cr}= the second moment of area of the fully-cracked section

The instantaneous deflection (Δ_i) of a simply supported beam which is reinforced by top and bottom steel bars and subjected to a bending moment can thus be calculated as follows:

$$f_r = 0.62\sqrt{f_c`} \qquad \textbf{(6-2)}$$

$$M_{cr} = \frac{f_r\, I_g}{y_t} \qquad \textbf{(6-3)}$$

$$y_u = \frac{\frac{bh^2}{2} + (n-1)(A_s d + A_s` d`)}{bh + (n-1)(A_s + A_s`)} \qquad \textbf{(6-4)}$$

$$I_g = \frac{bh^3}{12} + bh\left(\frac{h}{2} - y_u\right)^2 + (n-1)A_s(d - y_u)^2 + (n-1)A_s`(y_u - d`)^2 \qquad \textbf{(6-5)}$$

$$y_c = \frac{[(nA_s + (n-1)A_s`)^2 + 2b(nA_s d + (n-1)A_s` d`)]^{0.5} - (nA_s + (n-1)A_s`)}{b} \qquad \textbf{(6-6)}$$

$$I_{cr} = \frac{by_c{}^3}{12} + nA_s(d - y_c)^2 + (n-1)A_s`(y_c - d`)^2 \quad \textbf{(6-7)}$$

$$I_e = \left(\frac{M_{cr}}{M_a}\right)^3 I_g + \left[1 - \left(\frac{M_{cr}}{M_a}\right)^3\right] I_{cr} \ \leq I_g \quad \textbf{(6-8)}$$

$$\Delta_i = K\frac{M_a l^2}{E_c I} \quad \textbf{(6-9)}$$

Where:

K = a factor depending on support fixity and loading conditions

$I = I_g$ when $M_a \leq M_{cr}$ (section is un-cracked)

$I = I_e$ when $M_a > M_{cr}$ (section is cracked)

The additional long-term deflection (Δ_l) under sustained loading can be calculated using Branson`s Equation (Branson, 1977) by applying a multiplier factor (λ) to the instantaneous deflection. This multiplier factor includes the combined effects of creep and shrinkage on the deflection over time as given:

$$\lambda = \frac{\zeta}{1 + 50\rho`} \quad \textbf{(6-10)}$$

$$\Delta_l = \lambda\Delta_i \quad \textbf{(6-11)}$$

Where:

ζ = a time-dependent factor which can be determined from Figure 6-1

$\rho`$ = the compression reinforcement ratio $= A_s`/bd$

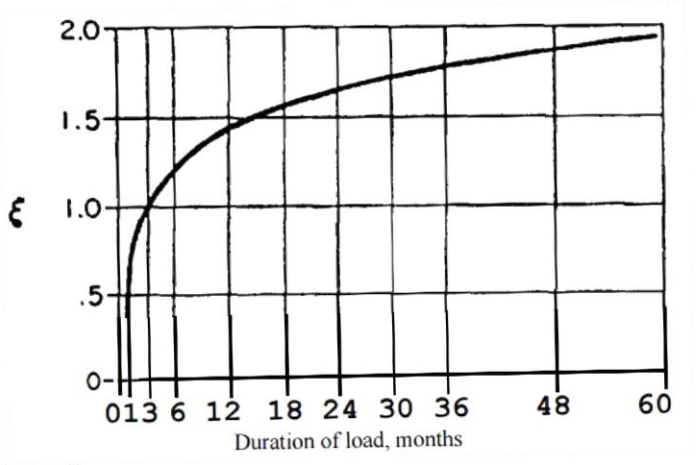

Figure 6-1 ACI multiplier factor for long-term deflection

Hence, the total deflection can be obtained by:

$$\Delta_t = \Delta_i + \lambda \Delta_i \quad \textbf{(6-12)}$$

Although the use of the multiplier factor method to calculate the long-term deflection is a simple method for practical purposes, research has shown that it does not always lead to accurate predictions due to time-dependent effects. As noted by many researchers (Gilbert, 1999, Ghali and Azarnejad, 1999, Taha and Hassanain, 2003, Araújo, 2005, Beeby et al., 2005, Vakhshouri and Nejadi, 2014), it is impossible to account for all the factors affecting long-term deflection with a single multiplier factor which depends only on time and compression reinforcement ratio. Using a single multiplier to predict the time-dependent deformations of concrete structures cannot represent and estimate all uncertainties arising from changes in the material properties, the geometry of the member, and the ambient conditions such as temperature and relative humidity. Therefore, several researchers have attempted to develop alternative methods in order to include other effects (e.g. high compressive strength and addition of additives) when predicting long-term deflections.

6.2.2 ACI-435

A different technique was proposed in ACI-435 for calculating the long-term deflection due to creep and shrinkage. This method is based on equations developed by Branson (1977) for the separate computation of deflections due to creep (Δ_{cr}) and shrinkage (Δ_{sh}) as follows:

$$\Delta_{cr} = \lambda_c \Delta_i \quad \textbf{(6-13)}$$

$$\Delta_{sh} = K_{sh} \phi_{sh} l^2 = K_{sh} \left[A_{sh} \times \frac{\varepsilon_{sh}(t, t_0)}{h} \right] l^2 \quad \textbf{(6-14)}$$

Where:

λ_c = the creep deflection constant:

$$\lambda_c = \frac{0.85\ \varphi(t, t_0)}{1 + 50\rho`} \quad \textbf{(6-15)}$$

K_{sh} = the shrinkage deflection constant:

$$K_{sh} = \begin{matrix} 0.5\ \ (for\ cantilevers) \\ 0.13\ \ (for\ simple\ beams) \end{matrix} \quad \textbf{(6-16)}$$

A_{sh} = the shrinkage deflection multiplier:

$$A_{sh} = \begin{cases} 0.7(\rho - \rho`)^{\frac{1}{3}}\left(\frac{\rho - \rho`}{\rho}\right)^{1/2} & (for\ \rho - \rho` \leq 3.0\%) \\ 0.7\rho^{1/3} \quad (for\ \rho` = 0) \\ 1.0 \quad (for\ \rho - \rho` > 3.0\%) \end{cases} \qquad \textbf{(6-17)}$$

$\varphi(t, t_0)$ = the creep coefficient at time t (days), which can be obtained from the method in ACI-209 for normal concrete:

$$\varphi(t, t_0) = \left[\frac{t^{0.6}}{10 + t^{0.6}}\right]\varphi_u \qquad \textbf{(6-18)}$$

$$\varphi_u = 2.35\gamma_{cr} \qquad \textbf{(6-19)}$$

γ_{cr} = the creep modification factor for nonstandard conditions:

$$\gamma_{cr} = K_{t0}^c K_{RH}^c K_{vs}^c K_s^c K_\psi^c K_\alpha^c \qquad \textbf{(6-20)}$$

$\varepsilon_{sh}(t, t_0)$ = the shrinkage strain at time t (days), which can be obtained from the method in ACI-209 for normal concrete:

$$\varepsilon_{sh}(t, t_0) = \left[\frac{t}{35 + t}\right]\varepsilon_{sh_u} \qquad \textbf{(6-21)}$$

$$\varepsilon_{sh_u} = 780 \times 10^{-6}\gamma_{sh} \qquad \textbf{(6-22)}$$

γ_{sh} = the shrinkage modification factor for nonstandard conditions:

$$\gamma_{sh} = K_{tc}^{sh} K_{RH}^{sh} K_{vs}^{sh} K_s^{sh} K_\psi^{sh} K_\alpha^{sh} K_c^{sh} \qquad \textbf{(6-23)}$$

The resulting total deflection is therefore:

$$\Delta_t = \Delta_i + \Delta_{cr} + \Delta_{sh} \qquad \textbf{(6-24)}$$

Although the calculation steps in this method can be used to compute separate values for the deflections due to creep and shrinkage, some parameters (e.g. cracking and tension stiffening) which can also influence long-term deflection are not considered. Researchers have indicated that this method might be preferable for use in some practical applications when a portion of the live load is considered as a sustained load. However, it still needs to be developed to provide more accurate predictions.

6.2.3 CSA

Similar to the ACI-318 approach, the Canadian Standard Association recommended the use of the multiplier factor approach in the Design of Concrete Structures (CSA-A23.3) for estimating the long-term deflection of reinforced concrete members subject to sustained service loads. This deflection can be estimated using the following equation:

$$\Delta_l = \left(\frac{S_t}{1 + 50\rho`}\right) \Delta_i \qquad \textbf{(6-25)}$$

The value of S_t is determined according to the duration of the loading as shown in Table 6-1, where it can be seen that the value of S_t increases with the duration of the sustained load until it reaches a maximum of 2 for $t \geq 5$ years.

Table 6-1 Values of the multiplier factor S_t for long-term deflection calculations

Duration of the sustained load	S_t
3 months	1.0
6 months	1.2
12 months	1.4
5 years or more	2.0

6.2.4 AS3600

The Australian Standard for Concrete Structures (AS3600) proposed a simple approach for calculating the additional long-term deflection caused by creep and shrinkage. This method can be used to approximate the long-term curvature (k_l) of a beam by multiplying the short-term curvature (k_i) by a multiplier factor (k_{cs}):

$$k_{cs} = \left[2 - 1.2\left(\frac{A_{sc}}{A_{st}}\right)\right] \geq 0.8 \qquad \textbf{(6-26)}$$

$$k_l = k_{cs} k_i \qquad \textbf{(6-27)}$$

$$k_i = \frac{M_s}{E_c I_{ef}} \qquad \textbf{(6-28)}$$

$$I_{ef} = \frac{I_{cr}}{1 - \left(1 - \frac{I_{cr}}{I_u}\right)\left(\frac{M_{cr}}{M_s}\right)^2} \leq 0.6 I_u \quad \textbf{(6-29)}$$

$$M_{cr} = Z f_{ct,f} \quad \textbf{(6-30)}$$

Where:

A_{sc} = the area of steel in the compression zone

A_{st} = the area of steel in the tension zone

M_s = the sustained moment

M_{cr} = the first cracking moment

I_u and I_c = the second moments of area of the un-cracked and cracked sections

Z = the section modulus

$f_{ct,f}$ = the flexural tensile strength of concrete

As discussed earlier, many researchers believe that using a multiplier factor to calculate the long-term deflection fails to adequately estimate the final deflection of concrete structures. This is because the actual effect of each of the parameters that can cause long-term deflection are not considered separately. More specifically, the multiplier approach ignores the effects of the creep and shrinkage characteristics of the concrete, the loss of tension stiffening over time, the age at first loading and the environmental conditions. Furthermore, relating the final deflection of concrete structures to the short-term deflection is fundamentally incorrect, as, for example, shrinkage can lead to a considerable deflection over time even when no load is applied.

Another approach has been recommended in the Australian Standard (AS3600) that was originally proposed in 2001 (Gilbert, 2001a) and then subsequently modified in 2012 (Gilbert, 2012) by Raymond Gilbert to include the effects of cracking and tension stiffening. In this approach, the long-term curvature due to creep and shrinkage are calculated separately for un-cracked and fully-cracked sections. Then, similar to the method in Eurocode 2, the average curvature is obtained from:

$$k_{avrg} = \xi\, k_{cr} + (1 - \xi)\, k_{uncr} \quad \textbf{(6-31)}$$

$$\xi = 1 - \left(\frac{M_{cr.t}}{M_s}\right)^2 \quad \textbf{(6-32)}$$

Where:

$M_{cr.t}$ = the first cracking moment at the time under consideration = 0.7 M_{cr}

In addition, for any cross section, and at any time, the curvature induced by creep (k_c) can be estimated from:

$$k_c(t, t_0) = k_i \frac{\varphi_c(t, t_0)}{\alpha} \quad \textbf{(6-33)}$$

Where α is a term used to account for the effect of cracking and the quantity of reinforcement. It is expressed as:

For cracked reinforced concrete sections ($M_s \geq M_{cr}$), $\alpha = \alpha_{cr}$:

$$\alpha_{cr} = [0.48\rho^{-0.5}]\left[1 + (125\rho + 0.1)\left(\frac{A_{sc}}{A_{st}}\right)^{1.2}\right] \quad \textbf{(6-34)}$$

For un-cracked reinforced concrete sections ($M_s < M_{cr}$), $\alpha = \alpha_{uncr}$:

$$\alpha_{uncr} = [1 - 15\rho]\left[1 + (140\rho - 0.1)\left(\frac{A_{sc}}{A_{st}}\right)^{1.2}\right] \quad \textbf{(6-35)}$$

$$\rho = \frac{A_{st}}{bd_o} \quad \textbf{(6-36)}$$

Where:

d_o = the depth from the extreme compressive reinforcement to the centroid of the tensile reinforcement

Hence, the final curvature due to creep is given by:

$$(k_c)_{avrg} = \xi\,(k_c)_{cr} + (1 - \xi)\,(k_c)_{uncr} \quad \textbf{(6-37)}$$

The curvature induced by shrinkage can be estimated from:

For a cracked section:

$$(k_{sh})_{cr} = 1.2\left[1 - 0.5\frac{A_{sc}}{A_{st}}\right]\left[\frac{\varepsilon_{sh}}{d_o}\right] \quad \textbf{(6-38)}$$

For an un-cracked section:

$$(k_{sh})_{uncr} = [100\rho - 2500\rho^2]\left[\frac{d_o}{0.5D} - 1\right]\left[1 - \frac{A_{sc}}{A_{st}}\right]^{1.3}\left[\frac{\varepsilon_{sh}}{D}\right] \qquad \rho \leq 0.01 \qquad \textbf{(6-39)}$$

$$(k_{sh})_{uncr} = [40\rho - 0.35]\left[\frac{d_o}{0.5D} - 1\right]\left[1 - \frac{A_{sc}}{A_{st}}\right]^{1.3}\left[\frac{\varepsilon_{sh}}{D}\right] \qquad \rho > 0.01 \qquad \textbf{(6-40)}$$

Hence, the final curvature due to shrinkage is given by:

$$(k_{sh})_{avrg} = \xi\,(k_{sh})_{cr} + (1 - \xi)\,(k_{sh})_{uncr} \qquad \textbf{(6-41)}$$

The overall long-term curvature can be calculated using the expression:

$$k(t) = (k_c)_{aveg} + (k_{sh})_{aveg} \qquad \textbf{(6-42)}$$

and the deflection can be calculated from:

$$\Delta = KL^2(k_L + 10k_M + k_R) \qquad \textbf{(6-43)}$$

Where:

K = the deflection coefficient factor which depends on the loading case and bending moment diagram

L = the span of the member

k_L and k_R = the curvature at the left and right supports

k_M = the curvature at the mid-span

Gilbert (2001a) stated that the equations for α and k_{sh} were developed empirically to fit the results obtained from a parametric study of the creep and shrinkage induced change in curvature under sustained load using the age-adjusted Effective Modulus Method (AEMM). Although the accuracy of this approach has been tested by the author using experimental results from several beam and slab tests, there have been no evaluations or recommendations presented by other researchers in the literature to confirm the suitability and accuracy of this approach.

6.2.5 Eurocode 2

Based on the CEB-FIB MC90, the Eurocode 2 (EC2) approach was proposed to predict the deformations (curvature, strain, deflection, etc.) of beams subjected to bending. Expression 7.18 of Eurocode 2 is used to determine the deformation parameter (α) as shown below:

$$\alpha = \xi\,\alpha_{II} + (1-\xi)\alpha_{I} \quad \textbf{(6-44)}$$

Where:

α_I and α_{II}= the values of the deformation parameters calculated for un-cracked and fully-cracked stages

ξ = the distribution coefficient which takes into account the tension stiffening of the section. The factor ξ can be calculated from Expression 7.19 of EC2 as follows:

$$\xi = 1 - \beta\left(\frac{M_{cr}}{M_a}\right)^2 \quad \textbf{(6-45)}$$

Where:

β = a coefficient which takes into account the influence of the duration and type of loading (β = 1 for short-term loading and 0.5 for long-term or repeated loading).

M_{cr} = the first cracking moment

M_a = the applied moment

$$M_{cr} = \frac{f_{ctm}\,I_u}{(h - x_u)} \quad \textbf{(6-46)}$$

ξ= 0 when $M_a \le M_{cr}$ (section is un-cracked)

$\xi = 1 - \beta\left(\frac{M_{cr}}{M_a}\right)^2$ when $M_a > M_{cr}$ (section is cracked)

The Eurocode 2 method can be used to predict the total long-term curvature of beams under sustained loading and includes the effects of creep and shrinkage separately. The effect of loss of tension stiffening with time is considered by including the distribution factor ξ in the calculations. In addition, the effect of creep is included by modifying the modulus of elasticity of the concrete using the Effective Modulus Method (EMM) which is based on the value of creep coefficient over time as shown below:

$$E_{c,eff}(t_0,t) = \frac{E_{c28}}{1+\varphi(t_0,t)} \quad \textbf{(6-47)}$$

$$\frac{1}{r_c} = \xi\frac{M_a}{E_{c,eff}I_c} + (1-\xi)\frac{M_a}{E_{c,eff}I_u} \quad \textbf{(6-48)}$$

Where:

E_{c28} = the 28-day tangent modulus of elasticity of concrete = $1.05E_{cm}$

$\varphi(t_0,t)$ = the creep coefficient at time t

Whereas the curvature due to shrinkage effect is calculated using:

$$\frac{1}{r_{sh}} = \xi\,\varepsilon_{sh}(t_0,t)\,\alpha_e\frac{S_c}{I_c} + (1-\xi)\,\varepsilon_{sh}(t_0,t)\,\alpha_e\frac{S_u}{I_u} \qquad \textbf{(6-49)}$$

Where:

$\varepsilon_{sh}(t_0,t)$ = the shrinkage strain at time t

α_e = the effective modular ratio = $E_s/E_{c,eff}$

I_u and I_c = the second moments of area of the un-cracked and cracked sections:

$$x_u = \frac{\frac{bh^2}{2} + (\alpha-1)(A_s d + A_{s2}d_2)}{bh + (\alpha-1)(A_s + A_{s2})} \qquad \textbf{(6-50)}$$

$$I_u = \frac{bh^3}{12} + bh\left(\frac{h}{2} - x_u\right)^2 + (\alpha-1)A_s(d-x_u)^2 + (\alpha-1)A_{s2}(x_u-d_2)^2 \qquad \textbf{(6-51)}$$

$$x_c = \frac{[(\alpha_e A_s + (\alpha_e-1)A_{s2})^2 + 2b(\alpha_e A_s d + (\alpha_e-1)A_{s2}d_2)]^{0.5} - (\alpha_e A_s + (\alpha_e-1)A_{s2})}{b} \qquad \textbf{(6-52)}$$

$$I_c = \frac{b{x_c}^3}{12} + \alpha_e A_s(d-x_c)^2 + (\alpha_e-1)A_{s2}(x_c-d_2)^2 \qquad \textbf{(6-53)}$$

S_u and S_c = the first moments of area of the reinforcement about the centroid of the un-cracked and cracked sections:

$$S_u = A_s(d-x_u) - A_{s2}(x_u-d_2) \qquad \textbf{(6-54)}$$

$$S_c = A_s(d-x_c) - A_{s2}(x_c-d_2) \qquad \textbf{(6-55)}$$

The total long-term curvature is calculated using the expression:

$$\frac{1}{r} = \frac{1}{r_c} + \frac{1}{r_{sh}} \qquad \textbf{(6-56)}$$

Where:

$\frac{1}{\mathrm{r}}$ = total long-term curvature

$\frac{1}{r_c}$ = the curvature due to creep

$\frac{1}{r_{sh}}$ = the curvature due to shrinkage

Hence, the total long-term deflection is:

$$\Delta = KL^2\frac{1}{r} \qquad \textbf{(6-57)}$$

The creep coefficient $\varphi(t_0, t)$ and shrinkage strain $\varepsilon_{sh}(t, t_0)$ at time t can be obtained from the method in FIB Model Code (2010) for normal concrete and are given by:

$$\varphi(t, t_0) = \emptyset_{c,RH}(h)\, \beta_c(f_{cm28})\, \beta_c(t_0)\, \beta_c(t, t_0) \quad \textbf{(6-58)}$$

$$\varepsilon_{sh}(t, t_0) = \emptyset_{s,RH}(h)\, \beta_s(f_{cm28})\, \beta_s(t, t_0) \quad \textbf{(6-59)}$$

Where:

$\emptyset_{RH}(h)$ = correction factor for ambient relative humidity

$\beta(f_{cm28})$ = correction factor for compressive strength

$\beta_c(t_0)$ = correction factor for loading age

$\beta(t, t_0)$ = time function

This approach has been recommended by many researches due to its accuracy in predicting experimental results. This can be attributed to the separate computation of the deflections due to creep and shrinkage and its inclusion of a distribution factor to account for the effects of cracking and tension stiffening. In this approach, it is clear that all the parameters which influence long-term deflection are considered.

Another simplified approach was also presented in technical reports published by MPA The Concrete Centre (2006) and Concrete Society (2005) according to Eurocode 2 for predicting the long-term deflection of beams which is based on an elastic analysis of a section. The general idea behind this approach is to reduce the stiffness of the section to account for cracking, creep and shrinkage. In this method, the effects of shrinkage and cracking are included in the calculation of an adjusted effective modulus of elasticity ($E^*_{c,eff}$):

$$E^*_{c,eff} = \frac{\mathrm{K}\, E_c}{1 + \varphi(t, t_0)} \quad \textbf{(6-60)}$$

$$\frac{1}{r} = \frac{M_a}{E^*_{c,eff} I_u} \quad \textbf{(6-61)}$$

The fixed value of the factor K = 0.5 is used to account for the effects of shrinkage and cracking. This approach has been proposed to simplify the calculations for

practical purposes and its effectiveness will be assessed in the next sections where predictions will be compared with experimental results.

6.3 Comparison of the Code Procedures

In this section, a simple comparison between the existing code procedures presented in the last section has been made in order to evaluate the accuracy and suitability of these methods. As these code procedures have been proposed to predict the long-term deflection of normal concrete structures, the experimental results (Exp) for the NC beam tested in this research have been used in the comparison. The results are presented in Table 6-2.

Table 6-2 Predictions from the existing code procedures for the long-term deflection of NC beams

Code procedures	Long-term deflection (mm)				Exp/Pre
	Exp	Prediction			
		Shrinkage	Creep	Total	
ACI-318	18.30	-	-	22.91	0.798
ACI-435		3.35	35.13	38.48	0.475
CSA		-	-	22.91	0.798
AS3600		-	-	47.21	0.387
Gilbert (2012)		6.38	13.06	19.44	0.941
Eurocode 2 (Cracked analysis)		6.23	11.93	18.16	1.007
Eurocode 2 (Elastic analysis)		-	-	19.53	0.937

It is clear from the results that all the methods which follow the multiplier factor approach failed to predict accurate values of long-term deflection (ACI-318, CSA and AS3600). Greater accuracy can be seen in the results from the methods which consider the effect of all the factors which influence long-term deflection (Gilbert (2012) and Eurocode 2). As mentioned earlier, Gilbert modified his approach and followed a route similar to the Eurocode 2 method. Based on these results and in line with the recommendations of many researchers, the Eurocode 2 approach was

selected for the analytical investigation in this research. Modifications to this method have been proposed to include the effects of recycled aggregate and steel fibres on the behaviour of concrete.

6.4 Limitations and Modifications

The main aim of this section is to assess the suitability of the Eurocode 2 methods for predicting the long-term concrete response when recycled aggregate and steel fibres are incorporated. Each calculation step will be reviewed and its limitations and appropriate modifications are presented. The assessment of each step is based on a comparison between the results from the analytical methods and those obtained from experiments.

6.4.1 Cracked section analysis approach

6.4.1.1 Effect of recycled aggregate

In this section, the method of Eurocode 2 for predicting the long-term deflection of reinforced concrete beams made with recycled aggregate is discussed. It was found that the code predictions showed good agreement with the experimental results from the normal concrete beams. However, it can be seen that as the replacement ratio of RA increased, the predictions from the Eurocode 2 method became less accurate and underestimated the short-term and long-term experimental values as shown in Figure 6-2.

This underestimation of beams deflection by the code is due to the difference between the tension stiffening behaviour of the RAC beams and the NC beam (as discussed in Section 5.4.1) which is not taken into account in the code calculations. At 90 days, the code predictions are still within 10% of the measured values, however, by extrapolation based on the trends of the measured and predicted curves, the error in the ultimate deflections will be greater and is likely to exceed the normally acceptable ±20% error for this type of prediction.

More specifically, the Eurocode 2 approach incorporates the effect of the loss of tension stiffening using a fixed value for the factor β (β= 1 for short-term loading and 0.5 for long-term or repeated loading) which does not vary for different types of concrete. Therefore, based on the experimental results from this study of the long-term tension stiffening tests and the recommendations of Whittle and Jones (2004)

and Scott and Beeby (2012), in order to account for the effect of the tension stiffening behaviour on the flexural response, modifications to the Eurocode 2 method are proposed to address the effect of the addition of RA.

The results indicate that as the level of RA is increased, the value of β should be reduced to below 0.5 when calculating long-term deflections. Based on the experimental results, β values of 0.4 and 0.3 are proposed for concrete with 50% and 100% RA, respectively. These values were obtained through back-calculation from the long-term experimental deflections. The application of these proposed values of β gave more accurate predictions for long-term deflections when the experimental results of the short-term deflections were used in the calculations (which avoids any error arising from the prediction of short-term deflection) as shown in Figure 6-2 and summarised in Table 6-3.

Modifying the tension stiffening factor β in the Eurocode 2 method is thought to be the best way of including the effect of RA in the calculations for long-term flexural behaviour. Other methods have been proposed in the literature based on modifying the properties of the concrete. However, these are not sufficient as they do not consider the influence of RA on other parameters such as the bond-slip action and the deformation of the micro-cracks which develop between the reinforcement and the concrete matrix which are two of the main parameters that affect the long-term flexural behaviour of concrete structures.

In terms of crack width, Forth (2014) highlighted the effect of tension stiffening (in the concrete between cracks) on the average strain in the steel in his comparison of the two formulae presented in Eurocode2 (flexural) and Eurocode 2 Part 3 (axial); it is the average strain in the steel which is used to calculate the crack width in Eurocode 2. It therefore seems more reasonable that modifying the tension stiffening parameter is also a better approach to calculating crack width than simply modifying the tensile strength of the concrete.

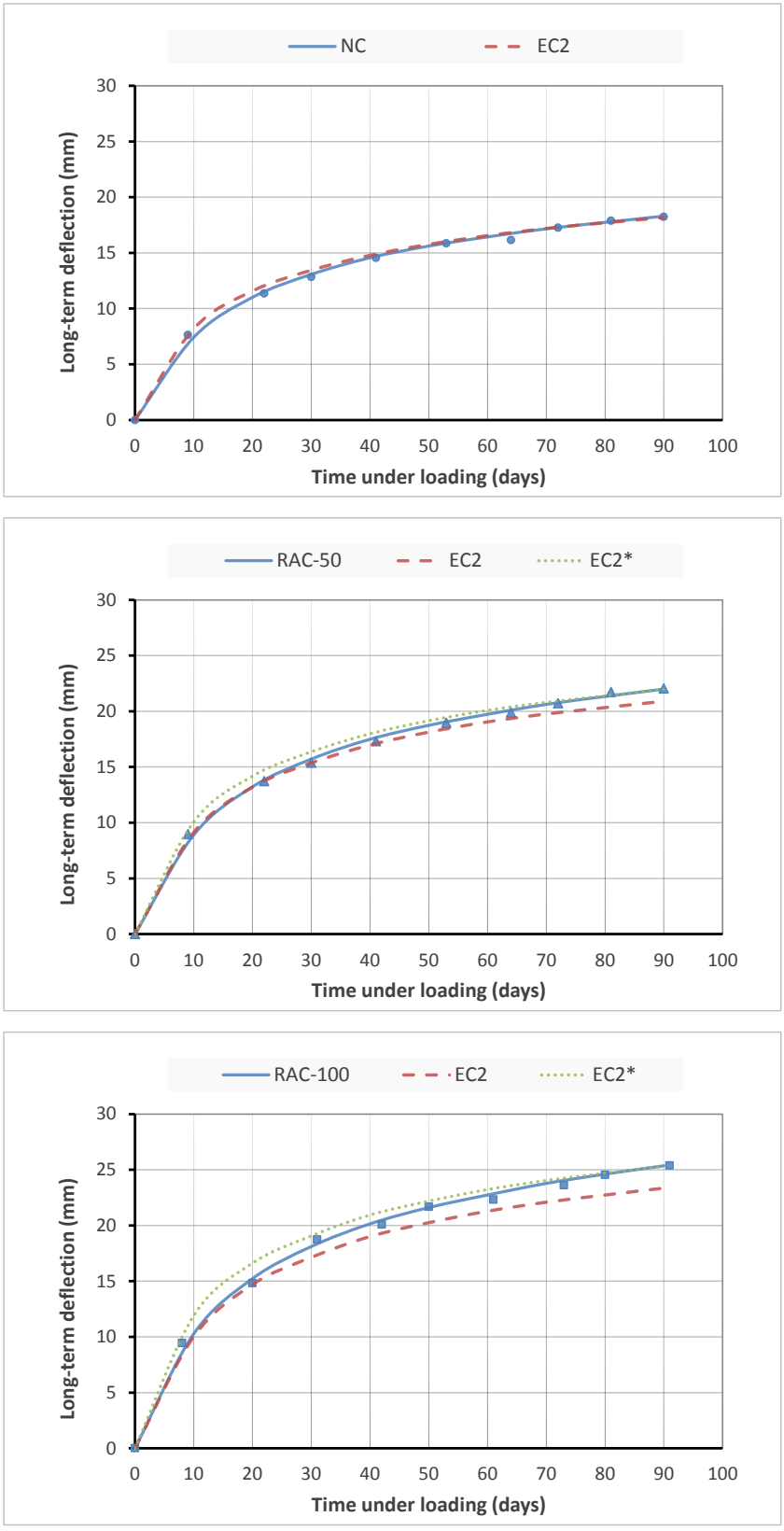

Figure 6-2 Comparison of the experimental and predicted long-term deflection of NC and RAC beams tested

6.4.1.2 Effect of steel fibres

The assessment of the suitability of the Eurocode 2 method for predicting the long-term deflection of reinforced concrete beams with steel fibres is discussed here. The assessment comprised two main steps:

- Firstly, examining the effect of steel fibres on long-term tension stiffening and how this effect is accounted for in the Eurocode 2 method.
- Secondly, assessing how the calculations in the Eurocode 2 method can consider the effect of steel fibres on the stiffness of the cracked section and the movement of the neutral axis with time due to creep, shrinkage and cracking.

Regarding the first step, as discussed earlier, it is necessary to include the effect of steel fibres on the long-term loss of tension stiffening in the calculation of long-term deflections for accurate results. Based on the results discussed in Section 5.4.2, the incorporation of steel fibres significantly reduces the rate of the loss of tension stiffening. Therefore, similar to the method used for RAC, it is suggested that this be taken into account through modification of the factor β, and as the steel fibre content increases, the value of β should exceed 0.5 in the calculation of long-term deflection.

According to the results from the tension stiffening tests, the relationship between the recycled aggregate and steel fibre contents on tension stiffening is almost linear. A similar relationship can be assumed to represent their relationship to the value of β. In order to estimate the appropriate values of β when steel fibres are incorporated, an interpolation analysis was carried out based on the results of the tension stiffening tests and the proposed values of β for NC and RAC. β values of 0.65 and 0.8 were derived for concrete made with 0.5% and 1.0% steel fibre contents, respectively. Statistical multiple regression analysis was used to develop a function for the combined effect of RA and steel fibres on β based on the replacement percentage of RA ($RP\%$) and the volume fraction of steel fibres ($V_f\%$) as follows:

$$\beta = 0.5 - 0.2RP\% + 30V_f\% \qquad (R^2 = 0.98) \qquad \textbf{(6-62)}$$

The correlation coefficient calculated (R^2=0.98) reflects the high strength of the relationship between the dependent and independent variables.

As mentioned earlier, considering the effect of steel fibres on the tension stiffening behaviour of concrete is not sufficient on its own to account for the role of steel fibres in enhancing the long-term flexural behaviour of reinforced concrete beams. The effect of steel fibres on the stiffness of the cracked section and the movement of the neutral axis with time due to creep, shrinkage and cracking, still need to be considered in the calculations.

The Eurocode 2 calculations employ the Effective Modulus of Elasticity Method (EMM) to account for the stiffness of the cracked section and hence the movement of the neutral axis with time. When using this method for analysing the cracked stage, it is assumed that the concrete below the neutral axis in the tension zone carries no stress and therefore does not creep. Consequently, the movement of the neutral axis with time is assumed to be due only to the creep in the compression zone; the effective modulus of elasticity with time is thus a function of compressive creep only as defined by Eq. (6-47).

This assumption can be accepted for both normal and recycled aggregate concrete without fibres as the general behaviour of the strain profiles is similar (the percentage change in strain over time was similar in both the tension and compression zones of both materials as discussed in Section 5.6.1). In contrast, the long-term strain development was different when steel fibres were incorporated (as discussed in Section 5.6.2). It was found that the effect of steel fibres on reducing strain was greater in the tension zone than in the compression zone. It is thought that the crack bridging by steel fibres which greatly enhances both the tensile response of concrete and concrete section stiffness leads to the differences in the strain profiles observed.

The same findings were also concluded by Nakov (2014) when some beams with different steel fibre contents were experimentally tested under sustained load. It was noticed that the addition of steel fibres to concrete does not have any significant effect on the time-dependent concrete compressive strains (3.4-7.2%). On the other hand, a great influence was noticed in the long-term tensile strains development. The SFRAC beams exhibited 19-62.8% smaller strains in the tension zone and the results showed that this effect increases with increasing the fibre content as shown in Figure 6-3.

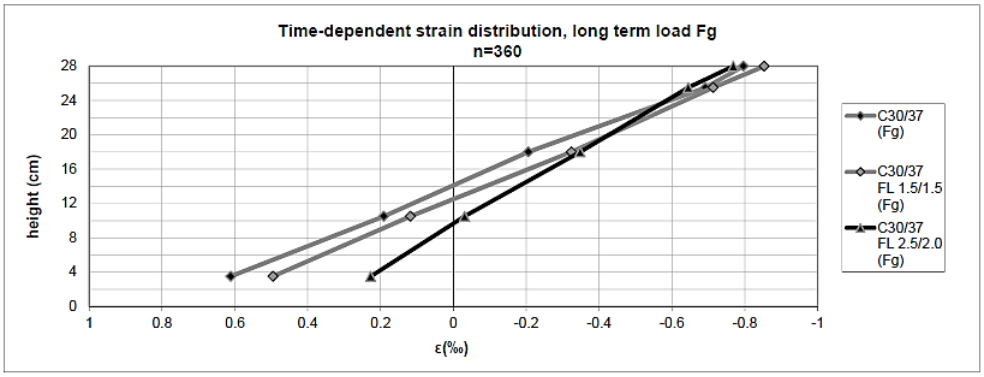

Figure 6-3 Time-dependent strain distribution for SFRAC beams after 360 days under sustained load (Nakov, 2014)

Consequently, when steel fibres are incorporated, the tensile creep of the concrete below the neutral axis cannot be neglected as it plays the main role in determining the movement of the neutral axis with time. The considerable reduction in the strains in the tensile zone make the section stiffer and controls movement of the neutral axis with time, the combination of which results in less deflection.

A review of the Eurocode 2 method without any modification to consider the effect of steel fibres found that the Eurocode 2 predictions for long-term deflections highly overestimated the experimental results as presented in Figures 6-3 to 6-5 and Table 6-3. Therefore, as discussed in the last section, a modification is needed to take into account the effect of steel fibres on the development of strain. Based on the fundamental assumption of the Effective Modulus of Elasticity Method, a factor (ψ) is proposed to account for the effect of steel fibres on the long-term strain in the tension zone (tensile creep) and the stiffness of the section as follows:

$$E_{c,eff}(t_0,t) = \frac{E_{c28}}{1+\psi\,\varphi(t_0,t)} \qquad \textbf{(6-63)}$$

Using the experimental results for long-term deflections, a statistical regression analysis was used to develop an expression for the factor (ψ) as a function of the volume fraction of steel fibres was determined via back-calculation as given below:

$$\psi = 1 - 40V_f\% \qquad (R^2 = 1) \qquad \textbf{(6-64)}$$

By applying this factor in the Effective Modulus of Elasticity Method and including the proposed values of tension stiffening factor (β), good agreement was obtained

between the calculated and measured values for the long-term deflection of all the beams tested as summarised in Table 6-3 and shown in Figures 6-4 and 6-5.

Table 6-3 Calibration of experimental and predicted long-term deflections using the cracked section analysis approach

Specimen	Long-term deflection (mm)			Exp/EC2*
	Exp	EC2	EC2*	
NC	18.30	18.16	18.16	1.007
SFC-0-0.5	16.40	18.57	16.34	1.004
SFC-0-1.0	14.94	19.42	14.79	1.010
RAC-50	21.99	20.19	21.98	1.000
SFRAC-50-0.5	19.72	21.84	19.53	1.010
SFRAC-50-1.0	17.98	22.95	17.93	1.003
RAC-100	25.36	23.35	25.32	1.002
SFRAC-100-0.5	22.78	25.38	22.96	0.993
SFRAC-100-1.0	20.79	26.24	20.97	0.992

EC2* = the modified Eurocode 2 cracked section analysis approach

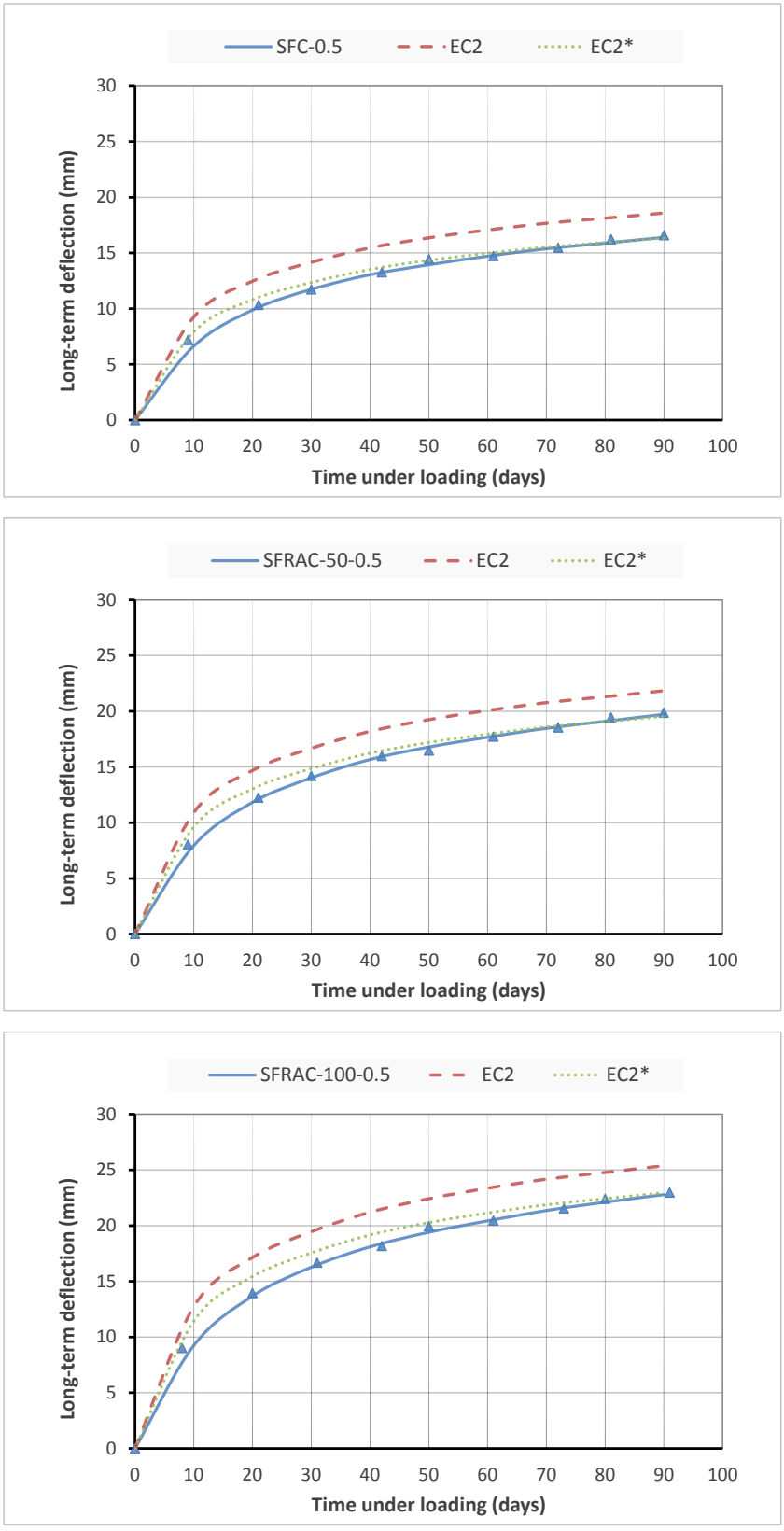

Figure 6-4 Comparison of the experimental and predicted long-term deflection of beams with 0.5% steel fibres

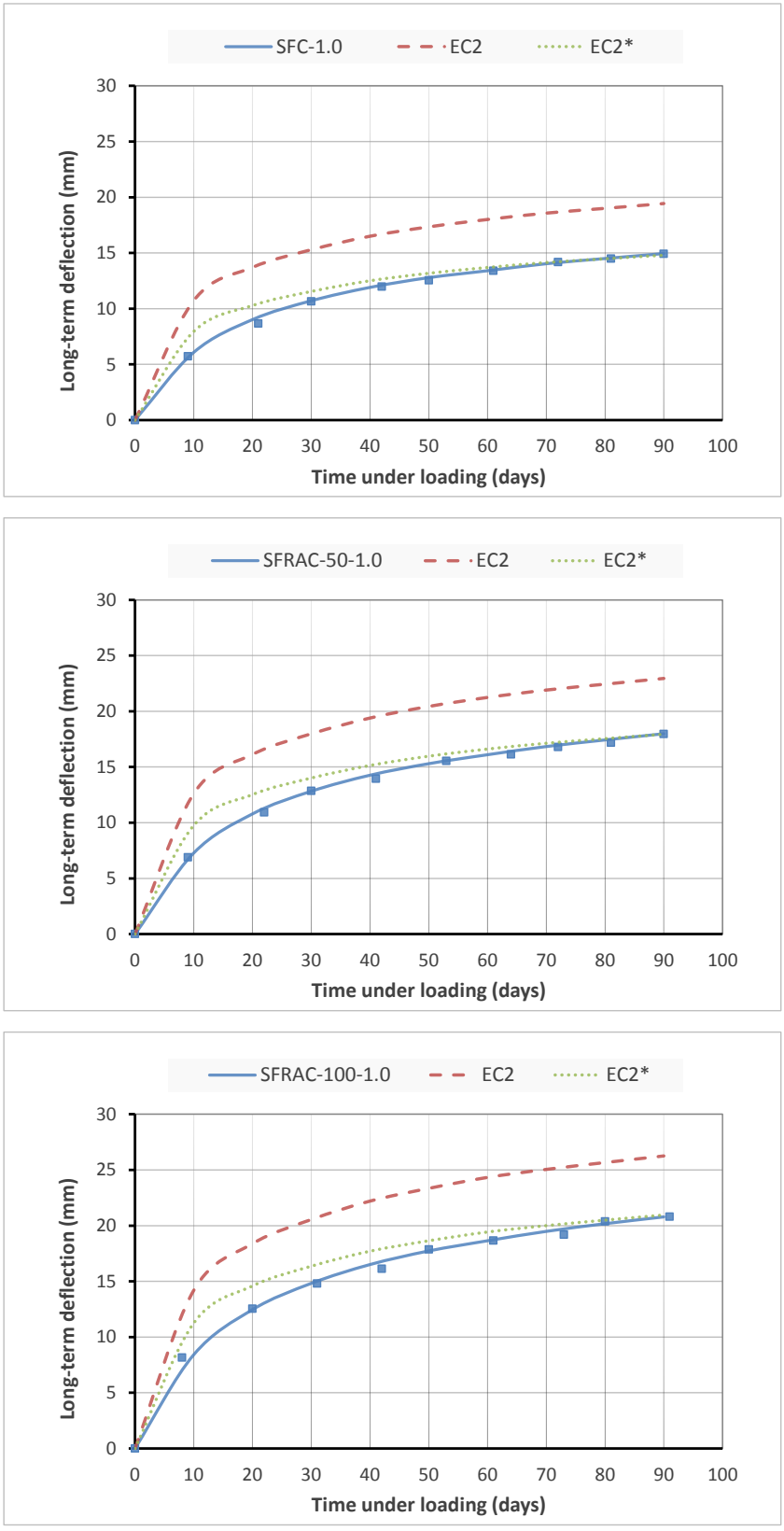

Figure 6-5 Comparison of the experimental and predicted long-term deflection of beams with 1.0% steel fibres

According to the figures presented, it can be seen that even after the calibration, there is still a slight overestimation compared to the experimentally measured deflections, particularly for the period of the first 30 days. The overestimation increases with increasing replacement percentage of RA and steel fibre content. This can be attributed to the way the loss of tension stiffening is considered in the calculations. Gilbert (2011), based on the results of his own experiments and those of Scott and Beeby (2005), stated that using a constant value for the tension stiffening factor β for all periods of loading is incorrect and recommended that the factor β should be taken as 0.7 up to 28 days and 0.5 after that for normal concrete specimens. Therefore, based on this recommendation and the results of tests for the reduction rate of tension stiffening over time presented and discussed in Chapter 5, another values for the factor β can be proposed similarly for the early stage of loading when recycled aggregate and steel fibres are incorporated.

6.4.2 Elastic analysis approach

An elastic approach is proposed in Eurocode 2 to simplify the calculation steps in the Eurocode 2 approach for practical purposes and for inclusion in elastic finite element analyses. In this method, the concrete stiffness is reduced to model the effects of shrinkage and cracking as defined by Eqs. (6-60) and (6-61).

Where the factor K (K = 0.5) is used to account for the effects of shrinkage and cracking. One criticism of this proposed approach concerns its use of a single fixed factor of 0.5 to account for the combined effects of shrinkage and cracking, as shrinkage and cracking are influenced by many parameters (e.g. changes in material properties, geometry of members, reinforcement details and ambient conditions) which cannot be represented by a single factor.

Therefore, a calibration was made between the experimental results of this study for long-term deflection and the predictions from this approach. The results confirmed that using a fixed single factor (K = 0.5) to compensate for the effects of shrinkage and cracking on the long-term deflection gave incorrect results for all the beams. Therefore, a back-calculation from the experimental results was carried out in order to determine the appropriate value of this factor for each beam. The results are presented in Figures 6-6 to 6-8 and summarised in Table 6-4.

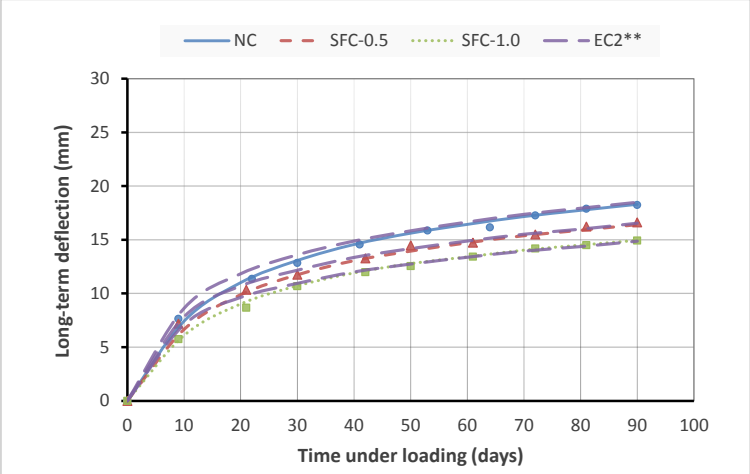

Figure 6-6 Comparison between the experimental and elastic analysis results for the long-term deflection of NC, SFC-0.5 and SFC-1.0 beams

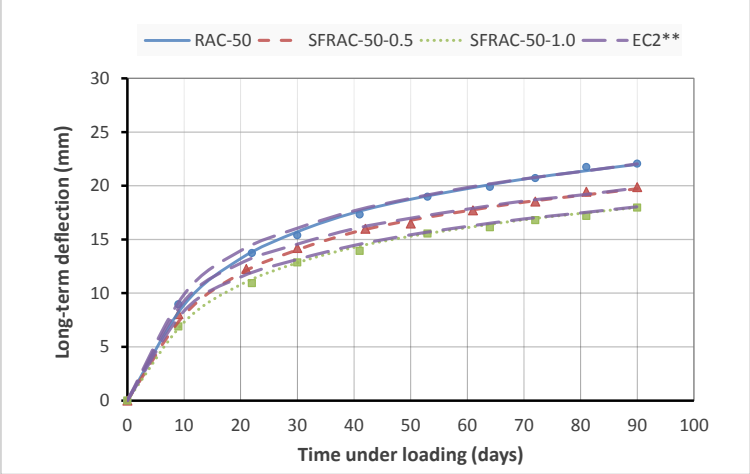

Figure 6-7 Comparison between the experimental and elastic analysis results for the long-term deflection of RAC-50, SFRAC-50-0.5 and SFRAC-50-1.0 beams

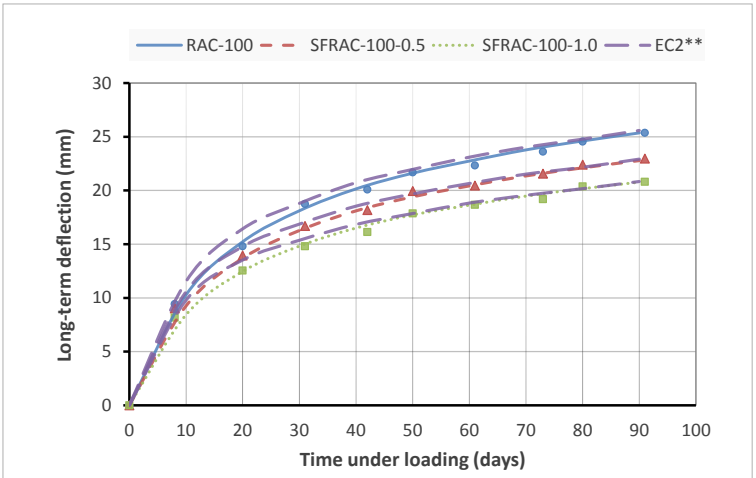

Figure 6-8 Comparison between the experimental and elastic analysis results for the long-term deflection of

It is clear from the results that a variable value for the factor K in the range 0.45-0.74 seems to be more reasonable than the assumption of a fixed value of K = 0.5. The value of the factor K decreases with increasing replacement percentage of RA which increases the deflection predicted; this is in line with experimental data for the effect of RA on shrinkage and cracking. In contrast, the value of K increases as the content of the steel fibres increases which is in line with the fact that steel fibres enhance the stiffness of the cracked section and reduce the shrinkage of the concrete leading to lower deflection. A statistical regression analysis indicated there was a high degree of correlation (R^2=0.99) between the dependent and independent variables, and the relationship between the factor K and the replacement percentage of RA ($RP\%$) and volume fraction of steel fibres ($V_f\%$) was found to be:

$$K = 0.55 - 0.1RP\% + 19V_f\% \qquad (R^2 = 0.99) \qquad \textbf{(6-65)}$$

Table 6-4 Long-term deflection results of elastic analysis approach

Specimen	*K*	Long-term deflection (mm)		Exp/EC2**
		Exp	EC2**	
NC	0.55	18.30	18.48	0.990
SFC-0-0.5	0.66	16.40	16.54	0.992
SFC-0-1.0	0.74	14.94	14.87	1.005
RAC-50	0.51	21.99	22.05	0.997
SFRAC-50-0.5	0.62	19.72	19.80	0.996
SFRAC-50-1.0	0.70	17.98	18.04	0.997
RAC-100	0.45	25.36	25.59	0.991
SFRAC-100-0.5	0.55	22.78	22.92	0.994
SFRAC-100-1.0	0.64	20.79	20.83	0.998

EC2** = the modified Eurocode 2 elastic analysis approach

The values for K presented in Table 6-4 were determined according to the parameters of this research and may not be applicable for predicting the long-term deflection of other beams e.g. with different material properties, geometries or reinforcement details. As discussed earlier, there are many parameters which can influence the value of K, therefore, more comprehensive data is needed to develop and generalise the proposed theoretical relationship to take into account the effect of these parameters. A formula which takes into account the effect of other parameters on the value of K would make this simplified approach more reliable and applicable which would be of benefit for practical purposes when more simplification in the calculations is preferred.

All the curves of the long-term deflection results were statistically extrapolated in order to estimate the ultimate deflection after 20 years of loading. This is to investigate trends in the accuracy of the predictions in comparison with the experimental results at the ultimate. No significant error was noticed in the accuracy of predictions during this period of time and the worst case recorded 12% error which does not exceed the normally acceptable error ±20% for this type of prediction.

Another statistical method for extrapolating this type of hyperbolic results was suggested by Ross (1937) and Lorman (1940) and recommended by Neville et al. (1983) and Daud (2016), was also used as shown below:

$$\Delta(t, t_0) = \frac{(t - t_0)}{\mathrm{A} + \mathrm{B} * (t - t_0)} \qquad \textbf{(6-66)}$$

Where:

$\Delta(t, t_0)$ = the deflection at anytime

$(t - t_0)$ = time under loading (days)

A and B = constants

When $(t - t_0)$ reaches infinity, the ultimate deflection will be $1/\mathrm{B}$. Hence, the limiting deflection can be found from the experimental results that have been obtained by plotting the relationship between $[(t - t_0)/\Delta(t, t_0)]$ and $(t - t_0)$ for each case. The slope of this linear relationship represents the constant B, and the intercept of the ordinate is the constant A. The estimations of this method for the

extrapolated long-term deflections after 20 years of loading did not show any significant error more than 8% in comparison with the experimental results.

6.5 Numerical Analysis Program

In this section, a numerical analysis program which has been developed using the MATLAB language for predicting the long-term deflection of reinforced concrete beams is presented. This program is based on the cracked section analysis approach from Eurocode 2 and includes the modifications proposed earlier to account for the effects of incorporating recycled aggregate and steel fibres. As the calculation steps are complicated and are performed as a function of time, the program has been designed to simplify the analytical calculations and present the final results for the long-term deflection in tables and figures. The flowchart of the program, results of the beams tested in this research and an example of numerical calculations are presented in the Appendix.

The program was developed to predict long-term deflections and to be used for validating the proposed analytical approach using the results available from previous investigations. More specifically, this means that the influence of other design parameters could be investigated such as:

- The dimensions of the section.
- The reinforcement details.
- The materials properties.
- The level of sustained load.
- The source of RA.
- The type of steel fibres.
- The ambient conditions.

Moreover, the program can be developed to include any proposed methods to predict materials properties, time-dependent deformations and instantaneous deflections when recycled aggregate and steel fibres are incorporated in concrete.

6.6 Comparison of the Proposed Modifications

The comparison of the proposed analytical approach was carried out by using the numerical program discussed above with the results from previous experimental

investigations presented in the literature. Several experimental studies on the separate effects of incorporating RA and steel fibres on the long-term flexural behaviour of reinforced concrete beams have been presented in the literature. However, many of these papers have not contained the data required for the analytical analysis (e.g. creep and shrinkage results). Therefore, only the results from those papers which included a complete set of data and others got by contacting with the authors were used for the comparison. The results are presented in Table 6-5. A comparison between the experimental values for long-term deflection (Exp) and the predictions from the proposed calculation method (Pre) is presented in Figure 6-9. The average and the standard deviation for Exp/Pre are 1.01 and 1.56%, respectively. These results indicate that the proposed modifications result in more accurate predictions of long-term deflection and good agreement with experimental results is obtained for a range of parameters and experimental conditions.

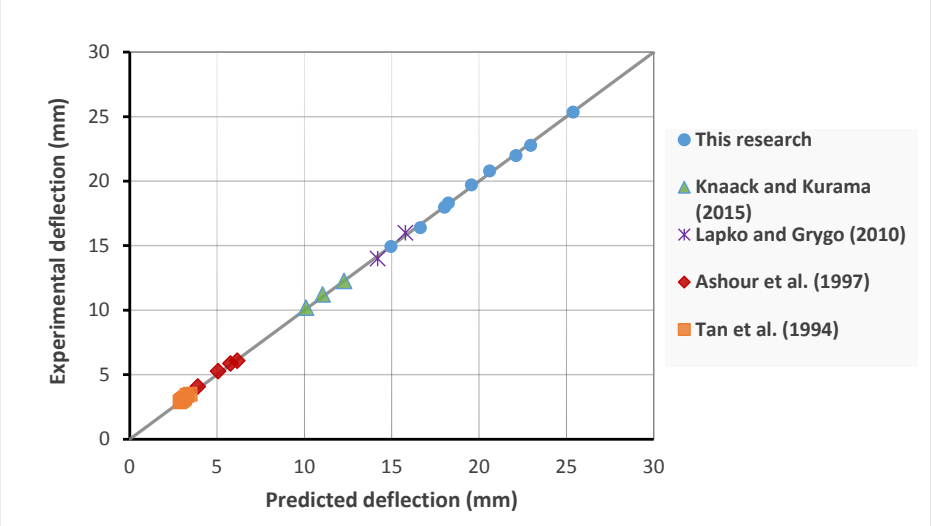

Figure 6-9 Comparison between experimental and predicted results

Table 6-5 Comparison between experimental and predicted results using the proposed calculation method

Study	Specimen	Long-term deflection (mm)		
		Exp	Pre	Exp/Pre
This research	NC	18.30	18.16	1.007
	SFC-0-0.5	16.40	16.34	1.004
	SFC-0-1.0	14.94	14.79	1.010
	RAC-50	21.99	21.98	1.000
	SFRAC-50-0.5	19.72	19.53	1.010
	SFRAC-50-1.0	17.98	17.93	1.003
	RAC-100	25.36	25.32	1.002
	SFRAC-100-0.5	22.78	22.96	0.993
	SFRAC-100-1.0	20.79	20.97	0.992
Knaack and Kurama (2015b)	CC-0-28	10.19	10.31	0.988
	CC-50-28	11.22	11.24	0.998
	CC-100-28	12.27	12.25	1.002
Łapko and Grygo (2010)	NC	14.00	14.19	0.987
	RAC	16.00	15.78	1.014
Ashour et al. (1997)	BS-0.0-0.5	6.08	6.14	0.991
	BS-0.75-0.5	5.27	5.05	1.044
	BS-1.5-0.5	4.08	3.89	1.049
	BS-0.75-0	5.88	5.76	1.021
Tan et al. (1994b)	A-50-0	3.50	3.45	1.014
	B-50-0.5	3.20	3.14	1.017
	C-50-1.0	3.10	3.07	1.009
	D-50-1.5	2.90	2.88	1.005
	C-65-1.0	3.40	3.28	1.037
	C-80-1.0	3.00	2.97	1.010
Average				1.01
Standard deviation				1.56%

6.7 Conclusion

The main conclusions drawn from the analytical investigation presented in this chapter are summarised as follows:

- The comparison showed that the methods which employ a multiplier factor (ACI-318, CSA and AS3600) fail to predict accurate values for the long-term deflection of normal concrete beams. Improved accuracy was noted for methods which take into account the effect of all factors that influence long-term deflection (Gilbert 2012 and Eurocode 2).
- The predictions from the Eurocode 2 method underestimated long-term deflection of beams made with RA. This underestimation increased with increasing levels of RA and time. The error at ultimate is expected to exceed the normally acceptable error of $\pm$20% for these types of predictions.
- The underestimation arises from the difference in the tension stiffening behaviour of RAC compared to NC which is not taken into account in the code method for predicting deflection. Therefore, modifications were proposed to address the effect of the addition of RA.
- The assessment of the accuracy of the Eurocode 2 method predictions showed that the effect of steel fibres on enhancing the long-term tension stiffening behaviour, and increasing the stiffness of cracked sections, was not considered effectively in the calculation steps.
- A method similar to that proposed for including the effects of RAC was suggested for modifying the factor β to include the effect of steel fibres on long-term tension stiffening.
- Based on the fundamental assumption of the Effective Modulus of Elasticity Method, a factor (ψ) was proposed, to account for the effect of the addition of steel fibres on reducing the strains in the tension zone (tensile creep) and enhancing the stiffness of the section.
- An assessment of the elastic analysis approach in Eurocode 2 showed that the use of a single constant factor K to account for the effects of shrinkage and cracking is fundamentally incorrect, as shrinkage and cracking are influenced by many parameters.

- A relationship between K and the replacement percentage of RA ($RP\%$) and volume fraction of steel fibres ($V_f\%$) was proposed. Many other parameters can influence the value of K, therefore, more data is still needed to develop and generalise this theoretical relationship.
- A numerical analysis program in the MATLAB language for predicting the long-term deflection of reinforced concrete beams has been developed. This program is based on the cracked section analysis approach of Eurocode 2 and includes the proposed modifications of this research.
- This program was used for validating the applicability of proposed analytical approach by using the results of this research and that are available from previous investigations for different design parameters.
- The results of the comparison exercise demonstrated the capability of the proposed modifications to give more accurate predictions, and good agreement with the experimental results available was obtained for a range of parameters and conditions.

Chapter 7 : Finite Element Analysis

7.1 Introduction

There are many commercial finite element analysis (FEA) software packages available for the analysis of concrete structures. However, the majority do not provide any materials models which include the effects of creep and shrinkage of the concrete in long-term analyses. In this research, the Midas FEA (V1.1) software released by MIDAS Information Technology Co. Ltd was used. This program has tools for geometry modelling and mesh generation, a powerful pre/post processor and an analysis solver. Furthermore, it provides a number of material constitutive models, allows for time-dependent materials properties and behaviours, and includes a wide range of analysis cases (including long-term analysis) for advanced analysis of civil structures.

In this chapter, a three-dimensional finite element analysis (FEA) of the long-term flexural performance of reinforced concrete beams is presented. The FEA approach was developed to account for the effects of recycled aggregate and steel fibres on the long-term deflection of beams. The proposed FEA approach was verified by comparing the obtained predictions with experimental results.

7.2 Description of Finite Element Model

A description of the steps taken to construct the model including forming the model, defining the materials, generating the elements and meshing, applying the boundary conditions and loads, and creating the analysis case, is presented in this section. The following sections have been written based on the explanations presented in the MIDAS Co. publications for users (MIDAS, 2010).

7.2.1 Geometry modelling

The geometry model is principally formed by defining the interlocking relationship between the various geometric elements. Midas FEA provides a wide range of functions to model different geometric entities (Curves, Surfaces and Solids) in various features (3-D lines or Arched curves, Planar or Conical faces, Box or

Conical solids, etc.) to simulate different types of concrete structures. In order to construct the beam models for this research, the Solid Box, 3-D line and 3-D rectangle curve tools were used to model the concrete sections, longitudinal steel bars and stirrups, respectively. A full-size beam model with the same dimensions and positions of reinforcement as the specimens constructed in the laboratory (see Figure 4-23) was created as shown in Figure 7-1.

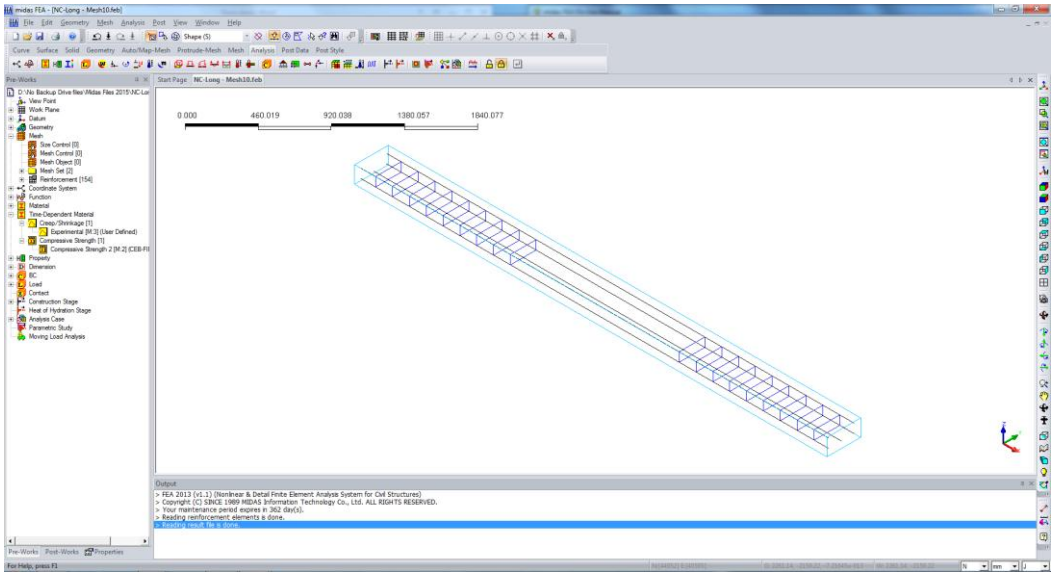

Figure 7-1 Modelling of concrete and reinforcement

7.2.2 Constitutive models for materials

Midas FEA has a number of constitutive models for defining the properties and behaviour of materials. In the case of this research, two materials models were needed to define the two types of materials in the beams (concrete and reinforcement) as described in the following sections.

7.2.2.1 Concrete

The Elastic material model was selected for the concrete as it is the only option available in Midas FEA which can take into account the time-dependent behaviours of concrete (creep and shrinkage). With this model, structural properties such as the Elastic Modulus, Poisson's Ratio and Weight Density can be entered manually or selected directly from a material library based on the grade of the concrete and the relevant international design code.

Midas FEA allows for the inclusion of creep, shrinkage and the increase in compressive strength with time of concrete. Several different functions are provided to specify creep, shrinkage and compressive strength using a number of code approaches, or alternatively data can be entered manually based on experimental results.

7.2.2.1.1 Creep

Figure 7-2 illustrates the definition of the creep function where the total of the initial elastic strain and the creep strain under a constant uni-axial stress is obtained from the following equation:

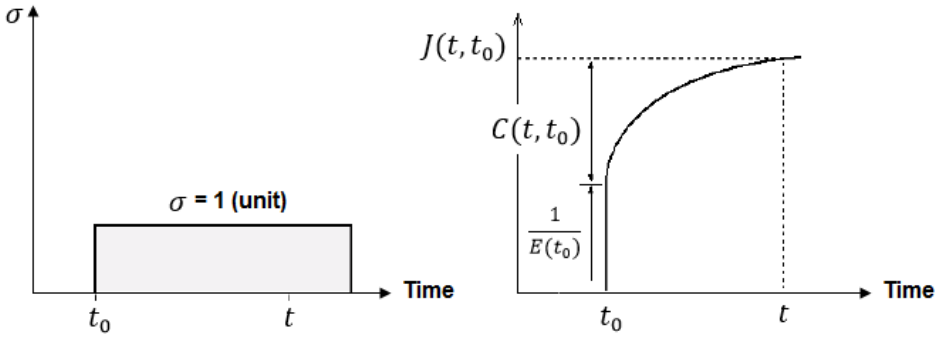

Figure 7-2 Definition of the creep function (MIDAS, 2010)

$$\varepsilon(t) = \varepsilon_i(t_0) + \varepsilon_c(t,t_0) = \sigma.J(t,t_0) \quad \textbf{(7-1)}$$

$$J(t,t_0) = \frac{1}{E(t_0)} + C(t,t_0) \quad \textbf{(7-2)}$$

Where:

$\varepsilon(t)$ = the total strain for a unit applied stress σ

$\varepsilon_i(t_0)$ = the initial elastic creep strain due to the applied stress

$\varepsilon_c(t,t_0)$ = the creep strain at time t

$J(t,t_0)$ = the creep function

$C(t,t_0)$ = the specific creep at time t

The creep function also can be expressed as:

$$J(t,t_0) = \frac{1+\varphi(t,t_0)}{E(t_0)} \quad \textbf{(7-3)}$$

Where:

$\varphi(t, t_0)$ = the creep coefficient which represents the ratio between the creep and elastic deformations.

Hence, the relationship between the specific creep and creep coefficient is given by:

$$C(t, t_0) = \frac{\varphi(t, t_0)}{E(t_0)} \qquad \textbf{(7-4)}$$

The User Defined function in Midas FEA allows the user to specify the creep function by entering data for the specific creep, creep function or creep coefficient. In this research, the experimental data for the creep coefficient over time was used to model the creep deformation of normal concrete and when recycled aggregate and steel fibres were incorporated as shown in Figure 7-3.

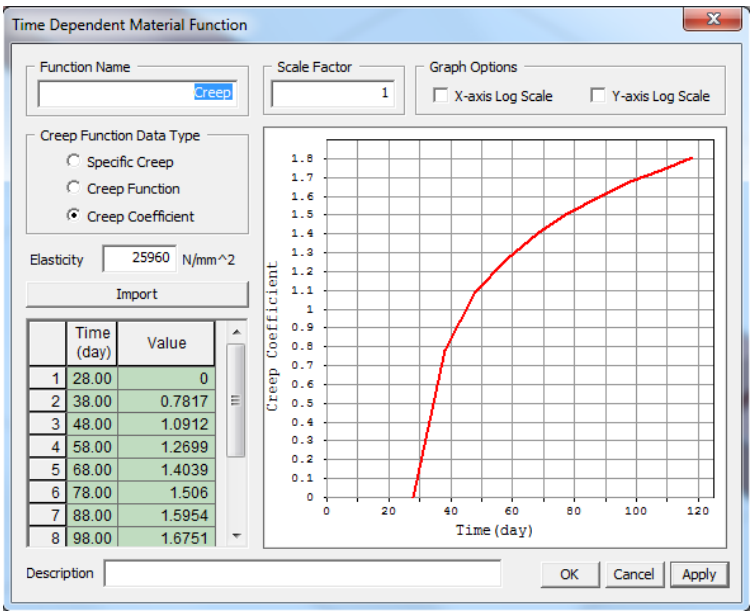

Figure 7-3 Creep function of concrete

It should be noted that the time of the load application in the experiments was taken into account when the creep function was defined. With concrete, the later the load is applied, the smaller the immediate elastic and creep deformations due to the improvement in concrete compressive strength with time. This is important because

the creep deformation of the concrete elements in the model in the time-dependent analyses is based on the age of the element.

7.2.2.1.2 Shrinkage

Shrinkage is a function of time and is independent of the stresses in the concrete members that are induced by the applied loading. The shrinkage strain from time (t_0) to time (t) can be expressed as:

$$\varepsilon_{sh}(t, t_0) = \varepsilon_{\infty} \,.\, f(t, t_0) \qquad \textbf{(7-5)}$$

Where:

ε_{∞} = the shrinkage at the final time
$f(t, t_0)$ = a function of time

In contrast to thermal strains and creep strains, shrinkage strains are non-mechanical strains. Therefore, shrinkage strains for a given stage are calculated from the characteristic curves for shrinkage as follows:

$$\varepsilon_{sh}(t_2, t_1) = \varepsilon_{sh}(t_2, t_0) - \varepsilon_{sh}(t_1, t_0) \qquad \textbf{(7-6)}$$

Where:

$\varepsilon_{sh}(t_2, t_0)$ = the shrinkage strain from t_0 to t_2
$\varepsilon_{sh}(t_1, t_0)$ = the shrinkage strain from t_0 to t_1

Concrete stresses due to shrinkage are obtained by subtracting the shrinkage strains from the strains due to displacement and multiplying by the modulus of elasticity as follows:

$$\sigma_{sh} = \varepsilon_{sh} \times E_{c,eff} \qquad \textbf{(7-7)}$$

It should be noted that if a structural member is not restrained in the axial direction, then shrinkage leads to a direct displacement without generating any creep stress. Otherwise, stresses caused by shrinkage when the member is restrained can induce creep without the need for external loading. Shrinkage strains are thus influenced by both boundary conditions and time.

In this research, the User Defined function was used to specify the concrete shrinkage by entering the experimental data for shrinkage strains with time. This

was done for normal concrete and when recycled aggregate and steel fibres were incorporated as shown in Figure 7-4. Another technique was also proposed and used in this study to consider the effect of non-uniform distribution of shrinkage which will be discussed later.

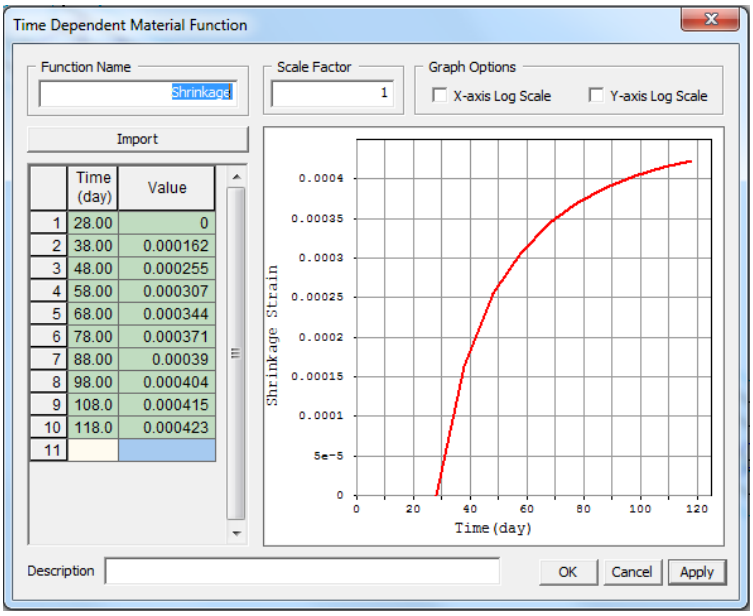

Figure 7-4 Shrinkage function of concrete

7.2.2.1.3 Compressive strength

Midas FEA changes the concrete compressive strength according to the age of the concrete members. During the calculations, Midas FEA automatically refers to the time-dependent concrete compressive strength values defined in the model construction. The compressive strength development function can be defined based on a number of different international code specifications, in this research, the CEB-FIP code function was used.

According to the computational theory behind the elastic model used, the concrete is considered to be in the elastic stage (un-cracked) for the analysis. This assumption is not actually correct for the real case of the concrete beams tested as they were already in the post-cracking stage (cracked sections). The limitations and the resulting modification of this approach will be discussed in detail in next sections.

7.2.2.2 Reinforcement

The reinforcement (longitudinal bars and stirrups) was defined in the analysis using the Von Mises model. The mechanical properties such as the Elastic Modulus was taken from the experimental results and Poisson's Ratio, Expansion Coefficient and Weight Density were taken from the data obtained from the manufacturer. Moreover, the initial yield stress obtained experimentally was used to define the behaviour.

7.2.3 Property of sections

After defining the materials properties, the next step in the modelling was to define the section properties and assign the materials to the sections. Midas FEA provides various section types and sub-types to create and manage the properties of the different sections of concrete structures. In this step, the concrete part of the beam was defined with a three-dimensional solid property and the concrete material model (discussed in the last section) was assigned to this section.

For the reinforcement, as three different sizes of bars were used in the beams tested (∅16, ∅12 and ∅8mm), three one-dimensional bar properties and sections were defined. The reinforcement material model (discussed in the last section) was assigned to all the sizes of bar and the reinforcement type was selected. The cross-sectional area of each type of bar was defined differently.

7.2.4 Element types

In this research, solid elements and reinforcement elements were used to simulate the concrete sections and the steel bars respectively. Details of each element type are presented in the next sections.

7.2.4.1 Concrete elements

Solid elements are generally used to model large structures such as concrete members, car engines, thick walls, rubber sections, etc. Three solid element geometries are available in Midas FEA: tetrahedron, pentahedron and hexahedron. Solid elements can be used for both static (linear & nonlinear) and dynamic analyses.

Solid elements can have a linear or quadratic shape function as shown in Figure 7-5. The “Linear elements” available include the 8-noded hexahedron, 6-noded pentahedron and 4-noded tetrahedron and the “Quadratic elements” are the 20-noded hexahedron, 15-noded pentahedron and 10-noded tetrahedron. Linear or Quadratic hexahedron elements generally give more accurate stress and strain results than tetrahedron and pentahedron elements. It is highly recommended that Linear or Quadratic hexahedron elements are used in the parts of the model where detailed analysis results are required.

Therefore, Quadratic hexahedron elements were used to model the concrete in this research. Figure 7-5 shows the directions of the ECS axes for the three types of solid element. In the case of a hexahedron, the x-axis is parallel to a line connecting the mid-point of Node 1 and Node 4 to the mid-point of Node 2 and Node 3. For a tetrahedron or pentahedron, the x-axis is parallel to the direction from Node 1 to Node 2.

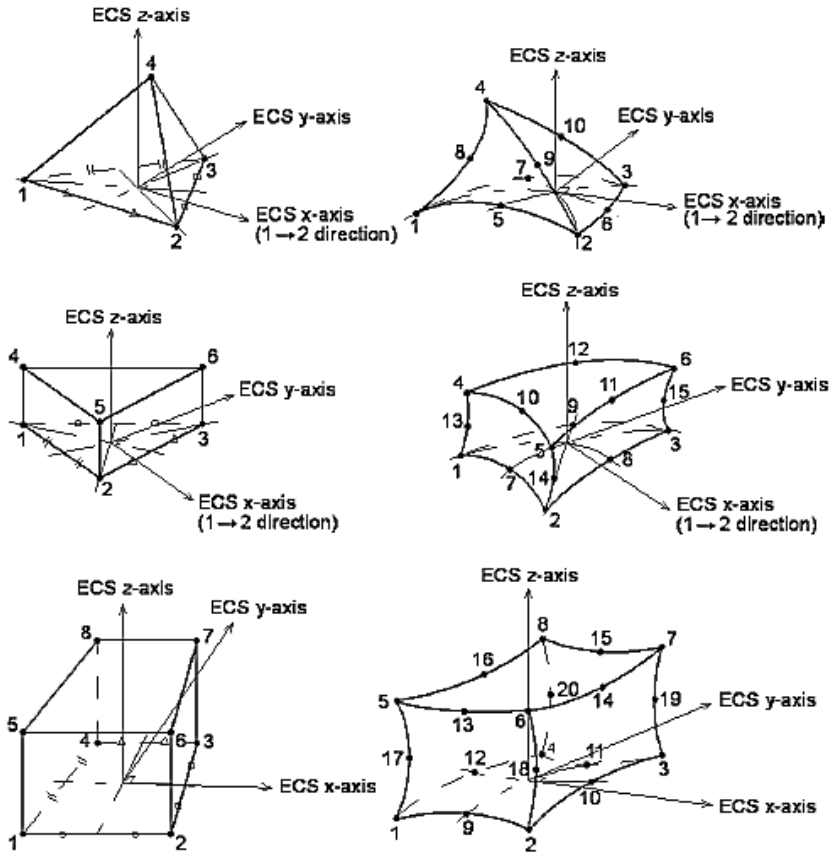

Figure 7-5 Linear and Quadratic shape functions of solid elements (MIDAS, 2010)

7.2.4.2 Reinforcement elements

Rather than defining the reinforcement with distinct elements, Midas FEA provides the concept of embedded reinforcement. In this concept, the stiffness of the reinforcement is added to the stiffness of the elements within which the reinforcement is located. The elements in which the reinforcement is embedded are called “mother elements”. The following should be noted when embedded reinforcement is used:

- The user defines the reinforcement location and the software calculates the intersection of the reinforcement with the mother elements.
- The reinforcement does not have separate degrees of freedom.
- The reinforcement is assumed to be perfectly bonded to the mother elements.
- The strain in the reinforcement is obtained from the displacements of the mother elements.

The two types of embedded reinforcement elements are Bar and Grid elements. The location, shape and material properties are the required inputs for defining the reinforcement. Depending on the type of mother element, the bar reinforcement is represented as either a line or a point.

In this research, Bar elements were used to define the steel bars and stirrups and lines were used as the mother elements were solids. With all solid element types, bar reinforcements can be represented by a straight 2-node line or a second order 3-node curve and can consist of one or more reinforcement sections. The user defines the reinforcement sections, and in the pre-processing phase the intersections between the bar sections and the mother elements are computed.

7.2.5 Meshing

The use of a rectangular shaped mesh is highly recommended for obtaining good results in the finite element analysis for reinforced concrete members. Therefore, cubic elements of size 25x25x25mm and 12.5x12.5x12.5mm were used (according to an investigation to the mesh sensitivity which will present in a next section) to mesh the concrete for all the specimens. The beam model comprised 12096 and 48384 elements of 20-node quadratic hexahedron respectively. The mesh was generated using the Map-Mesh Solid function as shown in Figure 7-6.

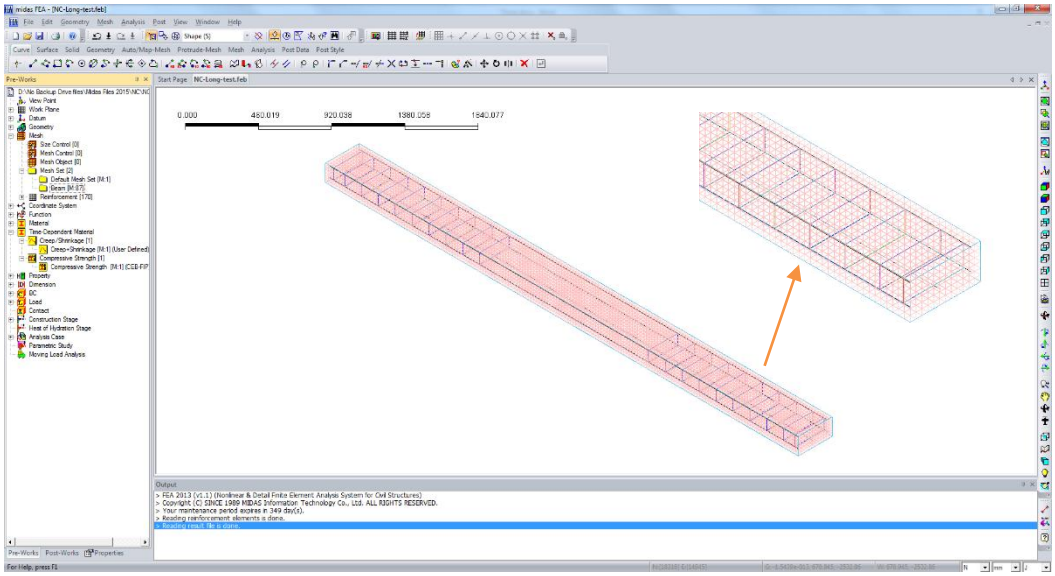

Figure 7-6 Mesh of the beam model

The reinforcement was modelled with embedded bar reinforcement elements using the Auto-Mesh Edge function. The reinforcement bar sections for both the steel bars and the stirrups were represented by 2-node lines with an equal interval length of 50mm. They were defined as bars within a solid based on the concrete mother elements. This technique of embedding the bars makes the finite element mesh of the reinforcement can be generated directly from the lines of the bar sections without having to determine the location of the reinforcement. Furthermore, the software can automatically define the location of the reinforcement segments and calculate the contribution of each bar segment to the stiffness and internal forces in the mother element.

7.2.6 Loading and Boundary conditions

The beam specimens were loaded experimentally by applying two concentrated loads. The finite element models of the beams were loaded at the same locations using a single line of node forces as shown in Figure 7-7. The load was applied as a concentrated line load directly to the nodes of the concrete elements using the node force function. The nodes at the edge of the beam had an applied nodal force of half the value of the interior nodes. The total value of the applied loads on all the nodes was 23KN, similar to the experiments.

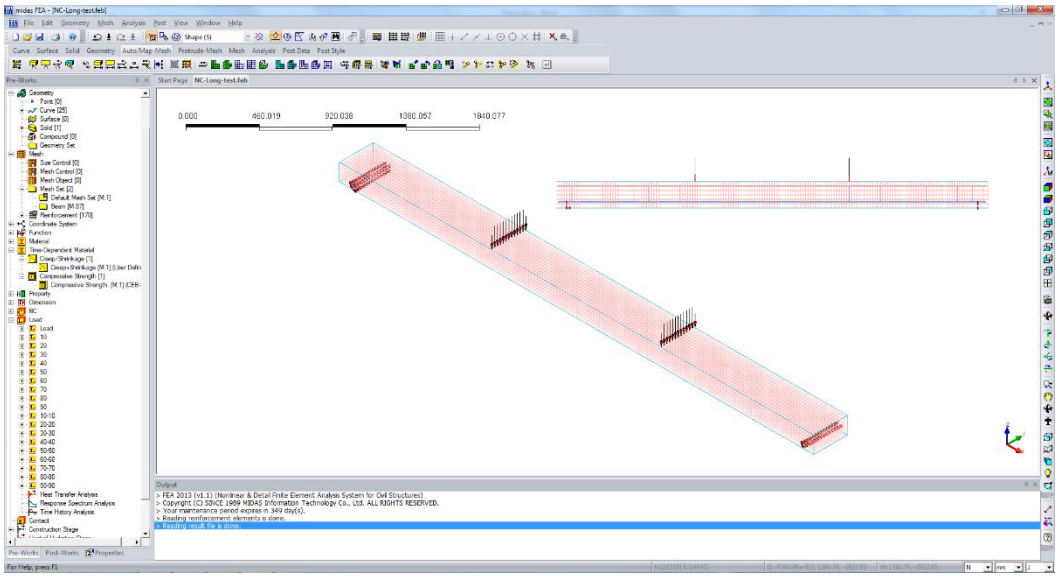

Figure 7-7 Loading and boundary conditions of the beam model

In terms of the boundary conditions, as the full-size beams were modelled, a single line of node constraints at each end of the beam was required to simulate the condition of restraint on the simply supported beam. In order to define the degrees of freedom (DOF) at each support, the transitions were restrained in three dimensions at one of the supporting points (pinned) and restrained in two directions and released in the axial direction at the second supporting point (roller). The rotations about all axes were not constrained at either of the supporting points.

7.2.7 Analysis case

Concrete structures are built in a number of stages thus the structural configuration, loadings, boundary conditions and even the physical properties of the structural elements may change during construction stages. In the case of concrete structural systems, the materials properties are known to change with time due to time-dependent deformation. As a result, the true behaviour of concrete structures may be different from the predicted behaviour if the time-dependent properties are not taken into account. Therefore, in this research, the analysis of the construction stage included the effect of the time-dependent properties of concrete.

Midas FEA allows for the following time-dependent properties of concrete to be included in construction stage analyses:

- Creep deformation.
- Shrinkage deformation.
- Compressive strength gain with time.

The following steps are carried out in the procedure used in Midas FEA for performing time-dependent analysis of the construction stages:

1. Create the structural model: form the shape, define the materials, assign elements, generate the mesh and apply the loads and boundary conditions.
2. Define the time-dependent materials properties.
3. Compose the construction stages based on the required element ages.
4. Specify the desired analysis conditions and carry out the structural analysis.

The various construction stages can be created by activating and/or deactivating elements, boundary conditions and loads. Sub-time steps can be used for the analysis of each construction stage, and loads can be added or deleted at each time step. As concrete structures are sensitive to time-dependent properties, the ages of the elements need to be assigned for each construction stage.

Figure 7-8 illustrates how construction stages are used in Midas FEA. The duration of each construction stage can be specified (a duration of '0' is possible) and the first and last steps are created once the construction stage has been defined. The activation and deactivation of elements, boundary conditions and loadings are carried out within the time duration of each stage.

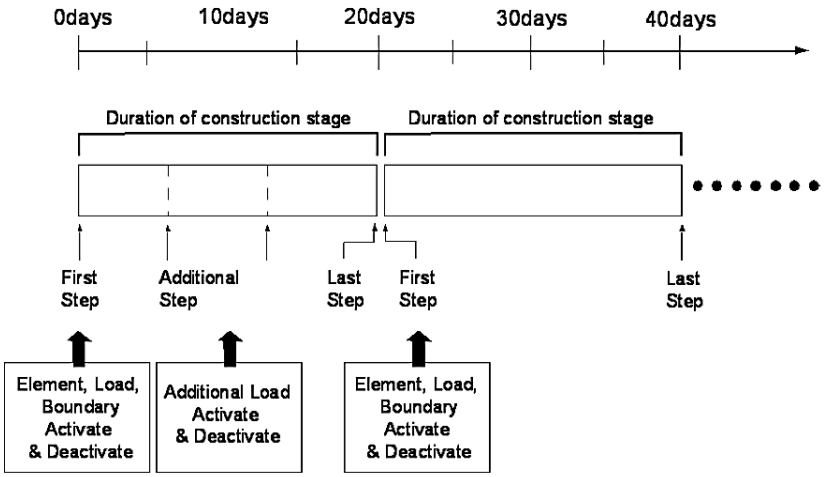

Figure 7-8 Composing of construction stages (MIDAS, 2010)

In this research, ten construction stages were composed. The first stage (element age = 28 days) comprised the initial elastic analysis. The remaining nine stages were created for the long-term analysis of the structure, each one comprising 10 days, such that the total duration of the analysis was 90 days (final element age = 118 days). Figure 7-9 shows how the construction stages were composed. The model elements, boundary conditions and loads were active for all stages. The ages of the elements were defined such that the effect of the time-dependent properties of concrete could be included in the analyses.

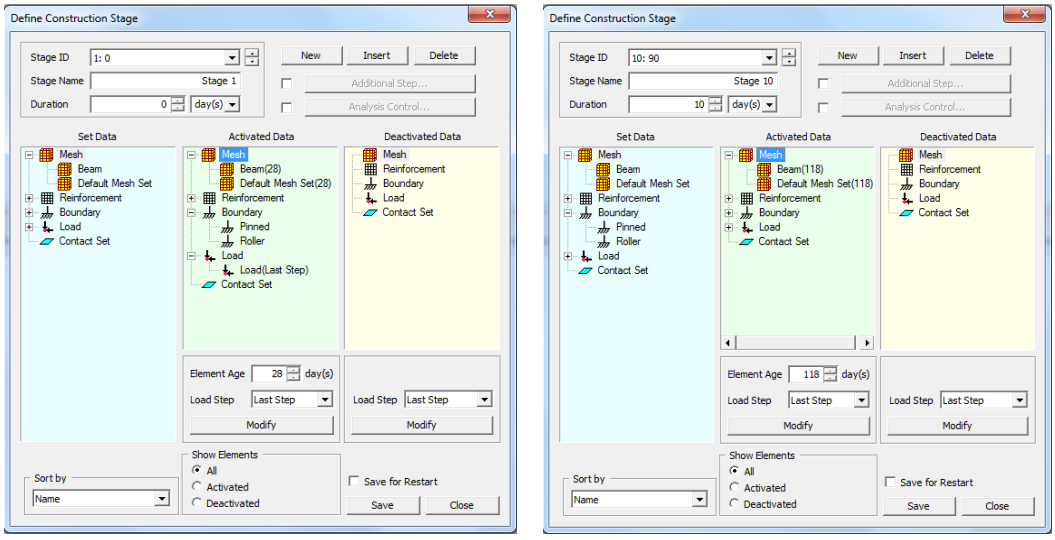

Figure 7-9 Composition of the construction stages

7.3 Development of the FEA Approach

As described earlier, the material constitutive model used to define the concrete was the Elastic model. This model is the only option can be used in Midas FEA which allows for the inclusion of time-dependent materials properties (mainly creep and shrinkage) in the analysis. However, this model does not accurately reflect the actual behaviour of cracked reinforced concrete beams under sustained load. The Elastic model is applicable for concrete in the elastic stage (un-cracked stage), but this research is on the long-term flexural behaviour of cracked beams.

The elastic model for un-cracked concrete does not take into account the effect of cracking on the stiffness of the section (including the tension stiffening response) or the different effect of shrinkage on the deflection of cracked beams. Cracking can reduce the stiffness of the section, change the creep behaviour and the tension

stiffening response with time. Moreover, the effect of shrinkage varies through the depth of the section when the section is cracked, as discussed and proven in several studies (Daud, 2016; Al-deen and Ranzi, 2015; Havlin, 2014; Marí et al., 2010; Mu et al., 2008). To confirm this, a long-term analysis was carried out using Midas FEA of the normal concrete specimen (NC) without any modification to the Elastic model. The results of this analysis were compared with the experimental results as shown in Figure 7-10.

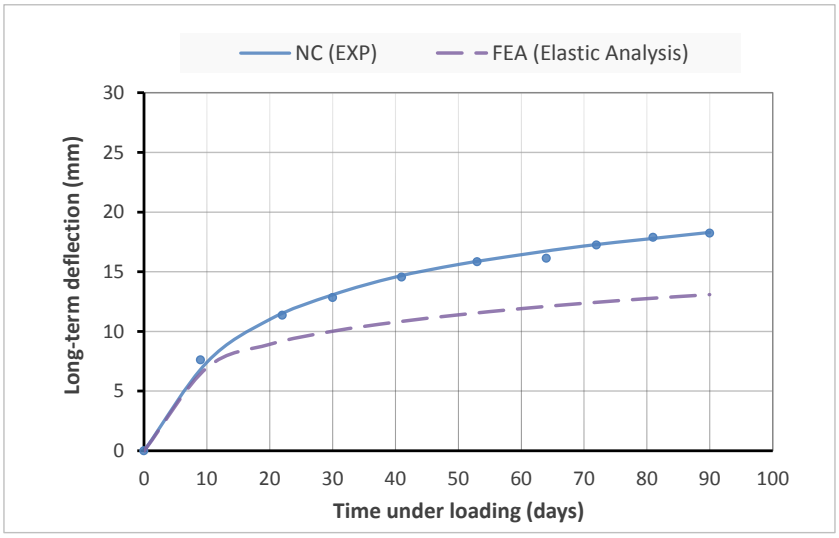

Figure 7-10 Comparison between experimental results for NC with FEA predictions using an elastic model for the concrete

It is clear from the figure that the results of the FEA analysis significantly underestimate the experimental results. This is because there are no cracks considered in the concrete section in the model which makes the section much stiffer in the analysis and reduces the deflection. In addition, the assumption that the concrete is not cracked means the effect of shrinkage is uniformly distributed through the depth of the section; this also reduces the deflection. Some modifications have been developed in this study to improve the accuracy of the simulations and the results.

In order to include the effect of cracking on the stiffness of the section with time, the CEB-FIB Model Code (2010) suggests that the modulus of elasticity of the concrete can be multiplied by a factor of 0.85. This method effectively takes into account the initial plastic strains in the elastic analysis. However, the proposed reduction factor

should not be taken as a fixed value for all types of concrete as each type of concrete has a different degree of initial cracking.

In this research, as the incorporation of recycled aggregate and steel fibres influenced the tension stiffening behaviour (see section 5.4) and the degree of cracking (see Section 5.5), it is proposed that different reduction factors can be used according to the replacement percentage of RA and the volume fraction of steel fibres.

The stiffness reduction should increase with increasing amounts of RA (as the number and width of cracks increases) and decrease with increasing steel fibres content (as the number and width of cracks decreases). Also, the stiffness reduction factor should include the different effect of incorporating the RA and steel fibres on the tension stiffening response.

Thus, an analytical investigation similar to that presented in the previous chapter (Section 6.4.2) was carried out. In this case, the effect of shrinkage was included in the calculations and the appropriate values of the reduction factor were determined to compensate for the effects of cracking only. The values obtained for the reduction factor (K^*) are presented in Table 7-1. A statistical regression analysis was used to identify the relationship between the parameters as follow:

$$K^* = 0.85 - 0.1RP\% + 10V_f\% \qquad (R^2 = 0.99) \qquad \textbf{(7-8)}$$

Using these values of K^*, good agreement with the experimental results for long-term deflection was obtained. The values in Table 7-1 were therefore used in the proposed finite element analysis approach.

In addition, the modification proposed in Section 6.4.1.2 for including the effect of steel fibres on stiffness of the section was also used. With this modification, the factor (ψ) is used in the calculations in the Effective Modulus Method (EMM) where (ψ) is a function of the volume fraction of steel fibres as given:

$$E_{c,eff}(t_0, t) = \frac{K^* E_{c28}}{1 + \psi\, \varphi(t_0, t)} \qquad \textbf{(7-9)}$$

$$\psi = 1 - 40V_f\% \qquad \textbf{(7-10)}$$

Table 7-1 Values of the reduction factor K^* for the elastic analysis

Specimen	RP (%)	V_f (%)	K*
NC	0	0	0.85
SFC-0-0.5	0	0.5	0.90
SFC-0-1.0	0	1.0	0.95
RAC-50	50	0	0.83
SFRAC-50-0.5	50	0.5	0.88
SFRAC-50-1.0	50	1.0	0.93
RAC-100	100	0	0.80
SFRAC-100-0.5	100	0.5	0.85
SFRAC-100-1.0	100	1.0	0.90

To take into account the hypothesis that the effect of shrinkage varies through the depth of the cracked section, the model employed a non-uniform distribution of shrinkage between the cracked and un-cracked part of the section. Based on the experimental results, the average cracked depth was taken to be the 75mm of all the beams. In accordance with the concept of the computational theory of shrinkage in Midas FEA, shrinkage strains are converted to compressive stresses at each time stage as follows:

$$\sigma_{sh}(t_2, t_0) = [\varepsilon_{sh}(t_2, t_0) - \varepsilon_{sh}(t_1, t_0)] \times E_{c,eff}(t_2, t_0) \quad \textbf{(7-11)}$$

These compressive stresses were applied externally to both ends of the beams as shown in Figure 7-11. A stress equal to 100% of the shrinkage stress was applied to the un-cracked part and a stress equal to 20% of the shrinkage stress was applied to the cracked part of the concrete section (Based on an investigation conducted on this point and will be presented later in this Chapter).

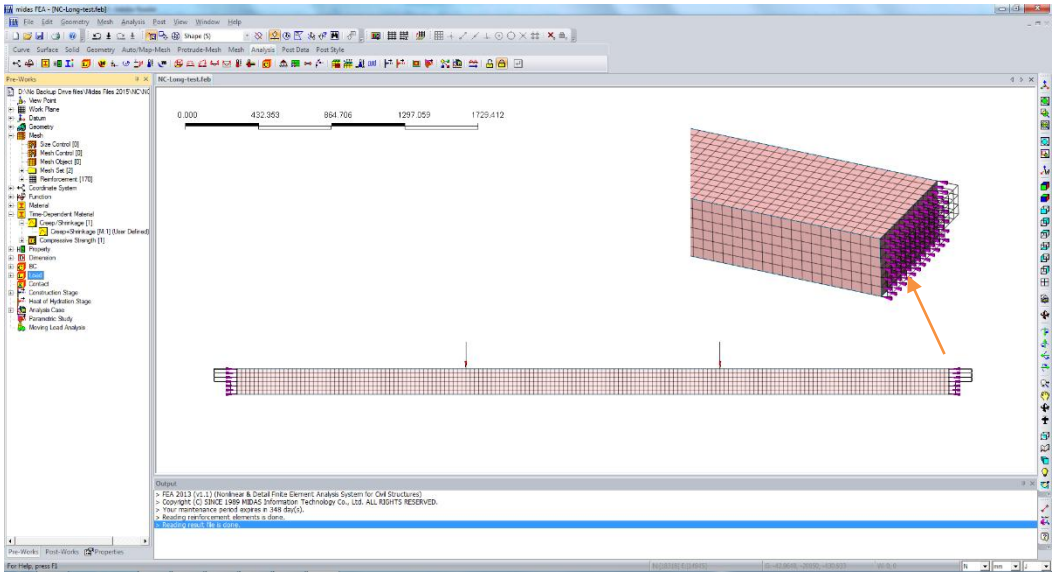

Figure 7-11 Definition of shrinkage as a non-uniform compressive stress

7.4 Results and Verification

This section compares the results of the modified FEA approach with the experimental data for the full-size beams tested. Comparisons are made between the results for long-term deflection at mid-span and concrete surface strains in the compression and tension zones. The data from the FEA predictions were extracted for the locations where measurements were taken during the experiments to enable direct comparison.

7.4.1 Long-term deflection

The mid-span deflection of the beams was measured in the experiments using an LVDT and data were collected from the FEA for the same location. A comparison between the experimental results and FEA predictions is shown in Figure 7-12. As can be seen in the figure, there is good agreement between the results for all the specimens. It has thus been demonstrated that the proposed FEA approach is capable of accurately predicting the long-term deflection of normal concrete specimens and those with and without recycled aggregate and steel fibres. By including the effect of the time-dependent properties of concrete on the long-term flexural behaviour of cracked beams, predictions are improved.

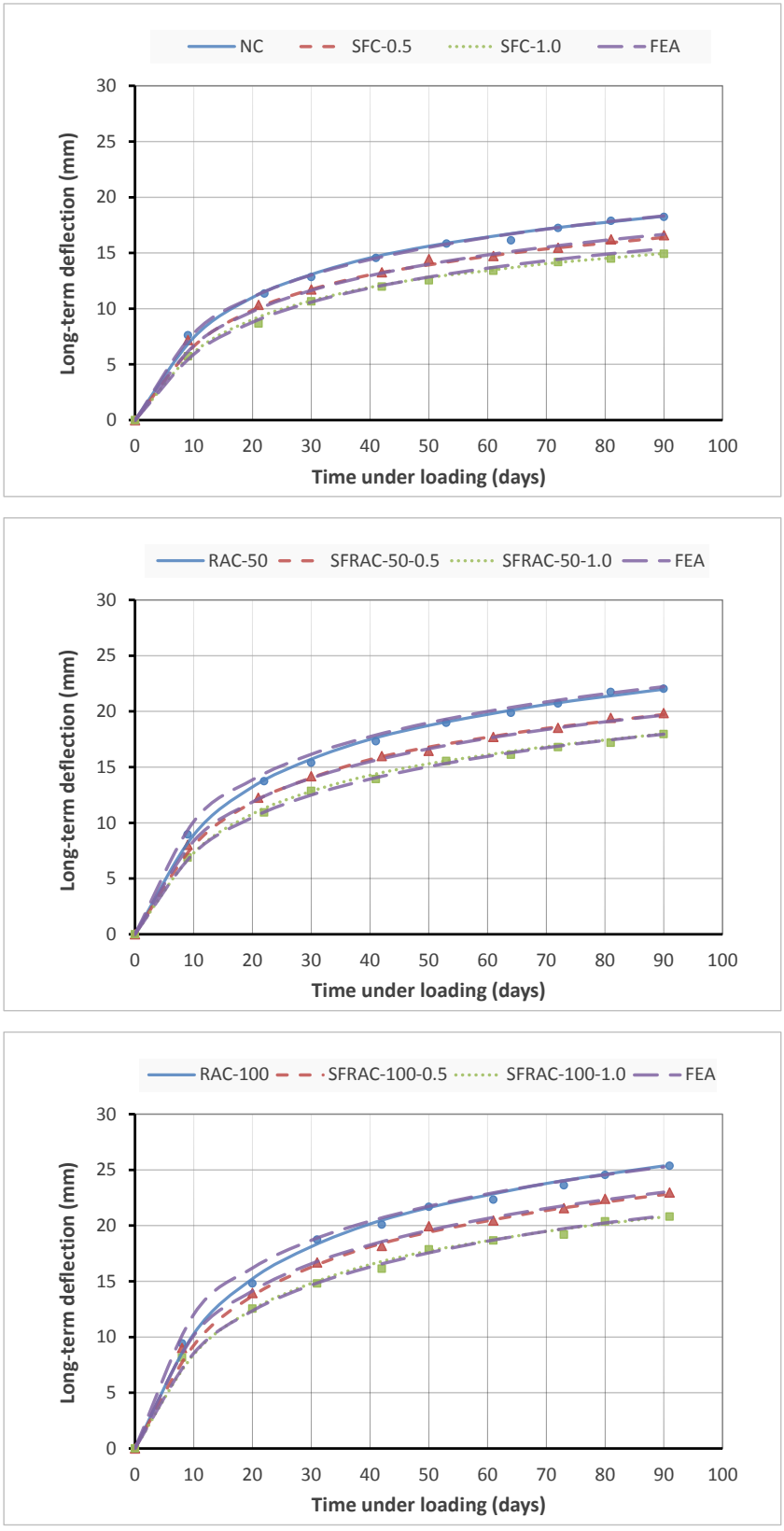

Figure 7-12 Comparison between the experimental and FEA results for long-term deflection

7.4.2 Concrete surface strains

The concrete surface strains at the compression and tension zones were measured experimentally using Demec points and a hand-held mechanical strain gauge. The average of readings for the flexural zone (between the loading points) at four different heights were recorded. Data were output from the FEA for the same locations. A comparison between the experimental results and the FEA predictions for all the beams tested are presented in Figures 7-13 and 7-14 where data for the strain at the height of the top and bottom longitudinal bars are shown. As shown in these figures, there was good agreement between the results. The FEA predictions presented in these figures were obtained from the analysis with the finest mesh size; the effect of mesh size will be discussed in the next section.

7.4.3 Verification

To expand the verification of the suitability of the modified FEA approach, beams from previous experimental investigations presented in the literature were also modelled. Using the same modified approach to model the selected beams and comparing between the obtained predictions of FEA and those recorded from the experiments allowed to validate the applicability of the proposed approach for a range of parameters and experimental conditions. The results of this verification are presented in Table 7-2. The average and the standard deviation for Exp/Pre are 0.995 and 2.51%, respectively. These results indicate that the developed FEA approach resulted in accurate predictions of long-term deflection and showed a good potential capability for use in modelling the beams under different parameters and conditions.

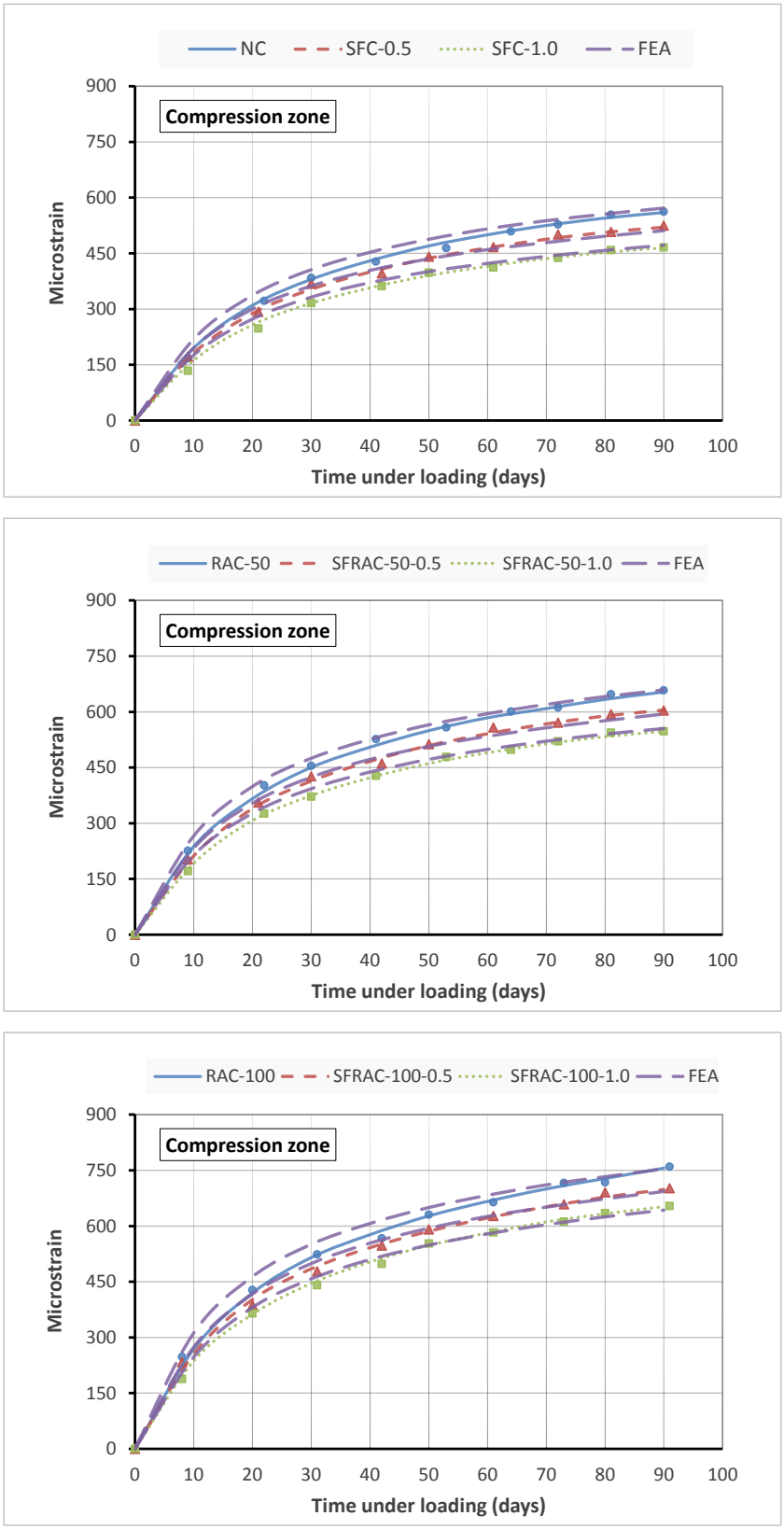

Figure 7-13 Comparison between the experimental and FEA results for concrete surface strains in the compression zone

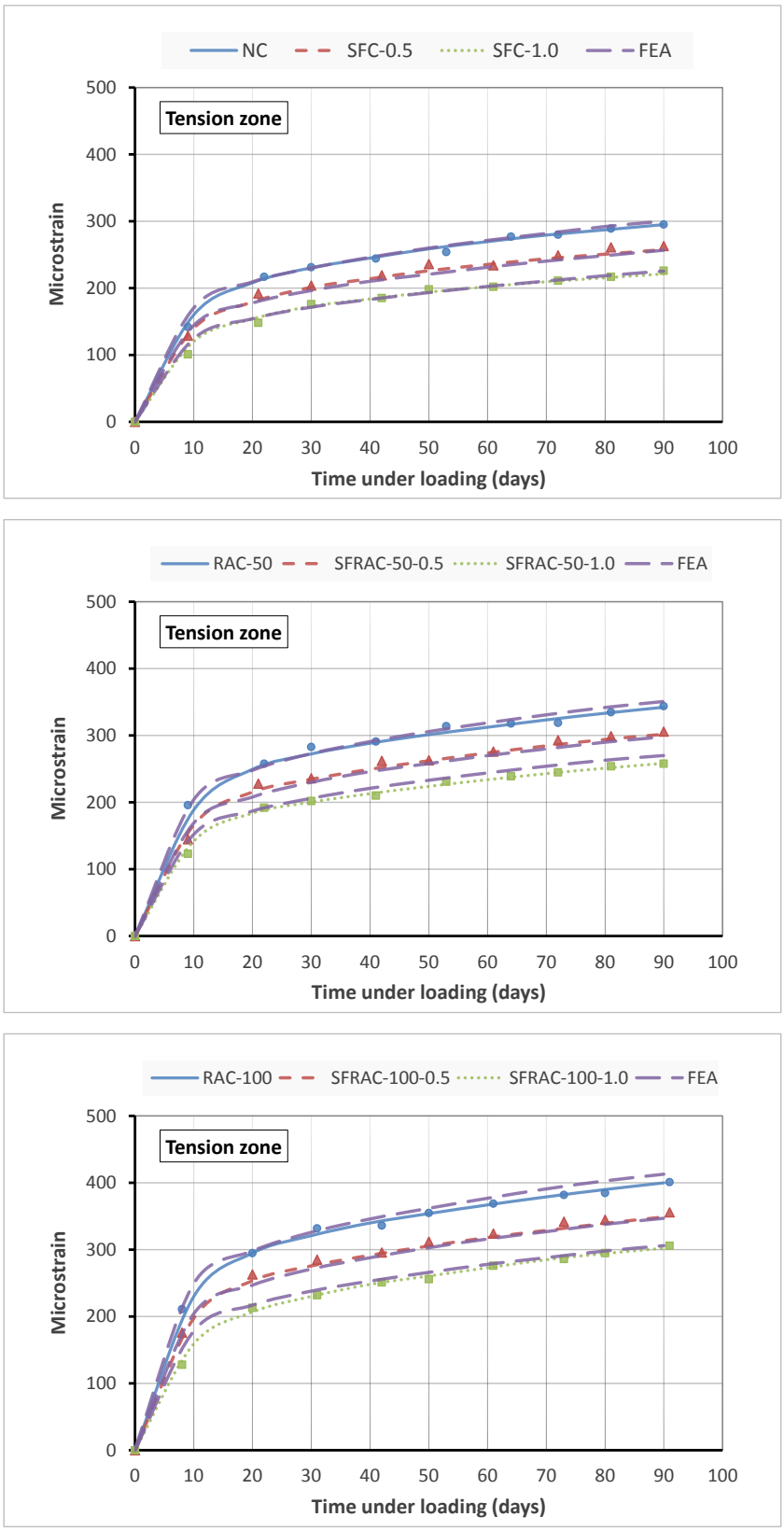

Figure 7-14 Comparison between the experimental and FEA results for concrete surface strains in the tension zone

Table 7-2 Comparison between experimental and predicted results using the modified FEA approach

Study	Specimen	Long-term deflection (mm)		
		Exp	Pre	$\mathrm{Exp}/\mathrm{Pre}$
This research	NC	18.30	18.33	0.998
	SFC-0-0.5	16.40	16.66	0.984
	SFC-0-1.0	14.94	15.38	0.971
	RAC-50	21.99	22.22	0.989
	SFRAC-50-0.5	19.72	19.67	1.002
	SFRAC-50-1.0	17.98	17.95	1.001
	RAC-100	25.36	25.25	1.004
	SFRAC-100-0.5	22.78	23.00	0.991
	SFRAC-100-1.0	20.79	20.87	0.996
Knaack and Kurama (2015b)	CC-0-28	10.19	9.96	1.023
	CC-50-28	11.22	11.43	0.980
	CC-100-28	12.27	12.54	0.978
Łapko and Grygo (2010)	NC	14.00	14.55	0.962
	RAC	16.00	16.75	0.955
Ashour et al. (1997)	BS-0.0-0.5	6.08	6.39	0.951
	BS-0.75-0.5	5.27	4.99	1.05
	BS-1.5-0.5	4.08	4.00	1.02
Tan et al. (1994b)	A-50-0	3.50	3.47	1.008
	B-50-0.5	3.20	3.15	1.015
	C-50-1.0	3.10	3.02	1.026
Average				0.995
Standard deviation				2.51%

7.5 Investigation of Model Parameters

The influence of various modelling parameters were investigated including element size, reduction value in the stiffness, effective value of shrinkage at cracking and crack depth. These parameters were investigated in some detail in order to assess their sensitivity on the accuracy of the predictions. Experimental and model results for four beam specimens (NC, SFC-1.0, RAC-100 and SFRAC-100-1.0) were selected to carry out this investigation. There was no significant difference between the conclusions drawn for the beams investigated, so the results for the NC beam specimen are presented and discussed here for illustrative purposes.

7.5.1 Mesh size

Mesh sensitivity is not considered be an issue when using Midas FEA. The software provides several options for generating meshes. They can be created based on user specifications or through automatic mesh generation functions in the software. Nevertheless, mesh sensitivity was investigated using three different mesh sizes: 50, 25 and 12.5mm cubes and the influence of mesh size on the predictions for long-term deflection and concrete surface strains was inspected.

After completing the analyses, the first item examined was the calculation time. The analysis of the beam model with an element size of 50mm took 202 seconds, while the analyses of models with mesh sizes of 25 and 12.5mm took 452 and 2274 seconds respectively. Figure 7-15 shows the predictions from calculations using the modified FEA approach for long-term deflection for the three different mesh sizes. It can be seen that the difference in predictions was ±2% and that the predicted long-term deflection decreased with increasing mesh size.

Figure 7-16 shows the mesh sensitivity of the predictions for concrete surface strains in the compression and tension zones. There is a noticeable difference in the predictions of up to 40%. This is due to the method used in the software for calculating the average deformation of each element and how that is converted to the surface strain of the element. As the mesh size increases, the volume and the area of each face of the element increases. The concrete surface strains change significantly through the depth of the section, and with increasing mesh size, the accuracy of the predictions decreases.

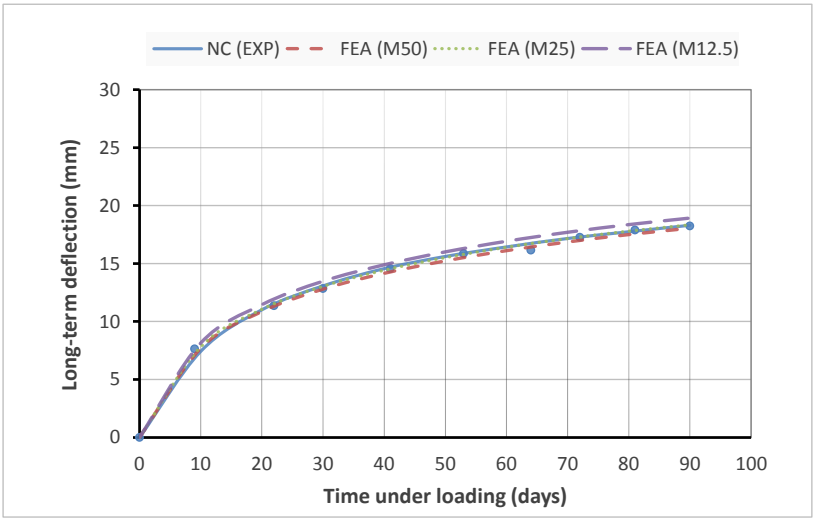

Figure 7-15 Mesh sensitivity of the predictions for long-term deflection

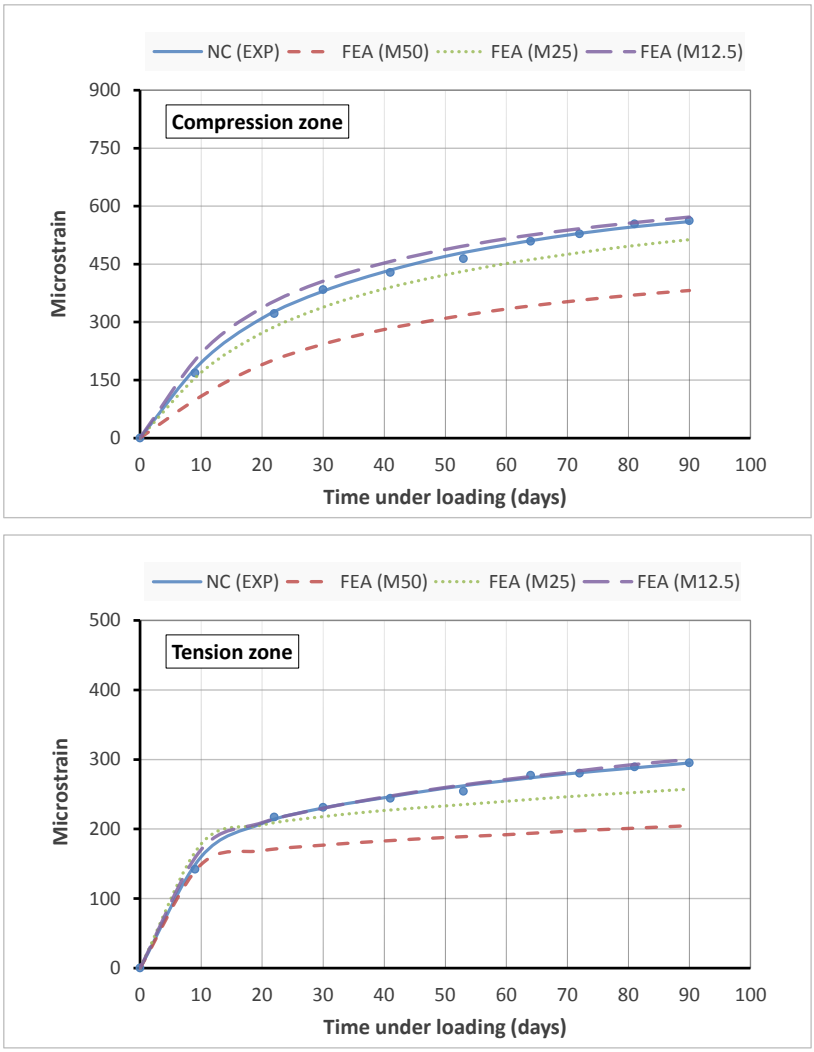

Figure 7-16 Mesh sensitivity of the predictions for concrete surface strains in the compression and tension zones

7.5.2 Effective reduction in stiffness

As mentioned earlier, the suggestion of the CEB-FIB Model Code (2010) to reduce the modulus of elasticity of concrete was followed in order to take into account the effect of cracking on the stiffness of the section in case of the elastic analysis. In this investigation, the sensitivity of the value of this reduction to the accuracy of the results was examined. Three different reduction values were used to carry out the analysis for all the beams assessed. The reduction values proposed in Table 7-1 represent the accurate results for all the beams.

Figure 7-17 presents the sensitivity of the reduction values to the predictions of the FEA approach for long-term deflection of the NC beam specimens. The results of using three different reduction values: K^*= 0.90, 0.85 and 0.80 for this specimen showed that increasing or decreasing the reduction value by 5% can result in 8% more or less in the predictions of the long-term deflection. Therefore, this remarkable effect should be considered when this proposed FEA approach would be used.

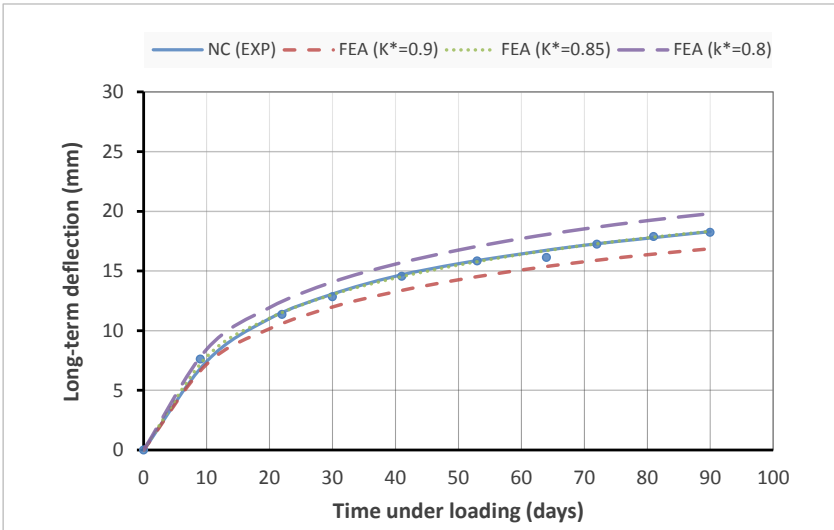

Figure 7-17 Effect of reduction value in stiffness on the predictions for long-term deflection

7.5.3 Shrinkage effect at cracking

The effect of shrinkage on cracked concrete sections has been investigated in several studies (Daud, 2016; Al-deen and Ranzi, 2015; Havlin, 2014; Marí et al., 2010; Mu et al., 2008). However, there is no available data for the magnitude of this

effect. Daud (2016) found that there is a relationship between the effective shrinkage in the cracked section and the number of cracks. It was concluded that as the number of cracks increases, the effective shrinkage at cracking decreases and at the stabilised crack stage, 20% shrinkage stress was confirmed as the effective percentage. In this research, all beams were loaded to the stabilised cracking stage; the same percentage was used and the slight difference in the degree of cracking was considered when the shrinkage stresses were calculated. The value of the effective modulus of elasticity ($E_{c,eff}$) can be used to take into account this difference and the same effective percentage of shrinkage for all beams was determined.

In this investigation, three different percentages of the shrinkage stress (10%, 20% and 30%) were applied to the cracked sections, and the accuracy of the resulting predictions was evaluated. Figure 7-18 shows the effect of different levels of shrinkage stress on the predictions of the FEA approach for long-term deflection. It can be seen that the predictions assuming a 20% shrinkage stress agreed most closely with the experimental results. Increasing the applied shrinkage stress by 10% resulted in a reduction in accuracy of 6%. A similar result was obtained for all the beams assessed, where the 20% shrinkage stresses were determined to give the best correlation.

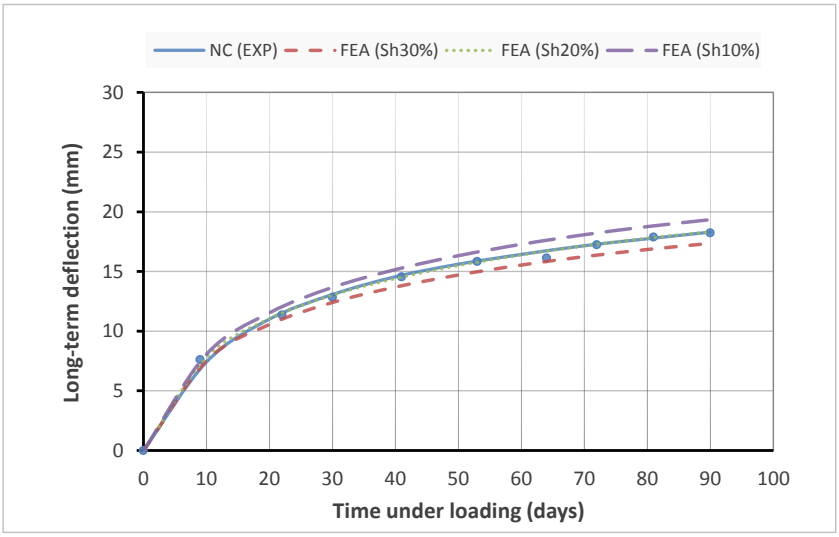

Figure 7-18 Effect of shrinkage in the cracked region on the predictions for long-term deflection

7.5.4 Depth of cracking

As the non-uniform distribution of shrinkage is related to the depth of cracking in the section, the effect of the crack depth assumed in the model on the accuracy of the predictions was assessed. Three different depths of cracked section (50, 75 and 100 mm) were investigated. Figure 7-19 illustrates the influence of crack depth on the accuracy of the long-term deflection predictions. The results show that increasing the crack depth by 25mm, increases the predictions for long-term deflection by 8%. By increasing the crack depth, the amount of shrinkage decreases in the lower part of the section (the part in tension) which acts to compress the section, hence the deflection increases. This confirms that the crack depth assumed must be chosen carefully to provide accurate predictions. In this research, good agreement was obtained between the experimental results and the FEA predictions when the average crack depth observed experimentally (75mm) was used.

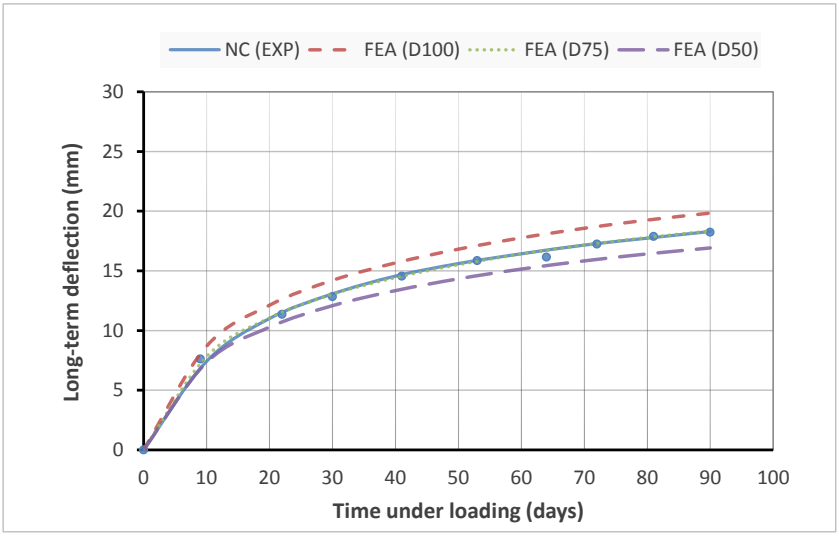

Figure 7-19 Influence of crack depth on the predictions for long-term deflection

7.6 Parametric Study

The primary aim of this parametric study was to investigate the effect of various structural parameters on the long-term deflection of reinforced concrete beams containing recycled aggregate and steel fibres. In particular, using the developed FEA approach, the influences of compression reinforcement amount, concrete

cover and predicted values of shrinkage and creep were studied. Specimens (NC) and (SFRAC-50-1.0) were selected to perform this study.

7.6.1 Compression reinforcement amount

As non-symmetrical reinforcement is considered to be one of the main factors affecting long-term deflection, the effects of different compression reinforcement amounts on the long-term deflection of reinforced beams prepared with recycled aggregate and steel fibres were examined. Four different amounts of compression reinforcement were used (A_s`= 0, 0.5A_s, A_s and 2A_s) in order to investigate the effect of this factor.

Figure 7-20 shows that when there was no compression reinforcement in the beam the long-term deflection recorded the highest value. It can be clearly noticed that on increasing the compression reinforcement amount by 50% of the tensile reinforcement, the long-term deflection decreased by 20%. In addition, the presence of compression reinforcement with an equivalent amount of 100% and 200% from tensile reinforcement could reduce the long-term deflection by 47% and 92% respectively. This can be due to the significant role of the compression reinforcement amount in restraining shrinkage and controlling creep values in the compression zone, which increase the stiffness of the section with time. The effect of this factor showed almost the same percentages for all the beams assessed for this investigation.

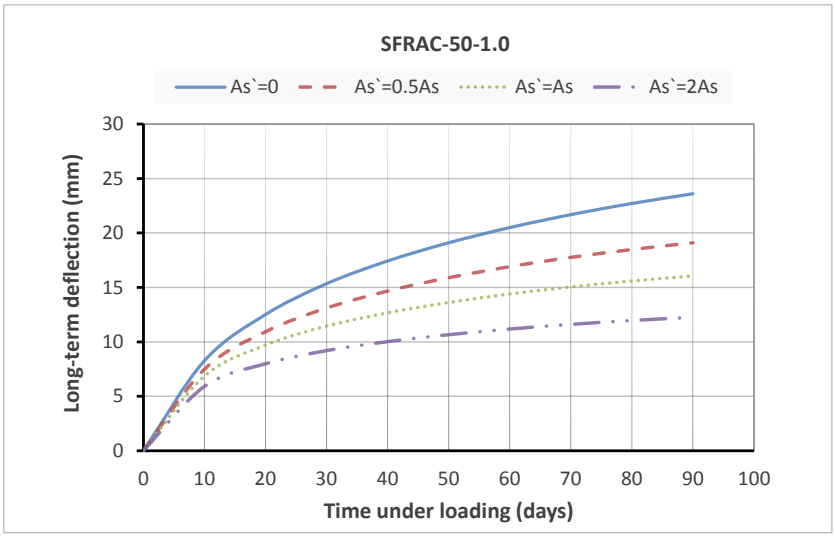

Figure 7-20 Effect of the compression reinforcement amount on the long-term deflection of SFRAC-50-1.0 specimen

7.6.2 Concrete cover

This line of investigation was to examine the influence of concrete cover on long-term deflection of beams incorporating recycled aggregate and steel fibres. Three different concrete cover values (15, 25 and 35mm) were used for this investigation. The results indicated that increasing the concrete cover by 10mm and 20mm could considerably increase the long-term deflection, by 22% and 44% respectively, as presented in Figure 7-21. This can be assumed to be due to the reduction in the effective depth of the section from increasing the concrete cover and its effect on reducing the stiffness of the section. This can also suggest that reducing the stiffness of the section by increasing the concrete cover has a greater influence on increasing long-term deflection than the additional contribution of the cover in enhancing tension stiffening, bond strength and cracking pattern.

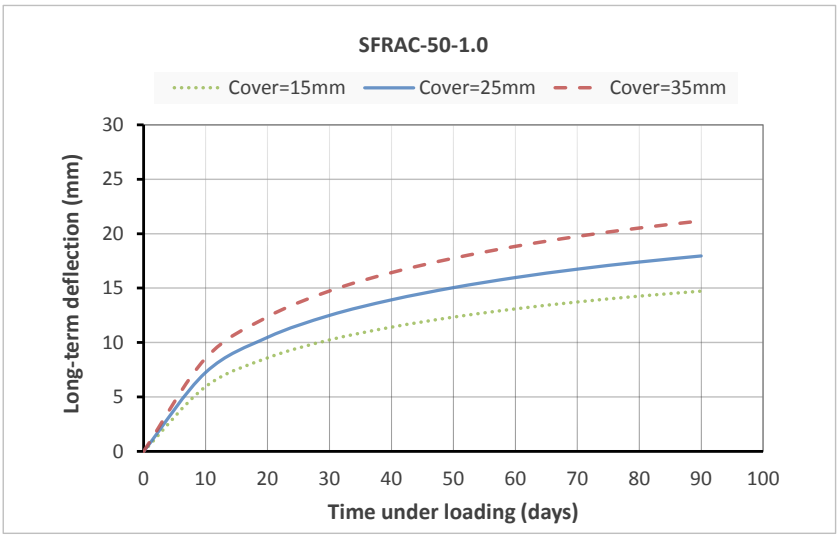

Figure 7-21 Effect of concrete cover on the long-term deflection of SFRAC-50-1.0 specimen

7.6.3 Experimental and predicted shrinkage and creep

As shrinkage and creep are the main parameters in the calculation of the long-term deflection of concrete members, a comparison was made using the experimental and predicted values of shrinkage and creep. The models of ACI-209 and CEB-FIB 2010 were used to predict the values of shrinkage and creep for the NC specimen and then used in the data entered in the developed FEA approach to predict the long-term deflection of the beam.

Firstly, the results of the predictions showed that both models overestimated shrinkage values compared to the experimental results, as shown in Figure 7-22. Moreover, it was evident that the CEB-FIB 2010 model exhibited a remarkable overestimation during the first 20 days. However, in the creep coefficient, the results of the CEB-FIB 2010 model showed a good agreement with the experimental results and ACI-209 was underestimated, as presented in Figure 7-23. This obvious difference in the results of shrinkage and creep can definitely affect the final results of the long-term deflection of beams.

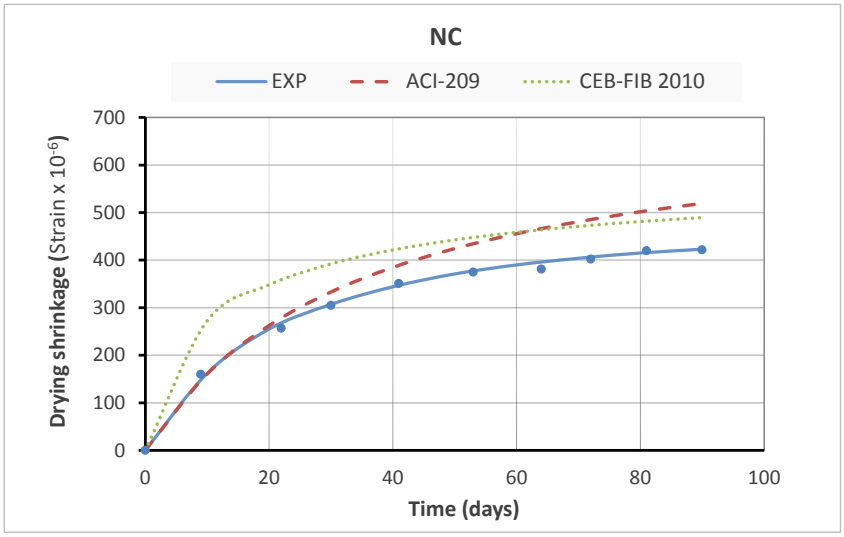

Figure 7-22 Comparison of experimental and predicted shrinkage for NC specimen

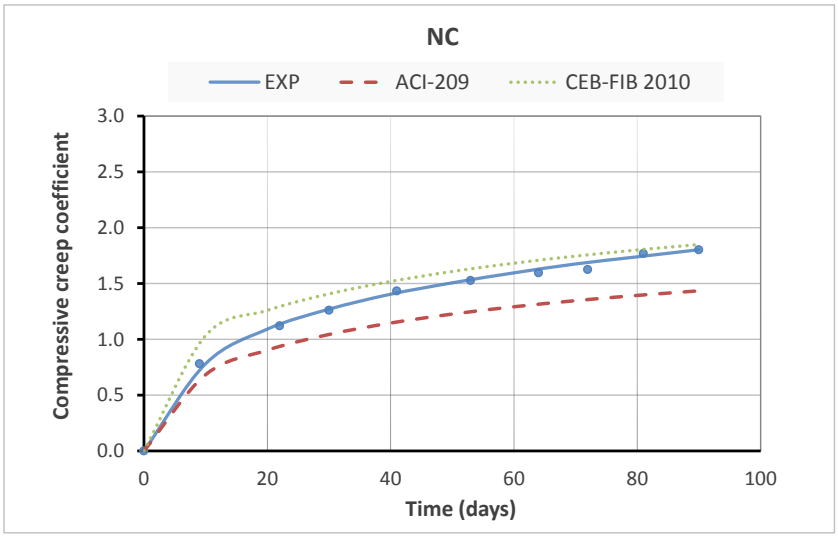

Figure 7-23 Comparison of experimental and predicted creep for NC specimen

Figure 7-24 presents the results of the long-term deflection for the NC specimen. The results were obtained by using the developed FEA approach with the experimental and predicted values for shrinkage and creep. It can be seen that when using the ACI-209 predictions the long-term deflection was underestimated by 12%. However, using the predictions of the CEB-FIB 2010 resulted in a slight overestimation by 4%. Accuracy in the results for long-term deflection directly depends on the predictions of shrinkage and creep.

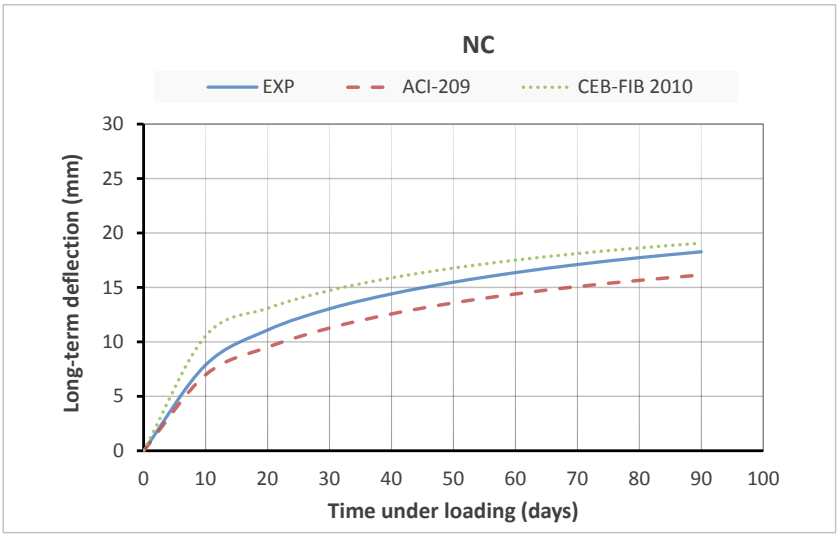

Figure 7-24 Effect of using the experimental and predicted shrinkage and creep values on the long-term deflection for NC specimen

7.7 Conclusion

In this chapter, a finite element analysis approach has been developed for using Midas FEA to predict the long-term deflection of reinforced cracked beams incorporating recycled aggregate and steel fibres. The following conclusions can be drawn:

- Midas FEA provides an elastic constitutive model for concrete which includes the effect of time-dependent properties. However, this model does not accurately reflect the behaviour of cracked concrete.
- In order to develop a new FEA approach, the suggestion in the CEB-FIB Model Code of including the effect of cracking on the stiffness of the section by reducing the modulus of elasticity was followed.

- The hypothesis of a non-uniform distribution of shrinkage through the depth of the section proposed in other studies was also examined and employed.
- The predictions of the developed FEA approach were verified through comparison with the experimental results from this study and data selected from previous investigations. Good agreement was obtained for the long-term deflections and concrete surface strains which indicates that the developed approach is suitable and accurate for a range of different parameters and experimental conditions.
- The influence of a number of model parameters on the accuracy of the FEA predictions was investigated. The mesh sensitivity study showed that with increasing element size, the accuracy of the predictions decreased. Although there was no significant influence on the predictions for long-term deflection, element size had a notable effect on the predictions for concrete surface strains.
- The results of the effect of the different reduction values in the stiffness of the section showed that increasing or decreasing the reduction value has a significant influence on the predictions of the long-term deflection.
- The investigation of the amount of shrinkage at cracking indicated that with an increase in the percentage of shrinkage applied to the cracked section, the predictions for long-term deflection decreased.
- The influence of the assumed depth of cracking on the accuracy of the predictions was also investigated. The results showed that with an increase in the crack depth, the predictions for the long-term deflection decreased.
- A parametric study was carried out to investigate the influence of some structural parameters on the long-term deflection of beams by using the developed FEA approach. The results showed that the amount of compression reinforcement and concrete cover have significant effects on the long-term deflection values.
- The comparison study of using the experimental and predicted shrinkage and creep showed that using the predictions of ACI-209 in the FEA approach resulted in underestimated long-term deflection of beams. However, using the predictions of CEB-FIB 2010 exhibited better results.

Chapter 8 : Conclusions and Recommendations for Further Research

8.1 Introduction

The long-term flexural behaviour of cracked reinforced concrete beams incorporating recycled aggregate and steel fibres was studied in this research. To achieve the research objectives, the study was divided into three phases: an experimental investigation, an analytical investigation and a finite element analysis. The final conclusions have been presented into three sections in accordance with the primary phases of this research.

8.2 Conclusions

The final concluding remarks of this research have been dawn as follows:

8.2.1 Concluding remarks from the experimental investigation

- All strength properties along with the modulus of elasticity of concrete deteriorated with the incorporation of RA. This is attributed to the presence of adhered mortar, clay brick and tiles in the RA, which have poorer properties than NA particles. In contrast, adding steel fibres considerably enhanced the mechanical properties of the normal and recycled aggregate concrete tested.
- The drying shrinkage and creep deformations of concrete significantly increased by the incorporation of RA while adding steel fibres to both NC and RAC resulted in noticeable reductions in drying shrinkage and tensile creep strains. However, it had less effect on compressive creep.
- The substitution of NA by RA increased the loss of tension stiffening over time. On the other hand, the addition of steel fibres to NC and RAC had a significant influence on the reduction in tension stiffening over time.
- The experimental results indicated that the incorporation of RA had a noticeable effect on increasing the first cracking loads and the short-term deflection of beams and the inclusion of steel fibres had considerable effect on reducing these aspects.

- In terms of the cracking patterns observed at the stabilised cracking stage, the RAC beams had wider and more closely spaced cracks than the NC beams. In contrast, the SFRC beams made with NC and RAC had fewer narrower cracks compared to those without steel fibres.
- The measured long-term deflections indicated that increasing the replacement percentage of RA results in significant increases in long-term deflection. However, the addition of steel fibres reduced the long-term deflection for all the NC and RAC beams tested.
- The results for concrete surface strains showed that steel fibres have a greater effect on reducing strains in the tension zone than in the compression zone.
- According to the results obtained, it can be deduced that the incorporation of 50% RA with 0.5% steel fibres or 100% RA with 1.0% steel fibres could result in concrete with similar strength properties, time-dependent deformations and flexural behaviour to conventional concrete.
- The addition of steel fibres to recycled aggregate concrete successfully enhances the properties of the concrete and the flexural behaviour of RAC beams. In particular it improves the serviceability (short and long-term deflections and cracking behaviour) sufficiently to overcome the restrictions that limit the use of RAC in construction applications.

8.2.2 Concluding remarks from the analytical investigation

- A comparison between the existing code procedures for predicting the long-term deflection of concrete beams showed that the methods which employ a multiplier factor approach (ACI-318, CSA and AS3600) fail to make accurate predictions.
- Significant improvements in accuracy were noted for the methods which take into account the effects of all the parameters that influence long-term deflection (Gilbert, 2012 and Eurocode 2).
- The evaluation of the suitability of the Eurocode 2 method for predicting the long-term behaviour of concrete members showed the code underestimated the long-term deflection of RAC beams and overestimated when steel fibres were added.

- Modifications to the value of (β) were proposed to account for the different tension stiffening behaviour of beams with RA and steel fibres. In addition, a statistical regression analysis was carried out to determine the combined effect of RA and steel fibres on the relationship of (β).
- Based on the fundamental assumption of the Effective Modulus of Elasticity Method, a factor (ψ) was proposed to account for the effect of incorporating steel fibres on reducing strains in the tension zone (tensile creep) and enhancing long-term section stiffness.
- A numerical analysis program was developed using the MATLAB language for predicting the long-term deflection of reinforced concrete beams. This program is based on the cracked section analysis approach in Eurocode 2 and included the proposed modifications to account for the effects of incorporating recycled aggregate and steel fibres.
- The applicability of this program was validated by investigating the influence of various design parameters on the predictions. Data obtained from previous studies were used along with the experimental results from this study, and the results showed that the proposed modifications and numerical program gave accurate results for a range of conditions.

8.2.3 Concluding remarks from the finite element analysis

- A 3D finite element analysis approach was developed for predicting the long-term deflection of cracked reinforced concrete beams. The approach includes consideration of the effects of incorporating recycled aggregate and steel fibres in concrete.
- The proposed FEA approach based on modifying an elastic constitutive model for defining the concrete materials properties to include the effect of the time-dependent properties of the materials.
- In order to develop the approach, the suggestion in the CIB-FIB Model Code of including the effect of cracking on the stiffness of the section by reducing the modulus of elasticity was employed.
- The technique of a non-uniform distribution of shrinkage through the depth of the section was included. Applying 20% of the shrinkage stress to cracked section was confirmed as the effective value for accurate predictions at the stabilised cracking stage for beams.

- The predictions of the developed FEA approach were verified through comparison with the experimental results from this study and data selected from previous investigations. Good agreement was obtained for the long-term deflections and concrete surface strains which indicates that the developed approach is suitable and accurate for a range of different parameters and experimental conditions.
- The influence of various model parameters on the accuracy of the FEA predictions was investigated. The influence of mesh sensitivity, reduction value in the stiffness, effective shrinkage in the cracked section and depth of cracking on the long-term deflection were addressed.
- A parametric study was carried out to investigate the influence of some structural parameters on the long-term deflection of beams by using the developed FEA approach. The results showed that the amount of compression reinforcement and concrete cover have significant effects on the long-term deflection values.
- The comparison study of using the experimental and predicted shrinkage and creep showed that using the predictions of ACI-209 in the FEA approach resulted in underestimated long-term deflection of beams. However, using the predictions of CEB-FIB 2010 exhibited better results.

Finally, the findings of this research indicated that the addition of steel fibres to the RAC succeed in overcoming the negative effect of replacing RA on the properties of concrete, in particular, the time-dependent performance. This combination will be potentially a viable alternative which allows for increasing the use of RA in constructions and solve several environmental issues. In addition, this research provided valuable experimental results, analytical and finite element investigations and developments which help researchers and engineers and improve the code guidelines to expand the scope of using SFRAC for structural applications.

8.3 Recommendations for Further Research

The following are recommended areas for further research:

- In this research, CDW was used as the recycled aggregate. It is recommended that other types of recycled aggregate such as RCA are

tested to examine the effects of diversity of resources and variability in aggregate characteristics.

- The durability performance of RAC is still not well known. Thus more research needs to be conducted in this area.
- It is recommended that the effects of adding other shapes of steel fibre and other types of fibre such as glass or synthetic are studied to examine which is structurally and economically the most effective type.
- This research focused on the flexural behaviour of beams. It is recommended that the long-term flexural behaviour of different concrete structures such as slabs and deep beams are investigated.
- The effect of different boundary conditions should be considered, for example by examining continuous beams and slabs, and different loading configurations.
- The influence of other parameters that affect the long-term flexural performance of concrete structures such as reinforcement ratios and ambient conditions requires more investigation.
- Additional experimental results are needed to fully validate the proposed modifications to the Eurocode2 method and the FEA approach for predicting the long-term deflection of concrete beams.
- Expansion of the numerical program developed in this research is recommended to include other proposed methods for predicting the strength properties, short-term deflection and time-dependent deformations of concrete made with recycled aggregate and steel fibres.
- In the future, the proposed FEA approach could be improved and implemented within commercial available software package

REFERENCES

ACI COMMITTEE 209. 2008. *Prediction of creep, shrinkage and temperature effect in concrete structures (ACI 209R-08).* American Concrete Institute, Farmington Hills, Michigan.

ACI COMMITTEE 318. 2014. *Building code requirements for structural concrete and commentary (ACI 318R-14)*. American Concrete Institute, Farmington Hills, Michigan.

ACI COMMITTEE 435. 1966. *Deflections of Reinforced Concrete Flexural Members (ACI 435R-95).* American Concrete Institute, Farmington Hills, Michigan.

ACI COMMITTEE 544. 2009. *Design Considerations for Steel Fiber Reinforced Concrete (ACI 544.4 R-09)*. American Concrete Institute, Farmington Hills, Michigan.

AJDUKIEWICZ, A. & KLISZCZEWICZ, A. 2002. Influence of recycled aggregates on mechanical properties of HS/HPC. *Cement and Concrete Composites,* 24, 269-279.

AJDUKIEWICZ, A. B. & KLISZCZEWICZ, A. T. 2007. Comparative tests of beams and columns made of recycled aggregate concrete and natural aggregate concrete. *Journal of Advanced Concrete Technology,* 5, 259-273.

AKBARNEZHAD, A., ONG, K., ZHANG, M., TAM, C. & FOO, T. 2011. Microwave-assisted beneficiation of recycled concrete aggregates. *Construction and Building Materials,* 25, 3469-3479.

AKINKUROLERE, O. 2010. Experimental investigation on the influence of steel fiber on the compressive and tensile strength of recycled aggregate concrete. *Journal of Engineering and Applied Sciences,* 5, 264-268.

AL-DEEN, S. & RANZI, G. 2015. Effects of non-uniform shrinkage on the long-term behaviour of composite steel-concrete slabs. *International Journal of Steel Structures,* 15, 415-432.

AL-OWAISY, L. S. R. & SHALLAL, M. A. 2007. Strength and elasticity of steel fiber reinforced concrete at high temperatures. *Journal of Engineering and Development,* 11.

ALENGARAM, U. J., SALAM, A., JUMAAT, M. Z., JAAFAR, F. F. & SAAD, H. B. 2011. Properties of high-workability concrete with recycled concrete aggregate. *Materials Research,* 14, 248-255.

ALSAYED, S. H. 1993. Flexural deflection of reinforced fibrous concrete beams. *ACI Structural Journal,* 90.

ALTUN, F., HAKTANIR, T. & ARI, K. 2007. Effects of steel fiber addition on mechanical properties of concrete and RC beams. *Construction and Building Materials,* 21, 654-661.

ARAÚJO, J. 2005. Simplified procedures for calculation of instantaneous and long-term deflections of reinforced concrete beams. *Revista Engenharia Civil da Universidade do Minho***,** 57-68.

AREZOUMANDI, M., SMITH, A., VOLZ, J. S. & KHAYAT, K. H. 2015. An experimental study on flexural strength of reinforced concrete beams with 100% recycled concrete aggregate. *Engineering Structures,* 88, 154-162.

ASHOUR, S. A., MAHMOOD, K. & WAFA, F. F. 1997. Influence of steel fibers and compression reinforcement on deflection of high-strength concrete beams. *ACI Structural Journal,* 94, 611-624.

ASHOUR, S. A., WAFA, F. F. & KAMAL, M. I. 2000. Effect of the concrete compressive strength and tensile reinforcement ratio on the flexural behavior of fibrous concrete beams. *Engineering Structures,* 22, 1145-1158.

BAI, W. H. & SUN, B. X. 2010. Experimental study on flexural behavior of recycled coarse aggregate concrete beam. *Applied Mechanics and Materials*, 543-548.

BALUGARU, P. & SHAH, S. 1992. Fiber-reinforced cement. *Composites*.

BEEBY, A. 1990. Fixings in cracked concrete. The probability of coincident occurrence and likely crack width.

BEEBY, A., SCOTT, R. & JONES, A. 2005. Revised code provisions for long-term deflection calculations. *Proceedings of the Institution of Civil Engineers-Structures and Buildings,* 158, 71-75.

BEGUM, R. A., SIWAR, C., PEREIRA, J. J. & JAAFAR, A. H. 2006. A benefit–cost analysis on the economic feasibility of construction waste minimisation: the case of Malaysia. *Resources, Conservation and Recycling*, 48, 86-98.

BENTUR, A. & MINDESS, S. 2006. *Fibre reinforced cementitious composites*. CRC Press.

BERNDT, M. 2009. Properties of sustainable concrete containing fly ash, slag and recycled concrete aggregate. *Construction and Building Materials,* 23, 2606-2613.

BISCHOFF, P. H. 2000. Comparison of tension stiffening for plain and steel fibre reinforced concrete. *Proceedings of the RILEM symposium on fibre-reinforced concretes*, 2000. 633-641.

BISCHOFF, P. H. 2001. Effects of shrinkage on tension stiffening and cracking in reinforced concrete. *Canadian Journal of Civil Engineering,* 28, 363-374.

BISCHOFF, P. H. 2003. Tension stiffening and cracking of steel fiber-reinforced concrete. *Journal of Materials in Civil Engineering,* 15, 174-182.

BRANSON, D. E. 1977. *Deformation of Concrete Structures*. McGraw-Hill Companies.

BRITISH STANDARDS INSTITUTION 1992. *BS882: Specification for aggregates from natural sources for concrete.* London: British Standards Institution.

BRITISH STANDARDS INSTITUTION 2000a. *BS EN 12350-2: Testing fresh concrete – Part-2: Slump test*. British Standards Institution.

BRITISH STANDARDS INSTITUTION 2000b. *BS EN 12390-2:2000: Testing hardened concrete. Making and curing specimens for strength tests.* British European Standard.

BRITISH STANDARDS INSTITUTION 2001. *BS EN 10002-1:2001: Tensile testing of metallic materials. Method of test at ambient temperature.* British Standards Institution.

BRITISH STANDARDS INSTITUTION 2002. *BS EN 1008:2002: Mixing Water for Concrete. Specification for Sampling, Testing and Assessing the Suitability of Water, Including Water Recovered from Processes in the Concrete Industry, as Mixing Water in Concrete*. British Standards Institution.

BRITISH STANDARDS INSTITUTION, 2004. *Eurocode 2: Design of Concrete Structures: Part 1-1: General Rules and Rules for Buildings, BS EN 1992-1-1:2004*. British Standards Institution.

BRITISH STANDARDS INSTITUTION 2006a. *BS EN 14889-1: Fibres for concrete*. British Standards Institution.

BRITISH STANDARDS INSTITUTION 2006b. *Concrete – Complementary British Standard to BS EN 206-1-Part 1: Method of Specifying and Guidance for the Specifier*. British Standards Institution.

BRITISH STANDARDS INSTITUTION 2009a. *BS EN 12390-5:2009: Testing hardened concrete. Flexural strength of test specimens.* British Standards Institution.

BRITISH STANDARDS INSTITUTION 2009b. *BS EN 12390-6: Tensile splitting strength of test specimens. Testing hardened concrete*. British Standards Institution. 1-14.

BRITISH STANDARDS INSTITUTION 2011a. *BS EN 197-1:2011: Cement, composition, specifications and conformity criteria for common cements.* London, England: British Standard Institution.

BRITISH STANDARDS INSTITUTION 2011b. *BS EN 12390-3:2009: Testing hardened concrete: Compressive strength of test specimens*. British Standards Institution.

BRITISH STANDARDS INSTITUTION 2012. *BS EN 934-2:2009+A1:2012: Admixtures for concrete, mortar and grout. Concrete admixtures. Definitions, requirements, conformity, marking and labeling*. British Standards Institution.

BRITISH STANDARDS INSTITUTION 2013. *BS EN 12390: Testing hardened concrete – Part 13: Determination of secant modulus of elasticity in compression*. Brussels, Belgium: European Committee for Standardization.

BUYLE-BODIN, F. & HADJIEVA-ZAHARIEVA, R. 2002. Influence of industrially produced recycled aggregates on flow properties of concrete. *Materials and Structures,* 35, 504-509.

CARNEIRO, J. A., LIMA, P. R. L., LEITE, M. B. & TOLEDO FILHO, R. D. 2014. Compressive stress–strain behavior of steel fiber reinforced-recycled aggregate concrete. *Cement and Concrete Composites,* 46, 65-72.

CASUCCIO, M., TORRIJOS, M., GIACCIO, G. & ZERBINO, R. 2008. Failure mechanism of recycled aggregate concrete. *Construction and Building Materials,* 22, 1500-1506.

CEB-FIP, MC90. 1990. Design of concrete structures. *British Standard Institution,* London.

CEB-FIB MODEL CODE. 2010. Design Code for Concrete Structures, volume 1. *International Federation for Structural Concrete (fib)*, Lausanne.

CHEN, Z.-P., HUANG, K.-W., ZHANG, X.-G. & XUE, J.-Y. 2010. Experimental research on the flexural strength of recycled coarse aggregate concrete. *2010 International Conference on Mechanic Automation and Control Engineering (MACE)*. IEEE, 1041-1043.

CHERN, J.-C. & YOUNG, C.-H. 1990. Study of factors influencing drying shrinkage of steel fiber reinforced concrete. *ACI Materials Journal,* 87.

CHOI, W.-C. & YUN, H.-D. 2013. Long-term deflection and flexural behavior of reinforced concrete beams with recycled aggregate. *Materials & Design,* 51, 742-750.

CHUNXIANG, Q. & PATNAIKUNI, I. 1999. Properties of high-strength steel fiber-reinforced concrete beams in bending. *Cement and Concrete Composites,* 21, 73-81.

COELHO, A. & DE BRITO, J. 2011. Distribution of materials in construction and demolition waste in Portugal. *Waste Management & Research,* 29, 843-853.

CORINALDESI, V. 2011. Structural concrete prepared with coarse recycled concrete aggregate: From investigation to design. *Advances in Civil Engineering,* 2011.

CORINALDESI, V. & MORICONI, G. 2009a. Behaviour of cementitious mortars containing different kinds of recycled aggregate. *Construction and Building Materials,* 23, 289-294.

CORINALDESI, V. & MORICONI, G. 2009b. Influence of mineral additions on the performance of 100% recycled aggregate concrete. *Construction and Building Materials,* 23, 2869-2876.

COPPLE, F. 1981. Costs and Energy Considerations. National Seminar on PCC Pavement Recycling and Rehabilitation.

CSA COMMITTEE A23.3. 2003. *Design of concrete structurers*. Canadian Standards Association CSA, Rexdale, Ont.

DAUD, S. 2016. *Long-Term Behaviour of Cracked Reinforced Concrete Beams Under Sustained and Repeated Loading* Ph.D. Thesis, University of Leeds.

DAUD, S., FORTH, J. P. & NIKITAS, N. 2015. Time-dependent behaviour of reinforced concrete beams under sustained and repeated loading. *Development,* 998, 10002695.

DE BRITO, J. & SAIKIA, N. 2012. *Recycled aggregate in concrete: Use of industrial, construction and demolition waste*. Springer Science & Business Media.

DE JUAN, M. S. & GUTIÉRREZ, P. A. 2004. Influence of recycled aggregate quality on concrete properties. *International conference on use of recycled materials in building and structures*, Barcelona, Spain, 2004.

DE JUAN, M. S. & GUTIÉRREZ, P. A. 2009. Study on the influence of attached mortar content on the properties of recycled concrete aggregate. *Construction and Building Materials,* 23, 872-877.

DE OLIVEIRA JÚNIOR, L. Á., DE LIMA ARAÚJO, D., TOLEDO FILHO, R. D., FAIRBAIRN, E. D. M. R., DE MORAES, E. & SOUZA DE ANDRADE, M. A. 2016. Tension stiffening of steel-fiber-reinforced concrete. *Acta Scientiarum Technology,* 38, 456-463.

DE OLIVEIRA, M. B. & VAZQUEZ, E. 1996. The influence of retained moisture in aggregates from recycling on the properties of new hardened concrete. *Waste Management,* 16, 113-117.

DOMINGO, A., LÁZARO, C., GAYARRE, F., SERRANO, M. & LOPEZ-COLINA, C. 2010. Long term deformations by creep and shrinkage in recycled aggregate concrete. *Materials and Structures,* 43, 1147-1160.

EGUCHI, K., TERANISHI, K., NAKAGOME, A., KISHIMOTO, H., SHINOZAKI, K. & NARIKAWA, M. 2007. Application of recycled coarse aggregate by mixture to concrete construction. *Construction and Building Materials,* 21**,** 1542-1551.

ELSAIGH, W. & ST KEARSLEY, F. 2002. Effect of steel fibre content on properties of concrete. *Beton, South Africa,* 102**,** 8-12.

EPA. Environmental Protection Agency. Available in: <http://www.epa.gov> [accessed January 2014].

ETXEBERRIA, M., MARI, A. & VAZQUEZ, E. 2007. Recycled aggregate concrete as structural material. *Materials and Structures,* 40, 529-541.

EUROSTAT. Waste statistics in Europe. Available in: <http://epp.eurostat.ec.europa.eu/> [accessed in July 2014].

FAN, Y., XIAO, J. & TAM, V. W. 2014. Effect of old attached mortar on the creep of recycled aggregate concrete. *Structural Concrete,* 15, 169-178.

FATHIFAZL, G., RAZAQPUR, A. G., ISGOR, O. B., ABBAS, A., FOURNIER, B. & FOO, S. 2011. Creep and drying shrinkage characteristics of concrete produced with coarse recycled concrete aggregate. *Cement and Concrete Composites,* 33, 1026-1037.

FERREIRA, L., DE BRITO, J. & BARRA, M. 2011. Influence of the pre-saturation of recycled coarse concrete aggregates on concrete properties. *Magazine of Concrete Research,* 63, 617-627.

FIELDS, K. & BISCHOFF, P. H. 2004. Tension stiffening and cracking of high-strength reinforced concrete tension members. *Structural Journal,* 101, 447-456.

FISHER, C. & WERGE, M. 2009. *EU as a Recycling Society.* ETC. SCP Working Paper 2/2009.

FONSECA, N., DE BRITO, J. & EVANGELISTA, L. 2011. The influence of curing conditions on the mechanical performance of concrete made with recycled concrete waste. *Cement and Concrete Composites,* 33, 637-643.

FORTH, J. P. & MARTIN, A. J. 2014. Design of Liquid Retaining Concrete Structures. 3rd Edition, *Whittles Publishing*.

GHALI, A. & AZARNEJAD, A. 1999. Deflection prediction of members of any concrete strength. *Structural Journal,* 96, 807-817.

GHALI, A., FAVRE, R. & ELBADRY, M., 2006. *Concrete structures: Stresses and deformations: Analysis and design for serviceability*. CRC Press.

GILBERT, R. 2001a. Deflection calculation and control – Australian code amendments and improvements. *Special Publication,* 203, 45-78.

GILBERT, R. 2001b. Shrinkage, cracking and deflection – the serviceability of concrete structures. *Electronic Journal of Structural Engineering,* 1, 2-14.

GILBERT, R. 2011. The serviceability limit states in reinforced concrete design. *Procedia Engineering,* 14, 385-395.

GILBERT, R. 2012. Creep and shrinkage induced deflections in RC beams and slabs. *Special Publication,* 284, 1-16.

GILBERT, R. I. 1999. Deflection calculation for reinforced concrete structures – why we sometimes get it wrong. *Structural Journal,* 96, 1027-1032.

GILBERT, R.I. & RANZI, G., 2010. *Time-dependent behaviour of concrete structures*. CRC Press.

GOMES, M. & DE BRITO, J. 2009. Structural concrete with incorporation of coarse recycled concrete and ceramic aggregates: Durability performance. *Materials and Structures,* 42, 663-675.

GOMEZ-SOBERON, J. M. 2002. Porosity of recycled concrete with substitution of recycled concrete aggregate: An experimental study. *Cement and Concrete Research,* 32, 1301-1311.

GONZÁLEZ-FONTEBOA, B. & MARTÍNEZ-ABELLA, F. 2008. Concretes with aggregates from demolition waste and silica fume. Materials and mechanical properties. *Building and Environment,* 43, 429-437.

GONZÁLEZ-FONTEBOA, B., MARTÍNEZ-ABELLA, F., EIRAS-LÓPEZ, J. & SEARA-PAZ, S. 2011. Effect of recycled coarse aggregate on damage of recycled concrete. *Materials and Structures,* 44, 1759-1771.

GRIBNIAK, V., KAKLAUSKAS, G., KAČIANAUSKAS, R., ATKOČIŪNAS, J., MANG, H. A., NORKUS, A., TAMULEVIČIUS, S., KVEDARAS, A. K. & RAUDYS, Š. 2009. *Shrinkage influence on tension-stiffening of concrete structures.* Vilniaus Gedimino technikos universitetas.

GUL, M., BASHIR, A. & NAQASH, J. A. 2014. Study of modulus of elasticity of steel fiber reinforced concrete. *International Journal of Engineering and Advanced Technology,* 3, 304-309.

GUPTA, A., MANDAL, S. & GHOSH, S. 2011. Direct compressive strength and elastic modulus of recycled aggregate concrete. *International Journal of Civil & Structural Engineering,* 2, 292-304.

HAMEED, M. & CHINI, A. 2010. Impact of transportation on cost and energy for recycled concrete aggregate. Accessed online, 3, 13.

HANSEN, T. C. & NARUD, H. 1983. Strength of recycled concrete made from crushed concrete coarse aggregate. *Concrete International,* 5, 79-83.

HAVLIN, K.J., 2014. Finite element simulation of long-term behaviour of post-tensioned composite slabs. *The UNSW Canberra at ADFA Journal of Undergraduate Engineering Research*, *6*(1).

HEERALAL, M., KUMAR, P. R. & RAO, Y. 2009. Flexural fatigue charecteristics of steel fiber reinforced recycled aggregate concrete.

HUGHES, B. P. 1981. Experimental test results for flexure and direct tension of fibre cement composites. *International Journal of Cement Composites and Lightweight Concrete,* 3, 13-18.

IGNJATOVIĆ, I. S., MARINKOVIĆ, S. B., MIŠKOVIĆ, Z. M. & SAVIĆ, A. R. 2013. Flexural behavior of reinforced recycled aggregate concrete beams under short-term loading. *Materials and Structures,* 46, 1045-1059.

JALILIFAR, H., SAJEDI, F. & KAZEMI, S. 2016. Investigation on the mechanical properties of fiber reinforced recycled concrete. *Civil Engineering Journal,* 2, 13-22.

JAMES, M. N., CHOI, W. & ABU-LEBDEH, T. 2011. Use of recycled aggregate and fly ash in concrete pavement. *American Journal of Engineering and Applied Sciences,* 4.

JOHNSTON, C. D. & COLEMAN, R. A. 1974. Strength and deformation of steel fiber reinforced mortar in uniaxial tension. *Special Publication,* 44, 177-194.

KANG, H., KIM, W., KWAK, K. & HONG, G. 2014. Flexural testing of reinforced concrete beams with recycled concrete aggregates. *ACI Structural Journal,* 111, 607.

KANG, T. H., KIM, W., MASSONE, L. M. & GALLEGUILLOS, T. A. 2012. Shear-flexure coupling behavior of steel fiber-reinforced concrete beams. *ACI Structural Journal,* 109, 435.

KATZ, A. 2003. Properties of concrete made with recycled aggregate from partially hydrated old concrete. *Cement and Concrete Research,* 33, 703-711.

KHALFALLAH, S. & GUERDOUH, D. 2014. Tension stiffening approach in concrete of tensioned members. *International Journal of Advanced Structural Engineering,* 6, 1-6.

KHAN, A. 1984. Recycled concrete – a source for new aggregate. *Cement, Concrete and Aggregates,* 6, 17-27.

KNAACK, A. M. & KURAMA, Y. C. 2014. Behavior of reinforced concrete beams with recycled concrete coarse aggregates. *Journal of Structural Engineering,* 141, B4014009.

KNAACK, A. M. & KURAMA, Y. C. 2015a. Creep and shrinkage of normal-strength concrete with recycled concrete aggregates. *ACI Materials Journal,* 112.

KNAACK, A. M. & KURAMA, Y. C. 2015b. Sustained service load behavior of concrete beams with recycled concrete aggregates. *ACI Structural Journal,* 112, 565.

KOSMATKA, S. H., KERKHOFF, B. & PANARESE, W. C. 2011. *Design and control of concrete mixtures*. Portland Cement Association.

KOU, S.-C. & POON, C.-S. 2008. Mechanical properties of 5-year-old concrete prepared with recycled aggregates obtained from three different sources. *Magazine of Concrete Research,* 60, 57-64.

KOU, S.-C., POON, C.-S. & AGRELA, F. 2011a. Comparisons of natural and recycled aggregate concretes prepared with the addition of different mineral admixtures. *Cement and Concrete Composites,* 33, 788-795.

KOU, S.-C., POON, C.-S. & ETXEBERRIA, M. 2011b. Influence of recycled aggregates on long term mechanical properties and pore size distribution of concrete. *Cement and Concrete Composites,* 33, 286-291.

KOU, S. & POON, C. 2012. Enhancing the durability properties of concrete prepared with coarse recycled aggregate. *Construction and Building Materials,* 35, 69-76.

KOU, S. C., POON, C. S. & CHAN, D. 2008. Influence of fly ash as a cement addition on the hardened properties of recycled aggregate concrete. *Materials and Structures,* 41, 1191-1201.

KRISHNA, T. S. 2015. An experimental investigation on flexural behavior of recycle aggregate fiber reinforcement concrete. *International Research Journal of Engineering and Technology. e-ISSN*, 2395-0056.

KUMAR, D. N., RAO, T. V., MADHU, T., SAROJA, P. & PRASAD, D. 2014. An experimental study of recycled concrete with polyporpylene fiber. *International Journal of Innovative Research in Advanced Engineering*, 2349-2163.

ŁAPKO, A. & GRYGO, R. 2010. Long term deformations of recycled aggregate concrete (RAC) beams made of recycled concrete. *Modern buildings materials structures and techniques, proceedings of the 10th international conference, 2010.*

LEE, G.-Y. & KIM, W. 2009. Cracking and tension stiffening behavior of high-strength concrete tension members subjected to axial load. *Advances in Structural Engineering,* 12, 127-137.

LEE, S.-C., CHO, J.-Y. & VECCHIO, F. J. 2013. Tension-stiffening model for steel fiber-reinforced concrete containing conventional reinforcement. *ACI Structural Journal,* 110, 639-648.

LI, J., XIAO, H. & ZHOU, Y. 2009. Influence of coating recycled aggregate surface with pozzolanic powder on properties of recycled aggregate concrete. *Construction and Building Materials,* 23, 1287-1291.

LI, Z. 2011. *Advanced concrete technology*. John Wiley & Sons.

LIM, T., PARAMISIVAM, P. & LEE, S. 1987. Bending behavior of steel-fiber concrete beams. *Structural Journal,* 84, 524-536.

LIMBACHIYA, M., KOULOURIS, A., ROBERTS, J. & FRIED, A. 2004. Performance of recycled aggregate concrete. *Proceedings of RILEM international symposium on environment-conscious materials and systems for sustainable development,* 2004. 127-136.

LIMBACHIYA, M., MEDDAH, M. S. & OUCHAGOUR, Y. 2012. Use of recycled concrete aggregate in fly-ash concrete. *Construction and Building Materials,* 27, 439-449.

LORMAN, W. R. 1940. Theory of Concrete Creep. *Proc. Am. Soc. Test. Mater,* 40**,** 1082-1102.

MALHOTRA, V. 1978. Recycled concrete – A new aggregate. *Canadian Journal of Civil Engineering,* 5, 42-52.

MANGAT, P. & AZARI, M. M. 1984. A theory for the free shrinkage of steel fibre reinforced cement matrices. *Journal of Materials Science,* 19, 2183-2194.

MANGAT, P. & AZARI, M. M. 1985. A theory for the creep of steel fibre reinforced cement matrices under compression. *Journal of Materials Science,* 20, 1119-1133.

MANGAT, P. & AZARI, M. M. 1988. Shrinkage of steel fibre reinforced cement composites. *Materials and Structures,* 21, 163-171.

MARÍ, A. R., BAIRÁN, J. M. & DUARTE, N. 2010. Long-term deflections in cracked reinforced concrete flexural members. *Engineering Structures,* 32, 829-842.

MARUYAMA, I., SOGO, M., SOGABE, T., SATO, R. & KAWAI, K. 2004. Flexural properties of reinforced recycled concrete beams. *Proceedings of the international RILEM conference on the use of recycled materials in buildings and structures*, Barcelona, Spain, 2004. Citeseer, 8-11.

MAS, B., CLADERA, A., DEL OLMO, T. & PITARCH, F. 2012. Influence of the amount of mixed recycled aggregates on the properties of concrete for non-structural use. *Construction and Building Materials,* 27, 612-622.

MATIAS, D. & DE BRITO, J. 2004. Influence of the shape of the coarse recycled concrete aggregates on the workability and strength of concrete. *Structural Concrete*, 187-194.

MEDA, A., MINELLI, F. & PLIZZARI, G. A. 2012. Flexural behaviour of RC beams in fibre reinforced concrete. *Composites Part B: Engineering,* 43, 2930-2937.

MIDAS 2010. *FEA analysis and algorithm manual. Nonlinear and Detail FE Analysis System for Civil Structures*. Midas Information and Technology.

MITCHELL, D., ABRISHAMI, H. H. & MINDESS, S. 1996. The effect of steel fibers and epoxy-coated reinforcement on tension stiffening and cracking of reinforced concrete. *Materials Journal,* 93, 61-68.

MONTEIRO, P. 2006. *Concrete: Microstructure, properties, and materials*. McGraw-Hill Publishing.

MU, R., FORTH, J., BEEBY, A. & SCOTT, R. 2008. Modelling of shrinkage induced curvature of cracked concrete beams. *Tailor made concrete solutions* (Walraven, J. C. and Steelhurst, D. (eds)). Abingdon, UK: Taylor & Francis, 573-578.

MUKAI, T. & KIKUCHI, M. 1978. Studies on utilization of recycled concrete for structural members (Part 1, Part 2). Summaries of technical papers of annual meeting, Architectural Institute of Japan, 1978. 85-86.

NAGATAKI, S., GOKCE, A. & SAEKI, T. 2000. Effects of recycled aggregate characteristics on performance parameters of recycled aggregate concrete. *Special Publication,* 192, 53-72.

NAGATAKI, S., GOKCE, A., SAEKI, T. & HISADA, M. 2004. Assessment of recycling process induced damage sensitivity of recycled concrete aggregates. *Cement and Concrete Research,* 34, 965-971.

NAKOV, D., 2014. *Time-Dependent Behaviour of SFRC Elements under Sustained and Repeated Variable Loads.* Doctoral dissertation, University" Ss. Cyril and Methodius, Macedonia.

NEVILLE, A. M., DILGER, W. H. & BROOKS, J. J. 1983. *Creep of Plain and Structural Concrete*, Construction press.

NEVILLE, A. M. 1995. *Properties of concrete*.

PAWADE, E. P. Y., PANDE, D. A. & NAGARNAIK, D. P. 2011. Effect of steel fibers on modulus of elasticity of concrete. *International Journal of Advanced Engineering Sciences and Technologies,* 1, 169-177.

PEPE, M. 2015. *A conceptual model for designing recycled aggregate concrete for structural applications*. Springer.

POON, C., SHUI, Z., LAM, L., FOK, H. & KOU, S. 2004a. Influence of moisture states of natural and recycled aggregates on the slump and compressive strength of concrete. *Cement and Concrete Research,* 34, 31-36.

POON, C. S., SHUI, Z. & LAM, L. 2004b. Effect of microstructure of ITZ on compressive strength of concrete prepared with recycled aggregates. *Construction and Building Materials,* 18, 461-468.

PRASAD, M. & RATHISH KUMAR, P. 2007. Strength studies on glass fiber reinforced recycled aggregate concrete. *Asian Journal of Civil Engineering (Building and Housing),* 8, 677-690.

RAHAL, K. 2007. Mechanical properties of concrete with recycled coarse aggregate. *Building and Environment,* 42, 407-415.

RAO, M. C., BHATTACHARYYA, S. & BARAI, S. 2011. Influence of field recycled coarse aggregate on properties of concrete. *Materials and Structures,* 44, 205-220.

RILEM T.C. 162-TDF. 2002. Test and design methods for steel fibre reinforced concrete. *Materials and structures*, *35*, pp.579-582.

ROSS, A. 1937. Concrete Creep Data. *Structural Engineer,* 15**,** 314-326.

WU, M. H. Q. 2010. *TENSION STIFFENING IN REINFORCED CONCRETE– INSTANTANEOUS AND TIME-DEPENDENT BEHAVIOUR.* PhD thesis UNIVERSITY OF NEW SOUTH WALES, SYDNEY.

SAFIUDDIN, M., ALENGARAM, U. J., RAHMAN, M. M., SALAM, M. A. & JUMAAT, M. Z. 2013. Use of recycled concrete aggregate in concrete: A review. *Journal of Civil Engineering and Management,* 19, 796-810.

SAGOE-CRENTSIL, K. K., BROWN, T. & TAYLOR, A. H. 2001. Performance of concrete made with commercially produced coarse recycled concrete aggregate. *Cement and Concrete Research,* 31, 707-712.

SANTOS, J. R., BRANCO, F. A. & DE BRITO, J. 2002. Compressive strength, modulus of elasticity and drying shrinkage of concrete with coarse recycled concrete. *XXXIAHS World Congress on Housing*, Coimbra, Portugal, 2002. 1685-1691.

SARSAM, K. & AL-AZZAWI, Z. M. K. 2010. Mechanical properties of high-strength fiber reinforced concrete.

SATO, R., MARUYAMA, I., SOGABE, T. & SOGO, M. 2007. Flexural behavior of reinforced recycled concrete beams. *Journal of Advanced Concrete Technology,* 5, 43-61.

SCOTT, R. H. & BEEBY, A. W. 2005. Long-term tension-stiffening effects in concrete. *ACI Structural Journal,* 102, 31.

SCOTT, R. H. & BEEBY, A. W. 2012. Evaluation and management of tension stiffening. *Special Publication,* 284, 1-18.

SENARATNE, S., GERACE, D., MIRZA, O., TAM, V. W. & KANG, W.-H. 2016. The costs and benefits of combining recycled aggregate with steel fibres as a sustainable, structural material. *Journal of Cleaner Production*, 112, 2318-2327.

SHAH, S. P. & RANGAN, B. V. 1971. Fiber reinforced concrete properties. *Journal Proceedings*, 1971. 126-137.

SHENDE, A., PANDE, A. & PATHAN, M. G. 2012. Experimental study on steel fiber reinforced concrete for M-40 Grade. *International Refereed Journal of Engineering and Science,* 1, 043-048.

SILVA, R., DE BRITO, J. & DHIR, R. 2015. Prediction of the shrinkage behavior of recycled aggregate concrete: A review. *Construction and Building Materials,* 77, 327-339.

SOUTSOS, M., LE, T. & LAMPROPOULOS, A. 2012. Flexural performance of fibre reinforced concrete made with steel and synthetic fibres. *Construction and Building Materials,* 36, 704-710.

SRI, R. & TAM, C. 1985. Properties of concrete made with crushed concrete as coarse aggregate. *Magazine of Concrete Research,* 37.

STANDARDS AUSTRALIA 2009. *Concrete structures AS3600-2009.* Sydney, Australia: Standards Australia.

SWAMY, F. & SA'AD, A. 1981. Deformation and ultimate strength in flexure of reinforced. *ACI Journal*.

SWAMY, R. & STAVRIDES, H. 1979. Influence of fiber reinforcement on restrained shrinkage and cracking. J*ournal Proceedings,* 1979, 443-460.

TAHA, M. R. & HASSANAIN, M. A. 2003. Estimating the error in calculated deflections of HPC slabs: A parametric study using the theory of error propagation. *ACI Special Publications,* 210, 65-92.

TAM, V. W., TAM, C. & WANG, Y. 2007. Optimization on proportion for recycled aggregate in concrete using two-stage mixing approach. *Construction and Building Materials,* 21, 1928-1939.

TAM, V. W. 2008. Economic comparison of concrete recycling: A case study approach. Resources, *Conservation and Recycling*, 52, 821-828.

TAN, K.-H., PARAMASIVAM, P. & TAN, K.-C. 1994a. Creep and shrinkage deflections of RC beams with steel fibers. *Journal of Materials in Civil Engineering,* 6, 474-494.

TAN, K., PARAMASIVAM, P. & TAN, K. 1994b. Instantaneous and long-term deflections of steel fiber reinforced concrete beams. *ACI Structural Journal,* 91, 384-393.

TAN, K. H. & SAHA, M. K. 2005. Ten-year study on steel fiber-reinforced concrete beams under sustained loads. *ACI Structural Journal,* 102, 472-480.

TANGCHIRAPAT, W., BURANASING, R., JATURAPITAKKUL, C. & CHINDAPRASIRT, P. 2008. Influence of rice husk–bark ash on mechanical properties of concrete containing high amount of recycled aggregates. *Construction and Building Materials,* 22, 1812-1819.

THOMAS, J. & RAMASWAMY, A. 2007. Mechanical properties of steel fiber-reinforced concrete. *Journal of Materials in Civil Engineering,* 19, 385-392.

TOPCU, I. B. 1997. Physical and mechanical properties of concretes produced with waste concrete. *Cement and Concrete Research,* 27, 1817-1823.

VAKHSHOURI, B. & NEJADI, S. 2014. Limitations and uncertainties in the long-term deflection calculation of concrete structures. Vulnerability, uncertainty, and risk: Quantification, mitigation, and management, 2014. ASCE, 535-546.

VASANELLI, E., MICELLI, F., AIELLO, M. A. & PLIZZARI, G. 2013. Long term behavior of FRC flexural beams under sustained load. *Engineering Structures,* 56, 1858-1867.

VIEIRA, J., CORREIA, J. & DE BRITO, J. 2011. Post-fire residual mechanical properties of concrete made with recycled concrete coarse aggregates. *Cement and Concrete Research,* 41, 533-541.

VYTLAČILOVÁ, V. 2011. The fibre reinforced concrete with using recycled aggregates. *International Journal Of Systems Applications, Engineering & Development,* 5.

WHITTLE, R. & JONES, T. 2004. *Technical Report No. 59: Influence of tension stiffening on deflection of reinforced concrete structures*. Camberley: The Concrete Society.

WRAP. Perfomance Related approach to use recycled aggregates. Oxon: *Waste and Resources Action Programme*; 2007.

WU, H. & GILBERT, R. 2008. An experimental study of tension stiffening in reinforced concrete members under short-term and long-term loads. *UNICIV Report no*.

XIAO, J. & FALKNER, H. 2007. Bond behaviour between recycled aggregate concrete and steel rebars. *Construction and Building Materials,* 21, 395-401.

XIAO, J., LI, L., TAM, V. W. & LI, H. 2014. The state of the art regarding the long-term properties of recycled aggregate concrete. *Structural Concrete,* 15, 3-12.

YANG, J., DU, Q. & BAO, Y. 2011. Concrete with recycled concrete aggregate and crushed clay bricks. *Construction and Building Materials,* 25, 1935-1945.

YEHIA, S., HELAL, K., ABUSHARKH, A., ZAHER, A. & ISTAITIYEH, H. 2015. Strength and durability evaluation of recycled aggregate concrete. *International Journal of Concrete Structures and Materials,* 9, 219-239.

YOUNIS, K. H. & PILAKOUTAS, K. 2013. Strength prediction model and methods for improving recycled aggregate concrete. *Construction and Building Materials,* 49, 688-701.

ZAHARIEVA, R., BUYLE-BODIN, F., SKOCZYLAS, F. & WIRQUIN, E. 2003. Assessment of the surface permeation properties of recycled aggregate concrete. *Cement and Concrete Composites,* 25, 223-232.

ZERBINO, R. L. & BARRAGÁN, B. E. 2012. Long-term behavior of cracked steel fiber-reinforced concrete beams under sustained loading. *ACI Materials Journal,* 109.

APPENDIX

A.1 Numerical Analysis Program

A numerical analysis program has been developed using the MATLAB language for predicting the long-term deflection of reinforced concrete beams. This program is based on the cracked section analysis approach from Eurocode 2 and includes the modifications proposed in this research to account for the effects of incorporating recycled aggregate and steel fibres.

Figure A-1 provides a flowchart of the program. As the calculation steps are complicated and are performed as a function of time, the program has been designed to simplify the analytical calculations and present the final results for the long-term deflection in tables and figures. The results from the analytical program of the beams tested in this research are presented in Figures A-2 to A-5.

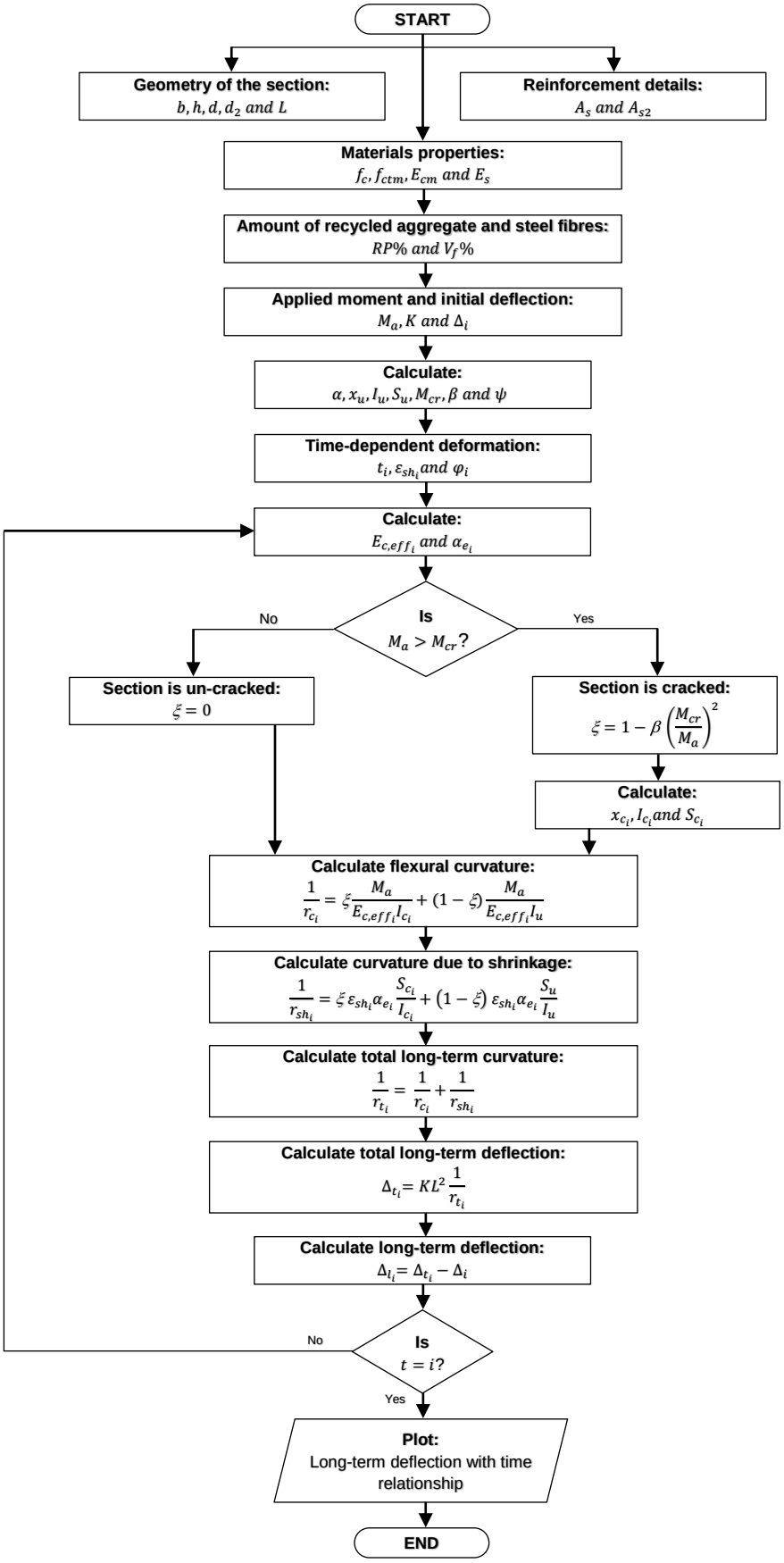

Figure A- 1 Flowchart of the numerical analysis program

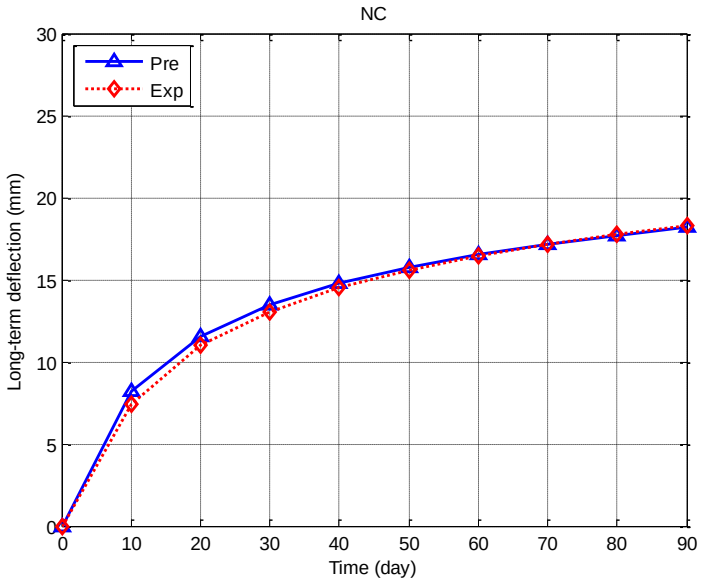

Figure A- 2 Predictions from the analytical program for the NC beam

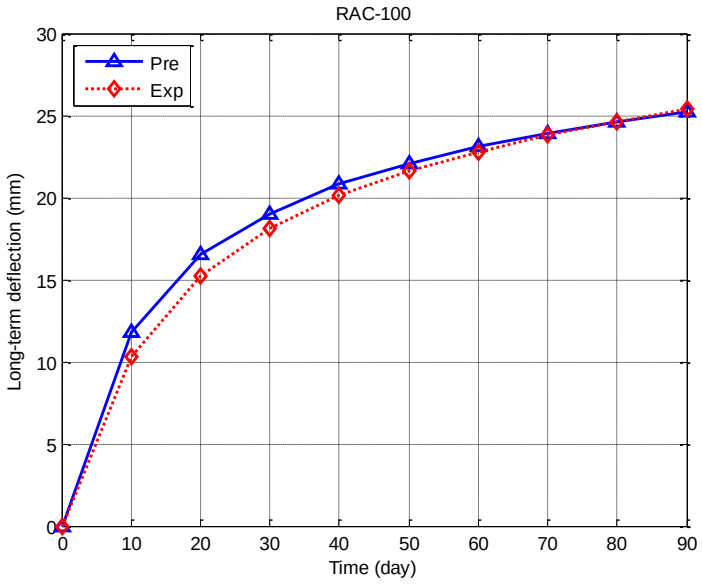

Figure A- 3 Predictions from the analytical program for the RAC-100 beam

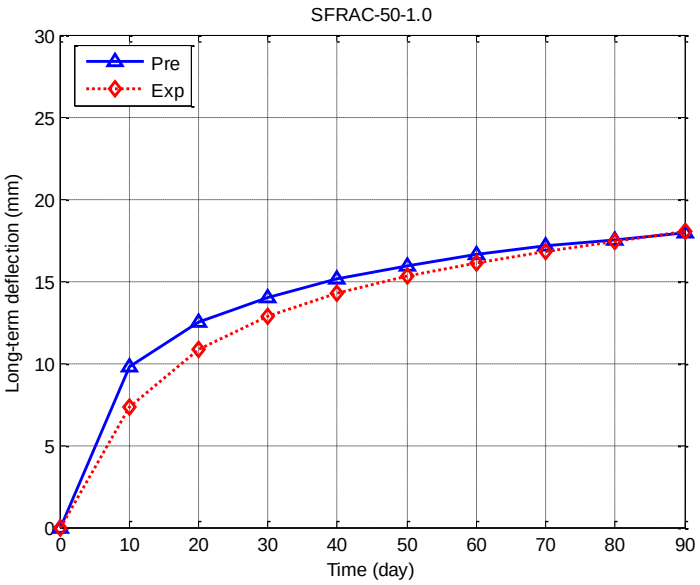

Figure A- 4 Predictions from the analytical program for the SFRAC-50-1.0 beam

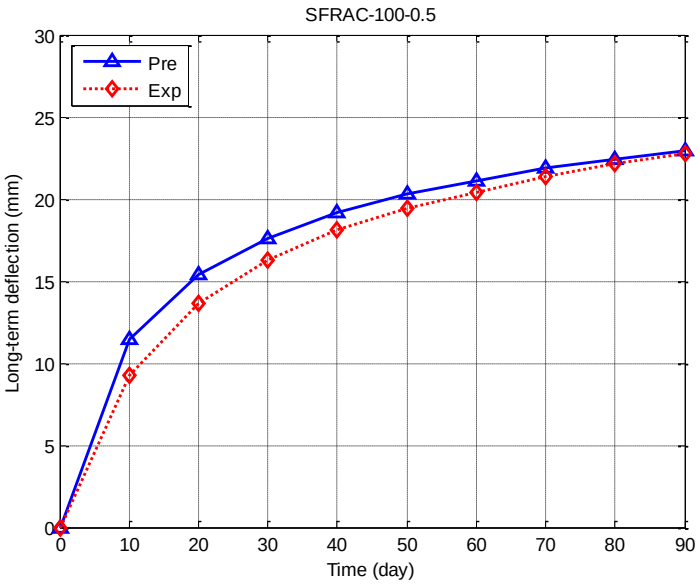

Figure A- 5 Predictions from the analytical program for the SFRAC-100-0.5 beam

A.2 Example of Numerical Calculations

Data for the SFRAC-50-1.0 beam has been selected to explain the calculation steps within the numerical program. The equations and calculation steps for predicting the long-term deflection of this beam at 90-days of loading are shown below (one loop). The following input data was obtained from the experimental results for the material properties and time-dependent deformations:

- Geometry of the section:

  $L = 4000\ mm \qquad b = 300\ mm \qquad h = 150\ mm$

  $d = 114\ mm \qquad d_2 = 34\ mm$

- Reinforcement details:

  $A_s = 603.2\ mm^2 \qquad A_{s2} = 226.2\ mm^2$

- Materials properties:

  $f_{ck} = 44.18\ MPa$

  $f_{ctm} = 0.3{f_{ck}}^{2/3} \ \ or \ \ 0.9f_{ctm,sp} \ \ or \ \ \frac{f_{ctm,fl}}{1.5} = 4.28\ MPa$

  $E_{cm} = 27{,}600\ MPa$

  $E_s = 200{,}000\ MPa$

- Amount of recycled aggregate and steel fibres:

  $RP\% = 50\% \qquad V_f\% = 1.0\%$

- Applied moment and initial deflection:

  $M_a = 16.535\ KN.m$

  $K = 0.104$

  $\Delta_i = 26.65\ mm$

- Time-dependent deformation:

  $t = 90$

  $\varepsilon_{sh} = 0.000408$

  $\varphi = 1.8556$

- Calculation:

  $$\alpha = \frac{E_s}{E_{cm}} = 7.246$$

  $$x_u = \frac{\frac{bh^2}{2} + (\alpha - 1)(A_s d + A_{s2} d_2)}{bh + (\alpha - 1)(A_s + A_{s2})} = 76.77\ mm$$

$$I_u = \frac{bh^3}{12} + bh\left(\frac{h}{2} - x_u\right)^2 + (\alpha - 1)A_s(d - x_u)^2 + (\alpha - 1)A_{s2}(x_u - d_2)^2$$

$$= 92322902.33\ mm^4$$

$$S_u = A_s(d - x_u) - A_{s2}(x_u - d_2) = 12779.06\ mm^2$$

$$M_{cr} = \frac{f_{ctm}\, I_u}{(h - x_u)} = 5.396\ KN.m$$

$$\beta = 0.5 - 0.002RP\% + 0.3V_f\% = 0.7$$

$$\psi = 1 - 0.4V_f\% = 0.6$$

$$E_{c,eff} = \frac{1.05E_{cm}}{1 + \psi\, \varphi} = 13{,}712\ MPa$$

$$\alpha_e = \frac{E_s}{E_{c,eff}} = 14.585$$

$$M_a = 16.535 > M_{cr} = 5.396$$

$$\xi = 1 - \beta\left(\frac{M_{cr}}{M_a}\right)^2 = 0.9213$$

$$x_c$$

$$= \frac{[(\alpha_e A_s + (\alpha_e - 1)A_{s2})^2 + 2b(\alpha_e A_s d + (\alpha_e - 1)A_{s2}d_2)]^{0.5} - (\alpha_e A_s + (\alpha_e - 1)A_{s2})}{b}$$

$$= 55.027\ mm$$

$$I_c = \frac{b{x_c}^3}{12} + \alpha_e A_s(d - x_c)^2 + (\alpha_e - 1)A_{s2}(x_c - d_2)^2 = 48616852.59\ mm^4$$

$$S_c = A_s(d - x_c) - A_{s2}(x_c - d_2) = 30815.25\ mm^2$$

$$\frac{1}{r_c} = \xi\frac{M_a}{E_{c,eff}I_c} + (1 - \xi)\frac{M_a}{E_{c,eff}I_u} = 23.251 \times 10^{-6}\ mm^{-1}$$

$$\frac{1}{r_{sh}} = \xi\,\varepsilon_{sh}\alpha_e\frac{S_c}{I_c} + (1 - \xi)\,\varepsilon_{sh}\alpha_e\frac{S_u}{I_u} = 3.542 \times 10^{-6}\ mm^{-1}$$

$$\frac{1}{r_t} = \frac{1}{r_c} + \frac{1}{r_{sh}} = 26.793 \times 10^{-6}\ mm^{-1}$$

$$\Delta_t = KL^2\frac{1}{r_t} = 44.58\ mm$$

$$\Delta_l = \Delta_t - \Delta_i = 17.93\ mm$$

$$(\Delta_l)_{Exp} = 17.98\ mm$$

These calculation steps can be repeated in a loop for different time points to obtain the relationship between the long-term deflection and the time of loading as shown in Figure A-4.